

**Investigations on new and forgotten antischistosomal
drugs and praziquantel pharmacokinetics in
opisthorchiasis patients**

INAUGURALDISSERTATION

zur

Erlangung der Würde eines Doktors der Philosophie

vorgelegt der

Philosophisch-Naturwissenschaftlichen Fakultät

der Universität Basel

von

Alexandra Christina Probst

Basel, 2023

Genehmigt von der Philosophisch-Naturwissenschaftlichen Fakultät der Universität Basel
auf Auftrag von

Prof. Dr. Jennifer Keiser

Prof. Dr. Pascal Mäser

Prof. Dr. Marc Hübner

Basel, den 21. September 2021

Prof. Dr. Marcel Mayor

Dekan der Philosophisch-Naturwissenschaftlichen Fakultät

TABLE OF CONTENTS

Acknowledgements	ii
Summary	iv
Table of Abbreviations.....	vii
Chapter I: Introduction	1
1. Schistosomiasis	1
1.1 Epidemiology and burden of disease	1
1.2 Life cycle.....	3
1.3 Clinical presentation and diagnosis.....	4
1.4 Control strategies and treatment.....	7
1.5 Need for new drugs and challenges in antischistosomal drug discovery	10
1.5.1 Promising drug candidates	12
2. <i>Opisthorchis felineus</i>	15
2.1 Epidemiology of <i>O. felineus</i>	15
2.2 Life cycle of <i>O. felineus</i>	16
2.3 Clinical manifestation and treatment	17
2.3.1 Towards a better understanding of the treatment of opisthorchiasis with praziquantel.....	17
3. References	19
Chapter II: Aims and Objectives	28
Chapter III: Antischistosomal pyridobenzimidazoles	29
Chapter IV: SF ₅ -containing diarylureas as antischistosomals	42
Chapter V: Antischistosomal <i>A. annua</i> and <i>A. afro</i> extracts	60
Chapter VI: Ro 15-5458, a schistosomicidal acridanone hydrazone	67
Chapter VII: Praziquantel pharmacokinetics in <i>O.felineus</i> infected patients.....	76
Chapter VIII: General discussion	85
8. Rationale and objectives.....	85
8.1 A way forward for antischistosomal drugs.....	87
8.2 Insights into praziquantel pharmacokinetics of <i>O. felineus</i> infected patients	115
8.3 References	117
Curriculum vitae	119

ACKNOWLEDGEMENTS

The past three and a half years have been an enriching experience that not only resulted in a highly collaborative thesis but also many life-lessons learned and unforgettable memories. Therefore, I would like to take the opportunity to express my sincerest thanks to all people who have contributed to this work or supported and encouraged me.

First and foremost, I am immensely grateful to my supervisor, Prof. Jennifer Keiser, for giving me all the support a PhD student can wish for. Your open-mindedness, your ability to motivate people and your feedback-culture guided me along my scientific journey and together with your commitment against NTDs were a source of constant inspiration. Thank you, Jenny, for the trust you have placed in me from the very beginning.

I am indebted to my second supervisor and my examining committee. Thank you to Prof. Pascal Mäser for following my doctoral investigations and providing helpful advice during our annual meetings. Moreover, thank you to Prof. Marc Hübner for carefully reading my thesis and acting as a co-referee at my PhD defense. Finally, a special thanks to Prof. Jürg Utzinger for acting as faculty representative.

My collaborations were an origin of innovation and joy. My sincerest thanks to Prof. Conor Caffrey (University of California San Diego) who first introduced me to research on schistosomiasis. To his ongoing support and his great hospitality during my research stay in San Diego. I am tremendously grateful to Prof. Kelly Chibale (University of Cape Town) for the lively exchanges on antischistosomal pyridobenzimidazoles and to Dr. Godwin Dziwornu for introducing me to SAR studies and for keeping in touch over the friendly catch-up calls along my PhD journey. Further, I express my deepest thanks to Prof. Santi Vazquez (University of Barcelona) and Dr. Eugènia Pujol for the stimulating discussions and enthusiasm around diarylureas. My appreciation extends to Prof. Jonathan Vennerstrom and team (University of Nebraska), Prof. Sue Charman and team (Monash University), Prof. Olga Fedorova and team (Siberian State Medical University) as well as Prof. Frank van der Kooy (North-West University) for their valuable inputs and the excellent scientific exchanges.

My sincere thanks to the Zoom@Novartis program for bringing together talented young female researchers and to my mentor, Dr. Petra Feiertag, for engaging in insightful conversations and for opening doors of opportunities.

I am fortunate to have shared many engaging discussions, lunch- and coffee breaks as well as unforgettable group outings with my dear wormy friends. To all my former and current lab-wormies: Val, Flavio, Valentin, Jessi, Stefan, Tanja, Martina, Anna, Hannah, Pierre, Lavinia, Erin, Miriam and Dani, I have learned so much from you and enjoyed all the hours we spent together in the lab, thank you for your collaboration and friendship. Labwork would have not been possible without the continuous contribution from Cécile and her army of civil servants, thank you for your unconditional support. To my field- and office-wormies: Ladina, Chandni, Marta, Sophie, Imma, Jantine and Evi, I would not have had such an amazing time without you guys, thanks for spreading kindness and happiness. Lastly, a special thanks to my master student Robert for diving into our wormy world with boundless motivation.

A deep and honest thanks to Pascale and all animal care takers for their utmost important and excellent work. Further, I am grateful to Yvette and Anna for maintaining the snails and sharing their immense parasitological knowledge.

For their kindness and the nice working atmosphere they create as well as for their help with certain experiments, I would like to thank Susi and Sabine, Monica and Romina, the technical service crew, the ET department, the library team, the PhD community and many more, be it in house at Swiss TPH or externally.

Finally, I express my boundless gratitude to my family and friends – close and far – for patiently listening to all the wormy stories and encouraging me throughout this wonderful experience. I am immensely happy and grateful for having found love during the most unexpected time of my journey at SwissTPH. From the bottom of my heart, thank you, Mama & Papa, my sister Claudia, and thank you, Basil, for encouraging me to follow my dreams, for your endless love and patience, and for always standing by my side.

SUMMARY

Neglected tropical diseases (NTDs) are defined as a group of communicable diseases, most prevalent in tropical and subtropical regions of the world. Prevailing over the poorest populations that have limited access to sanitation, hygiene and education, NTDs affect more than one billion people worldwide and are endemic in 149 countries.

Schistosomiasis, caused by blood-dwelling trematode flatworms of the *Schistosoma* genus is a neglected parasitic disease. The tremendous disease burden of schistosomiasis is associated with anemia, malnutrition as well as impaired childhood development and causes high morbidity for more than 200 million infected individuals. Praziquantel (PZQ) is the sole drug currently available; morbidity reduction using preventive chemotherapy relies completely on PZQ. Apart from its lack of activity against developing stages of the worm and the fact that PZQ is rarely curative, its abundant use incurs the possibility of drug resistance. Thus, there is an urgent need to identify and develop novel therapeutic principles.

Opisthorchiasis, caused by the liver fluke *Opisthorchis felineus* is a food-borne trematodiasis with worldwide highest prevalence in Western Siberia. There are 12.5 million individuals at risk for an infection. The disease erupts upon dietary consumption of raw or undercooked fish infested with trematode larvae. It affects the hepatobiliary system and can lead to pancreatitis or even severe chronic infections such as hepatic abscesses. As for schistosomiasis, the drug of choice for the treatment of opisthorchiasis is praziquantel. The doses used are empirical and prescribed individually, the whole treatment scheme is very complicated and takes about three months to be accomplished; thus it makes it unavailable for many people.

My PhD thesis had two major aims. The first was to advance antischistosomal drug discovery by identifying novel chemical entities and by rescuing a forgotten lead candidate. The second was to elucidate the pharmacokinetic properties of praziquantel in *O. felineus* infected patients, laying the groundwork for a simplified standardized treatment scheme.

A first study we conducted to achieve the first aim; followed-up on an existing structure-activity relationship (SAR) program, the antischistosomal *in vitro* and *in vivo* activities of a 3rd generation pyridobenzimidazole (PBI) drug set were evaluated. We found high *in vitro* activities against *Schistosoma mansoni* newly transformed schistosomula (NTS) and adult worms, with IC₅₀ values of 0.08 – 1.43 μM. Upon promising results obtained from metabolic stability assays with liver microsomes (>80%), we engaged in efficacy testing using infected mice. Moderate to high worm burden reductions (WBR) of 36 – 90 % were obtained after single oral doses of four selected compounds. However, we observed a small therapeutic window although results obtained from cytotoxicity screens against CHO and HepG2 cells did not foresee toxicity.

In order to expand SAR studies around another promising chemotype, *N,N'*-diarylhureas, we investigated a novel series of analogs featuring the pentafluorosulfanyl group (SF₅). High *in vitro* activity, acceptable cytotoxicity profiles and high microsomal hepatic stability were found. IC₅₀ values for the most promising compounds were between 0.8 and 1.8 μM for NTS and 0.1 – 0.4 μM for adult *S. mansoni*. However, none of the compounds tested in *S. mansoni* infected mice revealed *in vivo* efficacy. Results obtained from an accompanying PK study, showed that all tested compounds were slowly absorbed and only reached maximal plasma concentration values after 24 h. There was no correlation between drug exposure and *in vivo* efficacy.

Extracts and fractions of the medicinal plants *Artemisia annua* and *Artemisia afra* were tested for their *in vitro* activity against *S. mansoni* NTS and adult worms. We comparatively evaluated a set of extracts and fractions and found low IC₅₀ values, especially for the *A. afra* (BB) hexane and DCM fractions. The findings suggest that *A. afra*, despite lacking the bioactive compound artemisinin found in *A. annua*, is more active than the latter, further warranting studies to identify novel molecules.

Our studies on the largely forgotten lead candidate, Ro 15-5458, found high *in vivo* efficacy across the whole development stage of *S. mansoni*, when the drug was administered as a single oral dose of 50 mg/kg. Low ED₅₀ of 5.3 and 15 mg/kg were obtained for mice harboring adult and juvenile infections, respectively. Ro 15-5458 was also tested against *S.*

haematobium and *S. japonicum*. We found an ED₅₀ value of 17 mg/kg in hamsters harboring a patent *S. haematobium* infection; however, the compound was inactive at up to 100 mg/kg in *S. japonicum* infected mice. *In vitro*, a de-ethylated and a glucuronidated product were identified and the metabolic stability was evaluated using microsomes and hepatocytes. The low *in vitro* activity against NTS and adult worms and the late onset of action correlated with results obtained from hepatic shift experiments conducted *S. mansoni* infected mice. Ro 15-5458 had a half-life of approximately 5 h and the maximal plasma concentration was reached after 3 h (8 µg/mL) when a 50 mg/kg oral dose was administered to healthy mice.

In the context of a randomized controlled, single-blinded dose finding trial in Tomsk, Siberia, we conducted, for the second aim of this thesis, a PK study in *O. felineus* infected patients and assessed the kinetic disposition of both praziquantel enantiomers (*R*-PZQ and *S*-PZQ) and the drug's main metabolite (*R-trans*-4-OH-PZQ). Single, ascending doses of 20, 40 and 60 mg/kg were compared to multiple dosing (3 x 60 mg/kg). Dried blood spots (DBS) collected over 24 h were analyzed using a validated LC-MS/MS method. Maximal plasma concentrations were reached after 1.5 h (1.72 µg/mL), 2 h (4.89 µg/mL) and 3 h (2.69 µg/mL) for *R*-, *S*- and *R-trans*-OH-PZQ, respectively, when praziquantel was given as a single 60 mg/kg dose. Highest exposure levels (AUC) were observed for the triple dose scheme with AUC values of 8.04, 27.75 and 36.38 µg/mL*h, respectively.

In conclusion, we present two sets of promising antischistosomal drug candidates, the PBIs and the *N,N'*-diarylureas. Our studies complement early drug discovery efforts around both chemotypes and provide insights for a next generation of optimized antischistosomal PBIs and *N,N'*-diarylureas. Additionally, extracts from medicinal plants such as *A. annua* and *A. afra* present potential alternatives to small molecules. Concurrently, Ro 15-5458 is an excellent lead candidate, efficacious alongside all stages of *S. mansoni* development, and further warrants investigations. Finally, praziquantel disposition in *O. felineus* infected individuals has been evaluated and in combination with the results from the efficacy study will be pivotal to establish an evidence based dosing recommendation.

TABLE OF ABBREVIATIONS

ADME	Absorption, Distribution, Metabolism, Elimination
AUC	Area under the curve
BW	Body weight
C _{max}	Maximal concentration
DALYs	Disability adjusted life years
DBS	Dried blood spot
DMSO	Dimethyl sulfoxide
ED ₅₀	Median effective dose
FCS	Fetal calf serum
FDA	US Food and Drug Administration
HPLC	High-performance liquid chromatography
IC ₅₀	Drug concentration required to inhibit parasite viability by 50%
IS	Internal standard
LC-MS	Liquid chromatography - Mass spectrometry
LLOQ	Lower limit of quantification
MMV	Medicines for Malaria Venture
MOA	Mechanism of action
MW	Molecular weight
NTD	Neglected Tropical Disease
NTS	Newly transformed schistosomula
PK/PD	Pharmacokinetic / Pharmacodynamic
PPP	Public Private Partnership
PZQ	Praziquantel
QC	Quality control
rac	Racemic / racemate
SAR	Structure-activity relationship
SD	Standard deviation
SI	Selectivity index
TPP	Target product profile
T _{1/2}	Half-life
T _{max}	Time at maximal concentration
WASH	Water, sanitation and hygiene
WBR	Worm burden reduction
WHO	World Health Organization

CHAPTER I: INTRODUCTION

Neglected tropical diseases (NTDs) are a diverse group of communicable diseases generally afflicting the world's poorest populations. They are most prevalent in tropical and subtropical regions and affect more than one billion people living in 149 countries (Houweling et al. 2016; Utzinger et al. 2012; WHO 2020). The consequences of being infected with one or more NTDs can lead to devastating effects over an entire life-course. They include, but are not limited to, impaired physical and cognitive development, unfavorable pregnancy outcomes and decreased productivity in the workplace. Moreover, social stigmatization poses an enormous burden on afflicted individuals and lastly, NTDs contribute to mortality. These factors slow down the economic growth and further promote poverty (Weiss 2008; Molyneux, Hotez, and Fenwick 2005)

Human helminthiasis cause the largest disease burden among all NTDs (Utzinger et al. 2012). Thus, given the tremendous impact of helminth-associated infections, and limited treatment options, this thesis focusses on two diseases caused by parasitic helminths, namely schistosomiasis and opisthorchiasis.

1. Schistosomiasis

Human schistosomiasis, also known as Bilharzia, is a neglected tropical disease with a tremendous global burden. It is caused by the blood dwelling trematodes of the genus *Schistosoma* and poses a risk to millions of people worldwide (Gryseels et al. 2006; Molyneux, Hotez, and Fenwick 2005). People living in rural settings in tropical and subtropical regions most affected by the disease that is not only associated with but also further promotes poverty (Molyneux, Hotez, and Fenwick 2005; Gray et al. 2011; King 2010).

1.1 Epidemiology and burden of disease

More than 90 percent of all schistosomiasis cases occur in sub-Saharan Africa (WHO 2021), with children and adolescents being infected more often and heavily than adults (Doehring

1988). Infections involve contaminated water bodies and occur during daily activities such as bathing, fishing, laundering or agricultural tasks (Colley et al. 2014; Hotez and Kamath 2009). Schistosomiasis causes a loss of 1.4 million disability-adjusted life years (DALYs) (Collaborators 2018). Death estimates vary between 24,000 and 200,000 cases annually (WHO 2021). Transmission has been reported from 78 countries (Figure 1) (WHO 2021), including a recent outbreak in Europe (Boissier et al. 2016; Rothe et al. 2021). The WHO estimates that at least 236.6 million people were infected with schistosomiasis in 2019, and approximately 10 percent of the world population is at risk for an infection (WHO 2021).

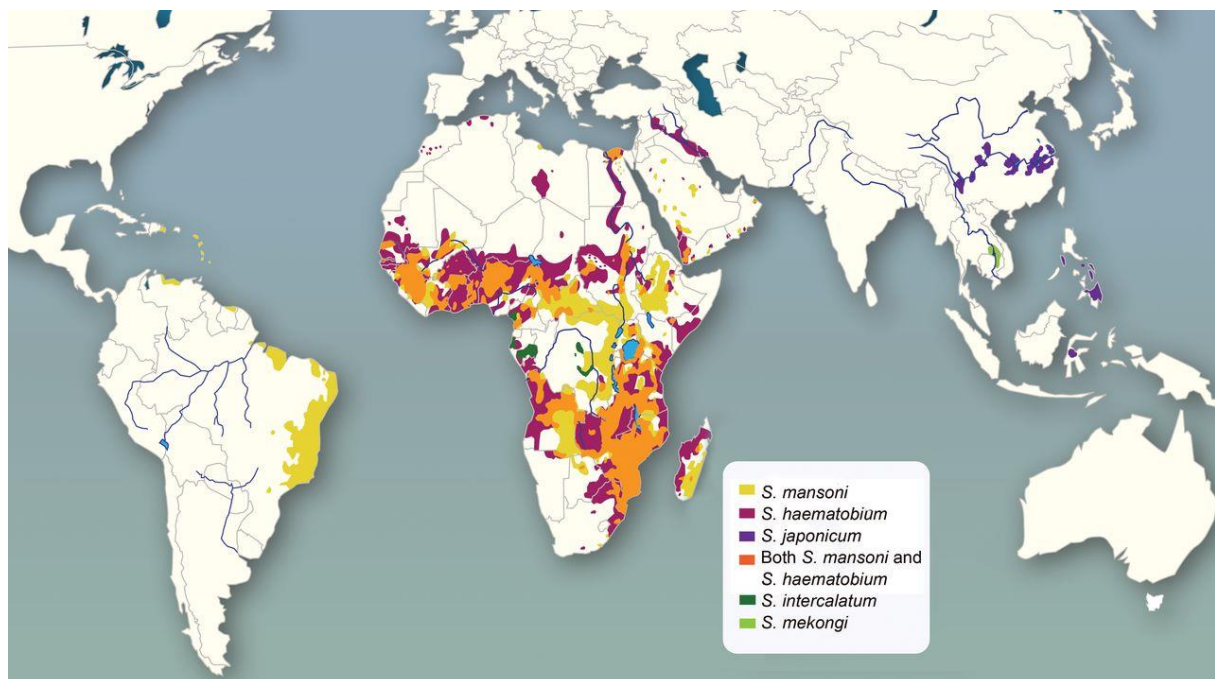


Figure 1: Global distribution of schistosomiasis (Weerakoon Kosala et al. 2015)

There are many different reasons, both behavioral and environmental, that promote disease transmission. Moreover, there is a high variability in prevalence and infection intensity across affected countries and even within small areas (Steinmann et al. 2006). It is worth noting, that the increase in water resource development projects has been associated with an increased prevalence of schistosomiasis cases. Since schistosomiasis has been introduced to previously non-endemic areas, calls to integrate health impact assessment and mitigation strategies have become louder (Steinmann et al. 2006).

Six medically important *Schistosoma* species infect humans. Of these, *Schistosoma haematobium*, *S. japonicum* and *S. mansoni* account for the highest burden of disease. *S. haematobium* is transmitted by *Bulinus* snails and causes the urogenital form of the disease; it is present in Africa and the Middle East. *S. japonicum* and *S. mansoni* both cause the intestinal form of the disease and are transmitted by *Biomphalaria* and *Oncomelania* snails, respectively. While *S. japonicum* accounts for schistosomiasis cases in China, the Philippines and Indonesia, *S. mansoni* infections are common in Africa, the Arabian peninsula, and South America. The remaining three species, namely *S. mekongi*, *S. guineensis* and related *S. intercalatum* are of local importance (Gryseels et al. 2006; Colley et al. 2014).

1.2 Life cycle

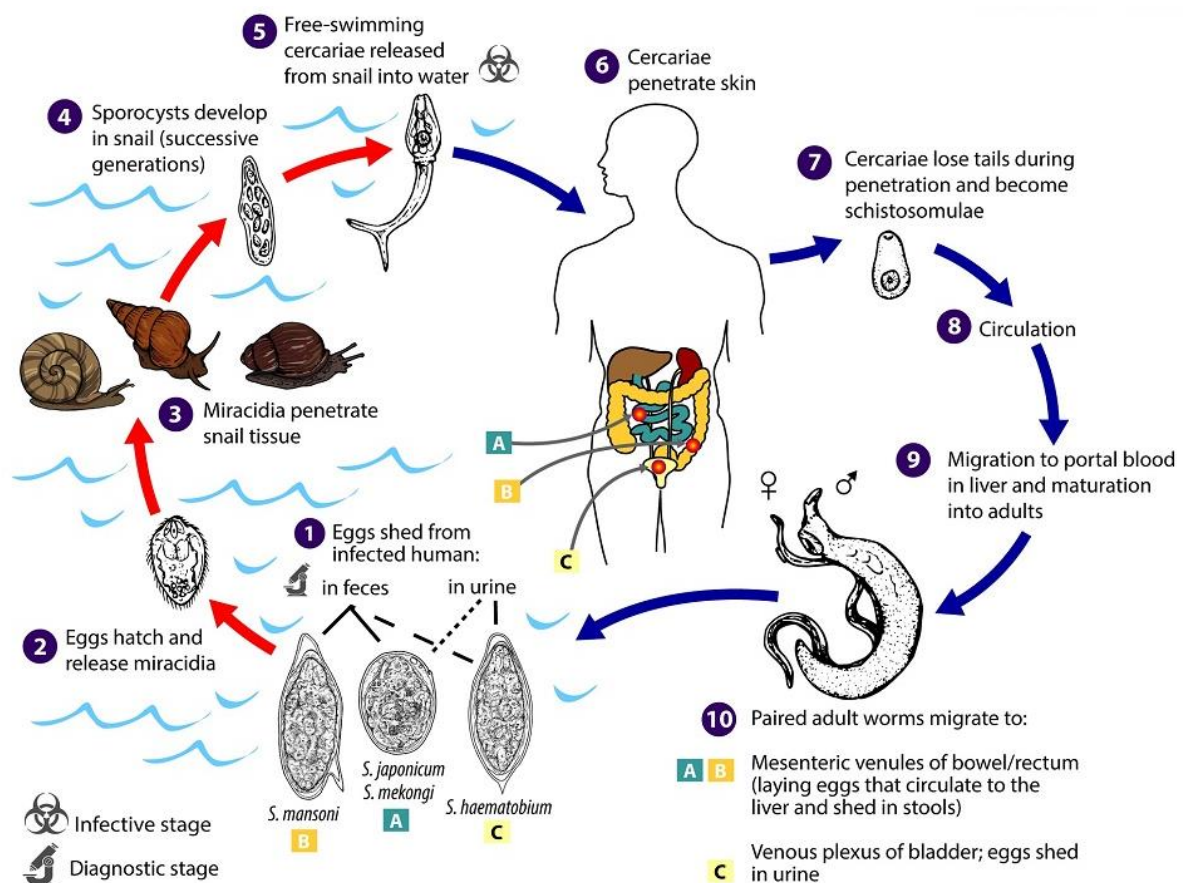


Figure 2: *Schistosoma* spp. life cycle (CDC 2021b).

Schistosomiasis is a water borne disease. Humans become infected upon penetration of the larval stage of *Schistosoma* spp., the cercariae, when in contact with contaminated fresh water bodies (Figure 2) (Gryseels et al. 2006). Using phototaxis and chemotaxis, cercariae seek the skin of a suitable host. They penetrate the host skin within 2 to 24 h and transform into schistosomula once they lose their forked tail (McKerrow and Salter 2002; Haas and Haeberlein 2009). The schistosomules travel along the vascular system towards the lungs where their transformation to juvenile worms occurs. Continuing their migration via venous system, they reach the host liver after four to six weeks and mature into male and female worms. Adult schistosomes live on average 3 - 10 years. They are approximately 7 – 20 mm in length, possess an oral and ventral sucker, reproductive organs and a blind digestive tract. The female worm is longer and thinner than the male worm and is held in the gynecophoric canal by the male. Upon mating, the paired schistosomes relocate to the portal and mesenteric veins, or in the case of *S. haematobium*, vesicular veins around the bladder. Female worms start to lay thousands of eggs daily, which are excreted with the urine (urogenital schistosomiasis) or feces (intestinal schistosomiasis). Upon contact with water, the eggs hatch into free-swimming miracidia, which then penetrate the intermediate snail host where they undergo asexual reproduction through mother and daughter sporocyst stages. Four to six weeks later the snails start to release cercariae and the lifecycle starts all over again (Colley et al. 2014).

1.3 Clinical presentation and diagnosis

Manifestation of schistosomiasis can be divided into acute and chronic schistosomiasis. Acute schistosomiasis, also known as Katayama Syndrome, often occurs on first contact with the parasite (tourists) or in case of a heavy reinfection. It is a systemic hypersensitivity reaction against schistosomula migration and egg deposition (Ross et al. 2007). The first symptom of an infection, an urticarial rash caused by the skin penetration of cercariae, can occur within hours and is also known as swimmer's itch. Other symptoms only occur within weeks or months and include fever, fatigue, myalgia, non-productive cough, eosinophilia, and patchy

infiltrates on chest radiography. Due to their rather non-specific nature, the acute stage of schistosomiasis is often missed or misdiagnosed (Gryseels et al. 2006).

Chronic schistosomiasis, independent of the species and stage of development, is caused by the host's immune response to eggs that are trapped in the tissues, rather than to the worms (Colley et al. 2014). Trapped eggs elicit a strong Th2-type immune response and in recruiting endothelial and immune cells such as eosinophils or macrophages induce the formation of granulomas. Eventually, trapped eggs die and form fibrotic plaques and sometimes even the development of necrosis (Fairfax et al. 2012). Thus, there is a strong correlation between the clinical pathology and the infection intensity of an infected individual. Further, it is thought that immune responses and host genetic factors may play a role (Pearce and MacDonald 2002; Colley et al. 2014).

Chronic schistosomiasis can occur in the form of urinary and intestinal schistosomiasis. The former, caused by *S. haematobium*, results in inflammation, ulceration and pseudopolyposis of the vesical and ureteral walls. In the early stage, urinary schistosomiasis is characterized by hematuria and dysuria, but can lead to severe complications including bacterial infections and renal dysfunction. Women may suffer from genital lesions, nodules in the vulva and vaginal bleeding, while hematospermia, orchitis and prostatitis can occur in man. Both sexes can suffer from pain during sexual intercourse and infertility (WHO 2017; Colley et al. 2014). Moreover, infections with *S. haematobium* have been associated with squamous-cell carcinoma of the bladder and an increased risk of an HIV infection (Colley et al. 2014; King et al. 1988; Kjetland et al. 2006). Abdominal pain, diarrhea and rectal bleeding are classical symptoms resulting from chronic intestinal schistosomiasis infections. Advanced cases often display an enlarged liver and spleen. These conditions can lead to death when complications occur (Colley et al. 2014). Finally, the disabling morbidities like chronic tissue inflammation and iron deficiency anemia, malnutrition, and impaired childhood development (including poor school performance) as well as increased susceptibility to co-infection with other parasitic diseases pose a significant health problem to at risk populations (King and Dangerfield-Cha 2008).

There are three different categories in which the current diagnostic tools fall into, namely (i) indirect methods such as interpretation of medical history and evaluation of clinical signs and symptoms; (ii) direct parasitological methods and (iii) immunological methods (van Lieshout, Polderman, and Deelder 2000; Colley et al. 2014).

The microscopic examination of species-specific eggs in stool (*S. mansoni* and *S. japonicum*) or urine (*S. haematobium*) samples remain the gold standard for diagnosing schistosomiasis (Gray et al. 2011). As quantitative methods are desired in epidemiological surveys and control programs (Danso-Appiah et al. 2013) the Kato-Katz thick smear (Katz, Chaves, and Pellegrino 1972) is widely employed for intestinal schistosomiasis, while a simple urine filtration is used to diagnose urinary schistosomiasis (Peters et al. 1976). In both cases, the number of eggs per gram of stool or per 10 mL of urine can be estimated, respectively (Gray et al. 2011). The specificity for both techniques is high, however, due to factors such as variable day-to-day egg output, these diagnostic tool have limited sensitivity when used in low or medium endemic areas (de Dood et al. 2018). Therefore, to increase sensitivity, it is recommended to collect and analyze several samples from the same person (Lamberton et al. 2014; Knopp et al. 2013; Gray et al. 2011).

The immunological techniques are based on either measuring the parasites and their products or the immune response of the infected host. They show superiority to the previous described microscopic evaluation in terms of sensitivity (van Lieshout, Polderman, and Deelder 2000). However, in an antibody-based assay it is not possible to distinguish between past and active infections. Thus, these tests are not suitable for the use in endemic populations (de Dood et al. 2018; van Lieshout, Polderman, and Deelder 2000). Another widely accepted method that, in turn is used for monitoring and mapping purposes, is the determination of circulating anodic (CAA) or cathodic (CCA) antigens via point-of-contact assays (POC CCA and POC CAA) (van Lieshout, Polderman, and Deelder 2000).

Finally, molecular techniques, such as amplification of DNA by PCR are generally the most specific and highly sensitive. They have the potential of diagnosing schistosomiasis in all

phases of the clinical disease but are far less suitable in the field due to high costs, infrastructure and specialized staff (Gray et al. 2011; Verweij and Stensvold 2014).

1.4 Control strategies and treatment

More than 100 years ago, schistosomiasis elimination has already been discussed. Despite huge efforts in transmission control and reduction of morbidities, schistosomiasis remains a public health threat with global elimination far off (Rollinson, Knopp, Levitz, Stothard, Tchuem Tchuente, et al. 2013; Fenwick and Jourdan 2016). Mass drug administration (MDA), so-called preventive chemotherapy (PC), has been identified as a key contributor to control and eventually eliminate schistosomiasis. This strategy aims to treat populations that are at high risk for infection, and to prevent transmission of the disease as well as to contribute towards reduction of morbidities (WHO 2021). Praziquantel is the drug of choice and will be discussed in more detail below. Although PC is a fundamental approach for the control of schistosomiasis (being employed since the 1980s) and has the advantage of treating large populations at low cost, elimination of schistosomiasis will only be feasible when incorporating complimentary approaches. These interventions include improved sanitation, access to safe drinking water and hygiene education (e.g. Water, Sanitation and Hygiene (WASH)), as well as innovative and intensified disease management (IDM) and snail control (Lo et al. 2017; Rollinson, Knopp, Levitz, Stothard, Tchuem Tchuente, et al. 2013).

In 2012, the WHO set a target to reach treatment coverage of at least 75% and up to 100% for at risk school-aged children by 2020. Additional targets included regional elimination in the Eastern Mediterranean Region, the Caribbean, Indonesia and the Mekong River Basin by 2015, and the Americas, Western Pacific Region and selected African Regions by 2020 (WHO 2012). These ambitious elimination targets were not met and, therefore, it is proposed to shift towards elimination of schistosomiasis as a global health threat by 2030 (WHO 2020). To reach this goal the pharmaceutical company Merck has promised to donate 250 million tablets of praziquantel annually for an unlimited amount of time (WHO 2017, 2020). According to data collected by the WHO, 95.3 million people were globally treated with praziquantel in 2018,

corresponding to a total coverage of 41.6 %. Thus, to reach the 2030 targets many roadblocks still need to be overcome.

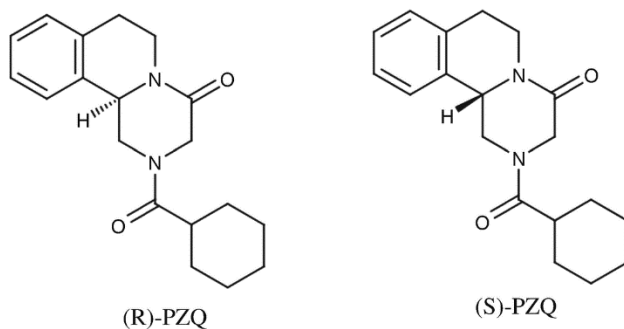


Figure 3: Enantiomers of praziquantel (PZQ): (R)-PZQ and (S)-PZQ

Praziquantel (Figure 3), the only drug recommended for treatment, is widely used in PC campaigns since its discovery by Bayer AG, Leverkusen and E. Merck, Darmstadt. The antischistosomal activity of the drug was first reported in 1977 by Gönner and Andrews and preliminary trials in humans infected with schistosomiasis were carried out soon after (Gönner and Andrews 1977). Praziquantel is active against all *Schistosoma* species. The orally administered drug is an acylated quinolone-pyrazin, commercially available as a racemate, *R*(-) and *S*(+) isomers, where mainly the *levo* form is schistosomicidal (Cioli and Pica-Mattocchia 2003; Meister et al. 2014). After oral application, PZQ is rapidly absorbed, with peak concentrations in the serum reached after 1-2 hours (Leopold et al. 1978). Praziquantel undergoes first pass metabolism and is eliminated in the urine and in the feces (Cioli and Pica-Mattocchia 2003).

Although PZQ has now been used since more than 40 years to treat schistosomiasis, the mechanism(s) of action have yet not been completely solved (Doenhoff, Cioli, and Utzinger 2008; Abdulla et al. 2009; Bergquist, Utzinger, and Keiser 2017). Only recently, a flatworm target for praziquantel, a transient receptor (TRP) channel in *S. mansoni* has been discovered (*Sm*.TRP_{PZQ}). Observations suggest that the exposure of adult worms to PZQ *in vitro* causes rapid, spastic paralysis of schistosome muscle, as well as vacuolation of the tegument (Park and Marchant 2020).

Due to its effectiveness and good safety profile, it can be given to pregnant woman and children (Friedman et al. 2018). Cure rates of 57 – 88 % and egg reduction rates of 95 % after a single oral 40 mg/kg dose of PZQ have been reported, depending on the *Schistosoma* species, age of participants, and the number of parasitological samples used for diagnosis (Fukushige et al. 2021).

However, major drawbacks of PZQ include its ineffectiveness against juvenile schistosomes, which means that developing infections are not treated during preventive chemotherapy campaigns, and trapped eggs in the tissues as well as the fact that it has a bitter taste, mainly caused by its S-isomer (Meyer et al. 2009; Kovač, Vargas, and Keiser 2017). Furthermore, due to the large size of the tablet, swallowing can be difficult for the younger age groups (Colley et al. 2014). Pediatric formulations are therefore under development (Bustinduy et al. 2016; Consortium 2021).

Finally, to rely on one drug only (that in fact has several limitations) to treat millions of people, risks the emergence of drug resistance development and treatment failures (Colley et al. 2014). At the same time, it is very likely that changes in immuno-epidemiology and genetics in *Schistosoma spp.* proceed slowly and over decades (Mutapi et al. 2017). It is known that resistance to praziquantel can be induced in the laboratory (Doenhoff et al. 2002). Nevertheless, there is not enough evidence regarding clinical praziquantel resistance. Case studies from Egypt and Senegal have reported low levels of praziquantel resistance against *S. mansoni* (Doenhoff et al. 2002), however, a recently published systematic review and meta-analysis found no evidence to support the concerns regarding praziquantel drug resistance (Fukushige et al. 2021). Yet, it should not be concluded that there will be no resistance development over the next 40 years. With praziquantel being widely used in PC campaigns, drug pressure might grow (Doenhoff, Cioli, and Utzinger 2008). Given that praziquantel does not show 100 % efficacy in terms of cure rate, not only parasite related factors but also host and drug related factors such as host liver health, and genetic polymorphisms of liver enzymes

involved in praziquantel metabolism as well as drug–drug interactions need to be further investigated (Zdesenko and Mutapi 2020).

1.5 Need for new drugs and challenges in antischistosomal drug discovery

Praziquantel is not a perfect drug to treat schistosomiasis and a good alternative seems still far off. It is of uppermost importance to identify additional or alternative drugs to praziquantel to fill the relatively empty drug pipeline of clinical candidates. In contrast, the pre-clinical pipeline is filled with several candidates, but key experiments are still missing for many of them. Promising drug candidates will be discussed in more detail below.

There are many challenges in the discovery of new antischistosomal agents, one of the most important being the rather long and complex life cycle of the parasite. Antischistosomal drug discovery relies heavily on phenotypic screening campaigns, with the main goal to identify drugs that are active against whole worms (and subsequently in animal models) rather than a specific target (Ramirez et al. 2007; Moreira-Filho et al. 2021). This approach requires a continuous maintenance of the parasite's life cycle including the infection of intermediate (snails) and definite host (mice or hamsters) (Lombardo et al. 2019). Not only does the approach rely on regular euthanasia of infected animals but also the number of worms that can be extracted from an infected rodent presents a limiting factor. Thus, so called first-pass screenings are often performed on newly transformed schistosomula, which can be easily obtained by mechanically transforming cercariae (Lombardo et al. 2019). On one hand, this approach allows for screening of multiple compounds (over a range of different concentrations), on the other hand, potential hits are missed due to variations in compound sensitivity towards different life stages of the parasite. With this limitation in mind, a recent study by Buchter and colleagues evaluated the reproducibility of a cell-free method to grow juvenile *S. mansoni* and validated its applicability for drug screening assays (Buchter, Schneeberger, and Keiser 2021). While reducing the use of animals in accordance with the 3Rs (reduce, refine, replace) of the animal protection principles (Keiser 2010), such a method also paves the way to include different development stages of the parasite into screening

campaigns. Taken together, the phenotypic screening of antischistosomal compounds, irrespective of the development stage of the parasite, is a semi-quantitative and time-consuming approach. Nevertheless, the approach has been very successful in identifying hits, defining structure activity relationship (SAR) and translating promising *in vitro* results into good activity in infection models of *Schistosoma* (Pasche, Laleu, and Keiser 2018b, 2018a; Maccesi et al. 2019).

Because of several shortcomings, such as the impossibility to maintain the complete parasite lifecycle *in vitro* (Wang, Chen, and Collins 2019; Buchter, Schneeberger, and Keiser 2021) or the lack of clonal organisms; as well as the scarcity of functional genomics tools (like established gene manipulation methods for the validation of potential targets), most industry-standard target-based drug screening approaches are not yet feasible in antischistosomal drug discovery (Ferreira, Oliva, and Andricopulo 2015; Caffrey and Secor 2011).

Over the past decade, innovative approaches have bolstered the drug discovery landscape for schistosomiasis. With the availability of the genomes of the three main schistosomes species affecting human health, new resources have emerged that are able to transform antischistosomal drug discovery research (Zhou et al. 2009; Berriman et al. 2009; Protasio et al. 2012; Young et al. 2012; Stroehlein et al. 2019; Luo et al. 2019). Additionally, transcriptomics and metabolomics have provided insights into gene-functionality and enabled target identification (Oliveira and Pierce 2015). Finally, computer-aided and artificial intelligence-based computational methods have contributed to the optimization of drug discovery efforts for schistosomiasis, as summarized in a recent review by Moreira-Filho and colleagues (Moreira-Filho et al. 2021).

The translation of hits from a screening campaign into animal testing comes with additional challenges. *S. mansoni* is the infection model most widely used in the laboratory (also at Swiss TPH). As mentioned before, the maintenance of the life cycle is time-consuming and requires planning well ahead of an experiment (Lombardo et al. 2019). Also, the infection variability of individual animals needs to be taken into account to some extent. Finally, unexpected events

such as unforeseen toxicity require a high degree of monitoring, flexibility and preparedness to modify study design *ad hoc*.

1.5.1 Promising drug candidates

As stated before, there is a pressing need for new antischistosomal drugs. Here I'll give a short introduction to the drug discovery landscape for schistosomiasis, focusing on drugs that were studied during my PhD (Figure 4).

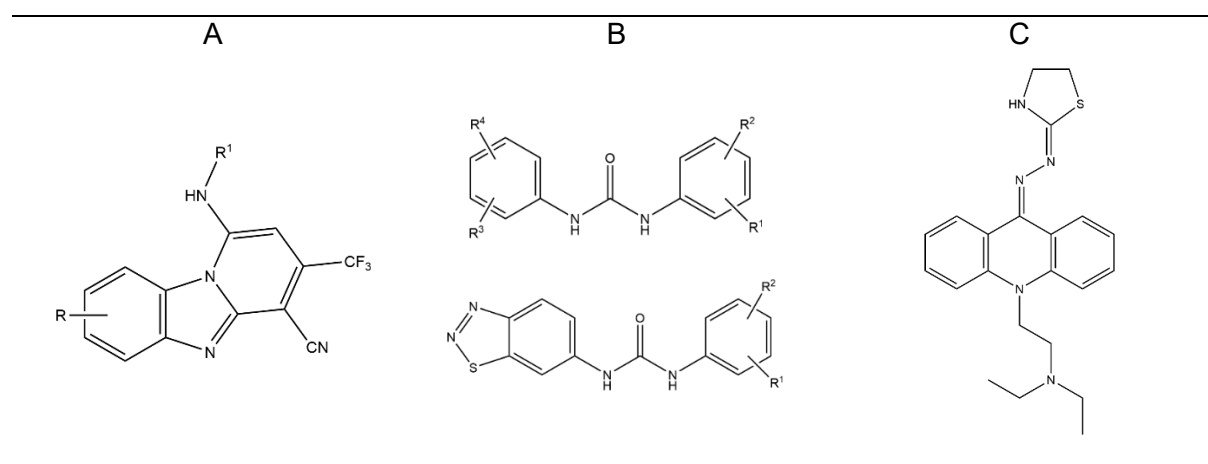


Figure 4: Chemical structures of the pyridobenzimidazole (A) and *N,N'*-diaryllurea (B) scaffolds, as well as Ro 15-5458, a 9-hydrazone acridanone (C).

Due to the lack of commercial interest, drug discovery efforts for schistosomiasis are mainly driven by academic research. It is therefore an attractive option to work with existing drugs rather than investigating complete new chemical entities in a *de-novo* development program (Caffrey and Secor 2011). Drug repurposing or repositioning, being the process of proposing new indications for marketed drugs or drugs that were abandoned during the various phases of discovery and development, presents a low-cost starting point for accelerating the search for new antischistosomal drugs (Panic et al. 2014; Sekhon 2013). This strategy has produced several interesting antimalarial drugs for the antischistosomal drug pipeline (Keiser and Utzinger 2012). Both parasites, the blood fluke *Schistosoma* and the protozoon *Plasmodium* share common characteristics (blood-dwelling, similarities in the digestion of hemoglobin) and are often co-endemic, especially in Africa (Caffrey and Secor 2011). Hence, it was suggested

to assess the potential auxillary effects of antimalarials against schistosomiasis (Keiser and Utzinger 2007). For example, artemisinin (a sesquiterpen lactone first isolated from *Artemisia annua*) and its semi-synthetic derivatives (artemether and artesunate) have been extensively studied against schistosomiasis in both, pre-clinical and clinical settings over the past years, and potent activities, especially during the juvenile development stages of *Schistosoma* spp. were reported (Panic and Keiser 2018; Lago et al. 2017). Medicinal chemistry driven drug discovery efforts have paved the way to synthetic alternatives, the ozonides and trioxaquinines, and improved the biopharmaceutical drug profile (Keiser and Utzinger 2012; Panic and Keiser 2018). While studies are underway to better characterize artemisinin-derived drugs such as the ozonides, it is important to remember that the potential use of compounds with dual activity in schistosomiasis patients might generate drug-resistant malaria parasites (with artemisinin-based combination therapies, ACTs, being the cornerstone for the treatment of malaria) and thus must be closely monitored.

In an *in vitro* screening setting tackling a panel of protozoa, a library of 1440 diverse compounds revealed moderate activity of the compound TDR15087, a pyrido[1,2-a]benzimidazole (PBI), towards *P. falciparum*. The pyridobenzimidazole core presented an attractive starting point for a structure-activity relationship program by exploring this new class of chemicals against malaria and subsequently engaging in an antischistosomal program (Singh et al. 2017; Okombo et al. 2017; Okombo et al. 2019; Mayoka, Njoroge, et al. 2019; Mayoka, Keiser, et al. 2019; Ndakala et al. 2011). First and second generation PBIs exhibited potent *in vitro* activities and promising *in vivo* efficacy, WBRs of 55 and 70 % were achieved when *S. mansoni* infected mice were given a single oral dose of 400 mg/kg (Okombo et al. 2017; Mayoka, Keiser, et al. 2019).

Efforts in accelerating drug discovery for neglected diseases, have put forth another compound library, the Open Access Malaria Box, consisting of 400 chemotypes with submicromolar activity against *Plasmodium falciparum* (Spangenberg et al. 2013). All compounds were screened against *S. mansoni* and low IC₅₀ values of 1.4 – 9.5 µM and 0.8 – 1.3 µM were

obtained for NTS and adult worms, respectively. MMV665852, a diarylurea was the most promising compound and exhibited moderate *in vivo* efficacy (WBR = 53 %) (Ingram-Sieber et al. 2014). Subsequent studies investigated derivatives of the lead compound and again found excellent *in vitro* activities but only low and moderate *in vivo* efficacy, calling for further exploration of this interesting class of chemicals (Yao et al. 2016; Wu et al. 2018; Cowan et al. 2015).

Finally, with likely no new drug candidate entering clinical testing in the near future, old antischistosomal lead candidates need revisiting. With praziquantel, being successfully adapted to mass drug administration campaigns short after its introduction; commercial drug discovery efforts for schistosomiasis were dropped by the pharmaceutical industry. In recent years though, two drugs from Hoffmann – La Roche, Ro 13-3978 and Ro 15-5458 have regained attention. The aryl hydantoin Ro 13-3978 was shown to be active against all major schistosomes species and had superior *in vivo* efficacy in a chronic *S. mansoni* mouse model when compared to praziquantel (Panic and Keiser 2018; Keiser et al. 2015). Ro 15-5458, a 9-acridanone hydrazone was reported to have ED₉₀ values below 100 mg/kg in rodents infected with all three major *Schistosoma* spp. (Stohler and Montavon 1984) and studies in experimentally infected *Cebus* and vervet monkeys, as well as baboons confirms the excellent antischistosomal efficacy (Sulaiman et al. 1989; Sturrock et al. 1987; Coelho and Pereira 1991).

In Chapter III, IV, V and VI, antischistosomal drugs from three different chemical classes, as well as plant-derived extracts from *Artemisia annua* and *Artemisia afra* are described and discussed. While Chapter III focusses on pyrido-[1,2-a]benzimidazoles (PBIs) that were first studied against malaria and later adapted to schistosomiasis drug discovery, Chapter IV explores the incorporation of a new bioisoster, the pentafluorosulfanyl group (SF₅), into a *N,N'*-diarylurea scaffold that has previously emerged as a promising antischistosomal entity through phenotypic screenings. In Chapter V different extracts and fractions from the medicinal plants *A. annua* and *A. afra* are studied for their *in vitro* antischistosomal potency. Finally, Ro 15-

5458, a potent lead candidate, is revisited in Chapter VI and the *in vivo* efficacy, metabolism and pharmacokinetic properties are characterized and discussed.

2. *Opisthorchis felineus*

The liver fluke *Opisthorchis felineus* is the causative agent of opisthorchiasis, a food-borne trematodiasis that affects humans and animals. *O. felineus* (Rivolta, 1894) belongs to the family Opisthorchiidae and is closely related to the trematode species *O. viverrini* (Poirier, 1886) and *Clonorchis sinensis* (Cobbold, 1875), which are regarded as important pathogens causing human disease. Opisthorchiasis due to *O. felineus* affects the hepatobiliary system of humans, domestic animals, as well as wild mammals and birds (Mordvinov et al. 2012). This thesis focuses on the infection transmitted by *O. felineus*.

2.1 Epidemiology of *O. felineus*

A total of 12.5 million people is at risk for an infection with *O. felineus* and estimates suggest that 1.6 million individuals are infected. The highest burden of disease accounts for people living in the Russian Federation, Siberia, the Ukraine and Kazakhstan (Keiser and Utzinger 2005; Keiser and Utzinger 2009; Petney et al. 2013). Located in the basins of the Ob and Irtysh rivers, an area of 14 regions in Western Siberia and four regions of Kazakhstan are accounted the largest endemic focus in the world (Yurlova et al. 2017). Systematic surveys in Western Siberia are performed since the late 1920s. Back then some regions (e.g. Tobolsk area, Tyumen, Tomsk, Omsk and Novosibirsk regions) had an opisthorchiasis prevalence of almost 100% (increasing gradient of prevalence from south to north). In the study-period of 2009-2013 the prevalence of *O. felineus* infections in humans decreased for some of the regions due to campaigns and education activities, according to state reports on the sanitary and epidemic welfare of populations in the Russian Federation (Yurlova et al. 2017). In other regions, due to growing population (migration due to work e.g. in the oil- and gas-industry) as well as touristic activities, the prevalence of opisthorchiasis infection increased and even spread to new areas (Yurlova et al. 2017; Fedorova et al. 2017). It is affirmed by the Russian scientific community that endemic areas have infection rates ranging from 10-45 %, thus exceeding the official

statistics from the Ministry of Health (Pakharukova and Mordvinov 2016). *O. felineus* infections have also been reported from countries belonging to the European Union (EU), but very little information is available. The most recent outbreaks have been documented for Germany, Greece and Italy (Pozio et al. 2013).

2.2 Life cycle of *O. felineus*

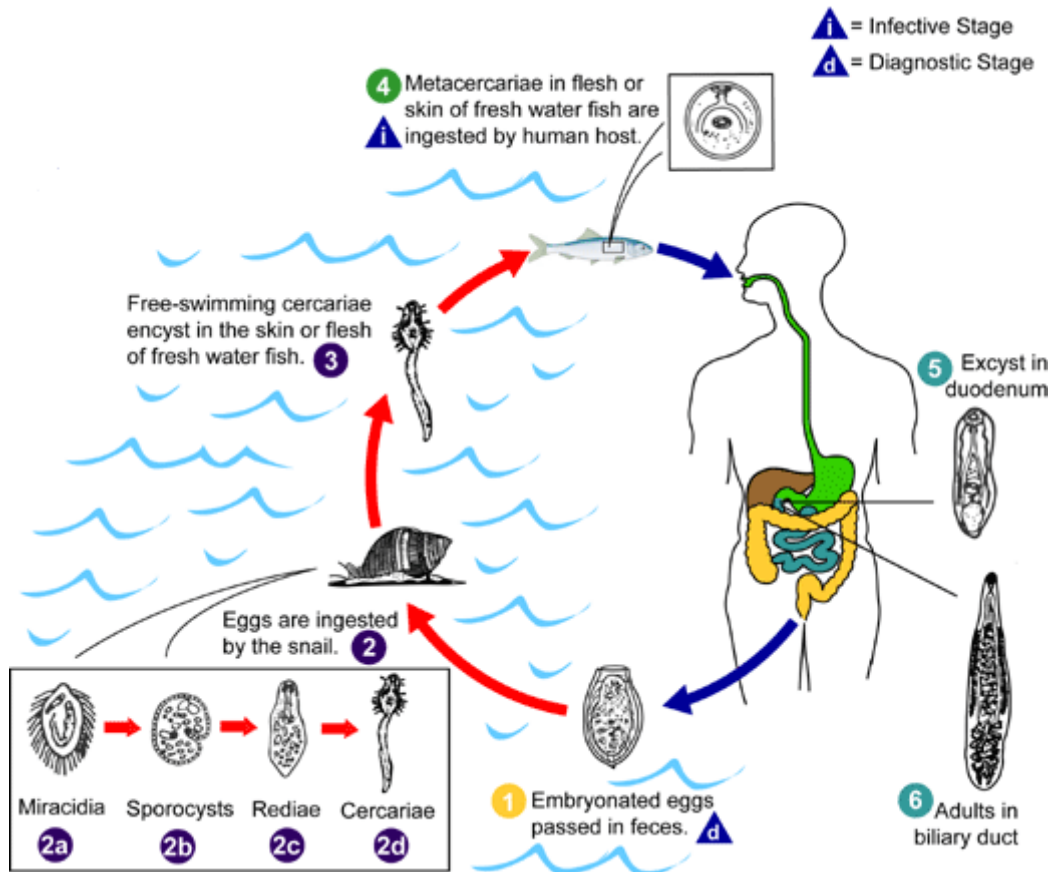


Figure 5: *O. felineus* life cycle (CDC 2021a)

O. felineus has a complex life cycle involving two intermediate hosts, being freshwater snails and fish, and a final host, the human (Figure 5). The snails belong to the genus *Bithynia*, three species are now recognized as first intermediate host of *O. felineus*, namely *Bithynia inflata*, *Bithynia leachi* and *Bithynia troscheli*. As for the second intermediate host, there are 23 species of carps (Cyprinidae) that have been identified so far. The adult *O. felineus* worm has a body length of 7-12 mm, and lives in the liver bile duct of fish-eating mammals. Eggs are produced by the worm and shed with the feces approximately 1-3 months after the infection. They are

ingested by freshwater snails. The larval stage, miracidium, develops to a sporocyst. After hatching, the sporocyst produces rediae, which then undergo maturation and transformation into cercariae (time range: ca. two months but can vary depending on the water temperature). Cercariae leave the snail and penetrate the skin of a fish; encystation takes place and subsequently cercariae undergo further development into metacercariae, which are the infective stage for the final host (time range: 3 weeks to 2 months). Once the final host, e.g. human eats raw fish infested with trematode larvae, flukes excyst in the gastrointestinal tract and infect the biliary tract, where they mature into adult worms. Of note is the lifespan of an adult liver fluke in the human body, which can reach over 20 years (Pakharukova and Mordvinov 2016; Yurlova et al. 2017; Pozio et al. 2013; Mordvinov et al. 2012).

2.3 Clinical manifestation and treatment

Depending on the severity, as well as the duration of the infection, individuals present with mild clinical symptoms ranging from abdominal pain, nausea, and dyspepsia to moderate symptoms such as pancreatitis and cholecystitis; and finally severe chronic infections being characterized by acute pancreatitis, hepatic abscesses and obstruction of the bile ducts, as summarized by Pozio and colleagues (Pozio et al. 2013). Of concern is the carcinogenic potential of *O. felineus*; different studies indicate a connection of liver cancer and opisthorchiasis in regions that have a high prevalence for the infection with *O. felineus* (Pakharukova and Mordvinov 2016). There is evidence that *O. felineus* infections are associated with a higher risk of acquiring cholangiocarcinoma (CCA) (Fedorova et al. 2020; Fedorova et al. 2017; Pakharukova and Mordvinov 2016) Praziquantel is the only drug that is officially registered for the treatment of opisthorchiasis in the Russian Federation.

2.3.1 Towards a better understanding of the treatment of opisthorchiasis with praziquantel

According to the Federal clinical guidelines “Opisthorchiasis in adults” and “Opisthorchiasis in children” (Ministry of Health Care of the Russian Federation, 2014), different doses of praziquantel are recommended for the treatment of the infection with *O. felineus*. Praziquantel

doses of 50, 60 and 75 mg/kg, divided into three intakes with dose intervals of four to six hours are recommended for adults, achieving an average efficacy of 83.3 % (Ministry of Health Care of the Russian Federation, 2014). For children older than four years, the guideline suggests a dosage of 50 mg/kg. As the therapy suggested by the clinical guidelines involves three stages of treatment (pre-treatment for up to 21 days employing antihistamines and spasmolytics, anthelmintic treatment with praziquantel, followed by rehabilitation with another round of antihistamines, spasmolytic and cholagogic drugs for up to three months) and should only be performed in in-patient departments it is unavailable for many patients, especially from remote villages. To reach the populations that need treatment against opisthorchiasis, it is of highest importance to assess the safety and efficacy of different short course treatment schemes as well as to elucidate the optimal doses of praziquantel by determining an exposure-response correlation in *O. felineus* infected patients. Working towards a better understanding of the treatment of opisthorchiasis with praziquantel, we studied the pharmacokinetic properties of both praziquantel enantiomers and its main metabolite, *R-trans-4-OH-PZQ* in *O. felineus* infected adults treated with ascending doses of racemic PZQ. Results are presented in Chapter VII.

References

- Abdulla, M. H., Ruelas, D. S., Wolff, B., Snedecor, J., Lim, K. C., Xu, F., Renslo, A. R., Williams, J., McKerrow, J. H., and Caffrey, C. R. 2009. 'Drug discovery for schistosomiasis: hit and lead compounds identified in a library of known drugs by medium-throughput phenotypic screening', *PLoS Negl Trop Dis*, 3: e478, doi:10.1371/journal.pntd.0000478.
- Bergquist, R., Utzinger, J., and Keiser, J. 2017. 'Controlling schistosomiasis with praziquantel: How much longer without a viable alternative?', *Infect Dis Poverty*, 6: 74, doi:10.1186/s40249-017-0286-2.
- Berriman, M., Haas, B. J., LoVerde, P. T., Wilson, R. A., Dillon, G. P., Cerqueira, G. C., Mashiyama, S. T., Al-Lazikani, B., Andrade, L. F., Ashton, P. D., Aslett, M. A., Bartholomeu, D. C., Blandin, G., Caffrey, C. R., Coghlan, A., Coulson, R., Day, T. A., Delcher, A., DeMarco, R., Djikeng, A., Eyre, T., Gamble, J. A., Ghedin, E., Gu, Y., Hertz-Fowler, C., Hirai, H., Hirai, Y., Houston, R., Ivens, A., Johnston, D. A., Lacerda, D., Macedo, C. D., McVeigh, P., Ning, Z., Oliveira, G., Overington, J. P., Parkhill, J., Perteua, M., Pierce, R. J., Protasio, A. V., Quail, M. A., Rajandream, M. A., Rogers, J., Sajid, M., Salzberg, S. L., Stanke, M., Tivey, A. R., White, O., Williams, D. L., Wortman, J., Wu, W., Zamanian, M., Zerlotini, A., Fraser-Liggett, C. M., Barrell, B. G., and El-Sayed, N. M. 2009. 'The genome of the blood fluke *Schistosoma mansoni*', *Nature*, 460: 352-8, doi:10.1038/nature08160.
- Boissier, J., Grech-Angelini, S., Webster, B. L., Allienne, J. F., Huyse, T., Mas-Coma, S., Toulza, E., Barré-Cardi, H., Rollinson, D., Kincaid-Smith, J., Oleaga, A., Galinier, R., Foata, J., Rognon, A., Berry, A., Mouahid, G., Henneron, R., Moné, H., Noel, H., and Mitta, G. 2016. 'Outbreak of urogenital schistosomiasis in Corsica (France): an epidemiological case study', *Lancet Infect Dis*, 16: 971-9, doi:10.1016/s1473-3099(16)00175-4.
- Buchter, V., Schneeberger, P. H. H., and Keiser, J. 2021. 'Validation of a human-serum-based in vitro growth method for drug screening on juvenile development stages of *Schistosoma mansoni*', *PLoS Negl Trop Dis*, 15: e0009313, doi:10.1371/journal.pntd.0009313.
- Bustinduy, A. L., Friedman, J. F., Kjetland, E. F., Ezeamama, A. E., Kabatereine, N. B., Stothard, J. R., and King, C. H. 2016. 'Expanding Praziquantel (PZQ) Access beyond Mass Drug Administration Programs: Paving a Way Forward for a Pediatric PZQ Formulation for Schistosomiasis', *PLoS Negl Trop Dis*, 10: e0004946, doi:10.1371/journal.pntd.0004946.
- Caffrey, C. R., and Secor, W. E. 2011. 'Schistosomiasis: from drug deployment to drug development', *Curr Opin Infect Dis*, 24: 410-7, doi:10.1097/QCO.0b013e328349156f.
- CDC. 2021a. 'Parasites - *Opisthorchis felinus* ', Accessed 01.08.2021. <https://www.cdc.gov/parasites/opisthorchis/biology.html>.
- CDC. 2021b. 'Parasites - Schistosomiasis ', Accessed 01.08.2021. <https://www.cdc.gov/parasites/schistosomiasis/biology.html>.
- Cioli, D., and Pica-Mattoccia, L. 2003. 'Praziquantel', *Parasitol Res*, 90: S3-S9, doi:10.1007/s00436-002-0751-z.
- Coelho, P. M., and Pereira, L. H. 1991. 'Schistosoma mansoni: preclinical studies with 9-Acridanone-hydrazones in Cebus monkeys experimentally infected', *Rev Inst Med Trop Sao Paulo*, 33: 50-7, doi:10.1590/s0036-46651991000100010.

- Collaborators, G. D. a. H. 2018. 'Global, regional, and national disability-adjusted life-years (DALYs) for 359 diseases and injuries and healthy life expectancy (HALE) for 195 countries and territories, 1990-2017: a systematic analysis for the Global Burden of Disease Study 2017', *Lancet*, 392: 1859-922, doi:10.1016/s0140-6736(18)32335-3.
- Colley, D. G., Bustinduy, A. L., Secor, W. E., and King, C. H. 2014. 'Human schistosomiasis', *Lancet*, 383: 2253-64, doi:10.1016/s0140-6736(13)61949-2.
- Consortium, Pediatric Praziquantel 2021. 'Schistosomiasis ', Accessed 29.07.2021. <https://www.pediatricpraziquantelconsortium.org/>.
- Cowan, N., Datwyler, P., Ernst, B., Wang, C., Vennerstrom, J. L., Spangenberg, T., and Keiser, J. 2015. 'Activities of N,N'-Diarylurea MMV665852 analogs against *Schistosoma mansoni*', *Antimicrob Agents Chemother*, 59: 1935-41, doi:10.1128/aac.04463-14.
- Danso-Appiah, A., Olliaro, P. L., Donegan, S., Sinclair, D., and Utzinger, J. 2013. 'Drugs for treating *Schistosoma mansoni* infection', *Cochrane Database Syst Rev*, doi:10.1002/14651858.CD000528.pub2.
- de Dood, C. J., Hoekstra, P. T., Mngara, J., Kalluvya, S. E., van Dam, G. J., Downs, J. A., and Corstjens, P. 2018. 'Refining Diagnosis of *Schistosoma haematobium* Infections: Antigen and Antibody Detection in Urine', *Front Immunol*, 9: 2635, doi:10.3389/fimmu.2018.02635.
- Doehring, E. 1988. 'Schistosomiasis in childhood', *Eur J Pediatr*, 147: 2-9, doi:10.1007/bf00442602.
- Doenhoff, M. J., Cioli, D., and Utzinger, J. 2008. 'Praziquantel: mechanisms of action, resistance and new derivatives for schistosomiasis', *Curr Opin Infect Dis*, 21: 659-67, doi:10.1097/QCO.0b013e328318978f.
- Doenhoff, M. J., Kusel, J. R., Coles, G. C., and Cioli, D. 2002. 'Resistance of *Schistosoma mansoni* to praziquantel: is there a problem?', *Trans R Soc Trop Med Hyg*, 96: 465-9, doi:10.1016/s0035-9203(02)90405-0.
- Fairfax, K., Nascimento, M., Huang, S. C., Everts, B., and Pearce, E. J. 2012. 'Th2 responses in schistosomiasis', *Semin Immunopathol*, 34: 863-71, doi:10.1007/s00281-012-0354-4.
- Fedorova, O. S., Fedotova, M. M., Zvonareva, O. I., Mazeina, S. V., Kovshirina, Y. V., Sokolova, T. S., Golovach, E. A., Kovshirina, A. E., Konovalova, U. V., Kolomeets, I. L., Gutor, S. S., Petrov, V. A., Hattendorf, J., Ogorodova, L. M., and Odermatt, P. 2020. 'Opisthorchis felinus infection, risks, and morbidity in rural Western Siberia, Russian Federation', *PLoS Negl Trop Dis*, 14: e0008421, doi:10.1371/journal.pntd.0008421.
- Fedorova, O. S., Kovshirina, Y. V., Kovshirina, A. E., Fedotova, M. M., Deev, I. A., Petrovskiy, F. I., Filimonov, A. V., Dmitrieva, A. I., Kudyakov, L. A., Saltykova, I. V., Odermatt, P., and Ogorodova, L. M. 2017. 'Opisthorchis felinus infection and cholangiocarcinoma in the Russian Federation: A review of medical statistics', *Parasitol Int*, 66: 365-71, doi:10.1016/j.parint.2016.07.010.
- Fenwick, A., and Jourdan, P. 2016. 'Schistosomiasis elimination by 2020 or 2030?', *Int J Parasitol*, 46: 385-8, doi:10.1016/j.ijpara.2016.01.004.
- Ferreira, L. G., Oliva, G., and Andricopulo, A. D. 2015. 'Target-based molecular modeling strategies for schistosomiasis drug discovery', *Future Med Chem*, 7: 753-64, doi:10.4155/fmc.15.21.

- Friedman, J. F., Olveda, R. M., Mirochnick, M. H., Bustinduy, A. L., and Elliott, A. M. 2018. 'Praziquantel for the treatment of schistosomiasis during human pregnancy', *Bull World Health Organ*, 96: 59-65, doi:10.2471/blt.17.198879.
- Fukushige, M., Chase-Topping, M., Woolhouse, M. E. J., and Mutapi, F. 2021. 'Efficacy of praziquantel has been maintained over four decades (from 1977 to 2018): A systematic review and meta-analysis of factors influence its efficacy', *PLoS Negl Trop Dis*, 15: e0009189, doi:10.1371/journal.pntd.0009189.
- Gönnert, R., and Andrews, P. 1977. 'Praziquantel, a new broad-spectrum antischistosomal agent', *Z Parasitenkd*, 52: 129-50, doi:10.1007/bf00389899.
- Gray, D. J., Ross, A. G., Li, Y.-S., and McManus, D. P. 2011. 'Diagnosis and management of schistosomiasis', *BMJ*, 342: d2651, doi:10.1136/bmj.d2651.
- Gryseels, B., Polman, K., Clerinx, J., and Kestens, L. 2006. 'Human schistosomiasis', *Lancet*, 368: 1106-18, doi:10.1016/s0140-6736(06)69440-3.
- Haas, W., and Haeberlein, S. 2009. 'Penetration of cercariae into the living human skin: *Schistosoma mansoni* vs. *Trichobilharzia szidati*', *Parasitol Res*, 105: 1061-6, doi:10.1007/s00436-009-1516-8.
- Hotez, P. J., and Kamath, A. 2009. 'Neglected tropical diseases in sub-saharan Africa: review of their prevalence, distribution, and disease burden', *PLoS Negl Trop Dis*, 3: e412, doi:10.1371/journal.pntd.0000412.
- Houweling, T. A., Karim-Kos, H. E., Kulik, M. C., Stolk, W. A., Haagsma, J. A., Lenk, E. J., Richardus, J. H., and de Vlas, S. J. 2016. 'Socioeconomic Inequalities in Neglected Tropical Diseases: A Systematic Review', *PLoS Negl Trop Dis*, 10: e0004546, doi:10.1371/journal.pntd.0004546.
- Ingram-Sieber, K., Cowan, N., Panic, G., Vargas, M., Mansour, N. R., Bickle, Q. D., Wells, T. N., Spangenberg, T., and Keiser, J. 2014. 'Orally active antischistosomal early leads identified from the open access malaria box', *PLoS Negl Trop Dis*, 8: e2610, doi:10.1371/journal.pntd.0002610.
- Katz, N., Chaves, A., and Pellegrino, J. 1972. 'A simple device for quantitative stool thick-smear technique in *Schistosomiasis mansoni*', *Rev Inst Med Trop Sao Paulo*, 14: 397-400.
- Keiser, J. 2010. 'In vitro and in vivo trematode models for chemotherapeutic studies', *Parasitology*, 137: 589-603, doi:10.1017/s0031182009991739.
- Keiser, J., Panic, G., Vargas, M., Wang, C., Dong, Y., Gautam, N., and Vennerstrom, J. L. 2015. 'Aryl hydantoin Ro 13-3978, a broad-spectrum antischistosomal', *J Antimicrob Chemother*, 70: 1788-97, doi:10.1093/jac/dkv016.
- Keiser, J., and Utzinger, J. 2005. 'Emerging Foodborne Trematodiasis', *Emerging Infectious Disease journal*, 11: 1507, doi:10.3201/eid1110.050614.
- Keiser, J., and Utzinger, J. 2007. 'Artemisinins and synthetic trioxolanes in the treatment of helminth infections', *Curr Opin Infect Dis*, 20: 605-12, doi:10.1097/QCO.0b013e3282f19ec4.
- Keiser, J., and Utzinger, J. 2009. 'Food-borne trematodiasis', *Clin Microbiol Rev*, 22: 466-83, doi:10.1128/cmr.00012-09.
- Keiser, J., and Utzinger, J. 2012. 'Antimalarials in the treatment of schistosomiasis', *Curr Pharm Des*, 18: 3531-8.

- King, C. H. 2010. 'Parasites and poverty: the case of schistosomiasis', *Acta Trop*, 113: 95-104, doi:10.1016/j.actatropica.2009.11.012.
- King, C. H., and Dangerfield-Cha, M. 2008. 'The unacknowledged impact of chronic schistosomiasis', *Chronic Illn*, 4: 65-79, doi:10.1177/1742395307084407.
- King, C. H., Keating, C. E., Muruka, J. F., Ouma, J. H., Houser, H., Siongok, T. K., and Mahmoud, A. A. 1988. 'Urinary tract morbidity in schistosomiasis haematobia: associations with age and intensity of infection in an endemic area of Coast Province, Kenya', *Am J Trop Med Hyg*, 39: 361-8, doi:10.4269/ajtmh.1988.39.361.
- Kjetland, E. F., Ndhlovu, P. D., Gomo, E., Mduluzza, T., Midzi, N., Gwanzura, L., Mason, P. R., Sandvik, L., Friis, H., and Gundersen, S. G. 2006. 'Association between genital schistosomiasis and HIV in rural Zimbabwean women', *Aids*, 20: 593-600, doi:10.1097/01.aids.0000210614.45212.0a.
- Knopp, S., Becker, S. L., Ingram, K. J., Keiser, J., and Utzinger, J. 2013. 'Diagnosis and treatment of schistosomiasis in children in the era of intensified control', *Expert Rev Anti Infect Ther*, 11: 1237-58, doi:10.1586/14787210.2013.844066.
- Kovač, J., Vargas, M., and Keiser, J. 2017. 'In vitro and in vivo activity of R- and S- praziquantel enantiomers and the main human metabolite trans-4-hydroxy-praziquantel against *Schistosoma haematobium*', *Parasit Vectors*, 10: 365, doi:10.1186/s13071-017-2293-3.
- Lago, E. M., Xavier, R. P., Teixeira, T. R., Silva, L. M., da Silva Filho, A. A., and de Moraes, J. 2017. 'Antischistosomal agents: state of art and perspectives', *Future Med Chem*, 10: 89-120, doi:10.4155/fmc-2017-0112.
- Lamberton, P. H., Kabatereine, N. B., Oguttu, D. W., Fenwick, A., and Webster, J. P. 2014. 'Sensitivity and specificity of multiple Kato-Katz thick smears and a circulating cathodic antigen test for *Schistosoma mansoni* diagnosis pre- and post-repeated-praziquantel treatment', *PLoS Negl Trop Dis*, 8: e3139, doi:10.1371/journal.pntd.0003139.
- Leopold, G., Ungethüm, W., Groll, E., Diekmann, H. W., Nowak, H., and Wegner, D. H. 1978. 'Clinical pharmacology in normal volunteers of praziquantel, a new drug against schistosomes and cestodes. An example of a complex study covering both tolerance and pharmacokinetics', *Eur J Clin Pharmacol*, 14: 281-91, doi:10.1007/bf00560463.
- Lo, N. C., Addiss, D. G., Hotez, P. J., King, C. H., Stothard, J. R., Evans, D. S., Colley, D. G., Lin, W., Coulibaly, J. T., Bustinduy, A. L., Raso, G., Bendavid, E., Bogoch, I. I., Fenwick, A., Savioli, L., Molyneux, D., Utzinger, J., and Andrews, J. R. 2017. 'A call to strengthen the global strategy against schistosomiasis and soil-transmitted helminthiasis: the time is now', *Lancet Infect Dis*, 17: e64-e69, doi:10.1016/s1473-3099(16)30535-7.
- Lombardo, F. C., Pasche, V., Panic, G., Endriss, Y., and Keiser, J. 2019. 'Life cycle maintenance and drug-sensitivity assays for early drug discovery in *Schistosoma mansoni*', *Nat Protoc*, doi:10.1038/s41596-018-0101-y.
- Luo, F., Yin, M., Mo, X., Sun, C., Wu, Q., Zhu, B., Xiang, M., Wang, J., Wang, Y., Li, J., Zhang, T., Xu, B., Zheng, H., Feng, Z., and Hu, W. 2019. 'An improved genome assembly of the fluke *Schistosoma japonicum*', *PLoS Negl Trop Dis*, 13: e0007612, doi:10.1371/journal.pntd.0007612.
- Maccesi, M., Aguiar, P. H. N., Pasche, V., Padilla, M., Suzuki, B. M., Montefusco, S., Abagyan, R., Keiser, J., Mourão, M. M., and Caffrey, C. R. 2019. 'Multi-center screening of the Pathogen Box collection for schistosomiasis drug discovery', *Parasit Vectors*, 12: 493, doi:10.1186/s13071-019-3747-6.

- Mayoka, G., Keiser, J., Häberli, C., and Chibale, K. 2019. 'Structure–Activity Relationship and in Vitro Absorption, Distribution, Metabolism, Excretion, and Toxicity (ADMET) Studies of N-aryl 3-Trifluoromethyl Pyrido[1,2-a]benzimidazoles That Are Efficacious in a Mouse Model of Schistosomiasis', *ACS Infect Dis*, 5: 418-29, doi:10.1021/acsinfecdis.8b00313.
- Mayoka, G., Njoroge, M., Okombo, J., Gibhard, L., Sanches-Vaz, M., Fontinha, D., Birkholtz, L. M., Reader, J., van der Watt, M., Coetzer, T. L., Lauterbach, S., Churchyard, A., Bezuidenhout, B., Egan, T. J., Yeates, C., Wittlin, S., Prudêncio, M., and Chibale, K. 2019. 'Structure-Activity Relationship Studies and Plasmodium Life Cycle Profiling Identifies Pan-Active N-Aryl-3-trifluoromethyl Pyrido[1,2- a]benzimidazoles Which Are Efficacious in an in Vivo Mouse Model of Malaria', *J Med Chem*, 62: 1022-35, doi:10.1021/acs.jmedchem.8b01769.
- McKerrow, J. H., and Salter, J. 2002. 'Invasion of skin by *Schistosoma cercariae*', *Trends Parasitol*, 18: 193-5, doi:10.1016/s1471-4922(02)02309-7.
- Meister, I., Ingram-Sieber, K., Cowan, N., Todd, M., Robertson, M. N., Meli, C., Patra, M., Gasser, G., and Keiser, J. 2014. 'Activity of praziquantel enantiomers and main metabolites against *Schistosoma mansoni*', *Antimicrob Agents Chemother*, 58: 5466-72, doi:10.1128/aac.02741-14.
- Meyer, T., Sekljic, H., Fuchs, S., Bothe, H., Schollmeyer, D., and Miculka, C. 2009. 'Taste, A New Incentive to Switch to (R)-Praziquantel in Schistosomiasis Treatment', *PLoS Negl Trop Dis*, 3: e357, doi:10.1371/journal.pntd.0000357.
- Molyneux, D. H., Hotez, P. J., and Fenwick, A. 2005. "'Rapid-impact interventions": how a policy of integrated control for Africa's neglected tropical diseases could benefit the poor', *PLoS Med*, 2: e336, doi:10.1371/journal.pmed.0020336.
- Mordvinov, V. A., Yurlova, N. I., Ogorodova, L. M., and Katokhin, A. V. 2012. 'Opisthorchis felinus and Metorchis bilis are the main agents of liver fluke infection of humans in Russia', *Parasitol Int*, 61: 25-31, doi:10.1016/j.parint.2011.07.021.
- Moreira-Filho, J. T., Silva, A. C., Dantas, R. F., Gomes, B. F., Souza Neto, L. R., Brandao-Neto, J., Owens, R. J., Furnham, N., Neves, B. J., Silva-Junior, F. P., and Andrade, C. H. 2021. 'Schistosomiasis Drug Discovery in the Era of Automation and Artificial Intelligence', *Front Immunol*, 12: 642383, doi:10.3389/fimmu.2021.642383.
- Mutapi, F., Maizels, R., Fenwick, A., and Woolhouse, M. 2017. 'Human schistosomiasis in the post mass drug administration era', *Lancet Infect Dis*, 17: e42-e48, doi:10.1016/s1473-3099(16)30475-3.
- Ndakala, A. J., Gessner, R. K., Gitari, P. W., October, N., White, K. L., Hudson, A., Fakorede, F., Shackelford, D. M., Kaiser, M., Yeates, C., Charman, S. A., and Chibale, K. 2011. 'Antimalarial Pyrido[1,2-a]benzimidazoles', *J Med Chem*, 54: 4581-89, doi:10.1021/jm200227r.
- Okombo, J., Brunschwig, C., Singh, K., Dziwornu, G. A., Barnard, L., Njoroge, M., Wittlin, S., and Chibale, K. 2019. 'Antimalarial Pyrido[1,2- a]benzimidazole Derivatives with Mannich Base Side Chains: Synthesis, Pharmacological Evaluation, and Reactive Metabolite Trapping Studies', *ACS Infect Dis*, 5: 372-84, doi:10.1021/acsinfecdis.8b00279.
- Okombo, J., Singh, K., Mayoka, G., Ndubi, F., Barnard, L., Njogu, P. M., Njoroge, M., Gibhard, L., Brunschwig, C., Vargas, M., Keiser, J., Egan, T. J., and Chibale, K. 2017. 'Antischistosomal Activity of Pyrido[1,2-a]benzimidazole Derivatives and Correlation

- with Inhibition of beta-Hematin Formation', *ACS Infect Dis*, 3: 411-20, doi:10.1021/acsinfecdis.6b00205.
- Oliveira, G., and Pierce, R. J. 2015. 'How has the genomics era impacted schistosomiasis drug discovery?', *Future Med Chem*, 7: 685-7, doi:10.4155/fmc.15.30.
- Pakharukova, M. Y., and Mordvinov, V. A. 2016. 'The liver fluke *Opisthorchis felinus*: biology, epidemiology and carcinogenic potential', *Trans R Soc Trop Med Hyg*, 110: 28-36, doi:10.1093/trstmh/trv085.
- Panic, G., Duthaler, U., Speich, B., and Keiser, J. 2014. 'Repurposing drugs for the treatment and control of helminth infections', *Int J Parasitol Drugs Drug Resist*, 4: 185-200, doi:10.1016/j.ijpddr.2014.07.002.
- Panic, G., and Keiser, J. 2018. 'Acting beyond 2020: better characterization of praziquantel and promising antischistosomal leads', *Curr Opin Pharmacol*, 42: 27-33, doi:10.1016/j.coph.2018.06.004.
- Park, S. K., and Marchant, J. S. 2020. 'The Journey to Discovering a Flatworm Target of Praziquantel: A Long TRP', *Trends Parasitol*, 36: 182-94, doi:10.1016/j.pt.2019.11.002.
- Pasche, V., Laleu, B., and Keiser, J. 2018a. 'Early antischistosomal leads identified from in vitro and in vivo screening of the Medicines for Malaria Venture Pathogen Box', *ACS Infect Dis*, doi:10.1021/acsinfecdis.8b00220.
- Pasche, V., Laleu, B., and Keiser, J. 2018b. 'Screening a repurposing library, the Medicines for Malaria Venture Stasis Box, against *Schistosoma mansoni*', *Parasit Vectors*, 11: 298, doi:10.1186/s13071-018-2855-z.
- Pearce, E. J., and MacDonald, A. S. 2002. 'The immunobiology of schistosomiasis', *Nat Rev Immunol*, 2: 499-511, doi:10.1038/nri843.
- Peters, P. A., Mahmoud, A. A., Warren, K. S., Ouma, J. H., and Siongok, T. K. 1976. 'Field studies of a rapid, accurate means of quantifying *Schistosoma haematobium* eggs in urine samples', *Bull World Health Organ*, 54: 159-62.
- Petney, T. N., Andrews, R. H., Saijuntha, W., Wenz-Mucke, A., and Sithithaworn, P. 2013. 'The zoonotic, fish-borne liver flukes *Clonorchis sinensis*, *Opisthorchis felinus* and *Opisthorchis viverrini*', *Int J Parasitol*, 43: 1031-46, doi:10.1016/j.ijpara.2013.07.007.
- Pozio, E., Armignacco, O., Ferri, F., and Gomez Morales, M. A. 2013. 'Opisthorchis felinus, an emerging infection in Italy and its implication for the European Union', *Acta Trop*, 126: 54-62, doi: 10.1016/j.actatropica.2013.01.005.
- Protasio, A. V., Tsai, I. J., Babbage, A., Nichol, S., Hunt, M., Aslett, M. A., De Silva, N., Velarde, G. S., Anderson, T. J. C., Clark, R. C., Davidson, C., Dillon, G. P., Holroyd, N. E., LoVerde, P. T., Lloyd, C., McQuillan, J., Oliveira, G., Otto, T. D., Parker-Manuel, S. J., Quail, M. A., Wilson, R. A., Zerlotini, A., Dunne, D. W., and Berriman, M. 2012. 'A Systematically Improved High Quality Genome and Transcriptome of the Human Blood Fluke *Schistosoma mansoni*', *PLoS Negl Trop Dis*, 6: e1455, doi:10.1371/journal.pntd.0001455.
- Ramirez, B., Bickle, Q., Yousif, F., Fakorede, F., Mouries, M. A., and Nwaka, S. 2007. 'Schistosomes: challenges in compound screening', *Expert Opin Drug Discov*, 2: S53-61, doi:10.1517/17460441.2.S1.S53.
- Rollinson, D., Knopp, S., Levitz, S., Stothard, J. R., Tchuem Tchuente, L. A., Garba, A., Mohammed, K. A., Schur, N., Person, B., Colley, D. G., and Utzinger, J. 2013. 'Time to

- set the agenda for schistosomiasis elimination', *Acta Trop*, 128: 423-40, doi:10.1016/j.actatropica.2012.04.013.
- Rollinson, D., Knopp, S., Levitz, S., Stothard, J. R., Tchuem Tchuenté, L. A., Garba, A., Mohammed, K. A., Schur, N., Person, B., Colley, D. G., and Utzinger, J. 2013. 'Time to set the agenda for schistosomiasis elimination', *Acta Trop*, 128: 423-40, doi:10.1016/j.actatropica.2012.04.013.
- Ross, A. G., Vickers, D., Olds, G. R., Shah, S. M., and McManus, D. P. 2007. 'Katayama syndrome', *Lancet Infect Dis*, 7: 218-24, doi:10.1016/s1473-3099(07)70053-1.
- Rothe, C., Zimmer, T., Schunk, M., Wallrauch, C., Helfrich, K., Gültekin, F., Bretzel, G., Allienne, J. F., and Boissier, J. 2021. 'Developing Endemicity of Schistosomiasis, Corsica, France', *Emerg Infect Dis*, 27: 319-21, doi:10.3201/eid2701.204391.
- Sekhon, B. S. 2013. 'Repositioning drugs and biologics: Retargeting old/existing drugs for potential new therapeutic applications', *J. Pharm. Ed. Res.*, 4: 1-15.
- Singh, K., Okombo, J., Brunschwig, C., Ndubi, F., Barnard, L., Wilkinson, C., Njogu, P. M., Njoroge, M., Laing, L., Machado, M., Prudencio, M., Reader, J., Botha, M., Nondaba, S., Birkholtz, L. M., Lauterbach, S., Churchyard, A., Coetzer, T. L., Burrows, J. N., Yeates, C., Denti, P., Wiesner, L., Egan, T. J., Wittlin, S., and Chibale, K. 2017. 'Antimalarial Pyrido[1,2-a]benzimidazoles: Lead Optimization, Parasite Life Cycle Stage Profile, Mechanistic Evaluation, Killing Kinetics, and in Vivo Oral Efficacy in a Mouse Model', *J Med Chem*, 60: 1432-48, doi:10.1021/acs.jmedchem.6b01641.
- Spangenberg, T., Burrows, J. N., Kowalczyk, P., McDonald, S., Wells, T. N., and Willis, P. 2013. 'The open access malaria box: a drug discovery catalyst for neglected diseases', *PLoS One*, 8: e62906, doi:10.1371/journal.pone.0062906.
- Steinmann, P., Keiser, J., Bos, R., Tanner, M., and Utzinger, J. 2006. 'Schistosomiasis and water resources development: systematic review, meta-analysis, and estimates of people at risk', *Lancet Infect Dis*, 6: 411-25, doi:10.1016/s1473-3099(06)70521-7.
- Stohler, H., and Montavon, M. 1984. '9-Acridanone-hydrazones, a novel class of broad spectrum schistosomicidal agents.', *XI International Congress for Tropical Medicine and Malaria 1984. Calgary.*: p. 148.
- Strohlein, A. J., Korhonen, P. K., Chong, T. M., Lim, Y. L., Chan, K. G., Webster, B., Rollinson, D., Brindley, P. J., Gasser, R. B., and Young, N. D. 2019. 'High-quality *Schistosoma haematobium* genome achieved by single-molecule and long-range sequencing', *Gigascience*, 8, doi:10.1093/gigascience/giz108.
- Sturrock, R. F., Bain, J., Webbe, G., Doenhoff, M. J., and Stohler, H. 1987. 'Parasitological evaluation of curative and subcurative doses of 9-acridanone-hydrazone drugs against *Schistosoma mansoni* in baboons, and observations on changes in serum levels of anti-egg antibodies detected by ELISA', *Trans R Soc Trop Med Hyg*, 81: 188-92, doi:10.1016/0035-9203(87)90210-0.
- Sulaiman, S. M., Ali, H. M., Homeida, M. M., and Bennett, J. L. 1989. 'Efficacy of a new Hoffmann-La Roche compound (Ro 15-5458) against *Schistosoma mansoni* (Gezira strain, Sudan) in vervet monkeys (*Cercopithecus aethiops*)', *Trop Med Parasitol*, 40: 335-36.
- Utzinger, J., Becker, S. L., Knopp, S., Blum, J., Neumayr, A. L., Keiser, J., and Hatz, C. F. 2012. 'Neglected tropical diseases: diagnosis, clinical management, treatment and control', *Swiss Med Wkly*, 142: w13727, doi:10.4414/smw.2012.13727.

- van Lieshout, L., Polderman, A. M., and Deelder, A. M. 2000. 'Immunodiagnosis of schistosomiasis by determination of the circulating antigens CAA and CCA, in particular in individuals with recent or light infections', *Acta Trop*, 77: 69-80, doi:10.1016/S0001-706X(00)00115-7.
- Verweij, J. J., and Stensvold, C. R. 2014. 'Molecular testing for clinical diagnosis and epidemiological investigations of intestinal parasitic infections', *Clin Microbiol Rev*, 27: 371-418, doi:10.1128/cmr.00122-13.
- Wang, J., Chen, R., and Collins, J. J., 3rd. 2019. 'Systematically improved in vitro culture conditions reveal new insights into the reproductive biology of the human parasite *Schistosoma mansoni*', *PLoS Biol*, 17: e3000254, doi:10.1371/journal.pbio.3000254.
- Weerakoon Kosala, G. A. D., Gobert Geoffrey, N., Cai, P., and McManus Donald, P. 2015. 'Advances in the Diagnosis of Human Schistosomiasis', *Clin Microbiol Rev*, 28: 939-67, doi:10.1128/CMR.00137-14.
- Weiss, M. G. 2008. 'Stigma and the Social Burden of Neglected Tropical Diseases', *PLoS Neg Trop Dis*, 2: e237, doi:10.1371/journal.pntd.0000237.
- WHO. 2012. 'Accelerating work to overcome the global impact of neglected tropical diseases: A roadmap for implementation', https://www.who.int/neglected_diseases/NTD_RoadMap_2012_Fullversion.pdf
- WHO. 2017. 'Integrating neglected tropical diseases into global health and development: fourth WHO report on neglected tropical diseases', <https://apps.who.int/iris/handle/10665/255011>
- WHO. 2020. 'Ending the neglect to attain the Sustainable Development Goals: A road map for neglected tropical diseases 2021–2030', https://www.who.int/neglected_diseases/Ending-the-neglect-to-attain-the-SDGs--NTD-Roadmap.pdf
- WHO. 2021. 'Schistosomiasis, Fact Sheet', Accessed 29.07.2021. <https://www.who.int/news-room/fact-sheets/detail/schistosomiasis>.
- Wu, J., Wang, C., Leas, D., Vargas, M., White, K. L., Shackleford, D. M., Chen, G., Sanford, A. G., Hemsley, R. M., Davis, P. H., Dong, Y., Charman, S. A., Keiser, J., and Vennerstrom, J. L. 2018. 'Progress in antischistosomal N,N'-diaryl urea SAR', *Bioorg Med Chem Lett*, 28: 244-48, doi:10.1016/j.bmcl.2017.12.064.
- Yao, H., Liu, F., Chen, J., Li, Y., Cui, J., and Qiao, C. 2016. 'Antischistosomal activity of N,N'-arylurea analogs against *Schistosoma japonicum*', *Bioorg Med Chem Lett*, 26: 1386-90, doi:10.1016/j.bmcl.2016.01.075.
- Young, N. D., Jex, A. R., Li, B., Liu, S., Yang, L., Xiong, Z., Li, Y., Cantacessi, C., Hall, R. S., Xu, X., Chen, F., Wu, X., Zerlotini, A., Oliveira, G., Hofmann, A., Zhang, G., Fang, X., Kang, Y., Campbell, B. E., Loukas, A., Ranganathan, S., Rollinson, D., Rinaldi, G., Brindley, P. J., Yang, H., Wang, J., Wang, J., and Gasser, R. B. 2012. 'Whole-genome sequence of *Schistosoma haematobium*', *Nat Genet*, 44: 221-5, doi:10.1038/ng.1065.
- Yurlova, N. I., Yadrenkina, E. N., Rastyazhenko, N. M., Serbina, E. A., and Glupov, V. V. 2017. 'Opisthorchiasis in Western Siberia: Epidemiology and distribution in human, fish, snail, and animal populations', *Parasitology International*, 66: 355-64, doi: 10.1016/j.parint.2016.11.017.
- Zdesenko, G., and Mutapi, F. 2020. 'Drug metabolism and pharmacokinetics of praziquantel: A review of variable drug exposure during schistosomiasis treatment in human hosts

and experimental models', *PLoS Negl Trop Dis*, 14: e0008649, doi:10.1371/journal.pntd.0008649.

Zhou, Y., Zheng, H., Chen, Y., Zhang, L., Wang, K., Guo, J., Huang, Z., Zhang, B., Huang, W., Jin, K., Dou, T., Hasegawa, M., Wang, L., Zhang, Y., Zhou, J., Tao, L., Cao, Z., Li, Y., Vinar, T., Brejova, B., Brown, D., Li, M., Miller, D. J., Blair, D., Zhong, Y., Chen, Z., Liu, F., Hu, W., Wang, Z.-Q., Zhang, Q.-H., Song, H.-D., Chen, S., Xu, X., Xu, B., Ju, C., Huang, Y., Brindley, P. J., McManus, D. P., Feng, Z., Han, Z.-G., Lu, G., Ren, S., Wang, Y., Gu, W., Kang, H., Chen, J., Chen, X., Chen, S., Wang, L., Yan, J., Wang, B., Lv, X., Jin, L., Wang, B., Pu, S., Zhang, X., Zhang, W., Hu, Q., Zhu, G., Wang, J., Yu, J., Wang, J., Yang, H., Ning, Z., Beriman, M., Wei, C.-L., Ruan, Y., Zhao, G., Wang, S., Liu, F., Zhou, Y., Wang, Z.-Q., Lu, G., Zheng, H., Brindley, P. J., McManus, D. P., Blair, D., Zhang, Q.-h., Zhong, Y., Wang, S., Han, Z.-G., Chen, Z., Wang, S., Han, Z.-G., Chen, Z., The Schistosoma japonicum Genome, S., Functional Analysis, C., Genome, a., evolution, a., Functional genomics, a., Sequencing, assembly, Paper, w., and Project, I. 2009. 'The Schistosoma japonicum genome reveals features of host-parasite interplay', *Nature*, 460: 345-51, doi:10.1038/nature08140.

CHAPTER II: AIMS AND OBJECTIVES

There is an urgent need for new and better treatment option for schistosomiasis. Although the blood dwelling parasite can cause lifelong impairment in already disadvantaged populations, no vaccine nor a fully effective drug targeting all *Schistosoma* species and development stages is available yet. Praziquantel with all its strengths has been the drug of choice for too many years, given its apparent weaknesses. My PhD project aimed to work towards the identification of better treatment options for schistosomiasis by exploring new and forgotten chemical scaffolds.

Furthermore, my PhD project aimed to elucidate the PK properties of praziquantel in adults infected with *Opisthorchis felineus*; a liver fluke most prevalent in Western Siberia, for which no standardized treatment recommendation is available yet.

In order to achieve these two main aims, following objectives were defined:

- 1) To expand the activity profile of the pyrido-[1,2-a]benzimidazole (PBI) scaffold by assessing the antischistosomal potency of a new drug series using different *in vitro* and *in vivo* techniques and analyzing the structure activity relationship (SAR).
- 2) To investigate the antischistosomal activity, structure-activity relationship and pharmacokinetic properties of SF₅-containing *N,N'*-diarylureas.
- 3) To evaluate extracts from the medicinal plants *Artemisia annua* and *Artemisia afra* for their *in vitro* activity against newly transformed schistosomula and adult *S. mansoni*.
- 4) To fully characterize the forgotten schistosomicidal lead candidate Ro 15-5458, employing efficacy, metabolism and pharmacokinetic studies.
- 5) To evaluate the pharmacokinetic profile of ascending doses of praziquantel in *Opisthorchis felineus* infected individuals from a clinical trial conducted in the Russian Federation.

CHAPTER III: ANTISCHISTOSOMAL PYRIDOBENZIMIDAZOLES

Expanding the activity profile of pyrido[1,2-a]benzimidazoles: Synthesis and evaluation of novel *N*¹-1-phenylethanamine derivatives against *Schistosoma mansoni*

Alexandra Probst,^{a,b} Kelly Chisanga,^c Godwin Akpeko Dziwornu,^c Cécile Haerberli,^{a,b} Jennifer Keiser,^{*,a,b} Kelly Chibale^{*,c,d,e}

^a Swiss Tropical and Public Health Institute, Socinstrasse 57, 4002 Basel, Switzerland

^b University of Basel, P.O. Box CH-4003, Basel, Switzerland

^c Department of Chemistry, University of Cape Town, Rondebosch 7701, South Africa

^d Institute of Infectious Diseases and Molecular Medicine, University of Cape Town, Rondebosch 7701, South Africa

^e South African Medical Research Council Drug Discovery Unit, University of Cape Town, Rondebosch 7701, South Africa

* Corresponding authors: jennifer.keiser@swisstph.ch; kelly.chibale@uct.ac.za

Alexandra Probst and Kelly Chisanga contributed equally to this work

Expanding the Activity Profile of Pyrido[1,2-*a*]benzimidazoles: Synthesis and Evaluation of Novel *N*¹-1-Phenylethanamine Derivatives against *Schistosoma mansoni*

Alexandra Probst,[▽] Kelly Chisanga,[▽] Godwin Akpeko Dziwornu, Cécile Haeberli, Jennifer Keiser,* and Kelly Chibale*



Cite This: *ACS Infect. Dis.* 2021, 7, 1032–1043



Read Online

ACCESS |



Metrics & More



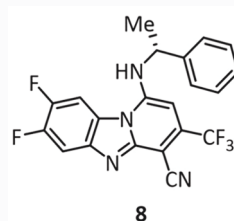
Article Recommendations



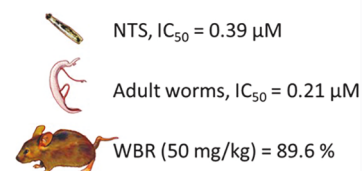
Supporting Information

ABSTRACT: Praziquantel is the only widely available drug to treat schistosomiasis. With very few candidates currently in the drug development pipeline, there is an urgent need to discover and develop novel antischistosomal drugs. In this regard, the pyrido[1,2-*a*]benzimidazole (PBI) scaffold has emerged as a promising chemotype in hit-to-lead efforts. Here, we report a novel series of antischistosomal PBIs with potent *in vitro* activity (IC₅₀ values of 0.08–1.43 μM) against *Schistosoma mansoni* newly transformed schistosomula and adult worms. Moreover, the current PBIs demonstrated good hepatic microsomal stability (>70% of drug remaining after 30 min) and were nontoxic to the Chinese hamster ovarian and human liver HepG2 cells, though toxicity (selectivity index, SI < 10) against the rat L6 myoblast cell line was observed. The compounds showed a small therapeutic window but were efficacious *in vivo*, exhibiting moderate to high worm burden reductions of 35.8–89.6% in *S. mansoni*-infected mice.

KEYWORDS: schistosomiasis, *Schistosoma mansoni*, pyrido[1,2-*a*]benzimidazole, antischistosomal lead, antischistosomal activity, 1-phenylethanamine



Antischistosomal activity profile



Schistosomiasis, one of the most prevalent neglected diseases of poverty, occurs in tropical and subtropical regions of the world. Approximately 800 million people are at risk of infection by one of the six *Schistosoma* species that infect humans, with *S. haematobium*, *S. japonicum*, and *S. mansoni* accounting for the highest disease burden.^{1,2} Exposure and activities related to infested waterbodies, as well as a lack of water supply and sanitation, are drivers for the transmission of the parasite.³ Only one drug, praziquantel (PZQ), is available for the treatment of schistosomiasis. PZQ is active against all *Schistosoma* species and has a good safety profile, but the drug is less effective against juvenile worms.^{4,5} Mass drug administration campaigns are entirely dependent on PZQ. Abundant use and no alternative treatment options raise questions attributed to treatment failures and resistance development.^{6–11} There is a pressing need for new drugs to fight schistosomiasis, and efforts are underway to identify novel chemical entities with antischistosomal activity.⁷ In contrast to many other neglected tropical diseases, drug discovery for schistosomiasis is primarily driven by academic institutions, but support by private–public partnerships, global alliances, and philanthropic institutions has moderately boosted the research landscape over the past decade.^{7,12}

Benzimidazole-based drugs, such as albendazole and thiabendazole, have become a cornerstone in chemotherapy against human and animal helminthic diseases worldwide. They

have shown broad-spectrum potency in treating many infections caused by cestodes, nematodes, and trematodes but also those caused by protozoans and certain microsporidia.^{13,14} However, there have been conflicting reports on the potential of benzimidazole anthelmintic drugs for the effective treatment of schistosomiasis.^{15–20} Notwithstanding, benzimidazole derivatives show promising scope as potential starting points in schistosomiasis drug discovery efforts.^{21–23}

In this regard, we have previously reported on the antischistosomal properties^{24,25} of pyrido[1,2-*a*]benzimidazole (PBI) derivatives, which have broad-spectrum biological properties including analgesic,²⁶ antipyretic,²⁶ antibacterial,²⁷ antiviral,²⁷ antimicrobial,²⁸ antifungal,²⁹ antimalarial,^{30–33} antimycobacterial,³⁴ and antitumor^{35,36} activities. A summary of the structure–activity relationship (SAR) studies for first and second generation schistosomicidal PBI analogs exemplified by the most potent analogs G1²⁴ and G2²⁵ is presented in Figure 1. Briefly, these compounds exhibited IC₅₀ values of 0.2–11 μM

Special Issue: Gut Pathogens

Received: May 6, 2020

Published: July 30, 2020



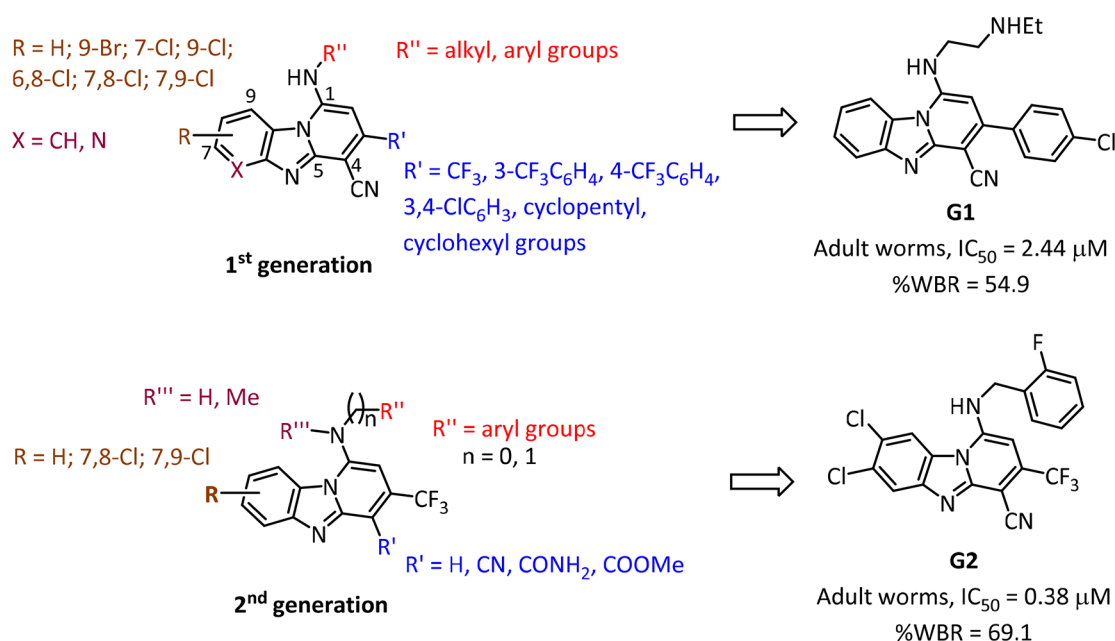
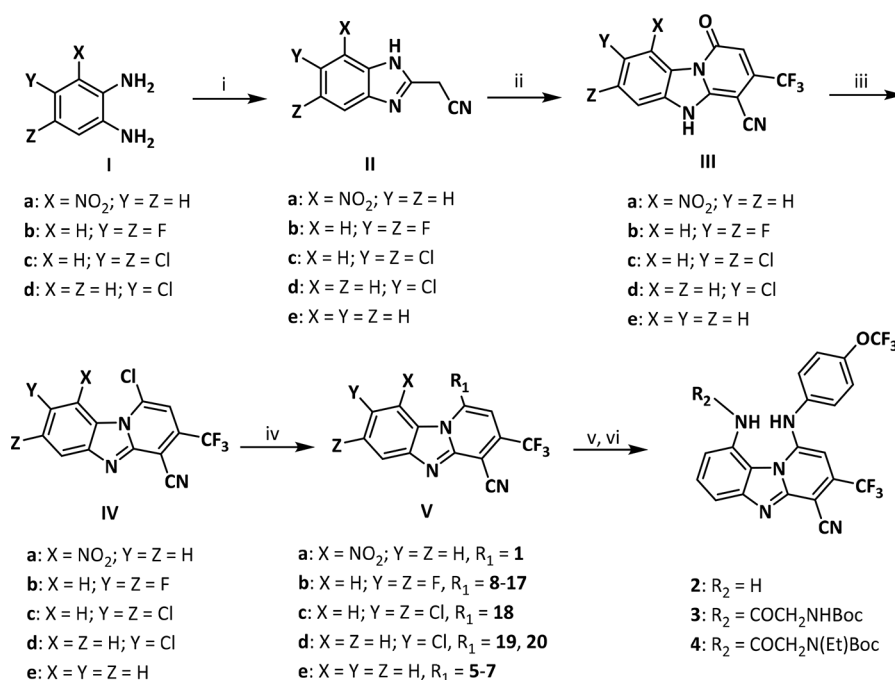


Figure 1. First and second generations of antischistosomal PBI derivatives.

Scheme 1. Synthesis of Target Compounds^{24,25 a}



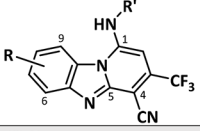
^aReagents and conditions: (i) ethyl cyanoacetate, DMF, 160 °C, 3 h; (ii) ethyl 4,4,4-trifluoro-3-oxobutanoate, NH₄OAc, 145 °C, 2 h; (iii) POCl₃, 130 °C, 3 h; (iv) appropriate amine, TEA, THF, 80 °C, microwave (150 W), 20 min, for **1** and **5-20**; (v) **1**, NH₄Cl, Fe, MeOH/H₂O (1:1), 65 °C, 45 min, for **2**; (vi) **2**, appropriate carboxylic acid, DCM, EDCl, DMAP, 0–25 °C, 6–12 h, for **3** and **4**.

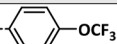
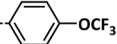
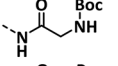
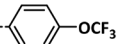
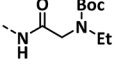
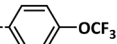
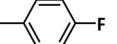
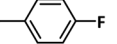
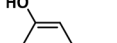
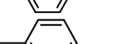
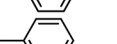
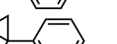
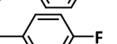
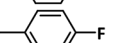
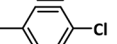
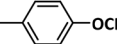
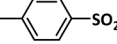
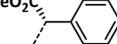
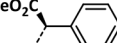
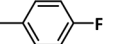
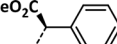
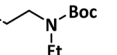
against adult *S. mansoni* and worm burden reductions (WBR) in the range of 26–69% after a single oral dose of 400 mg/kg given to mice harboring chronic *S. mansoni* infections. In this paper, to broaden the SAR scope, we describe investigations on novel PBI analogs incorporating N¹-1-phenylethanamines as potential antischistosomal drugs.

RESULTS AND DISCUSSION

Chemistry. The synthesis of the PBI core scaffold was achieved using previously described methods.^{27,30} Briefly,

condensation of a commercially available and appropriately substituted benzene-1,2-diamine (**I**) with ethyl 2-cyanoacetate under reflux conditions produced the 2-cyanomethylene benzimidazole intermediate (**II**), which underwent further condensation with ethyl 4,4,4-trifluoroacetoacetate, in the presence of anhydrous NH₄OAc, to yield the corresponding substituted 1-oxo-functionalized tricyclic PBI intermediate (**III**). Chlorination of **III** in the presence of phosphoryl chloride afforded the key intermediate **IV**, which upon amination produced the target compounds **1** and **5-20**. Reduction of

Table 1. *In Vitro* Antischistosomal Activities of the Synthesized Compounds^a


Compound	R	R'	NTS			<i>S. mansoni</i> adult				
			% Effect at 10 μ M (SD)	IC ₅₀ (μ M)	IC ₉₀ (μ M)	% Effect at 10 μ M (SD)	% Effect at 1 μ M (SD)	IC ₅₀ (μ M)	IC ₉₀ (μ M)	% Effect at 10 μ M + 45g/L Albumin (SD)
1	9-NO ₂	--- 	100.0 (0.0)			100.0 (0.0)	28.5 (3.0)			55.5 (4.9)
2	9-NH ₂	--- 	100.0 (0.0)			100.0 (0.0)	26.5 (6.0)			53.0 (11.3)
3		--- 	100.0 (0.0)	0.40	0.50	94.4 (3.0)	54.6 (0.0)			96.5 (4.9)
4		--- 	92.7 (10.3)			100.0 (0.0)	28.5 (3.0)			25.5 (6.4)
5	H	--- 	100.0 (0.0)			29.2 (0.0)				
6	H	--- 	100.0 (0.0)			60.3 (3.0)				
7	7,8-F	--- 	100.0 (0.0)	1.43	4.12	100.0 (0.0)	68.5 (3.0)			50.0 (9.9)
8	7,8-F	--- 	100.0 (0.0)	0.39	0.43	100.0 (0.0)	85.2 (0.0)	0.21	1.64	53.5 (4.9)
9	7,8-F	--- 	100.0 (0.0)	0.47		100.0 (0.0)	56.8 (6.0)			60.5 (17.7)
10	7,8-F	--- 	100.0 (0.0)	0.35		100.0 (0.0)	100.0 (0.0)	0.11	0.14	100.0 (0.0)
11	7,8-F	--- 	100.0 (0.0)	0.37	0.41	100.0 (0.0)	100.0 (0.0)	0.10	0.16	86.5 (2.1)
12	7,8-F	--- 	100.0 (0.0)	0.38	0.42	100.0 (0.0)	100.0 (0.0)	0.11	0.14	96.0 (2.8)
13	7,8-F	--- 	100.0 (0.0)	0.38	0.42	100.0 (0.0)	100.0 (0.0)	0.11	0.14	98.0 (2.8)
14	7,8-F	--- 	100.0 (0.0)			100.0 (0.0)	25.3 (0.0)			49.5 (0.7)
15	7,8-F	--- 	100.0 (0.0)			100.0 (0.0)	48.1 (5.0)			44.5 (16.3)
16	7,8-F	--- 	100.0 (0.0)	0.68	1.58	100.0 (0.0)	43.0 (3.0)			70.0 (11.3)
17	7,8-F	--- 	100.0 (0.0)	0.39	0.43	100.0 (0.0)	37.0 (0.0)			65.5 (12.0)
18	7,8-Cl	--- 	100.0 (0.0)			100.0 (0.0)	82.3 (3.0)	0.08		77.0 (12.7)
19	8-Cl	--- 	100.0 (0.0)			86.2 (3.0)	50.0 (3.0)			54.5 (23.0)
20	8-Cl	--- 	100.0 (0.0)	0.37		96.1 (6.0)	81.5 (0.0)	0.32	1.48	78.0 (0.0)
Praziquantel										0.1

^aNTS: newly transformed schistosomula; % effect = % reduction of viability; SD = standard deviation; blank cells = data not available.

the nitro group in compound 1 afforded 2, which underwent EDCI-mediated amide coupling reactions to obtain analogs 3 and 4 (Scheme 1).

***In Vitro* Antischistosomal Evaluation.** The synthesized compounds were initially evaluated for their activity against newly transformed schistosomula (NTS), followed by studies against adult *S. mansoni*, at an initial concentration of 10 μ M. All tested compounds inhibited the NTS and adult worms (except 5 and 6) viability by >75%. In more detail, against NTS, 12 compounds exhibited good activity with IC₅₀ values in the range of 0.35–1.43 μ M (Table 1). Of these, six compounds (8, 10, 11,

12, 13, and 20), as well as 18, were equally potent against adult worms with IC₅₀ values of 0.08–0.32 μ M.

From a SAR perspective, the *N*¹-1-phenylethylamine analogs demonstrated good activity against both NTS and adult worms. Among these, the *R*-enantiomer (as in 8, IC₅₀ = 0.21 μ M) exhibited better potency against adult worms than the *S*-enantiomer (as in 9), which showed <75% activity at 1 μ M. While the introduction of a cyclopropyl group (as in 10) at the benzylic position led to derivatives with potency against both the NTS and adult worms, the introduction of an ester group (as in 16 and 17) resulted in the loss of activity against adult worms. With regard to phenyl substituents, the activities of 11, 13, and

Table 2. *In Vitro* Cytotoxicity, Physicochemical, and *In Vitro* Microsomal Metabolic Stability Profiles^a

compound	cytotoxicity				HepG2 % tox. at 2 μ M (SD)	solubility (μ M) pH 7.4	metabolic stability m/r/h
	CHO IC ₅₀ μ M (SEM)	SI	L6 IC ₅₀ μ M (SD)	SI			
7	44.05 (2.42)		0.8 (0.2)		0 (7.2)		
8	7.57 (1.10)	37.8	0.9 (0.2)	4.2	0 (4.9)	<10	85/98/98.8
9	14.81 (2.21)		0.7 (0.2)		0 (7.5)	<10	89/97.2/98.7
10	26.49 (2.76)	264.9	0.5 (0.02)	4.2	0 (3.9)	50	96.4/99.4/99
11	7.49 (1.43)	74.9	0.7 (0.3)	6.7	0 (12.8)	<10	95/>99/>99
12	>50 (0)	>500	0.5 (0.06)	4.8	0 (42)	<10	>99/91/96
13	6.83 (1.07)	68.3	0.4 (0.2)	4.1	0 (18.3)	<10	>99/>99/>99
14	6.86 (1.57)		0.9 (0.2)		18.2 (12.9)	20	87/>99/>99
15	48.03 (1.98)		12.4 (3.5)		0 (12.1)	<10	
16	46.17 (0.39)		1.7 (0.7)		0 (13.7)	80	
17	45.70 (2.44)		1.9 (1.2)		0 (20.7)	80	
18	44.82 (2.66)	448.2	1.5 (0.3)	19.1	22.4 (11.6)	<10	96/80/89
19	49.68 (1.34)		1.4 (0.6)				
20	>50 (0)	>167	2.7 (0.6)	8.5			3.6/8.5/0.9
emetine	0.028 (0.004)				94.7 (5.2)		
podophyllotoxin			0.004 (0.001)				

^aCHO: Chinese hamster ovarian cell line; HepG2: human hepatoma G2 cells; L6: rat myoblast cell line; SI = selectivity index = IC₅₀ CHO or L6 divided by IC₅₀ adult *S. mansoni*. Solubility was determined by the turbidimetric kinetic solubility assay as previously described.³⁹ m/r/h: mouse/rat/human liver microsomes; values represent % drug remaining after 30 min of incubation. Standard deviations for the metabolic stability are shown in Table S2; blank cells = data not available.

Table 3. *In Vivo* Oral Efficacy of Key Compounds^a

compound	dose (mg/kg)	no. of mice cured/investigated	no. of mice that died	mean no. of worms (SD)	percentage of worm reduction (SD)	p-value
8	50	1/7 ^b	3	3.8 (3.3)	89.6 (9.1)	0.0027
8	25	0/8 ^c	3	13.6 (7.2)	47.5 (27.8)	>0.05
10	200	0/3	0	24.3 (3.5)	35.8 (9.3)	0.014
11	200	0/4	2	6.0 (2.8)	84.1 (7.5)	0.036
18	400	0/4	0	24.0 (4.3)	0	
20	400	0/4	0	10.0 (2.8)	43.2 (16.1)	0.029
control (C1)		0/8 ^d	0	17.6 (5.2)		
control (C2)		0/8 ^e	0	37.9 (7.2)		
control (C3)		0/8	0	20.1 (7.5)		
control (C4)		0/6	0	33.7 (4.5)		

^aSD: standard deviation. ^bResults were averaged from two experiments, in which C1 and C4 served as controls. ^cResults were averaged from two experiments, in which C3 and C4 served as controls. ^dC1 served as the control for 18 and 20; one mouse was not infected and was excluded from the analysis. ^eC2 served as the control for 10 and 11; blank cells = data not available.

14 suggest that large electron-withdrawing groups lead to loss of activity. Similarly, compound 15 bearing the bulky mesyl group substituent showed low activity against both NTS and adult worms.

On the benzimidazole scaffold, fluoro substitution potentiates activity, as evident for 11 and 12 compared to 5 and 6, respectively (Table 1). Like 11, chloro substituents (18) trigger activity, albeit against adult worms. Meanwhile, the *N*¹-4-trifluoromethoxy aniline-based analogs, 1–4, showed low activity against the adult worms. As previously shown, analogs with the *N*¹-alkylamino side chain (20) reveal good activity against both NTS and adult worms.

Finally, we investigated the activity of the synthesized compounds *in vitro* in a culture medium supplemented with albumin (45 g/L). Seven out of the 18 compounds that showed >75% activity against adult worms at 10 μ M showed similar activity in the albumin medium (Table 1). Generally, with the exception of 4 and 15, the test compounds exhibited >50% activity in the presence of albumin (Table 1). The data suggest that the activity of these compounds is not influenced by plasma

protein binding and therefore should be systemically available when given to experimental *S. mansoni* mouse models *in vivo*.^{37,38}

***In Vitro* Cytotoxicity and Hepatic Microsomal Metabolic Stability Evaluations.** Selected potent compounds were incubated with three mammalian cell lines, namely, the Chinese hamster ovarian (CHO) cells, human hepatoma (HepG2) cells, and rat myoblast L6 cells, to evaluate their *in vitro* cytotoxicity. For the CHO and L6 cells, IC₅₀ values were generated. Toxicity against the HepG2 cells was initially investigated at a single-point concentration of 2 μ M of drug. All tested compounds showed a low cytotoxic profile (0–22%) and were not progressed to IC₅₀ determinations. Similarly, the test compounds were noncytotoxic to the ovarian cells (selectivity index, SI > 10), but the selectivity indices (SI < 10) were generally much lower against the L6 muscle cells (except for 18, Table 2).

To prioritize compounds with potent *in vitro* antischistosomal activity and low cytotoxicity for *in vivo* efficacy studies (Table S1), their metabolic stability in mouse, rat, and human liver microsomes was evaluated. The percentage of compound

remaining after 30 min of coinubation with the microsomes was measured (Table 2), and the estimated half-life was calculated (Table S2). All test compounds, except for **20**, were stable with 80–100% of the compound remaining after the incubation period. The calculated half-lives were all above 150 min, except for **20**. Moreover, no apparent species differences could be observed in the rate of metabolism of the compounds. Further, the test compounds were poorly soluble (<50 μM at pH 7.4) in aqueous conditions, except compounds **16** and **17**, which were moderately soluble (80 μM), compared to **8** or **9** (<10 μM , Table 2).

In Vivo Oral Efficacy Evaluation. Seven compounds with high *in vitro* activity against NTS and adult *S. mansoni* were selected for *in vivo* efficacy studies in mice with an established chronic *S. mansoni* infection (Table 3). At an initial single oral dose of 400 mg/kg, all mice treated with **12** (also at 200 and 100 mg/kg) and **13** (also at 200 mg/kg) died prematurely. Of these mice, all showed reduced activity shortly after the oral application. Death occurred between 1 h postdosing (marked by tetanic muscle contractions) and 10 days postdosing. Interestingly, almost all worms were found dead in the liver of the dead mice. Furthermore, for mice that died 1 h postdosing (compound **12**), the onset of action, indicated by the shift of the worms from the mesenteric veins to the liver, was observed 1 h post-treatment, compared to that for praziquantel, which occurs 30 min after drug treatment.⁴⁰ Similarly, higher doses (400 and 200 mg/kg) of compounds **8**, **10**, and **11** resulted in toxicity and sudden deaths of the mice. However, therapeutic effects were observed after oral doses of 50 mg/kg for **8** and 200 mg/kg for **10** and **11**. Compound **8** showed a significant worm burden reduction of 89.6% ($p = 0.0027$) when mice were administered 50 mg/kg of drug, compared to the control. At the lower dose of 25 mg/kg, a moderate worm burden reduction of 47.5% was observed. A high worm burden reduction of 84.1% ($p = 0.036$) was achieved when compound **11** was given to the infected mice at a dose of 200 mg/kg. At the lower dose of 100 mg/kg, three treated mice ($n = 4$) died between days 1 and 5 postdosing; the fourth mouse was sacrificed due to a poor general condition. Notwithstanding, in the mice that died, worms were found dead in the liver. Compounds **10** and **20** showed modest but statistically significant activity of 35.8% ($p = 0.014$) and 43.2% ($p = 0.029$), respectively. Compound **18** showed no activity after a single oral dose of 400 mg/kg.

CONCLUSION

We demonstrated that the PBI scaffold is a promising antischistosomal chemotype. *N*¹-1-Phenylethanamine PBI analogs were highly active against NTS ($\text{IC}_{50} = 0.35\text{--}1.43 \mu\text{M}$) and adult *S. mansoni* (comparable to praziquantel, $\text{IC}_{50} = 0.1 \mu\text{M}$) *in vitro*. While we observed high cytotoxicity against rat L6 muscle cells, compounds showed low toxicity against CHO and HepG2 cells and high hepatic metabolic stability (>80%). Several derivatives showed significant activity *in vivo*. However, further structural optimizations are required, which must aim at increasing the therapeutic window and address the low aqueous solubility.

METHODS

All commercially available chemicals were purchased from either Sigma-Aldrich or Combi-Blocks. All solvents were dried by appropriate techniques. Unless otherwise stated, all solvents used were anhydrous. ¹H NMR spectra were recorded on a

Bruker Spectrometer at 300 or 400 MHz. Analytical thin-layer chromatography (TLC) was performed on aluminum-backed silica-gel 60 F254 (70–230 mesh) plates. Flash column chromatography was performed with Merck silica-gel 60 (70–230 mesh). Chemical shifts (δ) are given in ppm downfield from trimethylsilane (TMS) as the internal standard. Coupling constants, *J*, are recorded in hertz (Hz). Purity was determined by HPLC, and target compounds were confirmed to have >95% purity.

General Synthetic Procedure A (IIa–d). A suitably substituted 1,2-diaminobenzene (1.0 equiv) and ethyl cyanoacetate (3.0 equiv) in DMF (1.0 mL/0.100 g of sample) were stirred at 160 °C for 3 h. On completion, the reaction mixture was cooled to room temperature (25 °C), diluted with ethyl acetate, and washed with 20 mL portions of 5% lithium chloride (20 mL \times 3), distilled water (20 mL \times 3), and brine (10 mL \times 3) in a separatory funnel. The treated organic layer was dried on anhydrous MgSO_4 , concentrated, and finally dried *in vacuo*.

For **IIa**, the product was purified by trituration using toluene at 40–45 °C and filtered, and the residue was washed with diethyl ether and dried at ambient conditions.

2-(7-Nitro-1H-benzo[d]imidazole-2-yl)acetonitrile, IIa. Compound **IIa** was obtained from 3-nitro-1,2-diaminobenzene (**Ia**) (5.0 g, 32.65 mol, 1.0 equiv) and ethyl cyanoacetate (11.1 g, 97.45 mmol, 3.0 equiv) as a yellowish solid (5.4 g, 82% yield); Rf (EtOAc/hexane, 7:3) 0.43; ¹H NMR (300 MHz, DMSO-*d*₆) δ 8.2 (dd, *J* = 8.2, 1.0 Hz, 1H), 8.1 (dd, *J* = 8.0, 1.0 Hz, 1H), 7.4 (t, *J* = 8.1 Hz, 1H), 4.3 (s, 2H); HPLC-MS (ESI): purity = 99%, $t_R = 3.06$ min, m/z [$\text{M} - \text{H}$][−] = 200.9 [calcd for C₉H₆N₄O₂ m/z = 201.0413 (M − H)[−]].

2-(5,6-Difluoro-1H-benzo[d]imidazol-2-yl)acetonitrile, IIb. Compound **IIb** was obtained from 4,5-difluorobenzene-1,2-diamine (**Ib**) (3.48 g, 23.84 mmol, 1.0 equiv) and ethyl cyanoacetate (8.09 g, 71.49 mmol, 3.0 equiv) as a deep red solid (2.98 g, 65% yield); Rf (MeOH/DCM, 1:9) 0.32; ¹H NMR (300 MHz, DMSO-*d*₆) δ 12.8 (s, 1H), 7.6 (t, *J* = 9.7 Hz, 2H), 4.4 (s, 2H); HPLC-MS (ESI): purity = 90%, $t_R = 2.24$ min, m/z [$\text{M} - \text{H}$][−] = 192.1 [calcd for C₉H₄F₂N₃ m/z = 192.0373 (M − H)[−]].

2-(5,6-Dichloro-1H-benzo[d]imidazol-2-yl)acetonitrile, IIc. Compound **IIc** was obtained from 4,5-dichlorobenzene-1,2-diamine (**Ic**) (0.088 g, 0.50 mmol, 1.0 equiv) and ethyl cyanoacetate (0.170 g, 1.50 mmol, 3.0 equiv) as a brown solid (0.073 g, 65% yield); Rf (MeOH/DCM, 0.5:9.5) 0.30; ¹H NMR (400 MHz, DMSO-*d*₆) δ 12.9 (s, 1H), 7.9 (s, 2H), 4.4 (s, 2H); HPLC-MS (ESI): purity = 90%, $t_R = 4.01$ min, m/z [$\text{M} + \text{H}$]⁺ = 226.0 [calcd for C₉H₆Cl₂N₃ m/z = 225.9939 (M + H)⁺].

2-(6-Chloro-1H-benzo[d]imidazol-2-yl)acetonitrile, IIId. Compound **IIId** was obtained from 4-chloro-1,2-diaminobenzene (**Id**) (2.5 g, 17.53 mmol, 1.0 equiv) and ethyl cyanoacetate (5.6 mL, 0.053 mol, 3.0 equiv) as a brown solid (2.82 g, 84% yield); Rf (MeOH/DCM, 0.5:9.5) 0.26; ¹H NMR (400 MHz, acetonitrile-*d*₃) δ 12.9 (s, 1H), 7.6 (d, *J* = 1.9 Hz, 1H), 7.5 (d, *J* = 8.6 Hz, 1H), 7.2 (dd, *J* = 8.6, 1.9 Hz, 1H), 4.1 (s, 2H); HPLC-MS (ESI): purity = 86%, $t_R = 0.74$ min, m/z [$\text{M} - \text{H}$][−] = 190.0 [calcd for C₉H₅ClN₃ m/z = 190.0172 (M + H)⁺].

General Synthetic Procedure B (IIIa–e). An appropriate benzimidazole acetonitrile (1.0 equiv), the ethyl 4,4,4-trifluoroacetoacetate (1.2 equiv), and ammonium acetate (2.0 equiv) were stirred under reflux conditions at 145 °C for 2 h. Following completion of the reaction, the mixture was cooled to 70 °C, followed by the addition of 10 mL of acetonitrile and stirring the reaction product mixture for a further 10 min at that

temperature. The treated reaction mixture was cooled to room temperature (25 °C). The cooled reaction mixture was filtered; the resulting solid product was washed with cold acetonitrile (2–3 mL × 3) and dry ether (3–5 mL × 3), and finally, the product was dried at ambient conditions. The product was used in the subsequent step without further purification.

9-Nitro-1-oxo-3-(trifluoromethyl)-1,5-dihydrobenzo[4,5]-imidazo[1,2-a]pyridine-4-carbonitrile, IIIa. Compound IIIa was obtained from IIa (5.0 g, 25 mmol, 1.0 equiv), ethyl 4,4,4-trifluoro-3-oxobutanoate (0.29 g, 4.6 mL, 1.2 equiv), and ammonium acetate (3.9 mg, 50 mmol, 2.0 equiv) as a red solid (3.4 g, 42% yield); Rf (EtOAc/hexane, 8:2) 0.25; ¹H NMR (300 MHz, DMSO-*d*₆) δ 9.0 (d, *J* = 8.0 Hz, 1H), 8.3 (d, *J* = 8.3 Hz, 1H), 7.5 (t, *J* = 8.2 Hz, 1H), 6.4 (s, 1H); HPLC-MS (ESI): purity = 99%, *t*_R = 1.23 min, *m/z* [M + H]⁺ = 323.0 [calcd for C₁₃H₆F₃N₄O₃ *m/z* = 323.0392 (M + H)⁺].

7,8-Difluoro-1-oxo-3-(trifluoromethyl)benzo[4,5]imidazo[1,2-a]pyridine-4-carbonitrile, IIIb. Compound IIIb was obtained from IIb (2.86 g, 14.80 mmol, 1.0 equiv) and ethyl 4,4,4-trifluoro-3-oxobutanoate (3.26 g, 17.8 mmol, 1.2 equiv) as a brown solid (1.76 g, 86% yield); Rf (EtOAc/hexane, 7:3) 0.25; ¹H NMR (300 MHz, DMSO-*d*₆) δ 8.5 (dd, *J* = 10.3, 7.4 Hz, 1H), 7.7 (dd, *J* = 10.0, 7.0 Hz, 1H), 6.4 (s, 1H); HPLC-MS (ESI): purity = 99%, *t*_R = 2.69 min, *m/z* [M – H][–] = 312.0 [calcd for C₁₃H₃F₅N₃O *m/z* = 312.0196 (M – H)[–]].

7,8-Dichloro-1-oxo-3-(trifluoromethyl)benzo[4,5]imidazo[1,2-a]pyridine-4-carbonitrile, IIIc. Compound IIIc was obtained from IIc (0.113 g, 0.50 mmol, 1.0 equiv) and ethyl 4,4,4-trifluoro-3-oxobutanoate (0.110 g, 0.60 mmol, 1.2 equiv) and as gray solid (0.142 g, 82% yield); Rf (EtOAc/hexane 7:3) 0.36; ¹H NMR (300 MHz, DMSO-*d*₆) δ 8.7 (s, 1H), 7.7 (s, 1H), 6.5 (s, 1H); HPLC-MS (ESI): purity = 96%, *t*_R = 2.98 min, *m/z* [M + H]⁺ = 346.0 [calcd for C₁₃H₅Cl₂F₃N₃O *m/z* = 345.9762 (M + H)⁺].

8-Chloro-1-oxo-3-(trifluoromethyl)benzo[4,5]imidazo[1,2-a]pyridine-4-carbonitrile, III d. Compound III d was obtained from II d (1.90 g, 9.92 mmol, 1.0 equiv) and ethyl 4,4,4-trifluoro-3-oxobutanoate (2.19 g, 11.90 mmol, 1.2 equiv) as a yellow solid (2.16 g, 70% yield); Rf (MeOH/DCM, 0.5:9.5) 0.20; ¹H NMR (300 MHz, DMSO-*d*₆) δ 8.5 (d, *J* = 2.2 Hz, 1H), 7.7 (d, *J* = 8.6 Hz, 1H), 7.5 (dd, *J* = 8.4, 2.2 Hz, 1H), 6.4 (s, 1H); HPLC-MS (ESI): purity = 96%, *t*_R = 2.95 min, *m/z* [M + H]⁺ = 312.0 [calcd for C₁₃H₆ClF₃N₃O *m/z* = 312.0151 (M + H)⁺].

1-oxo-3-(Trifluoromethyl)benzo[4,5]imidazo[1,2-a]pyridine-4-carbonitrile, IIIe. Compound IIIe was obtained from IIe (1.25 g, 7.95 mmol, 1.0 equiv), ethyl 4,4,4-trifluoro-3-oxobutanoate (1.76 g, 9.54 mmol, 1.2 equiv), and ammonium acetate (1.23 g, 15.90 mmol, 2.0 equiv) as a brown solid (0.88 g, 40% yield); Rf (EtOAc/hexane, 3:7) 0.22; ¹H NMR (300 MHz, DMSO-*d*₆) δ 8.6 (dd, *J* = 7.8, 1.6 Hz, 1H), 7.6 (dd, *J* = 7.8, 1.6 Hz, 1H), 7.6–7.5 (dt, *J* = 7.8, 1.6 Hz, 1H), 7.3 (dt, *J* = 7.7, 1.7 Hz, 1H), 6.23 (s, 1H); HPLC-MS (ESI): purity = 98%, *t*_R = 2.57 min, *m/z* [M + H]⁺ = 278.0 [calcd for C₁₃H₇F₃N₃O *m/z* = 278.0541 (M + H)⁺].

General Synthetic Procedure C (IVa–e). A mixture of an appropriate hydroxy benzimidazole intermediate compound (1.0 equiv) and phosphoryl oxychloride (POCl₃: 20.0 equiv) was stirred at 130 °C for 3 h. On completion of the reaction, the reaction mixture was cooled to room temperature (25 °C). The excess POCl₃ was removed *in vacuo*. Ice cooled water (20 mL) was added to the treated reaction mixture with consistent stirring for 15 min. The mixture was neutralized using sodium bicarbonate; the crude product was filtered off, washed with

water, and dried at ambient conditions. The product was used in the subsequent step without further purification.

1-Chloro-9-nitro-3-(trifluoromethyl)benzo[4,5]imidazo[1,2-a]pyridine-4-carbonitrile, IVa. Compound IVa was obtained from IIIa (0.40 g, 1.4 mmol, 1.0 equiv) and POCl₃ (2.6 g, 28.0 mmol, 20.0 equiv) as a yellow solid (0.37 g, 78% yield); Rf (MeOH/DCM, 0.5:9.5) 0.25; ¹H NMR (400 MHz, DMSO-*d*₆) δ 7.8 (d, *J* = 8.1 Hz, 1H), 7.1 (t, *J* = 7.9 Hz, 1H), 6.8 (d, *J* = 7.9 Hz, 1H), 6.2 (s, 1H); HPLC-MS (ESI): purity = 96%, *t*_R = 1.04 min, *m/z* [M + H]⁺ = 341.0 [calcd for C₁₃H₅ClF₃N₄O₂ *m/z* = 341.0053 (M + H)⁺].

1-Chloro-7,8-difluoro-3-(trifluoromethyl)benzo[4,5]imidazo[1,2-a]pyridine-4-carbonitrile, IVb. Compound IVb was obtained from IIIb (0.93 g, 3.0 mmol, 1.0 equiv) and POCl₃ (9.11 g, 59.3 mmol, 20 equiv) as a yellow solid (0.93 g, 95% yield); Rf (EtOAc/hexane, 1.5:8.5) 0.17; ¹H NMR (300 MHz, DMSO-*d*₆) δ 8.8 (dd, *J* = 11.0, 7.4 Hz, 1H), 8.2 (dd, *J* = 10.7, 7.6 Hz, 1H), 7.9 (s, 1H); HPLC-MS (ESI): purity = 99%, *t*_R = 2.80 min, *m/z* [M + H]⁺ = 332.0 [calcd for C₁₃H₄ClF₅N₃ *m/z* = 332.0014 (M + H)⁺].

1,7,8-Trichloro-3-(trifluoromethyl)benzo[4,5]imidazo[1,2-a]pyridine-4-carbonitrile, IVc. Compound IVc was obtained from IIIc (0.080 g, 0.23 mmol, 1.0 equiv) and POCl₃ (0.71 g, 4.6 mmol, 20.0 equiv) as a yellow solid (0.080 g, 95% yield); Rf (EtOAc/hexane 1:9) 0.25; ¹H NMR (300 MHz, DMSO-*d*₆) δ 8.8 (s, 1H), 8.4 (s, 1H), 7.9 (s, 1H); HPLC-MS (ESI): purity = 99%, *t*_R = 5.04 min, *m/z* [M – H][–] = 361.9 [calcd for C₁₃H₂Cl₃F₃N₃ *m/z* = 361.9266 (M – H)[–]].

1,8-Dichloro-3-(trifluoromethyl)benzo[4,5]imidazo[1,2-a]pyridine-4-carbonitrile, IVd. Compound IVd was obtained from III d (1.2 g, 3.9 mmol, 1.0 equiv) and POCl₃ (1.3 g, 7.9 mmol, 1.5 equiv) as a yellow solid (0.7 g, 85% yield); Rf (EtOAc/hexane, 1.5:8.5) 0.21; ¹H NMR (600 MHz, DMSO-*d*₆) δ 8.7 (d, *J* = 1.1 Hz, 1H), 8.2 (d, *J* = 8.6 Hz, 1H), 7.9 (s, 1H), 7.7 (dd, *J* = 9.1, 1.1 Hz, 1H); HPLC-MS (ESI): purity = 91%, *t*_R = 1.13 min, *m/z* [M + H]⁺ = 329.9 [calcd for C₁₃H₅Cl₂F₃N₃ *m/z* = 329.9813 (M + H)⁺].

1-Chloro-3-(trifluoromethyl)benzo[4,5]imidazo[1,2-a]pyridine-4-carbonitrile, IVe. Compound IVe was obtained from IIIe (0.94 g, 3.39 mmol, 1.0 equiv) and POCl₃ (10.4 g, 67.82 mmol, 20 equiv) as a yellow solid (0.812 g, 81% yield); Rf (EtOAc/hexane, 1:9) 0.35; ¹H NMR (300 MHz, CDCl₃) δ 8.7 (dd, *J* = 7.8, 1.2 Hz, 1H), 8.6 (dd, *J* = 7.8, 1.2 Hz, 1H), 7.8 (dt, *J* = 7.8, 1.3 Hz, 1H), 7.6 (dt, *J* = 8.1, 1.2 Hz, 1H), 7.2 (s, 1H); HPLC-MS (ESI): purity = 99%, *t*_R = 3.25 min, *m/z* [M + H]⁺ = 296.0 [calcd for C₁₃H₆ClF₃N₃ *m/z* = 296.0202 (M + H)⁺].

General Synthetic Procedure D (1, 5–20). A mixture of the appropriate chloro intermediate (IVa–e: 1.0 equiv), the corresponding amine (2.0 equiv), and triethylamine (2.0 equiv) in tetrahydrofuran (THF) (2 mL/100 mg of sample) was irradiated under microwave conditions at 150 W and 80 °C for 25 min. The cooled reaction mixture was transferred to a round-bottom flask and concentrated *in vacuo*. The product was recrystallized in a minimum volume of acetone (or ethanol). Where purification was required, flash column chromatography with a 25–30% ethyl acetate (EtOAc) in hexane eluent system was used to purify the compound. The appropriate fractions were reconstituted, concentrated, and dried *in vacuo*.

9-Nitro-1-(4-(trifluoromethoxy)phenyl)amino)-3-(trifluoromethyl)benzo[4,5]imidazo[1,2-a]pyridine-4-carbonitrile, 1. Compound 1 was obtained from IVa (0.36 g, 1.07 mmol, 1.0 equiv) and 4-(trifluoromethoxy)aniline (0.38 g, 2.14 mmol, 2.0 equiv) as a yellow solid (0.24 g, 47% yield); Rf

(EtOAc/hexane, 4:6) 0.32; ^1H NMR (400 MHz, DMSO- d_6) δ 9.1 (d, J = 8.3 Hz, 1H), 8.4 (d, J = 8.2 Hz, 1H), 7.6 (t, J = 8.3 Hz, 1H), 7.5 (d, J = 8.5 Hz, 2H), 7.4 (d, J = 8.6 Hz, 2H), 6.4 (s, 1H); HPLC-MS (ESI): purity = 99%, t_{R} = 3.31 min, m/z $[\text{M} + \text{H}]^+ = 482.0$ [calcd for $\text{C}_{20}\text{H}_{10}\text{F}_6\text{N}_5\text{O}_3$ $m/z = 482.0688$ ($\text{M} + \text{H}$) $^+$].

1-((1-(4-Fluorophenyl)ethyl)amino)-4-(trifluoromethyl)benzo[4,5]imidazo[1,2-a]pyridine-3-carbonitrile, 5. Compound 5 was obtained from **IVe** (0.087 g, 0.31 mmol, 1.0 equiv) and 1-(4-fluorophenyl)ethan-1-amine (0.087 g, 0.63 mmol, 2.0 equiv) as a yellow solid (0.079 g, 64% yield), m.p. 181–183 °C; Rf (EtOAc/hexane, 3:7) 0.26; ^1H NMR (400 MHz, DMSO- d_6) δ 8.6 (dd, J = 7.8, 2.1 Hz, 1H), 8.3 (s, 1H), 7.9 (dd, J = 7.8, 2.0 Hz, 1H), 7.7 (dt, J = 7.6, 2.1 Hz, 1H), 7.6 (dd, J = 8.3, 5.6 Hz, 2H), 7.5 (m, 3H), 6.2 (s, 1H), 5.3 (q, J = 6.9 Hz, 1H), 1.8 (d, J = 6.7 Hz, 3H); HPLC-MS (ESI): purity = 99%, t_{R} = 3.05 min, m/z $[\text{M} + \text{H}]^+ = 399.1$ [calcd for $\text{C}_{21}\text{H}_{15}\text{F}_4\text{N}_4$ $m/z = 399.1233$ ($\text{M} + \text{H}$) $^+$].

(R)-1-((1-(4-Fluorophenyl)ethyl)amino)-4-(trifluoromethyl)benzo[4,5]imidazo[1,2-a]pyridine-3-carbonitrile, 6. Compound 6 was obtained from **IVe** (0.100 g, 0.36 mmol, 1.0 equiv) and *R*-1-(4-fluorophenyl)ethan-1-amine (0.100 g, 0.72 mmol, 2.0 equiv) as a yellow solid (0.092 g, 64% yield), m.p. 175–177 °C; Rf (MeOH/DCM, 1:9) 0.37; ^1H NMR (600 MHz, DMSO- d_6) δ 8.6 (dd, J = 7.8, 2.1 Hz, 1H), 8.0 (s, 1H), 7.9 (dd, J = 7.7, 1.8 Hz, 1H), 7.7 (m, 4H) 7.6 (dt, J = 7.8, 1.7 Hz, 1H), 7.5 (dt, J = 7.8, 1.7 Hz, 1H), 6.2 (s, 1H), 5.2 (q, J = 6.7 Hz, 1H), 1.8 (d, J = 6.7 Hz, 3H); HPLC-MS (ESI): purity = 98%, t_{R} = 2.95 min, m/z $[\text{M} + \text{H}]^+ = 399.1$ [calcd for $\text{C}_{21}\text{H}_{15}\text{F}_4\text{N}_4$ $m/z = 399.1233$ ($\text{M} + \text{H}$) $^+$].

(S)-1-((1-(2-Hydroxyphenyl)ethyl)amino)-3-(trifluoromethyl)benzo[4,5]imidazo[1,2-a]pyridine-4-carbonitrile, 7. Compound 7 was obtained from **IVe** (0.089 g, 0.29 mmol, 1.0 equiv) and 2-(1-aminoethyl)phenol (0.100 g, 0.57 mmol, 2.0 equiv) as a yellow solid (0.084 g, 68%), m.p. 231–233 °C; Rf (MeOH/DCM, 0.2:9.8) 0.21; ^1H NMR (400 MHz, DMSO- d_6) δ 10.1 (s, 1H), 8.7 (dd, J = 11.2, 7.2 Hz, 1H), 8.2 (s, 1H), 8.0 (dd, J = 11.0, 7.6 Hz, 1H), 7.5 (dd, J = 7.7, 1.7 Hz, 1H), 7.1 (td, J = 7.3, 1.7 Hz, 1H), 6.9 (dd, J = 8.2, 1.2 Hz, 1H), 6.8 (td, J = 7.5, 1.2 Hz, 1H), 6.4 (s, 1H), 5.2 (q, J = 6.7 Hz, 1H), 1.7 (d, J = 6.7 Hz, 3H); HPLC-MS (ESI): purity = 98%, t_{R} = 3.36 min, m/z $[\text{M} + \text{H}]^+ = 433.1$ [calcd for $\text{C}_{21}\text{H}_{14}\text{F}_3\text{N}_4\text{O}$ $m/z = 433.1088$ ($\text{M} + \text{H}$) $^+$].

(R)-7,8-Difluoro-1-((1-phenylethyl)amino)-4-(trifluoromethyl)benzo[4,5]imidazo[1,2-a]pyridine-3-carbonitrile, 8. Compound 8 was obtained from **IVb** (0.080 g, 0.24 mmol, 1.0 equiv) and 1-phenylethyl-1-amine (0.059 g, 0.48 mmol, 2.0 equiv) as an orange solid (0.052 g, 52% yield), m.p. 210–212 °C; Rf (EtOAc/hexane, 3:7) 0.20; ^1H NMR (400 MHz, DMSO- d_6) δ 8.7 (dd, J = 11.3, 7.2 Hz, 1H), 8.3 (d, J = 6.2 Hz, 1H), 8.0 (dd, J = 10.7, 7.7 Hz, 1H), 7.6 (dd, J = 7.5, 2.2 Hz, 2H), 7.4 (t, J = 7.3 Hz, 2H), 7.3 (dt, J = 7.4, 2.2 Hz, 1H), 6.2 (s, 1H), 5.2 (m, 1H), 1.8 (d, J = 6.7 Hz, 3H); HPLC-MS (ESI): purity = 99%, t_{R} = 2.98 min, m/z $[\text{M} + \text{H}]^+ = 417.1$ [calcd for $\text{C}_{21}\text{H}_{14}\text{F}_5\text{N}_4$ $m/z = 417.1139$ ($\text{M} + \text{H}$) $^+$].

(S)-7,8-Difluoro-1-((1-phenylethyl)amino)-4-(trifluoromethyl)benzo[4,5]imidazo[1,2-a]pyridine-3-carbonitrile, 9. Compound 9 was obtained from **IVb** (0.061 g, 0.18 mmol, 1.0 equiv) and 1-phenylethyl-1-amine (0.045 g, 0.37 mmol, 2.0 equiv) as a yellow solid (0.025 g, 34% yield), m.p. 193–195 °C; Rf (EtOAc/hexane, 3:7) 0.19; ^1H NMR (400 MHz, DMSO- d_6) δ 8.7 (dd, J = 11.3, 7.2 Hz, 1H), 8.3 (s, 1H), 8.0 (dd, J = 11.6, 7.7 Hz, 1H), 7.6 (dd, J = 7.5, 2.1 Hz, 2H), 7.4 (t, J = 7.3 Hz, 2H), 7.3 (dt, J = 7.3, 2.2 Hz, 1H), 6.2 (s, 1H), 5.2 (q, J

= 6.6 Hz, 1H), 1.8 (d, J = 6.8 Hz, 3H); HPLC-MS (ESI): purity = 97%, t_{R} = 2.98 min, m/z $[\text{M} + \text{H}]^+ = 417.1$ [calcd for $\text{C}_{21}\text{H}_{14}\text{F}_5\text{N}_4$ $m/z = 417.1139$ ($\text{M} + \text{H}$) $^+$].

7,8-Difluoro-1-((1-phenylcyclopropyl)amino)-3-(trifluoromethyl)benzo[4,5]imidazo[1,2-a]pyridine-4-carbonitrile, 10. Compound 10 was obtained from **IVb** (0.080 g, 0.24 mmol, 1.0 equiv) and 1-phenylcyclopropan-1-amine (0.063 g, 0.48 mmol, 2.0 equiv) as a yellow solid (0.066 g, 64% yield), m.p. 182–184 °C; Rf (EtOAc/hexane, 3:7) 0.17; ^1H NMR (400 MHz, DMSO- d_6) δ 9.0 (s, 1H), 8.9 (dd, J = 11.7, 7.3 Hz, 1H), 8.0 (dd, J = 11.0, 7.7 Hz, 1H), 7.3 (m, 5H), 6.2 (s, 1H), 1.6 (s, 4H); HPLC-MS (ESI): purity = 99%, t_{R} = 2.99 min, m/z $[\text{M} + \text{H}]^+ = 429.1$ [calcd for $\text{C}_{22}\text{H}_{14}\text{F}_3\text{N}_4$ $m/z = 429.1139$ ($\text{M} + \text{H}$) $^+$].

7,8-Difluoro-1-((1-(4-fluorophenyl)ethyl)amino)-3-(trifluoromethyl)benzo[4,5]imidazo[1,2-a]pyridine-4-carbonitrile, 11. Compound 11 was obtained from **IVb** (0.080 g, 0.26 mmol, 1.0 equiv) and 1-(4-fluorophenyl)ethan-1-amine (0.071 g, 0.51 mmol, 2.0 equiv) as a yellow solid (0.064 g, 56.5% yield), m.p. 182–185 °C; Rf (EtOAc/hexane, 1:1) 0.25; ^1H NMR (400 MHz, DMSO- d_6) δ 8.7 (dd, J = 11.5, 7.2 Hz, 1H), 8.3 (d, J = 6.2 Hz, 1H), 8.0 (dd, J = 10.9, 7.6 Hz, 1H), 7.7 (dd, J = 8.6, 5.6 Hz, 2H), 7.2 (t, J = 8.9 Hz, 2H), 6.2 (s, 1H), 5.2 (m, 1H), 1.8 (d, J = 6.7 Hz, 3H); HPLC-MS (ESI): purity = 98%, t_{R} = 2.95 min, m/z $[\text{M} + \text{H}]^+ = 435.0$ [calcd for $\text{C}_{21}\text{H}_{13}\text{F}_6\text{N}_4$ $m/z = 435.1044$ ($\text{M} + \text{H}$) $^+$].

(R)-7,8-Difluoro-1-((1-(4-fluorophenyl)ethyl)amino)-3-(trifluoromethyl)benzo[4,5]imidazo[1,2-a]pyridine-4-carbonitrile, 12. Compound 12 was obtained from **IVb** (0.046 g, 0.14 mmol, 1.0 equiv) and 1-(4-fluorophenyl)ethan-1-amine (0.039 g, 0.28 mmol, 2.0 equiv) as a yellow solid (0.029 g, 48% yield), m.p. 210–212 °C; Rf (EtOAc/hexane, 1:1) 0.24; ^1H NMR (400 MHz, DMSO- d_6) δ 8.7 (dd, J = 11.2, 7.3 Hz, 1H), 8.3 (d, J = 6.2 Hz, 1H), 8.0 (dd, J = 11.0, 7.7 Hz, 1H), 7.6 (dd, J = 8.6, 5.6 Hz, 2H), 7.2 (t, J = 8.9 Hz, 2H), 6.2 (s, 1H), 5.2 (m, 1H), 1.8 (d, J = 6.9 Hz, 3H); HPLC-MS (ESI): purity = 99%, t_{R} = 2.96 min, m/z $[\text{M} + \text{H}]^+ = 435.0$ [calcd for $\text{C}_{21}\text{H}_{13}\text{F}_6\text{N}_4$ $m/z = 435.1044$ ($\text{M} + \text{H}$) $^+$].

1-((1-(4-Chlorophenyl)ethyl)amino)-7,8-difluoro-3-(trifluoromethyl)benzo[4,5]imidazo[1,2-a]pyridine-4-carbonitrile, 13. Compound 13 was obtained from **IVb** (0.080 g, 0.26 mmol, 1.0 equiv) and 1-(4-chlorophenyl)ethan-1-amine (0.098 g, 0.51 mmol, 2.0 equiv) as a yellow solid (0.080 g, 68% yield), m.p. 182–184 °C; Rf (EtOAc/hexane, 1:1) 0.18; ^1H NMR (300 MHz, DMSO- d_6) δ 8.7 (dd, J = 11.4, 7.2 Hz, 1H), 8.3 (d, J = 6.4 Hz, 1H), 8.0 (dd, J = 11.0, 7.6 Hz, 1H), 7.6 (J = 8.5 Hz, 2H), 7.4 (d, J = 8.5 Hz, 2H), 6.2 (s, 1H), 5.3 (m, 1H), 1.8 (d, J = 6.7 Hz, 3H); HPLC-MS (ESI): purity = 99%, t_{R} = 3.35 min, m/z $[\text{M} - \text{H}]^- = 449.0$ [calcd for $\text{C}_{21}\text{H}_{11}\text{ClF}_5\text{N}_4$ $m/z = 449.0592$ ($\text{M} + \text{H}$) $^+$].

7,8-Difluoro-1-((1-(4-(trifluoromethoxy)phenyl)ethyl)amino)-3-(trifluoromethyl)benzo[4,5]-imidazo[1,2-a]pyridine-4-carbonitrile, 14. Compound 14 was obtained from **IVb** (0.081 g, 0.24 mmol, 1.0 equiv) and 1-phenylcyclopropan-1-amine (0.100 g, 0.49 mmol, 2.0 equiv) as a yellow solid (0.053 g, 44% yield), m.p. 213–215 °C; Rf (EtOAc/hexane, 3:7) 0.25; ^1H NMR (400 MHz, DMSO- d_6) δ 8.7 (dd, J = 11.3, 7.2 Hz, 1H), 8.3 (d, J = 6.2 Hz, 1H), 8.0 (dd, J = 10.7, 8.0 Hz, 1H), 7.7 (d, J = 7.7 Hz, 2H), 7.4 (d, J = 7.9 Hz, 2H), 6.2 (s, 1H), 5.3 (m, 1H), 1.8 (d, J = 6.7 Hz, 3H); HPLC-MS (ESI): purity = 99%, t_{R} = 3.06 min, m/z $[\text{M} + \text{H}]^+ = 501.0$ [calcd for $\text{C}_{22}\text{H}_{13}\text{F}_8\text{N}_4\text{O}$ $m/z = 501.0962$ ($\text{M} + \text{H}$) $^+$].

7,8-Difluoro-1-((1-(4-(methylsulfonyl)phenyl)ethyl)amino)-3-(trifluoromethyl)benzo[4,5]-imidazo[1,2-a]-

pyridine-4-carbonitrile, **15**. Compound **15** was obtained from **IVb** (0.084 g, 0.27 mmol, 1.0 equiv) and 1-(4-(methylsulfonyl)phenyl)ethan-1-amine (0.11 g, 0.54 mmol, 2.0 equiv) as a yellow solid (0.063 g, 46% yield), m.p. 261–263 °C; Rf (EtOAc/hexane, 0.5:9.5) 0.18; ¹H NMR (400 MHz, DMSO-*d*₆) δ 8.7 (dd, *J* = 11.3, 7.1 Hz, 1H), 8.4 (s, 1H), 8.0 (m, 3H), 7.9 (d, *J* = 8.5 Hz, 2H), 6.3 (s, 1H), 5.4 (q, *J* = 7.5 Hz, 1H), 3.2 (s, 3H), 1.8 (d, *J* = 6.7 Hz, 3H); HPLC-MS (ESI): purity = 99%, *t*_R = 3.43 min, *m/z* [M - H]⁻ = 493.0 [calcd for C₂₂H₁₄F₃N₄O₂S *m/z* = 493.0758 (M + H)⁺].

Methyl (*S*)-2-((3-Cyano-7,8-difluoro-4-(trifluoromethyl)benzo[4,5]imidazo[1,2-*a*]pyridin-1-yl)amino)-2-phenylacetate, **16**. Compound **16** was obtained from **VIb** (0.080 g, 0.26 mmol, 1.0 equiv) and methyl (*S*)-2-amino-2-phenylacetate (0.084 g, 0.51 mmol, 2.0 equiv) as a yellow solid (0.033 g, 28% yield), m.p. 228–230 °C; Rf (EtOAc/hexane, 4:6) 0.24; ¹H NMR (400 MHz, DMSO-*d*₆) δ 8.6 (dd, *J* = 9.4, 7.3 Hz, 1H), 8.5 (dd, *J* = 8.8, 7.5 Hz, 1H), 8.0 (s, 1H), 7.7 (dd, *J* = 7.4, 1.6 Hz, 2H), 7.5 (t, *J* = 8.2 Hz, 2H), 7.4 (dt, *J* = 7.3, 1.7 Hz, 1H), 6.3 (s, 1H), 6.0 (s, 1H), 3.8 (s, 3H); HPLC-MS (ESI): purity = 99%, *t*_R = 2.98 min, *m/z* [M - H]⁻ = 459.0 [calcd for C₂₂H₁₂F₃N₄O₂ *m/z* = 459.0880 (M + H)⁺].

Methyl (*R*)-2-((3-Cyano-7,8-difluoro-4-(trifluoromethyl)benzo[4,5]imidazo[1,2-*a*]pyridin-1-yl)amino)-2-phenylacetate, **17**. Compound **17** was obtained from **VIb** (0.12 g, 0.36 mmol, 1.0 equiv) and methyl (*R*)-2-amino-2-phenylacetate (0.12 g, 0.72 mmol, 2.0 equiv) as an orange solid (0.070 g, 42% yield), m.p. 232–235 °C; Rf (EtOAc/hexane, 4:6) 0.24; ¹H NMR (400 MHz, DMSO-*d*₆) δ 8.6 (dd, *J* = 9.4, 7.2 Hz, 1H), 8.5 (dd, *J* = 8.8, 7.6 Hz, 1H), 8.0 (s, 1H), 7.7 (dd, *J* = 7.4, 1.4 Hz, 2H), 7.5 (t, *J* = 7.5 Hz, 2H), 7.3 (dt, *J* = 7.3, 1.6 Hz, 1H), 6.3 (s, 1H), 6.0 (s, 1H), 3.8 (s, 3H); HPLC-MS (ESI): purity = 98%, *t*_R = 2.98 min, *m/z* [M - H]⁻ = 459.0 [calcd for C₂₂H₁₂F₃N₄O₂ *m/z* = 459.0880 (M + H)⁺].

7,8-Dichloro-1-((1-(4-fluorophenyl)ethyl)amino)-3-(trifluoromethyl)benzo[4,5]imidazo[1,2-*a*]pyridine-4-carbonitrile, **18**. Compound **18** was obtained from **VIc** (0.070 g, 0.19 mmol, 1.0 equiv) and 1-(4-fluorophenyl)ethan-1-amine (0.053 g, 0.38 mmol, 2.0 equiv) as a yellow solid (0.043 g, 48% yield), m.p. 224–226 °C; Rf (EtOAc/hexane, 3:7) 0.37; ¹H NMR (600 MHz, DMSO-*d*₆) δ 8.6 (s, 1H), 8.4 (s, 1H), 7.9 (s, 1H), 7.6 (dd, *J* = 8.5, 5.4 Hz, 2H), 7.2 (t, *J* = 8.9 Hz, 2H), 6.3 (s, 1H), 5.3 (m, 1H), 1.8 (d, *J* = 6.7 Hz, 3H); HPLC-MS (ESI): purity = 98%, *t*_R = 3.13 min, *m/z* [M + H]⁺ = 467.0 [calcd for C₂₁H₁₃Cl₂F₄N₄ *m/z* = 467.0453 (M + H)⁺].

Methyl (*R*)-2-((8-Chloro-4-cyano-3-(trifluoromethyl)benzo[4,5]imidazo[1,2-*a*]pyridin-1-yl)amino)-2-phenylacetate, **19**. Compound **19** was obtained from **IVd** (0.100 g, 0.30 mmol, 1.0 equiv) and methyl (*R*)-2-amino-2-phenylacetate (0.100 g, 0.60 mmol, 2.0 equiv) as an orange solid (0.121 g, 88%), m.p. 183–187 °C; Rf (EtOAc/hexane, 1:8) 0.25; ¹H NMR (600 MHz, DMSO-*d*₆) δ 8.59 (s, 1H), 7.9 (d, *J* = 2.3 Hz, 1H), 7.6 (d, *J* = 7.7 Hz, 1H), 7.5 (dd, *J* = 7.8, 2.3 Hz, 1H), 7.4 (dd, *J* = 7.2, 2.3 Hz, 2H), 7.4 (t, *J* = 7.4 Hz, 2H), 7.3 (dt, *J* = 7.4, 2.3 Hz, 1H), 6.2 (s, 1H), 5.9 (s, 1H), 3.7 (s, 3H); HPLC-MS (ESI): purity = 99%, *t*_R = 3.40 min, *m/z* [M + H]⁺ = 459.0 [calcd for C₂₂H₁₅ClF₃N₄O₂ *m/z* = 459.0836 (M + H)⁺].

tert-Butyl 2-((8-Chloro-4-cyano-3-(trifluoromethyl)benzo[4,5]imidazo[1,2-*a*]pyridin-1-yl)amino)ethyl(ethyl)carbamate, **20**. Compound **20** was obtained from compound **IVd** (0.115 g, 0.30 mmol, 1.0 equiv) and *tert*-butyl 2-aminoethyl(ethyl)carbamate (0.079 g, 0.36 mmol, 1.2 equiv) as a yellow solid (0.114 g, 79%), m.p. 197–199 °C; Rf (EtOAc/

hexane, 3:7) 0.21; ¹H NMR (600 MHz, DMSO-*d*₆) δ 8.6 (d, *J* = 2.1 Hz, 1H), 8.5 (dd, *J* = 8.8, 2.1 Hz, 1H), 7.84 (s, 1H), 7.5 (d, *J* = 8.5 Hz, 1H), 6.0 (s, 1H), 3.7 (t, *J* = 6.1 Hz, 2H), 3.5 (t, *J* = 6.3 Hz, 2H), 3.2 (q, *J* = 6.9 Hz, 2H), 1.2 (s, 9H), 1.0 (t, *J* = 8.7 Hz, 3H); HPLC-MS (ESI): purity = 99%, *t*_R = 1.28 min, *m/z* [M + H]⁺ = 482.0 [calcd for C₂₂H₂₄ClF₃N₅O₂ *m/z* = 482.1571 (M + H)⁺].

9-Amino-1-((4-(trifluoromethoxy)phenyl)amino)-3-(trifluoromethyl)benzo[4,5]imidazo[1,2-*a*]pyridine-4-carbonitrile, **2**. A mixture of compound **1** (0.22 g, 0.46 mmol, 1.0 equiv), ammonium chloride (0.26 g, 4.60 mmol 10.0 equiv), and iron (0.26 g, 4.60 mmol, 10.0 equiv) in a 1:1 methanol–water solution (2.0 mL) was stirred at 65 °C for 45 min. The reaction mixture was cooled to room temperature (25 °C) after which it was taken up in ethyl acetate (10.0 mL). The treated reaction mixture was filtered through Celite, washed with deionized water (20 mL × 3), dried with brine (10 mL × 2) and, finally, dried over MgSO₄. The organic layer was concentrated and dried *in vacuo*. The product was purified by flash-chromatography using EtOAc and obtained as a yellow solid (0.19 g, 90% yield), m.p. 223–226 °C; Rf (MeOH (NH₃)/DCM, 1:9) 0.28; ¹H NMR (400 MHz, acetonitrile-*d*₃) δ 7.8 (dd, *J* = 8.4, 0.8 Hz, 1H), 7.4 (m, 4H), 7.2 (dd, *J* = 8.4, 7.7 Hz, 1H), 6.8 (dd, *J* = 7.7, 0.8 Hz, 1H), 6.2 (s, 1H), 5.5 (s, 1H), 3.3 (s, 2H); HPLC-MS (ESI): purity = 97%, *t*_R = 1.22 min, *m/z* [M + H]⁺ = 452.0 [calcd for C₂₀H₁₂F₆N₅O *m/z* = 452.0946 (M + H)⁺].

General Synthetic Procedure V (3 and 4). A mixture of the corresponding carboxylic acid (1.5 equiv), *N,N*-dimethylpyridin-4-amine (DMAP) (1.5 equiv), and *N*-ethyl-*N'*-(3-dimethylaminopropyl)carbodiimide hydrochloride (EDCI) (1.5 equiv) in 0 °C cooled dichloromethane (1.0 mL per 100 mg of compound) was stirred at 0 °C for 5 min after which the temperature was increased to 17–25 °C (ambient temperature) for 15 min. The amine was added to the treated reaction mixture, and stirring was continued at that temperature for 1.5 h. The product was washed with three portions of 10 mL of deionized water, filtered, triturated with diethyl ether and, finally, dried at ambient conditions.

tert-Butyl 2-((4-Cyano-1-((4-(trifluoromethoxy)phenyl)amino)-3-(trifluoromethyl)benzo[4,5]imidazo[1,2-*a*]pyridin-9-yl)amino)-2-oxoethyl)carbamate, **3**. Compound **3** was obtained from compound **2** (0.06 g, 0.13 mmol, 1.0 equiv) and *tert*-butoxycarbonyl glycine (0.035 g, 0.20 mmol, 1.5 equiv) as an orange solid (0.029 g, 37% yield), m.p. 215–218 °C; Rf (MeOH/DCM, 1:9) 0.18; ¹H NMR (300 MHz, acetonitrile-*d*₃) δ 9.0 (s, 1H), 8.4 (dd, *J* = 8.3, 0.9 Hz, 1H), 8.3 (dd, *J* = 8.0, 1.2 Hz, 1H), 7.3 (m, 3H), 7.2 (d, *J* = 7.7 Hz, 2H), 6.1 (s, 1H), 4.1 (s, 2H), 1.5 (s, 9H); HPLC-MS (ESI): purity = 99%, *t*_R = 3.35 min, *m/z* [M - H]⁻ = 607.0 [calcd for C₂₇H₂₁F₆N₆O₄ *m/z* = 607.1528 (M - H)⁻].

tert-Butyl 2-((4-Cyano-1-((4-(trifluoromethoxy)phenyl)amino)-3-(trifluoromethyl)benzo[4,5]imidazo[1,2-*a*]pyridin-9-yl)amino)-2-oxoethyl(ethyl)carbamate, **4**. Compound **4** was obtained from compound **2** (0.06 g, 0.13 mmol, 1.0 equiv) and *N*-(*tert*-butoxycarbonyl)-*N*-ethylglycine (0.040 g, 0.20 mmol, 1.5 equiv) as a beige solid (0.072 g, 81% yield), m.p. 219–221 °C; Rf (EtOAc/hexane, 6:4) 0.35; ¹H NMR (300 MHz, acetonitrile-*d*₃) δ 9.0 (s, 1H), 8.4 (dd, 8.4, 1.1 Hz, 1H), 8.2 (dd, *J* = 8.0, 1.2 Hz, 1H), 7.3 (m, 3H), 7.2 (d, *J* = 7.6 Hz, 2H), 6.1 (s, 1H), 3.6 (s, 2H), 3.1 (q, *J* = 7.2 Hz, 2H), 1.5 (s, 9H), 1.2 (t, *J* = 6.5 Hz, 3H); HPLC-MS (ESI): purity = 99%, *t*_R = 3.37 min, *m/z* [M - H]⁻ = 635.0 [calcd for C₂₉H₂₅F₆N₆O₄ *m/z* = 635.1841 (M - H)⁻].

Compounds and Media. For *in vitro* assays with NTS and adult *S. mansoni*, the compounds were dissolved in DMSO (Sigma-Aldrich, Switzerland) at a concentration of 10 mM. For *in vivo* efficacy studies, solid compound was dissolved in tap water with Tween 80/ethanol (10%, 70:30). The formulation was then thoroughly vortexed and sonicated.

Hank Balanced Salt Solution (HBSS, 1×), M199 medium, RPMI 1640, and AlbuMax II were purchased from Gibco (Waltham MA, USA). Penicillin/streptomycin 10 000 U/mL and fetal calf serum (FCS) were purchased from Bioconcept AG (Allschwil, Switzerland). Podophyllotoxin (PTT) was commercially obtained from Sigma-Aldrich (Switzerland), and stock solutions (5 μg/mL) were prepared in L6 cells medium, supplemented with FCS and L-glutamine (Sigma-Aldrich, Switzerland).

Newly Transformed Schistosomula (NTS) and Adult *Schistosoma mansoni* Worms. The *S. mansoni* lifecycle is maintained at the Swiss Tropical and Public Health Institute (Swiss TPH), as described.⁴¹ To obtain cercariae from infected *Biomphalaria glabrata* snails, an in-house method was used. Briefly, infected snails were isolated in 24-well plates (filled with pond water) and placed under a strong light source for 3–4 h to initiate shedding of the cercariae. Cercariae were collected and mechanically transformed to newly transformed schistosomula (NTS), which were then kept in the incubator (37 °C and 5% CO₂) in medium 199, supplemented with 5% FCS and 1% penicillin/streptomycin, for at least 12 h to a maximum of 24 h until usage. Adult *S. mansoni* worms were collected by dissecting the mesenteric veins of infected mice at day 49 post-infection. Worms were incubated in supplemented RPMI medium (5% FCS, 100 U/mL penicillin, and 100 μg/mL streptomycin) at 37 °C and 5% CO₂ until usage.

In Vitro Phenotypic Screening Assays. For NTS and adult *S. mansoni* worms, transparent flat-bottom 96- and 24-well plates were used, respectively (Sarstedt, Switzerland). PBIs were initially tested at 10 μM in triplicate on NTS and repeated once; each well contained 30–40 NTS. Phenotypic reference points such as motility, morphology, and granularity were used for scoring the overall viability of incubated parasites (scores from 0 to 3).⁴¹ Parasites were judged via microscopic readout 72 h after incubation; compounds that showed high activity (75–100% reduction of viability) against NTS were subsequently tested at 1 and 0.37 μM for IC₅₀ determination. Identified hits from the NTS screening (>75% activity at 10 μM) were tested on *S. mansoni* adult worms. At least three worms (both sexes) were incubated with RPMI 1640 supplemented with 5% (v/v) FCS and 1% (v/v) penicillin/streptomycin at 37 °C and 5% CO₂ for 72 h at concentrations of 10, 1, and 0.1 μM, respectively.⁴¹ The experiment was conducted in duplicate and was not repeated; standard deviations were calculated from two wells. The influence on protein binding was tested at a 10 μM drug concentration by supplementing the medium with 45 g/L bovine serum albumin (at the human plasma concentration); the experiment was conducted in duplicate and repeated once.⁴² For all *in vitro* assays, negative controls (using the highest concentration of DMSO) were included.

Chinese Hamster Ovarian Cytotoxicity Assay. Compounds were screened for *in vitro* cytotoxicity against CHO mammalian cells, using the 3-(4,5-dimethylthiazol-2-yl)-2,5-diphenyltetrazolium bromide (MTT) assay. The reference standard, emetine, was prepared at 2 mg/mL in distilled water while stock solutions of the test compounds were prepared at 20 mg/mL in 100% DMSO with the highest concentration of

solvent to which the cells were exposed having no measurable effect on the cell viability. The initial concentration of the drugs and control was 100 μg/mL, which was serially diluted in complete medium with 10-fold dilutions to give six concentrations, the lowest being 0.001 μg/mL. Plates were incubated for 48 h with 100 μL of drug and 100 μL of cell suspension in each well and developed afterward by adding 25 μL of sterile MTT (Thermo Fisher Scientific) to each well, followed by 4 h of incubation in the dark. The plates were then centrifuged; the medium was aspirated off, and 100 μL of DMSO was added to dissolve crystals before reading absorbance at 540 nm. IC₅₀ values were then obtained from dose–response curves, using a nonlinear dose–response curve fitting analysis via GraphPad Prism v.4.0 software (La Jolla, USA). The assay was conducted in triplicate and once.

Rat Skeletal Myoblast L6 Cytotoxicity Assay. Rat skeletal myoblast L6 cells were seeded at 2 × 10⁴ cells/mL in a transparent flat bottom 96-well plate in RPMI 1640 supplemented with 10% FCS and 1.7 μM L-glutamine. Cells were incubated overnight at 37 °C and 5% CO₂ for their adherence to the well plate before compounds were added to the cells with 3-fold serial drug dilutions (concentration range: 100–0.0017 μM). Podophyllotoxin was used as a reference substance, starting at a concentration of 0.05 μg/mL. After 70 h, resazurin was added to the wells, and after another 2 h of incubation, the fluorescence was read using an excitation wavelength of 530 nm and an emission wavelength of 590 nm (SpectraMax, Molecular Devices; Softmax, version 5.4.6). Compounds were tested as singletons and repeated three times.^{43–45}

Human Hepatoma HepG2 Cells Cytotoxicity Assay. Caucasian hepatocellular carcinoma cells (HepG2) were maintained as previously described.⁴⁶ Cells were grown in Dulbecco's Modified Eagle's Medium (DMEM, HyClone) supplemented with 5% heat inactivated fetal bovine serum (HyClone) and 1% penicillin/streptomycin (Sigma-Aldrich) at 37 °C and 5% CO₂. Cell viability was monitored using a phase contrast microscope (40× magnification) with 0.2% Trypan-Blue. Cells were trypsinized with 1× Trypsin-EDTA (Sigma-Aldrich), and ~100 000 cells/well were plated in 96-well plates and grown for 24 h. The cells were drug treated and incubated for 48 h at 37 °C and 5% CO₂. Cytotoxicity was determined using the CytoSelect LDH Cytotoxicity Assay Kit (Cell Biolabs Inc., CBA-241). Absorbance was measured at 450 nm. Data obtained were analyzed in Excel, and experiments were performed in technical duplicates for three biological replicates (*n* = 3).

Metabolic Stability Assay. The metabolic stability assay was performed in duplicate in a 96-well microtiter plate. The test compounds (0.1 μM) were incubated (37 °C) in mouse, rat, and pooled human liver microsomes (final protein concentration of 0.4 mg/mL; XenoTech, Lenexa, KS) suspended in 0.1 M phosphate buffer (pH 7.4) for predetermined time points, in the presence and absence of the cofactor-reduced nicotinamide adenine dinucleotide phosphate (NADPH) (1 mM). The reactions were quenched by the addition of ice-cold acetonitrile containing an internal standard (carbamazepine, 0.0236 μg/mL). The samples were centrifuged, and the supernatant was analyzed employing liquid chromatography–tandem mass spectrometry (LC–MS/MS) (Agilent Rapid Resolution HPLC, AB SCIEX 4500 MS). The relative loss of the parent compound over time was monitored, and plots were prepared for each compound of Ln% remaining versus time to determine

the first-order rate constant for compound depletion. This was used to calculate the degradation half-life and *in vitro* intrinsic clearance value.

In Vivo Studies in *S. mansoni*-Infected Mice. For *in vivo* efficacy studies, female NMRI mice (age 3 weeks) weighing 20–22 g were purchased from Charles River, Germany. Mice were kept under environmentally controlled conditions (temperature ~ 25 °C; humidity ~ 70%; 12 h light and 12 h dark cycle) with access to water and rodent diet *ad libitum*. After 1 week of habituation, mice were infected by subcutaneously injecting approximately 100 *S. mansoni* cercariae in phosphate-buffered saline (PBS). Selected single doses (mg/kg) of chosen PBIs were administered to groups of four *S. mansoni* infected mice by oral gavage 7 weeks after infection. Untreated mice served as controls. Control and treated mice were euthanized by the CO₂ method 3 weeks post-drug administration. Worms were removed by picking; they were sexed and counted, and worm burden reduction was calculated.⁴⁷

Kinetic (Turbidimetric) Solubility. In this solubility assay method,³⁹ one intact PBS buffer tablet was dissolved in 1 L of water to make a phosphate buffered saline (PBS) solution constituting 0.14 M NaCl, 0.003 M KCl, and 0.01 M phosphate buffer (pH 7.4). The solution was then filtered through a 0.22 μm nylon filter to remove particulate contaminants. The pH was then verified using a pH meter. Test compounds were dissolved in DMSO to give 10 mM stock solutions. Starting from 8 to 0.25 mM (also referred to as predilution), serial dilutions of the compounds in DMSO were prepared in triplicate on a 96-well plate. A secondary dilution plate containing 196 μL of DMSO and PBS buffer in each well of the first six and last six columns of the 96-well plate, respectively, was prepared. After pipetting 4 μL aliquots from the predilution plate to corresponding wells in the secondary plate containing 196 μL of DMSO and PBS buffer (final volume of 200 μL in each well), secondary serial dilutions (5–200 μM) in DMSO and PBS buffer, also in triplicate, were prepared. The DMSO serial dilutions served as controls to ensure the test compounds in solution did not absorb electromagnetic radiation at the test wavelength. The plate was covered, placed in an oven maintained at 26 °C, and left to incubate for 2 h. A UV–visible Multiskan Go 1510-05438 spectrometer (Thermo Scientific) was then used to measure the absorbance values of the wells. The absorbance of the blank wells containing only DMSO and 2% DMSO in PBS was then subtracted from the absorbance values of cells containing the samples to get corrected values. Employing Excel, the corrected absorbance values were plotted as a function of concentration. For a compound soluble at all concentrations, a constant absorbance value of 0 at all concentrations is observed. For insoluble compounds, the precipitate formed at a certain concentration causes turbidity, the absorbance of which was measured by a UV–visible spectrometer. The concentration above which the test compound precipitates from solution causing a sustained upward deviation of absorbance values from zero was taken to be the solubility value.

Ethics. *In vivo* efficacy studies were carried out in accordance with Swiss national and cantonal regulations on animal welfare at the Swiss Tropical and Public Health Institute (Basel, Switzerland) under the permission number 2070.

Data Analysis. Drug effects from the *in vitro* assays were calculated from the mean viability values (±SD) of treated NTS or *S. mansoni* adult worms in relation to control parasite viability values. GraphPad Prism (Version 8.2.1(411)) was used to calculate IC₅₀ and IC₉₀ values from the NTS and adult *S. mansoni*

screening. IC₅₀ values against the mammalian cell line (L6) were generated using the Softmax software. Selectivity indices (SIs) were calculated by dividing the CHO or the L6 cytotoxicity IC₅₀, respectively, by the adult *S. mansoni* IC₅₀. *In vivo* worm burden reductions (WBRs) were assessed by calculating the mean values of living worms of each treatment group relative to the untreated mice; results were given in percentage (±SD). The Kruskal–Wallis test was employed for statistical significance in R (version 3.5.1).

■ ASSOCIATED CONTENT

Supporting Information

The Supporting Information is available free of charge at <https://pubs.acs.org/doi/10.1021/acsinfecdis.0c00278>.

Table S1, screening cascade (XLSX)

Table S2, summary data for all *in vitro* experiments (XLSX)

■ AUTHOR INFORMATION

Corresponding Authors

Kelly Chibale – Department of Chemistry, Institute of Infectious Diseases and Molecular Medicine, and South African Medical Research Council Drug Discovery Unit, University of Cape Town, Rondebosch 7701, South Africa; orcid.org/0000-0002-1327-4727; Email: Kelly.Chibale@uct.ac.za

Jennifer Keiser – Swiss Tropical and Public Health Institute, 4002 Basel, Switzerland; University of Basel, Basel, Switzerland; Email: Jennifer.keiser@swisstph.ch

Authors

Alexandra Probst – Swiss Tropical and Public Health Institute, 4002 Basel, Switzerland; University of Basel, Basel, Switzerland

Kelly Chisanga – Department of Chemistry, University of Cape Town, Rondebosch 7701, South Africa

Godwin Akpeko Dziwornu – Department of Chemistry, University of Cape Town, Rondebosch 7701, South Africa

Cécile Haeberli – Swiss Tropical and Public Health Institute, 4002 Basel, Switzerland; University of Basel, Basel, Switzerland

Complete contact information is available at: <https://pubs.acs.org/doi/10.1021/acsinfecdis.0c00278>

Author Contributions

[‡]The lead authorship of this work is equally shared between the first (A.P.) and second (K. Chisanga) authors.

Notes

The authors declare no competing financial interest.

■ ACKNOWLEDGMENTS

The University of Cape Town and South African Research Chairs Initiative of the Department of Science and Innovation, administered through the South African National Research Foundation, are gratefully acknowledged for support (K. Chibale). J.K. is grateful to the Swiss National Science Foundation for financial support (No. 320030_175585/1). We thank Dr. Dale Taylor of the Drug Discovery and Development Centre (H3D) for generating the cytotoxicity (CHO) data and Dr. Dina Coertzen and Meta Leshbane of the University of Pretoria Institute for Sustainable Malaria Control for the HepG2 results on the compounds.

REFERENCES

- (1) Colley, D. G., Bustinduy, A. L., Secor, W. E., and King, C. H. (2014) Human schistosomiasis. *Lancet* 383, 2253–2264.
- (2) McManus, D. P., Dunne, D. W., Sacko, M., Utzinger, J., Vennervald, B. J., and Zhou, X.-N. (2018) Schistosomiasis. *Nat. Rev. Dis. Prim.* 4, 13.
- (3) Steinmann, P., Keiser, J., Bos, R., Tanner, M., and Utzinger, J. (2006) Schistosomiasis and water resources development: Systematic review, meta-analysis, and estimates of people at risk. *Lancet Infect. Dis.* 6, 411–425.
- (4) Thétiot-Laurent, S. A.-L., Boissier, J., Robert, A., and Meunier, B. (2013) Schistosomiasis chemotherapy. *Angew. Chem., Int. Ed.* 52, 7936–7956.
- (5) Gönner, R., and Andrews, P. (1977) Praziquantel, a new broad-spectrum antischistosomal agent. *Z. Parasitenkd.* 52, 129–150.
- (6) Crellen, T., Walker, M., Lamberton, P. H. L., Kabatereine, N. B., Tukahebwa, E. M., Cotton, J. A., and Webster, J. P. (2016) Reduced efficacy of praziquantel against *Schistosoma mansoni* is associated with multiple rounds of mass drug administration. *Clin. Infect. Dis.* 63, 1151–1159.
- (7) Bergquist, R., Utzinger, J., and Keiser, J. (2017) Controlling schistosomiasis with praziquantel: how much longer without a viable alternative? *Infect. Dis. Poverty* 6, 74.
- (8) Pica-Mattocchia, L., and Cioli, D. (2004) Sex- and stage-related sensitivity of *Schistosoma mansoni* to *in vivo* and *in vitro* praziquantel treatment. *Int. J. Parasitol.* 34, 527–533.
- (9) Xiao, S. H., Catto, B. A., and Webster, L. T. (1985) Effects of praziquantel on different developmental stages of *Schistosoma mansoni* *in vitro* and *in vivo*. *J. Infect. Dis.* 151, 1130–1137.
- (10) Mäder, P., Rennar, G. A., Ventura, A. M. P., Grevelding, C. G., and Schlitzer, M. (2018) Chemotherapy for fighting schistosomiasis: past, present and future. *ChemMedChem* 13, 2374–2389.
- (11) Doenhoff, M. J., Cioli, D., and Utzinger, J. (2008) Praziquantel: mechanisms of action, resistance and new derivatives for schistosomiasis. *Curr. Opin. Infect. Dis.* 21, 659–667.
- (12) Utzinger, J., and Keiser, J. (2013) Research and development for neglected diseases: more is still needed, and faster. *Lancet Glob. Heal.* 1, e317–e318.
- (13) van den Enden, E. (2009) Pharmacotherapy of helminth infection. *Expert Opin. Pharmacother.* 10, 435–451.
- (14) Keiser, J., Engels, D., Büscher, G., and Utzinger, J. (2005) Triclabendazole for the treatment of fascioliasis and paragonimiasis. *Expert Opin. Invest. Drugs* 14, 1513–1526.
- (15) Schmidt, J. (1998) Effects of benzimidazole anthelmintics as microtubule-active drugs on the synthesis and transport of surface glycoconjugates in *Hymenolepis microstoma*, *Echinostoma caproni*, and *Schistosoma mansoni*. *Parasitol. Res.* 84, 362–368.
- (16) Khalil, S. S. (2000) On the schistosomicidal effect of triclabendazole an experimental study. *J. Egypt. Soc. Parasitol.* 30, 799–808.
- (17) Nessim, N. G., Hassan, S. I., William, S., and El-Baz, H. (2000) Effect of the broad spectrum anthelmintic drug flubendazole upon *Schistosoma mansoni* experimentally infected mice. *Arzneim. Forsch.* 50, 1129–1133.
- (18) William, S., Guirguis, F., and Nessim, N. G. (2003) Effect of simultaneous and/or consecutive administration of the broad spectrum anthelmintic flubendazole together with praziquantel in experimental *Schistosoma mansoni* infection. *Arzneim. Forsch.* 53, 532–537.
- (19) Keiser, J., El Ela, N. A., El Komy, E., El Lakkany, N., Diab, T., Chollet, J., Utzinger, J., and Barakat, R. (2006) Triclabendazole and its two main metabolites lack activity against *Schistosoma mansoni* in the mouse model. *Am. J. Trop. Med. Hyg.* 75, 287–291.
- (20) Ben, S. A., and Useh, M. F. (2017) A comparative study on the efficacy of praziquantel and albendazole in the treatment of urinary schistosomiasis in adult, cross river state, Nigeria. *Int. Health* 9, 288–293.
- (21) Nofal, Z. M., Fahmy, H. H., and Mohamed, H. S. (2002) Synthesis, antimicrobial and molluscicidal activities of new benzimidazole derivatives. *Arch. Pharmacol. Res.* 25, 28–38.
- (22) El Bialy, S. A., Taman, A., El-Beshbishi, S. N., Mansour, B., El-Malky, M., Bayoumi, W. A., and Essa, H. M. (2013) Effect of a novel benzimidazole derivative in experimental *Schistosoma mansoni* infection. *Parasitol. Res.* 112, 4221–4229.
- (23) Long, T., Neitz, R. J., Beasley, R., Kalyanaraman, C., Suzuki, B. M., Jacobson, M. P., Dissous, C., McKerrow, J. H., Drewry, D. H., Zuercher, W. J., Singh, R., and Caffrey, C. R. (2016) Structure-bioactivity relationship for benzimidazole thiophene inhibitors of polo-like kinase 1 (plk1), a potential drug target in *Schistosoma mansoni*. *PLoS Neglected Trop. Dis.* 10, e0004356.
- (24) Okombo, J., Singh, K., Mayoka, G., Ndubi, F., Barnard, L., Njogu, P. M., Njoroge, M., Gibbard, L., Bruntschwig, C., Vargas, M., Keiser, J., Egan, T. J., and Chibale, K. (2017) Antischistosomal activity of pyrido[1,2-a]benzimidazole derivatives and correlation with inhibition of β -hematin formation. *ACS Infect. Dis.* 3, 411–420.
- (25) Mayoka, G., Keiser, J., Häberli, C., and Chibale, K. (2019) Structure-activity relationship and *in vitro* absorption, distribution, metabolism, excretion, and toxicity (ADMET) studies of N-aryl 3-trifluoromethyl pyrido[1,2-a]benzimidazoles that are efficacious in a mouse model of schistosomiasis. *ACS Infect. Dis.* 5, 418–429.
- (26) Prostavkov, N. S., Varlamov, A. V., Shendrik, I. V., Anisimov, B. N., Krapivko, A. P., Lavani-Edogierie, S., and Fomichev, A. A. (1983) New method for the synthesis of pyrido[1,2-a]benzimidazole. *Chem. Heterocycl. Compd.* 19, 1102–1104.
- (27) Rida, S. M., Soliman, F. S. G., Badawey, E.-S. A. M., El-Ghazzawi, E., Kader, O., and Kappe, T. (1988) Benzimidazole condensed ring systems. I. syntheses and biological investigations of some substituted pyrido[1,2-a]benzimidazoles. *J. Heterocycl. Chem.* 25, 1087–1093.
- (28) Badawey, E. A., and Gohar, Y. M. (1992) Benzimidazole condensed ring systems. 8 (1). synthesis of some substituted 1-oxo-1h,5h-pyrido[1,2-a]benzimidazole-4-carbonitriles with anticipated antimicrobial activity. *Farmacol.* 47, 489–496.
- (29) Takeshita, H., Watanabe, J., Kimura, Y., Kawakami, K., Takahashi, H., Takemura, M., Kitamura, A., Someya, K., and Nakajima, R. (2010) Novel pyridobenzimidazole derivatives exhibiting antifungal activity by the inhibition of beta-1,6-glucan synthesis. *Bioorg. Med. Chem. Lett.* 20, 3893–3896.
- (30) Ndakala, A. J., Gessner, R. K., Gitari, P. W., October, N., White, K. L., Hudson, A., Fakorede, F., Shackelford, D. M., Kaiser, M., Yeates, C., Charman, S. A., and Chibale, K. (2011) Antimalarial pyrido[1,2-a]benzimidazoles. *J. Med. Chem.* 54, 4581–4589.
- (31) Singh, K., Okombo, J., Bruntschwig, C., Ndubi, F., Barnard, L., Wilkinson, C., Njogu, P. M., Njoroge, M., Laing, L., Machado, M., Prudencio, M., Reader, J., Botha, M., Nondaba, S., Birkholtz, L. M., Lauterbach, S., Churchyard, A., Coetzer, T. L., Burrows, J. N., Yeates, C., Denti, P., Wiesner, L., Egan, T. J., Wittlin, S., and Chibale, K. (2017) Antimalarial pyrido[1,2-a]benzimidazoles: lead optimization, parasite life cycle stage profile, mechanistic evaluation, killing kinetics, and *in vivo* oral efficacy in a mouse model. *J. Med. Chem.* 60, 1432–1448.
- (32) Okombo, J., Bruntschwig, C., Singh, K., Dziwornu, G. A., Barnard, L., Njoroge, M., Wittlin, S., and Chibale, K. (2019) Antimalarial pyrido[1,2-a]benzimidazole derivatives with Mannich base side chains: synthesis, pharmacological evaluation, and reactive metabolite trapping studies. *ACS Infect. Dis.* 5, 372–384.
- (33) Mayoka, G., Njoroge, M., Okombo, J., Gibbard, L., Sanches-Vaz, M., Fontinha, D., Birkholtz, L.-M., Reader, J., van der Watt, M., Coetzer, T. L., Lauterbach, S., Churchyard, A., Bezuidenhout, B., Egan, T. J., Yeates, C., Wittlin, S., Prudencio, M., and Chibale, K. (2019) Structure-activity relationship studies and plasmodium life cycle profiling identifies pan-active N-aryl-3-trifluoromethyl pyrido[1,2-a]benzimidazoles which are efficacious in an *in vivo* mouse model of malaria. *J. Med. Chem.* 62, 1022–1035.
- (34) Pieroni, M., Tipparaju, S. K., Lun, S., Song, Y., Sturm, A. W., Bishai, W. R., and Kozikowski, A. P. (2011) Pyrido[1,2-a]benzimidazole-based agents active against tuberculosis (TB), multi-drug-resistant (mdr) TB and extensively drug-resistant (xdr) TB. *ChemMedChem* 6, 334–342.
- (35) Badawey, E.-S. A. M., and Kappe, T. (1999) Benzimidazole condensed ring systems. xi. synthesis of some substituted cycloalkyl

pyrido[1,2-a]benzimidazoles with anticipated antineoplastic activity. *Eur. J. Med. Chem.* 34, 663–667.

(36) el-Hawash, S. A., Badawey el-S, A., and Kappe, T. (1999) Benzimidazole condensed ring systems. xii. synthesis and anticancer evaluation of certain pyrido[1,2-a]benzimidazole derivatives. *Die Pharmazie* 54, 341–346.

(37) Beckmann, S., Long, T., Scheld, C., Geyer, R., Caffrey, C. R., and Greveling, C. G. (2014) Serum albumin and α -1 acid glycoprotein impede the killing of *Schistosoma mansoni* by the tyrosine kinase inhibitor Imatinib. *Int. J. Parasitol.: Drugs Drug Resist.* 4, 287–295.

(38) Pasche, V., Laleu, B., and Keiser, J. (2018) Screening a repurposing library, the Medicines for Malaria Venture Stasis Box, against *Schistosoma mansoni*. *Parasites Vectors* 11, 298.

(39) Bevan, C. D., and Lloyd, R. S. (2000) A High-Throughput Screening Method for the Determination of Aqueous Drug Solubility Using Laser Nephelometry in Microtiter Plates. *Anal. Chem.* 72 (8), 1781–1787.

(40) Meister, I., Ingram-Sieber, K., Cowan, N., Todd, M., Robertson, M. N., Meli, C., Patra, M., Gasser, G., and Keiser, J. (2014) Activity of praziquantel enantiomers and main metabolites against *Schistosoma mansoni*. *Antimicrob. Agents Chemother.* 58, 5466–5472.

(41) Lombardo, F. C., Pasche, V., Panic, G., Endriss, Y., and Keiser, J. (2019) Life cycle maintenance and drug-sensitivity assays for early drug discovery in *Schistosoma mansoni*. *Nat. Protoc.* 14, 461–481.

(42) Pasche, V., Laleu, B., and Keiser, J. (2019) Early antischistosomal leads identified from *in vitro* and *in vivo* screening of the Medicines for Malaria Venture Pathogen Box. *ACS Infect. Dis.* 5, 102–110.

(43) Page, B., Page, M., and Noel, C. (1993) A new fluorometric assay for cytotoxicity measurements *in-vitro*. *Int. J. Oncol.* 3, 473–476.

(44) Ansar Ahmed, S., Gogal, R. M., and Walsh, J. E. (1994) A new rapid and simple non-radioactive assay to monitor and determine the proliferation of lymphocytes: an alternative to [³H]thymidine incorporation assay. *J. Immunol. Methods* 170, 211–224.

(45) Cowan, N., Dätwyler, P., Ernst, B., Wang, C., Vennerstrom, J. L., Spangenberg, T., and Keiser, J. (2015) Activities of N,N'-diarylurea MMV665852 analogs against *Schistosoma mansoni*. *Antimicrob. Agents Chemother.* 59, 1935–1941.

(46) Verlinden, B. K., Niemand, J., Snyman, J., Sharma, S. K., Beattie, R. J., Woster, P. M., and Birkholtz, L. M. (2011) Discovery of novel alkylated (bis)urea and (bis)thiourea polyamine analogues with potent antimalarial activities. *J. Med. Chem.* 54, 6624–6633.

(47) Xiao, S.-H., Keiser, J., Chollet, J., Utzinger, J., Dong, Y., Endriss, Y., Vennerstrom, J. L., and Tanner, M. (2007) *In vitro* and *in vivo* activities of synthetic trioxolanes against major human schistosome species. *Antimicrob. Agents Chemother.* 51, 1440–1445.

CHAPTER IV: SF₅-CONTAINING DIARYLUREAS AS ANTISCHISTOSOMALS

***In vitro*, *In vivo*, and absorption, distribution, metabolism, and excretion evaluation of SF₅-containing *N,N'*-diarylureas as antischistosomal agents**

Alexandra Probst,^{a,b} Eugènia Pujol,^c Cécile Häberli,^{a,b} Jennifer Keiser,^{a,b,#} Santiago Vázquez^{c#}

^a Swiss Tropical and Public Health Institute, Basel, Switzerland

^b University of Basel, Basel, Switzerland

^c Laboratori de Química Farmacèutica (Unitat Associada al CSIC), Facultat de Farmàcia i Ciències de l'Alimentació, and Institute of Biomedicine (IBUB), Universitat de Barcelona, Barcelona, Spain

Corresponding authors: jennifer.keiser@swisstph.ch, or svazquez@ub.edu

Alexandra Probst and Eugènia Pujol contributed equally to this work



In Vitro, *In Vivo*, and Absorption, Distribution, Metabolism, and Excretion Evaluation of SF₅-Containing *N,N'*-Diarylureas as Antischistosomal Agents

 Alexandra Probst,^{a,b}  Eugènia Pujol,^c Cécile Häberli,^{a,b}  Jennifer Keiser,^{a,b}  Santiago Vázquez^c

^aSwiss Tropical and Public Health Institute, Basel, Switzerland

^bUniversity of Basel, Basel, Switzerland

^cLaboratori de Química Farmacèutica (Unitat Associada al CSIC), Facultat de Farmàcia i Ciències de l'Alimentació, and Institute of Biomedicine (IBUB), Universitat de Barcelona, Barcelona, Spain

Alexandra Probst and Eugènia Pujol contributed equally to this work; these authors are listed in alphabetical order.

ABSTRACT In recent years, *N,N'*-diarylureas have emerged as a promising chemotype for the treatment of schistosomiasis, a parasite-caused disease that poses a considerable health burden to millions of people worldwide. Here, we report a novel series of *N,N'*-diarylureas featuring the scarcely explored pentafluorosulfanyl group (SF₅). Low 50% inhibitory concentration (IC₅₀) values for *Schistosoma mansoni* newly transformed schistosomula (0.6 to 7.7 μM) and adult worms (0.1 to 1.6 μM) were observed. Four selected compounds that were highly active in the presence of albumin (>70% at 10 μM), endowed with decent cytotoxicity profiles (selectivity index [SI] against L6 cells >8.5), and good microsomal hepatic stability (>62.5% of drug remaining after 60 min) were tested in *S. mansoni*-infected mice. Despite the promising *in vitro* worm-killing potency, none of them showed significant activity *in vivo*. Pharmacokinetic data showed a slow absorption, with maximal drug concentrations reached after 24 h of exposure. Finally, no direct correlation between drug exposure and *in vivo* activity was found. Thus, further investigations are needed to better understand the underlying mechanisms of SF₅-containing *N,N'*-diarylureas.

KEYWORDS *N,N'*-diarylureas, pentafluorosulfanyl, *Schistosoma mansoni*, antischistosomal, pharmacokinetics, structure-activity relationship

There are more than 200 million people enduring schistosomiasis and several million people currently living at risk for an infection. This neglected tropical disease is caused by the blood dwelling flatworm of the genus *Schistosoma*, with *Schistosoma haematobium*, *Schistosoma japonicum*, and *Schistosoma mansoni* being the main responsible species (1–2). Schistosomiasis causes a tremendous health burden, including malnutrition, anemia, learning deficiencies, and, in rare cases, death due to chronicity of the disease (2–3).

For more than four decades, treatment of schistosomiasis has relied on one drug only, praziquantel, patented in 1973 and widely used in preventive chemotherapy programs (4). It is inexpensive and safe and can be used in the treatment of all six *Schistosoma* species infecting humans. Major drawbacks include the inactivity of praziquantel against juvenile parasites and the rising concern of drug resistance (4–6). Therefore, there is an urgent need to develop new antischistosomal drugs able to effectively control this disease (7–8).

Over the past years, drug discovery efforts have focused on identifying new scaffolds through phenotypic screenings. Specifically, *N,N'*-diarylureas emerged as a new, promising chemotype, with the chlorinated, symmetrical urea MMV665852 (Fig. 1)

Citation Probst A, Pujol E, Häberli C, Keiser J, Vázquez S. 2021. *In vitro*, *in vivo*, and absorption, distribution, metabolism, and excretion evaluation of SF₅-containing *N,N'*-diarylureas as antischistosomal agents. *Antimicrob Agents Chemother* 65:e00615-21. <https://doi.org/10.1128/AAC.00615-21>.

Copyright © 2021 American Society for Microbiology. All Rights Reserved.

Address correspondence to Jennifer Keiser, jennifer.keiser@swisstph.ch, or Santiago Vázquez, svazquez@ub.edu.

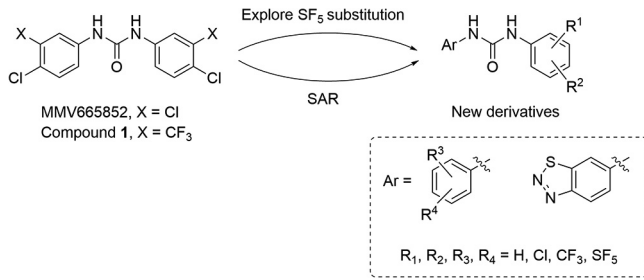
Received 25 March 2021

Returned for modification 17 April 2021

Accepted 22 July 2021

Accepted manuscript posted online 26 July 2021

Published 17 September 2021



62

N,N'

63

64

65

66

67

68

69

70

71

72

73

74

75

76

77

78

79

80

81

82

83

84

85

86

87

88

89

90

91

92

93

94

95

96

97

98

99

100

101

102

103

104

105

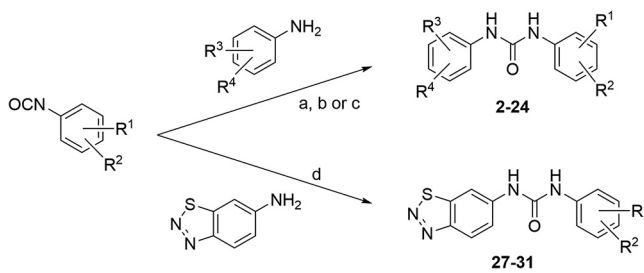
106

107

108

109

110



111

112

113

114

115

116

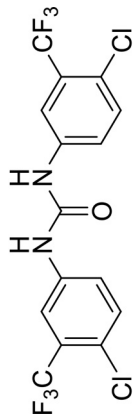
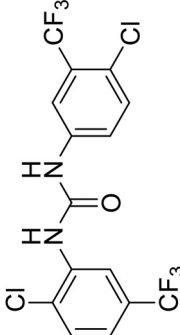
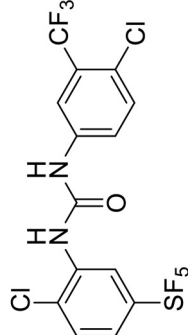
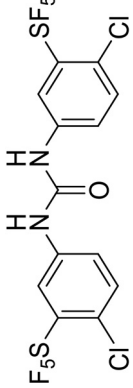
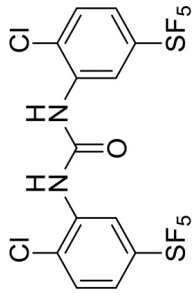
nBhR

-Eor by E

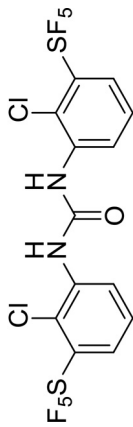
2C, f

ANNEX

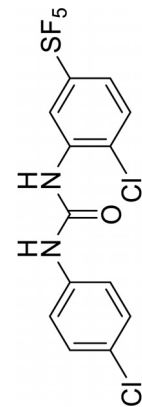
Table

Sl. No.	Chemical Structure	Concentration		Dose		Route	
		µg/ml	µg/l	mg/kg	mg/kg	µg/ml	µg/ml
1		0.01	0.01	0.01	0.01	0.01	0.01
2		0.01	0.01	0.01	0.01	0.01	0.01
3		0.01	0.01	0.01	0.01	0.01	0.01
4		0.01	0.01	0.01	0.01	0.01	0.01
5		0.01	0.01	0.01	0.01	0.01	0.01

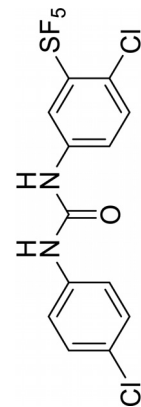
No	In		Out		In	Out	
	μM	μM	μM	μM		μM	μM
6	5	0	5	0	5	0	5



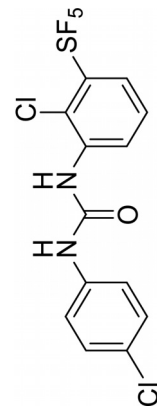
7



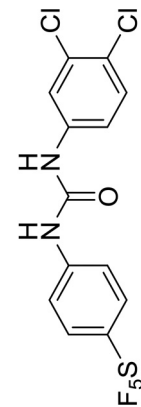
8



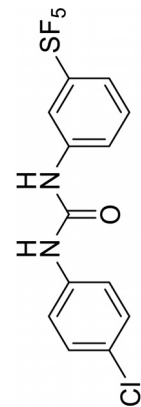
9

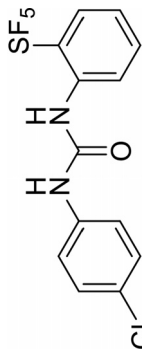
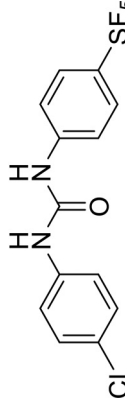
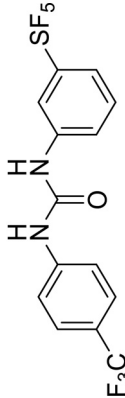
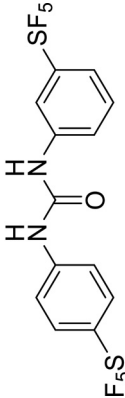
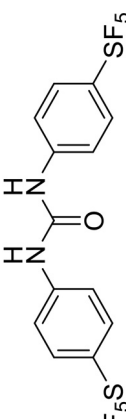
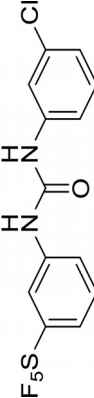


0

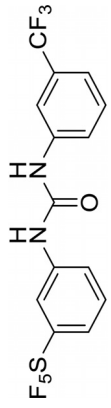


1

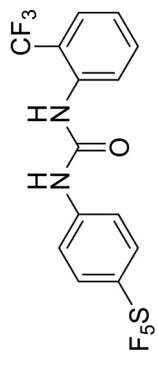


No.	Chemical Structure	C ₀ , μM ^b		C ₀ , μM ^b		C ₀ , μM ^b		C ₀ , μM ^b	
		>0	0	0	1	0	1	0	1
2		5	0	0	1	0	0	0	0
3		5	0	0	0	0	0	0	0
4		3	0	0	0	0	0	0	0
5		5	0	0	0	0	0	0	0
6		5	0	0	1	0	0	0	0
7		3	0	0	5	0	0	0	0

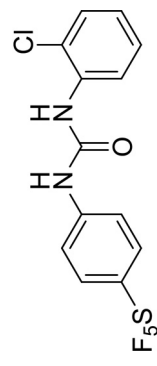
Sl. No.	Concentration		Solvent	Concentration		Solvent	Concentration	
	10 ⁻⁵ M	10 ⁻⁶ M		10 ⁻⁵ M	10 ⁻⁶ M		10 ⁻⁵ M	10 ⁻⁶ M
8	3	2	0	0	0	0	0	0



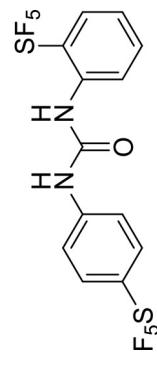
9	8	5	0	0	0	0	0	0
---	---	---	---	---	---	---	---	---



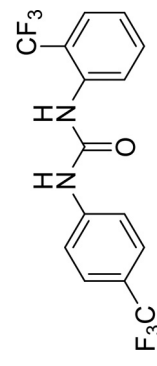
0	7	9	0	0	0	0	0	0
---	---	---	---	---	---	---	---	---



2	5	7	0	0	0	0	0	0
---	---	---	---	---	---	---	---	---



2	6	8	0	0	0	0	0	0
---	---	---	---	---	---	---	---	---



No	Chemical Structure	C ₉ , μM ^b		C ₉ , μM ^b		C ₉ , μM ^b		C ₉ , μM ^b	
		0	1	0	1	0	1	0	1
3		0	1	0	1	0	1	0	1
4		0	1	0	1	0	1	0	1
5		0	1	0	1	0	1	0	1
6		0	1	0	1	0	1	0	1
7		0	1	0	1	0	1	0	1

> 0 0 0 0 0 0

0

> 0

0

0

0

S. No.	Chemical Structure	In Vitro		In Vivo		In Vivo	
		IC ₅₀ (μM)	IC ₅₀ (μM)	IC ₅₀ (μM)	IC ₅₀ (μM)	IC ₅₀ (μM)	IC ₅₀ (μM)
1		0.0001	0.0001	0.0001	0.0001	0.0001	0.0001
2		0.0001	0.0001	0.0001	0.0001	0.0001	0.0001
3		0.0001	0.0001	0.0001	0.0001	0.0001	0.0001
4		0.0001	0.0001	0.0001	0.0001	0.0001	0.0001


S. No.	Chemical Structure	In Vitro		In Vivo		In Vivo	
		IC ₅₀ (μM)	IC ₅₀ (μM)	IC ₅₀ (μM)	IC ₅₀ (μM)	IC ₅₀ (μM)	IC ₅₀ (μM)
1		0.0001	0.0001	0.0001	0.0001	0.0001	0.0001

Table 1 *in vitro* ...

Time (h)	Concentration (μM)	...
0	0	...
1	2	...
4	5	...
5	10	...
6	20	...
9	50	...
24	100	...

...

Table 2 *in vivo* ...

Time (h)	Concentration (μM)
1	0	0.8	0	0
5	0	0.4	0	0
6	0	1.8	2	0
24	0	0.4	0	0
48	0.8	0.8	0	1
72	0.4	0.4	0	1

Table 3 *in vivo* ...

Time (h)	Concentration (μM)
1	0	0.8	0	0	0
5	0	0.4	0	0	0
6	0	1.8	2	0	0
24	0	0.4	0	0	0
48	0.8	0.8	0	1	1
72	0.4	0.4	0	1	1

...

№	Элемент	C_m гн	T_m ч	$Q_n \times 10^5$ гн	t_2 ч	Q_n
---	---------	----------	---------	----------------------	---------	-------

Элементы

Элементы

Элементы

Элементы

Элементы

Элементы

Элементы

Элементы

Элементы

Элементы

Элементы

Элементы

Элементы

Элементы

Элементы

Элементы

Элементы

Элементы

Элементы

Элементы

Элементы

Элементы

Элементы

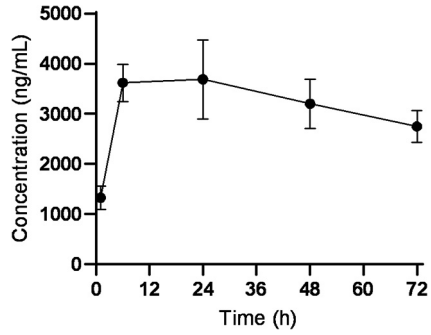
Элементы

Элементы

Элементы

Элементы

Элементы



E5 Ինտեգրումը հետևյալից
 է:

Ինտեգրումը հետևյալից է:
 $\int_0^{\infty} C(t) dt = \int_0^{\infty} \frac{C_0 e^{-\lambda t}}{\lambda} dt = \frac{C_0}{\lambda} \int_0^{\infty} e^{-\lambda t} dt = \frac{C_0}{\lambda} \left[-\frac{1}{\lambda} e^{-\lambda t} \right]_0^{\infty} = \frac{C_0}{\lambda} \left[0 - \left(-\frac{1}{\lambda}\right) \right] = \frac{C_0}{\lambda^2}$

Ինտեգրումը հետևյալից է:
 $\int_0^{\infty} C(t) dt = \int_0^{\infty} \frac{C_0 e^{-\lambda t}}{\lambda} dt = \frac{C_0}{\lambda} \int_0^{\infty} e^{-\lambda t} dt = \frac{C_0}{\lambda} \left[-\frac{1}{\lambda} e^{-\lambda t} \right]_0^{\infty} = \frac{C_0}{\lambda} \left[0 - \left(-\frac{1}{\lambda}\right) \right] = \frac{C_0}{\lambda^2}$

CHAPTER V: ANTISCHISTOSOMAL *A. ANNUA* AND *A. AFRA* EXTRACTS

***In vitro* antischistosomal activity of *Artemisia annua* and *Artemisia afra* extracts**

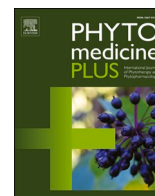
Lorencia Taljaard,^a Alexandra Probst,^{b,c} Robert Tornow,^{b,c} Jennifer Keiser,^{b,c} Richard K. Haynes,^a Frank van der Kooy^{a,*}

^a Centre of Excellence for Pharmaceutical Sciences, North-West University, Private Bag X6001, Potchefstroom, 2520, South Africa

^b Swiss Tropical and Public Health Institute, Basel, Switzerland.

^c University of Basel, Basel, Switzerland.

*Corresponding author: frank.vanderkooy@nwu.ac.za



In vitro antischistosomal activity of *Artemisia annua* and *Artemisia afra* extracts

Lorencia Taljaard^a, Alexandra Probst^{b,c}, Robert Tornow^{b,c}, Jennifer Keiser^{b,c},
Richard K. Haynes^a, Frank van der Kooy^{a,*}

^a Centre of Excellence for Pharmaceutical Sciences, North-West University, Private Bag X6001, Potchefstroom, 2520, South Africa

^b Swiss Tropical and Public Health Institute, Socinstrasse 57, P.O. Box, 4002, Basel, Switzerland

^c University of Basel, Petersplatz 1, P.O. Box, 4001, Basel, Switzerland

ARTICLE INFO

Keywords:

Artemisia afra
Artemisia annua
Schistosomiasis
Artemisinin
Active extract
In vitro assay

ABSTRACT

Background: Schistosomiasis, a neglected tropical disease, imposes substantial health and economic burdens on impoverished groups living in predominantly rural areas. Praziquantel (PZQ) is the only drug available for treatment, and it is not completely efficacious. *Artemisia annua* and *Artemisia afra* infusions were proposed to possess antischistosomal activities in a recently retracted publication of a clinical trial, leading to our investigation *in vitro*.

Objective: The objective was to identify the main components of the infusions and evaluate the *in vitro* antischistosomal activities of traditionally prepared infusions as well as hexane and dichloromethane (DCM) extracts of the infusions of *A. afra* and *A. annua*.

Methods: Infusions of *A. afra* and *A. annua* were submitted to liquid-liquid partitioning with n-hexane and DCM to provide samples for *in vitro* bioassays using newly transformed schistosomulas (NTS) and adult *Schistosoma mansoni* worms obtained from infected mice. The viability of the NTS and adult *S. mansoni* was visually scored via microscopic readout.

Results: Nine phytochemicals comprising coumarins and organic acids were identified. *A. afra* and *A. annua* infusions and extracts possess potent *in vitro* antischistosomal activities against NTS, at 100 g/ml. However, the *A. afra* infusions exhibited better activities against NTS than the *A. annua* infusion. The *A. afra* hexane- and DCM extracts presented IC₅₀ values that are similar to PZQ (1.5 g/ml) and approximately five times lower than the comparison drug artesunate (11.6 g/ml) against NTS. Low IC₅₀ values for both these extracts were also obtained in phenotypic assays with adult *S. mansoni*.

Conclusion: *A. afra* shows greater antischistosomal potential than *A. annua*. Thus, further studies are necessary to identify the active molecule(s) responsible for the notable antischistosomal activity of *A. afra*.

Introduction

The neglected tropical disease, schistosomiasis (bilharzia), is caused by the *Schistosoma* trematode fluke species of which *S. mansoni*, *S. japonicum*, and *S. haematobium* are the three main important parasites for human infection (Colley et al. 2014; CDC, 2018; McManus et al. 2018; WHO, 2021). Infectious cercariae penetrate the host's skin and transform into schistosomulas, which travel the vascular system and eventually reach the host's liver, where they mature into adult worms.

Fertilised eggs are produced by adult female worms inside the host's veins to either induce inflammation that leads to morbidity, or to be cast back into the environment (Colley et al. 2014).

Populations in rural tropical and sub-tropical regions are mainly affected (CDC, 2018; Colley et al. 2014; McManus et al. 2018; WHO, 2021). Malnutrition, anaemia, and underdeveloped cognitive function among infected children are common (CDC, 2018). Inadequate sanitation, unsafe water supply, food insecurity, and the widespread occurrence of parasites contribute to the vulnerability of endemic

Abbreviations: DCM, dichloromethane; IC₅₀, Half-maximal inhibitory concentration; NTS, newly transformed schistosomula; PZQ, Praziquantel.

* Corresponding author: Frank van der Kooy, Centre of Excellence for Pharmaceutical Sciences, North-West University, Private Bag X6001, Potchefstroom, 2520, South Africa. Tel.: 27 18 299 2236

E-mail address: frank.vanderkooy@nwu.ac.za (F. van der Kooy).

<https://doi.org/10.1016/j.phyplu.2022.100279>

Received 22 November 2021; Received in revised form 21 March 2022; Accepted 12 April 2022

Available online 14 April 2022

2667-0313/© 2022 The Author(s). Published by Elsevier B.V. This is an open access article under the CC BY-NC-ND license (<http://creativecommons.org/licenses/by-nc-nd/4.0/>).

communities to infection (Colley et al. 2014; McManus et al. 2018; WHO, 2021). However, prevalence is increasing due to migration patterns and increased tourism (WHO, 2021). For example, schistosomiasis remains a frequent infection among Europeans who travel to and migrate from susceptible areas (Lingscheid et al. 2017). Overall, some 800 million people are at risk of acquiring infection, with transmission occurring in 78 countries (Boubacar et al. 2017; WHO, 2021).

In 2019, the World Health Organization (WHO) estimated that 236 million people, of which 90% resided in Africa, required treatment. Current treatment consists mainly of praziquantel (PZQ), which is an effective and safe treatment option and is included in schistosomiasis control programmes (CDC, 2018; McManus et al. 2018). This drug is currently on the WHO's list of essential medicines and although effective against all adult *Schistosoma* flatworm species, it is, however, ineffective against the immature- and egg phase of the flatworms (WHO, 2019; Xiao et al. 2018). Even though it is considered the safest among all anthelmintic drugs, the potential for emergence of drug resistance and its effectiveness against only the adult stage of the parasite indicate that new and safe medications, effective against all stages, are needed (Cioli et al. 2014).

Certain antimalarial drugs, such as mefloquine and derivatives of artemisinin, extracted from *Artemisia annua* L. (Asteraceae), were shown to be effective against the immature schistosome stages rather than against the adult flatworms (Keiser et al. 2009; Bergquist et al. 2017). Ethanolic *A. annua* extracts have also been shown to possess lethal effects against adult *S. mansoni* worms *in vitro* (Abd Ellah et al. 2021). In experimental animals, the artemisinin derivative: artemether, was also shown to prevent the maturing of *S. mansoni* worms, if treatment is applied during the larval stages of the parasite (Xiao et al. 2000). Currently, artemisinin and its derivatives are used for treatment of malaria, and therefore the prospect that other *Artemisia* species might yield new antiparasitic compounds, including antischistosomal compounds, should be investigated (De Almeida et al. 2016; Gruessner et al. 2019). *Artemisia afra* Jacq. ex Willd. (Asteraceae) is closely related to *A. annua* but does not contain artemisinin (Van der Kooy et al. 2008; Du Toit and Van der Kooy, 2019). Reviews documenting the studies on *A. afra* indicated that *A. afra* has been tested for *in vitro* activity against *Plasmodium falciparum*, parasitic gastrointestinal nematodes, *Trypanosoma* species and *Leishmania donovani* with good to moderate activity (Liu et al. 2009; Du Toit and Van der Kooy, 2019). The fact that *A. afra* does not contain artemisinin but does show interesting activity against various parasites, therefore makes it a species of interest for further studies.

In a recent publication (Munyangi et al. 2018), it was reported that a clinical trial involving infusions prepared from leaves and twigs of both *A. annua* and *A. afra* might offer an alternative treatment for schistosomiasis, with *A. afra* being as efficacious as *A. annua* in eliminating *S. mansoni* parasite eggs, as indicated by the examination of patient faecal smears. Although the trial received a published critique highlighting serious shortcomings of the study and hence raising considerable doubts on the results observed (Argemi et al. 2019), followed by article retraction (Munyangi et al. 2020), our attention was drawn to the fact that despite no artemisinin being present in *A. afra* (van der Kooy et al. 2008), it could still display antischistosomal activity similar to that of *A. annua*, which does contain artemisinin.

We therefore decided to retrace the first steps of the pharmacological studies by assessing the *in vitro* antischistosomal activity of *A. annua* and *A. afra* infusions as well as hexane and DCM extracts, in order to investigate the role played by artemisinin in the antischistosomal activity, as was also suggested by Gruessner et al. (2019).

The aim of the current study was to comparatively evaluate traditionally prepared *A. afra* and *A. annua* infusions, n-hexane and DCM extracts prepared from the infusions, and the extracted infusions for their antischistosomal activities *in vitro*.

Material and methods

Chemicals and reagents

n-Hexane and DCM used for liquid-liquid partitioning of infusions were purchased from Merck (Darmstadt, Germany) and used without purification. Ultrapure water for the preparation of infusions was obtained from a Replife Ultrapure water system (Boston, MA, USA). Scopolin (CAS number: 531-44-2), scopoletin (92-61-5), chlorogenic acid (327-97-9), neochlorogenic acid (906-33-2), 4-caffeoylquinic acid (905-99-7), 1,5-dicaffeoylquinic acid (DCQA) (19870-46-3), 3,4-DCQA (14534-61-3), 3,5-DCQA (2450-53-5), 4,5-DCQA (57378-72-0), luteolin (491-70-3), and quercetin (117-39-5) were purchased from Alfa Biotechnology (Chengdu, China) and all were of 98% purity.

Plant material

Commercial *A. annua* (cultivar A3) plant material was donated by ANAMED International e.V. (Winnenden, Germany). *A. annua* is commercially cultivated to contain high levels of artemisinin, which can act as a chemical marker for species identification. LCMS analysis was conducted to quantify artemisinin and thereby positively identify the plant material.

Leaves and twigs of *A. afra* were collected at Bronkhorstbaai (BB), South Africa and in the Botanical Garden (BG) of North-West University in April 2019, after which the plant samples were oven-dried for seven days at 40 °C to remove moisture. All dried leaves were then separated from the twigs to obtain the material used for this study. Voucher herbarium specimen samples of both *A. afra* samples were deposited at the A.P. Goossens Herbarium at North-West University (PUC0015454 (*A. afra* BB) and PUC0015456 (*A. afra* BG)).

Preparation of plant material infusions and extracts

Infusions were prepared by adding leaf material (2 g) to boiling deionised water (200 ml). The mixture was allowed to infuse for 10 min, after which it was filtered. The filtrate (2 ml) was then again filtered through a polytetrafluoroethylene (PTFE) syringe filter (0.45 µm, 25 mm) into a high-performance liquid chromatography (HPLC) vial for chemical analysis. The remaining infusion was frozen at -80 °C, followed by freeze-drying to yield a primary dried infusion sample.

For liquid-liquid partitioning, infusions were prepared as described above. After the initial filtration, the infusion (200 ml) was cooled to room temperature (25 °C), transferred into a separating funnel, and sequentially extracted with n-hexane (200 ml) and DCM (200 ml). The organic extracts were evaporated to dryness using a rotary evaporator (Buchi R200). The dried organic extracts were reconstituted in 5 ml of methanol, of which 1 ml of each was transferred into HPLC vials for analysis, whereas the remaining solutions were again dried to yield the extracts for bioactivity testing. One ml of the residual aqueous extract (extracted infusion) was transferred into a HPLC vial for analysis, whilst the remaining liquid was frozen at -80 °C, followed by freeze-drying to yield a dried extracted infusion sample.

HPLC analysis

A Shimadzu iNexera LC-2040 HPLC equipped with a quaternary pump, autosampler, column oven, and photodiode array detector was used to analyse the samples. Separation and chemical fingerprinting were performed on an Agela C18 4.6 × 150 mm, 5 micron column (Agela Technologies, Tianjin, China). For the primary infusion samples, a stepwise gradient mobile system was used at a flow rate of 0.8 ml/min. The eluents consisted of water 0.1% formic acid (A) and methanol (MeOH) 0.1% formic acid (B). The gradient system started at 20% B at time 0-1, increased to 40% B after 6 min, where it was kept at 40% until 9 min, whereafter it increased to 60% after 11 min. It was kept at 60%

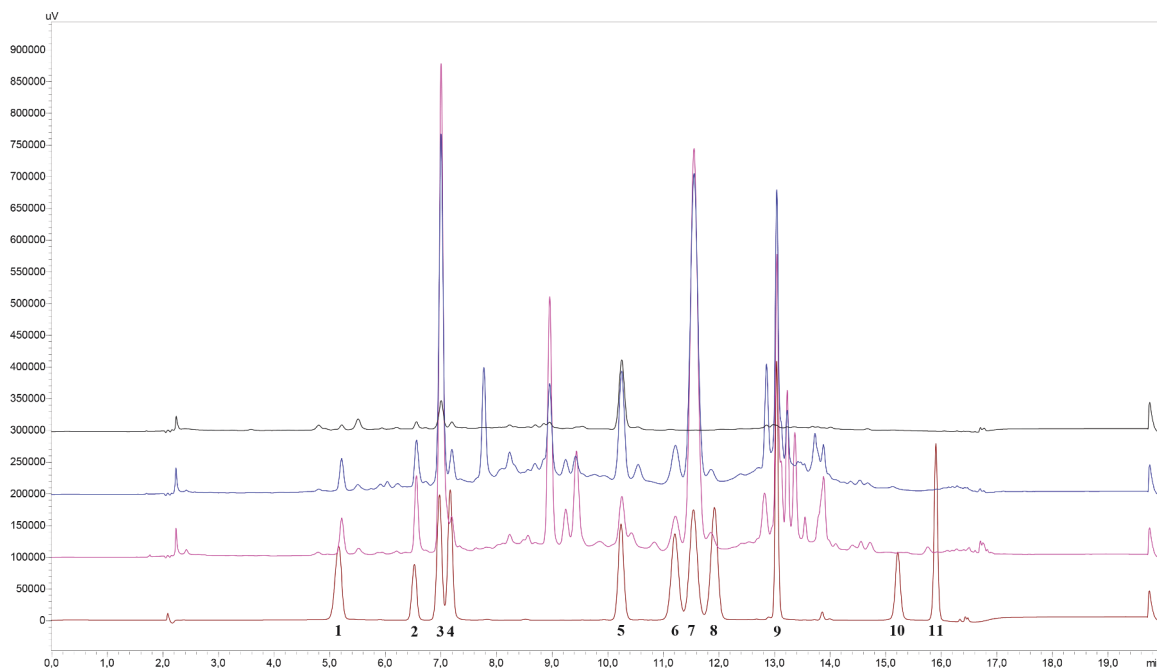


Fig. 1. Overlaid HPLC chromatograms of the infusions and the reference standard mixture (RSM). From top to bottom: *A. afra* (BG), *A. afra* (BB), *A. annua*, and RSM, as measured at 254 nm. The elution order for the reference standards is: [1] neochlorogenic acid, [2] scopoline, [3] chlorogenic acid, [4] 4-caffeoylquinic acid, [5] scopoletin, [6] 3,4-dicaffeoylquinic acid (DCQA), [7] 3,5-DCQA, [8] 1,5-DCQA, [9] 4,5-DCQA, [10] quercetin, and [11] luteolin.

until 13 min, increasing to 100% B at 14 min, where it was kept at 100% until 17 min. The system was re-equilibrated for 3 min at 20% B. For the hexane, DCM and extracted infusion samples the gradient started at 20% B, changing to 100% B after 20 min, and holding at 100% B until 25 min, after which the system was reconditioned at 20% B for 5 min. A mixture of the reference compounds was also analysed using these two chromatographic systems. The choice of reference compounds was based on literature regarding the major compounds found in *A. annua* infusions (Van der Kooy et al. 2008; Mouton and Van der Kooy, 2014; Du Toit and Van der Kooy, 2019).

Liquid chromatography mass spectrometry analysis

A validated method using an Agilent Ultivo electrospray ionisation triple quadrupole mass spectrometer was used to analyse all samples for artemisinin content (Lee et al., 2022). A Kinetix 2.6 μm C18 100 \times 2.1 mm column was used, and the gradient mobile system was as follows: 0.0 min 35% B, 1.0 min 35% B, 2.5 min 100% B, 3.9 min 100% B, 4.0 min. 35% B, and a post run time of 1.5 min to re-equilibrate the system. Total run time was 5.5 min. A multiple reaction monitoring (MRM) method with the following transitions was used for quantitation of artemisinin; 283.2 m/z to 265.1 m/z (collision energy 4 V) and 247.1 m/z. (collision energy 8 V). The optimized settings were as follow: gas temperature 300°C, N₂ gas flow 10 L/min, nebulizer pressure 35 psi, capillary voltage 4000V, fragmentor voltage 85V.

Drug-screening assay with *S. mansoni* newly transformed schistosomula (NTS) and adult worms

All samples were first diluted in 100% dimethyl sulfoxide (DMSO) (Sigma-Aldrich, Schaffhausen, Switzerland) to obtain stock solutions of 10 mg/ml. The dried *A. afra* (BB) infusion sample was equally divided (1:1) into two samples and the one dissolved in DMSO, as above, and the second in ultrapure water (Milli-Q® Advantage A10 purification system, Merck) to a concentration of 10 mg/ml. All stock solutions were vortexed and sonicated. For *in vitro* assays with NTS and adult *S. mansoni*, stock solutions were further diluted with supplemented M199 medium

(Gibco, Waltham, MA, USA) and supplemented RPMI 1640 medium (Gibco), respectively. Working solutions of 1 mg/ml and 100 $\mu\text{g/ml}$ were prepared.

NTS were obtained by mechanically transforming cercariae of *S. mansoni* (Liberian strain), which were obtained from infected intermediate host snails (*Biomphalaria glabrata*). Adult *S. mansoni* were collected by dissecting the mesenteric veins of infected mice at day 49 post-infection.

The phenotypic screening was conducted as described by Lombardo et al. (2019). In brief, approximately 30-40 NTS were incubated with the test samples in a final volume of 250 μl of M199 medium supplemented with 5% (v/v) fetal calf serum (FCS) (Bioconcept AG, Allschwil, Switzerland), 1% (v/v) penicillin/streptomycin (Sigma-Aldrich), and 1% (v/v) antibacterial/antifungal solution for up to 72 hrs at 37°C and 5% CO₂, using transparent flat-bottom 96 well plates (Sarstedt AG, Sevelen, Switzerland). The final drug concentration in the well was 100 $\mu\text{g/ml}$ or 10 $\mu\text{g/ml}$ depending on the working solution that was used. To determine the IC₅₀ of the samples, dose response assays in a concentration range of 6.25 $\mu\text{g/ml}$ to 100 $\mu\text{g/ml}$ and 0.621 $\mu\text{g/ml}$ to 10 $\mu\text{g/ml}$ were conducted, starting at a concentration of 100 $\mu\text{g/ml}$ and 10 $\mu\text{g/ml}$, respectively. Each sample was tested in triplicate, and the experiments were repeated once.

Phenotypic assays with adult worms were performed in a similar manner. At least three worms (both sexes) were incubated with RPMI 1640 supplemented with 5% FCS and 1% penicillin/streptomycin at 37°C and 5% CO₂ for 72 hrs at concentrations of 100 $\mu\text{g/ml}$ and 10 $\mu\text{g/ml}$, respectively. Transparent flat-bottom 24-well plates were used, and the total volume was 2 ml. The experiments were conducted in duplicate and repeated once.

For all assays, negative controls (using the highest concentration of DMSO without exceeding 1.5% (v/v)) were included. The viability of the NTS and adult *S. mansoni* was visually scored via microscopic readout at selected time points (24 h, 48 h, and 72 h), using reference points such as motility, morphology, and granularity. Drug effects were calculated (Microsoft Excel) from mean viability values (\pm SD) of treated parasites in relation to the control, and IC₅₀ values were calculated using GraphPad Prism (Version 8.2.1).

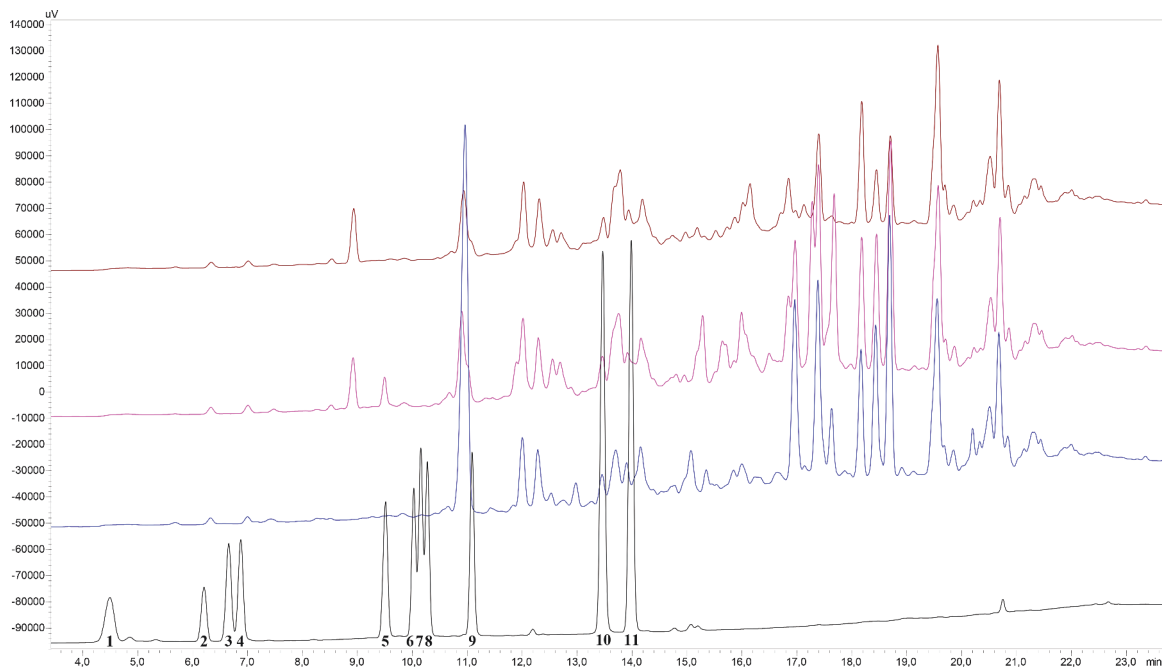


Fig. 2. Overlaid HPLC chromatograms of the hexane extracts of the infusions and the reference standard mixture (RSM). From top to bottom: *A. afra* (BG), *A. afra* (BB), *A. annua*, and RSM, as measured at 254 nm. The elution order for the reference standards is: [1] neochlorogenic acid, [2] scopoline, [3] chlorogenic acid, [4] 4-caffeoylquinic acid, [5] scopoletin, [6] 3,4-dicaffeoylquinic acid (DCQA), [7] 3,5-DCQA, [8] 1,5-DCQA, [9] 4,5-DCQA, [10] quercetin, and [11] luteolin.

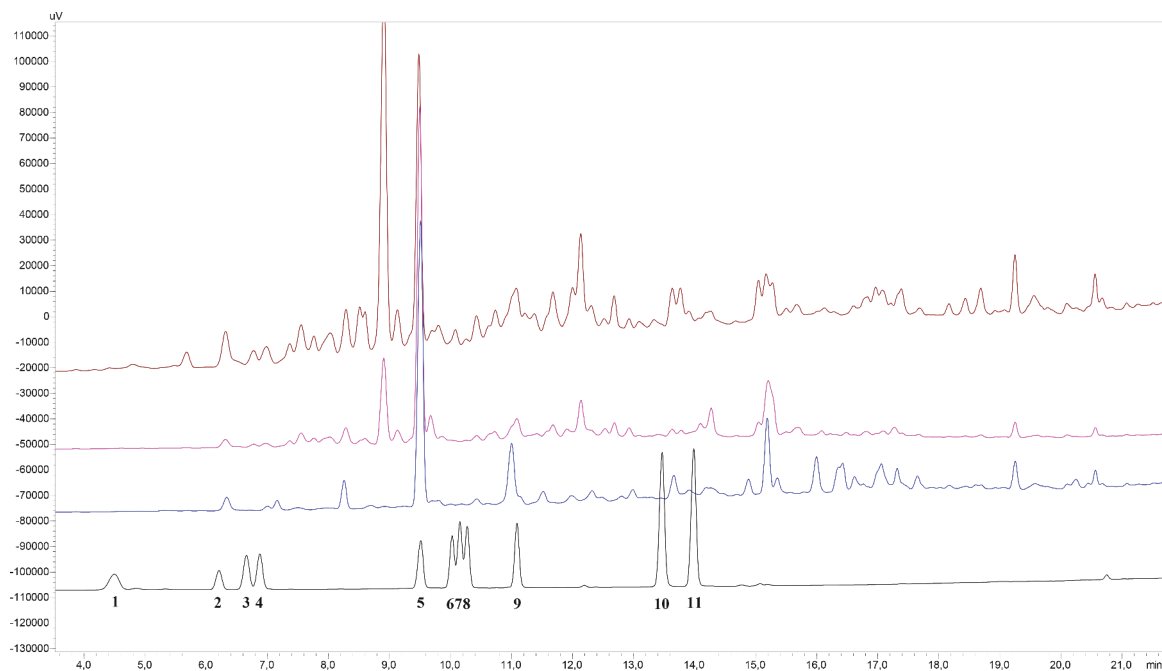


Fig. 3. Overlaid HPLC chromatograms of the DCM extracts of the infusions and the reference standard mixture (RSM). From top to bottom: *A. afra* (BG), *A. afra* (BB), *A. annua*, and RSM, as measured at 254 nm. The elution order for the reference standards is: [1] neochlorogenic acid, [2] scopoline, [3] chlorogenic acid, [4] 4-caffeoylquinic acid, [5] scopoletin, [6] 3,4-dicaffeoylquinic acid (DCQA), [7] 3,5-DCQA, [8] 1,5-DCQA, [9] 4,5-DCQA, [10] quercetin, and [11] luteolin.

Results and discussion

No trace of artemisinin could be found in both the *A. afra* samples, whereas the *A. annua* sample contained 0.36% artemisinin after extraction of all plant material samples with organic solvents and LCMS analysis as described by Lee et al. (2022). Analysis of the infusion samples confirmed that both the *A. afra* samples were devoid of artemisinin and the *A. annua* infusion contained 0.25% artemisinin, which

equates to an extraction efficiency of roughly 70%. Liquid partitioning with hexane and DCM extracted 91% and 9% respectively of the available artemisinin, with the extracted infusion sample of *A. annua* containing undetectable levels of artemisinin.

Fig. 1-4 illustrates the HPLC chromatograms of all samples as compared to 11 reference standards. The infusions contained neochlorogenic acid, scopoline, chlorogenic acid (major component), scopoletin, and four dicaffeoylquinic acids with 3,5- and 4,5-

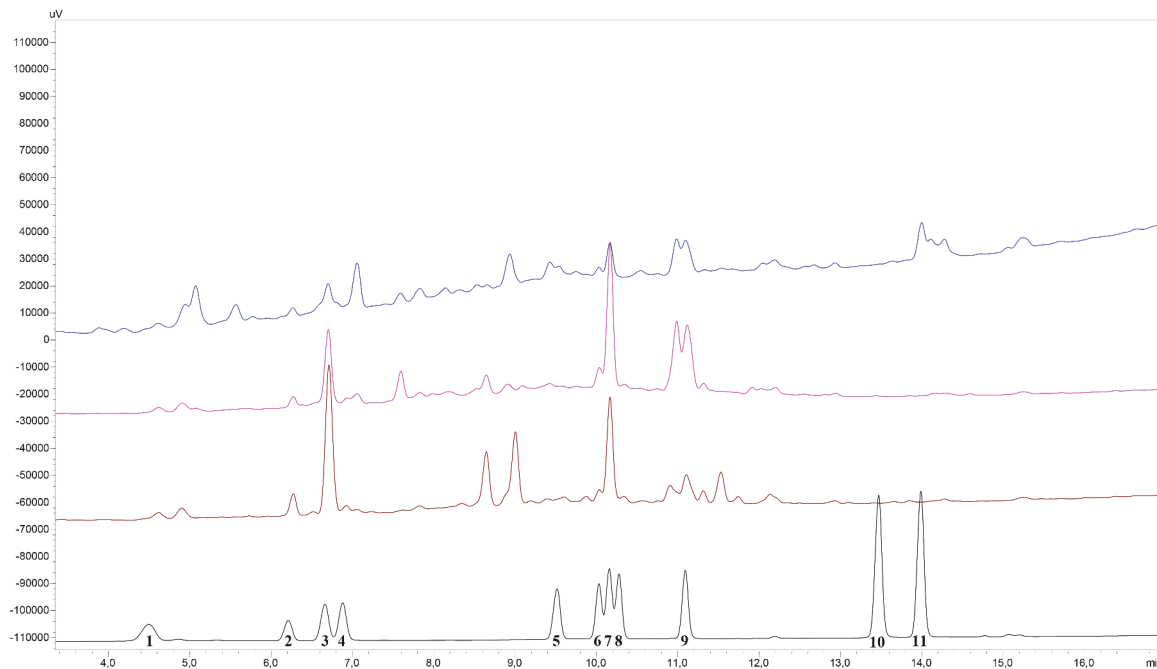


Fig. 4. Overlaid HPLC chromatograms of the remaining extracted infusions and the reference standard mixture (RSM). From top to bottom: *A. afra* (BG), *A. afra* (BB), *A. annua*, and RSM, as measured at 254 nm. The elution order for the reference standards is: [1] neochlorogenic acid, [2] scopoline, [3] chlorogenic acid, [4] 4-caffeoylquinic acid, [5] scopoletin, [6] 3,4-dicaffeoylquinic acid (DCQA), [7] 3,5-DCQA, [8] 1,5-DCQA, [9] 4,5-DCQA, [10] quercetin, and [11] luteolin.

Table 1
In vitro antischistosomal activities of *A. afra* and *A. annua* infusions and extracts.

Samples	NTS, % inhibition (SD)					<i>S. mansoni</i> adult worms, % inhibition (SD)				
	10 µg/ml 24 h	10 µg/ml 72 h	100 µg/ml 24 h	100 µg/ml 72 h	IC ₅₀ (µg/ ml) 72 h	10 µg/ml 72 h	100 µg/ml 24 h	100 µg/ml 48 h	100 µg/ml 72 h	IC ₅₀ (µg/ml) 72 h
<i>A. afra</i> (BG) -infusion	14.3*	15.4*		90.0 (10.0)			15.6*	24.1*	9.2 (5.3)	>100
<i>A. afra</i> (BB) -infusion	0.0*	1.4 (1.9)	80.7 (33.5)	100.0 (0.0)	17.8	1.2*	66.7 (15.3)	75.9 (4.8)	74.0 (2.2)	
<i>A. afra</i> (BB) -infusion [§]	10.3 (5.7)	12.0 (7.5)	100.0 (0.0)	100.0 (0.0)	29.1	11.7 (6.7)	19.6 (4.6)	35.2 (3.5)	42.7 (10.7)	>100
<i>A. afra</i> (BB) -extracted infusion		14.5 (4.1)		95.8 (36.7)	>50	4.9*				
<i>A. afra</i> (BB) -hexane extract	97.1 (4.0)	100.0 (0.0)	100.0*	100.0 (0.0)	1.8	41.25 (8.05)	100.0 (0.0)	100.0 (0.0)	100.0 (0.0)	10.4
<i>A. afra</i> (BB) -DCM extract	100.0 (0.0)	100.0 (0.0)	88.2*	100.0 (0.0)	1.7	28.85 (7.75)	100.0 (0.0)	100.0 (0.0)	100.0 (0.0)	8.9
<i>A. annua</i> -infusion		53.8 (34.5)		48.0 (25.7)	>50					
<i>A. annua</i> -extracted infusion		51.3 (43.7)		67.2 (26.5)						
<i>A. annua</i> -hexane extract		11.2 (7.0)		100.0 (0.0)	77.6					
<i>A. annua</i> -DCM extract		4.9 (6.8)		100.0 (0.0)	45.8					
Artesunate				100.0*	11.6*					
Praziquantel [#]					1.5					0.05

[§] dissolved in water;

* single experiment, no repetition;

[#] from Meister et al. (2014); NTS = newly transformed schistosomula; SD = standard deviation; IC₅₀ = Half-maximal inhibitory concentration; BG = botanical garden; BB = bronkhostbaai; DCM = dichloromethane; blank cells = data not available

dicaffeoylquinic acids as major components. The two flavonoids: luteolin and quercetin could not be detected in the infusion samples. The hexane extracts indicate that very small amounts, if any, of these marker compounds were extracted, and it mainly consists of as yet identified non-polar compounds. The DCM extracts transferred some of the marker molecules, most notably chlorogenic acid, into the organic phase. The extracted infusion samples contained most of the marker compounds, which indicates that these components might play a limited role in the observed bioactivity.

The results (Table 1) indicate that infusions of both *A. afra* and *A. annua* showed good activity, at 100 µg/ml, in the NTS bioassay. After

a treatment period of 72 hrs, *A. afra* (BG) afforded 90% inhibition, *A. afra* (BB) 100%, for both the DMSO- and water dissolved sample, and *A. annua* 48% inhibition. Further testing was conducted on *A. afra* (BB) and *A. annua* infusion samples, which yielded IC₅₀ values of 17.8 and 29.1 µg/ml for the two *A. afra* (BB) samples, respectively, and >50 µg/ml for the *A. annua* sample.

A. afra infusion samples were further submitted to bioassays conducted with adult *S. mansoni* worms, which overall delivered low to moderate inhibition, compared to the NTS bioassay results. Irrespective of the developmental stage of the parasite, it was interesting to note that by dissolving the *A. afra* (BB) infusion sample in DMSO, higher activities

resulted, with the highest being 75.9% inhibition at 100 g/ml after 48 h, whilst the same infusion sample dissolved in water only delivered, at the highest, 42.7% inhibition at 100 g/ml, together with an IC₅₀ value of 100 g/ml after 72 hrs of treatment.

No adult *S. mansoni* worm bioassays were conducted with the *A. annua* infusion, due to lower activity, at 100 g/ml, and a higher IC₅₀ value, as compared to *A. afra* infusions, in the NTS bioassay.

The various extracts (hexane, DCM, and extracted infusions) of *A. afra* (BB) and *A. annua* were also tested in NTS bioassays. Both the hexane- and DCM extract of *A. afra* (BB) as well as of *A. annua*, afforded 100% inhibition, at 100 g/ml after 72 h. The IC₅₀ values for the *A. afra* (BB) hexane- and DCM extract were found to be 1.8 and 1.7 g/ml, respectively, and for the *A. annua* hexane- and DCM extract 77.6 and 45.8 g/ml, respectively. Compared to the gold standard praziquantel (IC₅₀ 1.5 g/ml) (Meister et al. 2014) and to a semisynthetic comparator, artesunate (IC₅₀ 11.6 g/ml), both the hexane- and DCM extract of *A. afra* (BB) were therefore remarkably active.

Furthermore, the extracts of *A. afra* (BB) were also submitted to adult *S. mansoni* worm bioassays, which delivered 100% inhibition for both the hexane- and DCM extract at 100 g/ml, after 24 hrs, 48 hrs, and 72 hrs of treatment. The IC₅₀ values were found to be 10.4 and 8.9 g/ml after a 72 h incubation period for the *A. afra* (BB) hexane- and DCM extract, respectively.

Conclusion

The results indicate that *A. afra* is more active than *A. annua* against *S. mansoni*, and it seems that artemisinin plays a limited role in the observed bioactivity. The results also indicate that *A. afra* may contain highly active novel molecules with more in-depth research required to identify the molecule(s) responsible for these observed activities.

Declaration of competing interest

The authors declare no conflict of interest.

Ethical approval

The *S. mansoni* lifecycle is maintained at Swiss TPH and the animal work was carried out in accordance with Swiss national and cantonal regulations on animal welfare under the permission number 2070.

Acknowledgements

This work was financially supported by the Centre of Excellence for Pharmaceutical Sciences (PharmacenTM), North-West University. We would also like to thank ANAMED International e.V. for donating the *A. annua* plant material. JK is grateful for financial support from the Swiss National Science Foundation (No. 320030_175585).

References

- Abd Ellah, O.H., Ahmed, D.H., Abdel-Rahman, I.A., El-Kady, A.M., Mohamed, Y.M., 2021. Tegumental alterations in adult *Schistosoma mansoni* treated with ethanolic extracts of *Artemisia annua* in vitro. SVU-Int. J. Med. Sci. In press <https://doi.org/10.21608/svuijm.2021.59101.1066>.
- Argemi, X., Hansmann, Y., Gaudart, J., Gillibert, A., Caumes, E., Jaureguiberry, S., Meyer, N., 2019. Comment on "Effect of *Artemisia annua* and *Artemisia afra* tea infusions on schistosomiasis in a large clinical trial". Phytomedicine 62, 152943. <https://doi.org/10.1016/j.phymed.2018.12.027>.
- Bergquist, R., Utzinger, J., Keiser, J., 2017. Controlling schistosomiasis with praziquantel: how much longer without a viable alternative? Infect. Dis. Poverty 6, 74. <https://doi.org/10.1186/s40249-017-0286-2>.
- Boubacar, S., Diallo, I.M., Cisse, O., Ntenga, P., Kaba, Y., Fall, M., Basse, A.M., Ndiaye, M., Diop, A.G., Ndiaye, M.M., 2017. Schistosomiasis complications in tropical neurology: a review. Clin. Case Rep. Rev. 3, 1 4. <https://doi.org/10.15761/CCRR.1000338>.
- CDC (Center for Disease Control and Prevention), 2018. Parasites Schistosomiasis. <https://www.cdc.gov/parasites/schistosomiasis/index.html> (accessed 18 August 2021).
- Cioli, D., Pica-Mattocchia, L., Basso, A., Guidi, A., 2014. Schistosomiasis control: praziquantel forever? Mol. Biochem. Parasitol. 195, 23 29 <https://doi.org/10.1016/j.molbiopara.2014.06.002>.
- Colley, D.G., Bustinduy, A.L., Secor, W.E., King, C.H., 2014. Human schistosomiasis. Lancet 383, 2253 2264. [https://doi.org/10.1016/S0140-6736\(13\)61949-2](https://doi.org/10.1016/S0140-6736(13)61949-2).
- De Almeida, L.M.S., Carvalho, L.S.A.D., Gazolla, M.C., Silva Pinto, P.L., Silva, M.P.N.D., De Moraes, J., Da Silva Filho, A.A., 2016. Flavonoids and sesquiterpene lactones from *Artemisia absinthium* and *Tanacetum parthenium* against *Schistosoma mansoni* worms. Evid.-based Complement. Altern. Med. 2016, e9521349 <https://doi.org/10.1155/2016/9521349>.
- Du Toit, A., Van der Kooy, F., 2019. *Artemisia afra*, a controversial herbal remedy or a treasure trove of new drugs? J. Ethnopharmacol. 244, 112 127. <https://doi.org/10.1016/j.jep.2019.112127>.
- Gruessner, B.M., Cornet-Vernet, L., Desrosiers, M.R., Lutgen, P., Towler, M.J., Weathers, P.J., 2019. It is not just artemisinin: *Artemisia* spp. for treating diseases including malaria and schistosomiasis. Phytochem. Rev. 18, 1509 1527. <https://doi.org/10.1007/s11101-019-09645-9>.
- Keiser, J., Chollet, J., Xiao, S., Mei, J., Jiao, P., Utzinger, J., Tanner, M., 2009. Mefloquine -an aminoalcohol with promising antischistosomal properties in mice. PLOS Negl. Trop. Dis. 3, e350. <https://doi.org/10.1371/journal.pntd.0000350>.
- Lee, B.J., van Niekerk, S.E., Legoabe, L.J., van der Kooy, F., 2022. Validating a sensitive LCMS method for the quantitation of artemisinin in *Artemisia* spp. including material used in retracted clinical trials. J. Pharm. Biomed. Anal. 208, 114446 <https://doi.org/10.1016/j.jpba.2021.114446>.
- Lingscheid, T., Kurth, F., Clerinx, J., Marocco, S., Trevino, B., Schunk, M., 2017. Schistosomiasis in European travellers and migrants: analysis of 14 years TropNet surveillance data. Am. J. Trop. Med. Hyg. 97, 567 574 <https://doi.org/10.4269/ajtmh.17-0034>.
- Liu, N.Q., Van der Kooy, F., Verpoorte, R., 2009. *Artemisia afra*: a potential flagship for African medicinal plants? S. Afr. J. Bot. 75, 185 195. <https://doi.org/10.1016/j.sajb.2008.11.001>.
- Lombardo, F.C., Pasche, V., Panic, G., Endriss, Y., Keiser, J., 2019. Life cycle maintenance and drug-sensitivity assays for early drug discovery in *Schistosoma mansoni*. Nat. Protoc. 14, 461 481. <https://doi.org/10.1038/s41596-018-0101-y>.
- McManus, D.P., Dunne, D.W., Sacko, M., Utzinger, J., Vennervald, B.J., Zhou, X.N., 2018. Schistosomiasis. Nat. Rev. Dis. Primers 4, 13. <https://doi.org/10.1038/s41572-018-0013-8>.
- Meister, I., Ingram-Sieber, K., Cowan, N., Todd, M., Robertson, M.N., Meli, C., Patra, M., Gasser, G., Keiser, J., 2014. Activity of praziquantel enantiomers and main metabolites against *Schistosoma mansoni*. Antimicrob. Agents Chemother. 58, 5466 5472. <https://doi.org/10.1128/AAC.02741-14>.
- Mouton, J., Van der Kooy, F., 2014. Identification of cis- and trans- melilotoside within an *Artemisia annua* tea infusion. Eur. J. Med. Plants 4, 52 63. <https://doi.org/10.9734/EJMP/2014/6385>.
- Munyangi, J., Cornet-Vernet, L., Idumbo, M., Lu, C., Lutgen, P., Perronne, C., Weathers, P., 2018. Effect of *Artemisia annua* and *Artemisia afra* tea infusions on schistosomiasis in a large clinical trial. Phytomedicine 51, 233 240. <https://doi.org/10.1016/j.phymed.2018.10.014>.
- Munyangi, J., Cornet-Vernet, L., Idumbo, M., Lu, C., Lutgen, P., Perronne, C., Weathers, P., 2020. Retraction notice to Effect of *Artemisia annua* and *Artemisia afra* tea infusions on schistosomiasis in a large clinical trial. [PHYTOMEDICINE 51C (2018) 233 240]. Phytomedicine 78, 153303. <https://doi.org/10.1016/j.phymed.2020.153303>.
- Van der Kooy, F., Verpoorte, R., Meyer, J.J.M., 2008. Metabolomic quality control of claimed anti-malarial *Artemisia afra* herbal remedy and *A. afra* and *A. annua* plant extracts. S. Afr. J. Bot. 74, 186 189. <https://doi.org/10.1016/j.sajb.2007.10.004>.
- WHO (World Health Organization), 2019. World Health Organization Model List of Essential Medicine. <https://www.slideshare.net/NabinBist/world-health-organization-model-list-of-essential-medicines-21st-list-2019> (accessed 7 April 2020).
- WHO (World Health Organization), 2021. Fact sheets: Schistosomiasis. <https://www.who.int/news-room/fact-sheets/detail/schistosomiasis> (accessed 18 August 2021).
- Xiao, S., Chollet, J., Weiss, N.A., Bergquist, R.N., Tanner, M., 2000. Preventive effect of artemether in experimental animals infected with *Schistosoma mansoni*. Parasitol. Int. 49, 19 24. [https://doi.org/10.1016/s1383-5769\(00\)0028-3](https://doi.org/10.1016/s1383-5769(00)0028-3).
- Xiao, S., Sun, J., Chen, M., 2018. Pharmacological and immunological effects of praziquantel against *Schistosoma japonicum*: a scoping review of experimental studies. Infect. Dis. Poverty 7, 9. <https://doi.org/10.1186/s40249-018-0391-x>.

Efficacy, metabolism and pharmacokinetics of Ro 15-5458, a forgotten schistosomicidal 9-acridanone hydrazone

Alexandra Probst^{1,2}, Cécile Häberli^{1,2}, Dionicio Siegel³, Dave Huang³, Seth Vigneron³, Anh P. Ta³, Danielle E. Skinner³, Nelly El-Sakkary³, Jeremiah D. Momper³, Jon Gangoiti⁴, Yuxiang Dong⁵, Jonathan L. Vennerstrom⁵, Susan A. Charman⁶, Conor R. Caffrey³, Jennifer Keiser^{1,2,*}

¹ Department of Medical Parasitology and Infection Biology, Swiss Tropical and Public Health Institute, P.O. Box, CH-4002, Basel, Switzerland

² University of Basel, P.O. Box, CH-4003, Basel, Switzerland

³ Center for Discovery and Innovation in Parasitic Diseases, Skaggs School of Pharmacy and Pharmaceutical Sciences, University of California San Diego, 9500 Gilman Dr., La Jolla, CA 92093, the United States of America.

⁴ Biochemical Genetics and Metabolomics Laboratory, Department of Pediatrics, School of Medicine, University of California San Diego, 9500 Gilman Dr., La Jolla, CA 92093, the United States of America.

⁵ College of Pharmacy, University of Nebraska Medical Center, 986125 Nebraska Medical Center, Omaha, NE, the United States of America.

⁶ Centre for Drug Candidate Optimisation, Monash Institute of Pharmaceutical Sciences, Monash University, 381 Royal Parade, Parkville, Victoria 3052, Australia.

* Corresponding author: jennifer.keiser@swisstph.ch

Efficacy, metabolism and pharmacokinetics of Ro 15-5458, a forgotten schistosomicidal 9-acridanone hydrazone

Alexandra Probst^{1,2}, Cécile Häberli^{1,2}, Dionicio Siegel³, Jianbo Huang³, Seth Vigneron³, Anh P. Ta³, Danielle E. Skinner³, Nelly El-Sakkary³, Jeremiah D. Momper³, Jon Gangoiti⁴, Yuxiang Dong⁵, Jonathan L. Vennerstrom⁵, Susan A. Charman⁶, Conor R. Caffrey³ and Jennifer Keiser ^{1,2*}

¹Department of Medical Parasitology and Infection Biology, Swiss Tropical and Public Health Institute, PO Box, CH-4002, Basel, Switzerland; ²University of Basel, PO Box, CH-4003, Basel, Switzerland; ³Center for Discovery and Innovation in Parasitic Diseases, Skaggs School of Pharmacy and Pharmaceutical Sciences, University of California San Diego, 9500 Gilman Dr., La Jolla, CA 92093, USA; ⁴Biochemical Genetics and Metabolomics Laboratory, Department of Pediatrics, School of Medicine, University of California San Diego, 9500 Gilman Dr., La Jolla, CA 92093, USA; ⁵College of Pharmacy, University of Nebraska Medical Center, 986125 Nebraska Medical Center, Omaha, NE, USA; ⁶Centre for Drug Candidate Optimisation, Monash Institute of Pharmaceutical Sciences, Monash University, 381 Royal Parade, Parkville, Victoria 3052, Australia

*Corresponding author. E-mail: jennifer.keiser@swisstph.ch

Received 21 February 2020; returned 2 April 2020; revised 8 May 2020; accepted 10 May 2020

Background: Treatment of schistosomiasis, a neglected disease, relies on just one partially effective drug, praziquantel. We revisited the 9-acridanone hydrazone, Ro 15-5458, a largely forgotten antischistosomal lead compound.

Methods: Ro 15-5458 was evaluated in juvenile and adult *Schistosoma mansoni*-infected mice. We studied dose–response, hepatic shift and stage specificity. The metabolic stability of Ro 15-5458 was measured in the presence of human and mouse liver microsomes, and human hepatocytes; the latter also served to identify metabolites. Pharmacokinetic parameters were measured in naive mice. The efficacy of Ro 15-5458 was also assessed in *S. haematobium*-infected hamsters and *S. japonicum*-infected mice.

Results: Ro 15-5458 had single-dose ED₅₀ values of 15 and 5.3 mg/kg in mice harbouring juvenile and adult *S. mansoni* infections, respectively. An ED₅₀ value of 17 mg/kg was measured in *S. haematobium*-infected hamsters; however, the compound was inactive at up to 100 mg/kg in *S. japonicum*-infected mice. The drug-induced hepatic shift occurred between 48 and 66 h post treatment. A single oral dose of 50 mg/kg of Ro 15-5458 had high activity against all tested *S. mansoni* stages (1-, 7-, 14-, 21- and 49-day-old). *In vitro*, human hepatocytes produced *N*-desethyl and glucuronide metabolites; otherwise Ro 15-5458 was metabolically stable in the presence of microsomes or whole hepatocytes. The maximum plasma concentration was approximately 8.13 µg/mL 3 h after a 50 mg/kg oral dose and the half-life was approximately 4.9 h.

Conclusions: Ro 15-5458 has high activity against *S. mansoni* and *S. haematobium*, yet lacks activity against *S. japonicum*, which is striking. This will require further investigation, as a broad-spectrum antischistosomal drug is desirable.

Introduction

Schistosomiasis is a neglected tropical disease caused by blood-dwelling flatworms of the *Schistosoma* genus. Out of the six medically important species, *Schistosoma haematobium*, *Schistosoma japonicum* and *Schistosoma mansoni* account for the highest burden of disease.¹ Disabling morbidities such as anaemia, malnutrition and impaired child development, as well as increased susceptibility to co-infection with other parasitic diseases, pose

significant health problems.^{2–4} Control and treatment of schistosomiasis have been entirely dependent upon praziquantel for the past four decades. Although active against all medically important schistosomes, praziquantel is rarely curative, and has little to no effect on developing parasites. Further, its increasing use might trigger drug resistance.^{5,6} Thus, there is a need for new drugs.

In the 1980s, 9-acridanone hydrazones were investigated by Hoffmann La-Roche for the treatment of schistosomiasis. Ro 15-5458 was the lead candidate selected for further development.

Ro 15-5458 had ED₉₀ values below 100 mg/kg in mice and hamsters infected with *S. mansoni*, *S. haematobium* and *S. japonicum*.⁷ The excellent *in vivo* efficacy against *S. mansoni* was confirmed in baboons^{8,9} and Cebus monkeys.¹⁰ Although studies on the biochemical characterization and possible mode of action of Ro 15-5458 were carried out,^{11,12} considerable gaps in our understanding of this intriguing antischistosomal lead compound remain. In spite of its remarkable activity, Ro 15-5458 was not further investigated, probably because of the successful introduction of praziquantel as antischistosomal treatment in the market at that time. The aim of the present study was to further characterize and define the strengths and weaknesses of Ro 15-5458.

Materials and methods

Ethics

In vivo efficacy studies were carried out in accordance with Swiss national and cantonal regulations on animal welfare at the Swiss Tropical and Public Health Institute (Basel, Switzerland) under permission number 2070. At the University of California San Diego, use of hamsters was approved by the university's Institutional Animal Care and Use Committee. Pharmacokinetic (PK) studies were conducted at the Center for Drug Candidate Optimization, Monash University in accordance with the Australian Code of Practice for the Care and Use of Animals for Scientific Purposes. Study protocols were reviewed and approved by the Monash Institute of Pharmaceutical Sciences Animal Ethics Committee.

Vertebrate animals and parasites

For *in vivo* efficacy studies, female mice (NMRI strain; 3 weeks old; weight ~20–22 g) were purchased from Charles River, Germany. Golden Syrian LVG hamsters (Charles River, USA), exposed to 350 *S. haematobium* (Egyptian strain) cercariae and Swiss Webster mice (Taconic Inc, NY) exposed to 40 *S. japonicum* cercariae (Philippine strain) were ordered from the US NIH's Biomedical Research Institute (BRI). Rodents were kept under environmentally controlled conditions (temperature ~25°C; humidity ~70%; 12 h light, 12 h dark cycle) with free access to water and rodent diet, and acclimatized for 1 week before infection. Cercariae of *S. mansoni* (Liberian strain) were obtained from infected intermediate host snails (*Biomphalaria glabrata*) and mechanically transformed to newly transformed schistosomula (NTS) as described previously.¹³ Mice were infected by subcutaneously injecting approximately 100 *S. mansoni* cercariae.

For PK studies, the systemic exposure of Ro 15-5458 was studied in male Swiss outbred mice weighing 25.6–30.4 g. Mice had access to food and water *ad libitum* throughout the pre- and post-dose sampling period.

Ro 15-5458

Ro 15-5458 was synthesized as described (Material S1, available as [Supplementary data](#) at JAC Online).¹⁴ For *in vitro* assays, the compound was dissolved in DMSO (Sigma–Aldrich, Switzerland) at a concentration of 10 mM. For *in vivo* efficacy and PK studies, on the day of dosing, solid compound was dispersed in Tween-80 [7% (v/v) *nal*], after which ethanol [3% (v/v) *nal*] and Milli-Q water were added. The formulation was then vortexed and sonicated.

In vitro studies

Phenotypic screening of NTS and adult worms

For *S. mansoni* NTS and adults, and adult *S. japonicum* worms, transparent at-bottom 96- and 24-well plates were used, respectively (Sarstedt, Switzerland). Approximately 100 NTS per well were incubated in the

presence of 1.56–100 μM Ro 15-5458 in 250 μL of M199 medium (Gibco, USA) supplemented with 5% (v/v) FCS (Bioconcept AG, Switzerland), 1% (v/v) penicillin/streptomycin solution (Sigma–Aldrich, Switzerland) and 1% (v/v) antibacterial/antifungal¹³ solution for up to 72 h at 37°C and 5% CO₂. At least three adult worms (both sexes) were incubated with 10 and 100 μM Ro 15-5458 in 2 mL of RPMI 1640 (Gibco, USA) supplemented with 5% (v/v) FCS and 1% (v/v) penicillin/streptomycin for 72 h at 37°C and 5% CO₂.¹³

The activity of Ro 15-5458 on NTS and adults was judged by scoring the overall viability of the parasites.^{13,15} The possible influence of protein binding on activity was tested by supplementing the medium with 45 g/L BSA (AlbuMax II Lipid-Rich BSA, Gibco).¹⁶ Also, any long-term effect of Ro 15-5458 on adult worms was tested by incubating the worms at 10 and 100 μM for 48 h and, after extensive washing, continuing the incubation in medium only for a further 10 days.

The *ex vivo* assessment of viability of adult *S. mansoni* post exposure to Ro 15-5458 *in vivo* was also studied. After their perfusion from Ro 15-5458-treated mice, worms were washed and incubated in Basch medium¹⁷ supplemented with 5% FBS, 100 U/mL penicillin and 100 μg/mL streptomycin for up to 14 days.¹⁵ For all experiments, the highest concentration of DMSO served as a negative control. Experiments were conducted in duplicate and repeated at least once.

Metabolic stability of Ro 15-5458 incubated with mouse and human liver microsomes or human hepatocytes

The metabolic stability study of Ro 15-5458 in the presence of mouse and human liver microsomes (both obtained from Xenotech) was performed at Monash University. Ro 15-5458 was incubated at a final concentration of 1 μM at 37°C and a 0.4 mg/mL protein concentration. The metabolic reaction was initiated by the addition of an NADPH-regenerating system. Over a 60 min incubation period, the reaction was quenched at different time-points by adding acetonitrile containing diazepam as an internal standard followed by centrifugation to pellet the precipitated material (4500 g, 4 min, 21°C). Control samples (containing no NADPH) were included and quenched at 2, 30 and 60 min to monitor for potential degradation in the absence of the cofactor. The samples were analysed by LC-MS (Waters Xevo G2 QTOF instrument equipped with an Acquity UPLC system) under positive electrospray ionization, and MS data were acquired in the mass range of 80 to 1200 Da. The *in vitro* intrinsic clearance values (expressed as μL/min/mg protein) were calculated using the first-order degradation rate constant (h⁻¹) and the microsomal protein concentration (mg/μL). The metabolic stability of Ro 15-5458 in the presence of human hepatocytes was assessed by the contract research organization, WuXi AppTec (Shanghai, China), according to its standard protocols and under the auspices of the CDIPD-UCSD (Method S1).

Metabolite profiling following incubation of Ro 15-5458 with human hepatocytes in vitro

This study was performed by WuXi AppTec under the auspices of the CDIPD-UCSD. Cryopreserved human hepatocytes (In Vitro Technologies) were thawed and incubated for 120 min with 10 μM Ro 15-5458 in 200 μL of William's E medium containing 1 × 10⁶ cells/mL at 37°C, 5% CO₂. Samples were precipitated with a 2-fold volume of acetonitrile (containing 0.1% formic acid) and centrifuged at 3220 g for 20 min. The supernatant was removed and dried with N₂ gas at room temperature. The residue was reconstituted in 200 μL of 10% acetonitrile/0.1% formic acid and 15 μL was injected onto an Acquity UPLC HSS T3 column (1.8 μm, 2.1 × 100 mm) under the control of a Waters Xevo G2 QTOF MS system. MS/MS analyses were performed in positive electrospray ionization mode, and UPLC/MS^E was used as scan mode. The metabolites of Ro 15-5458 were detected and further characterized by LC-MSⁿ (*n* = 1–2). The metabolite structures were elucidated by comparative analysis of fragments between the parent and individual

metabolites. Samples were also monitored by UV absorbance for the purpose of estimating relative metabolite concentrations.

In vivo efficacy studies

S. mansoni

To investigate the dose–response relationship of Ro 15-5458, selected single doses (6.25, 12.5, 25, 50 and 100 mg/kg) were administered to groups of four *S. mansoni*-infected mice by oral gavage at 21 days (juvenile infection) or 49 days (adult infection) post infection. To determine the onset of action of Ro 15-5458 (hepatic shift), four mice infected with *S. mansoni* were treated with 17.5 mg/kg Ro 15-5458 on day 49 post infection. After 8, 24, 48 and 72 h, one mouse was euthanized and the worms in the mesenteric vein system were removed by picking.¹⁸ The livers were excised, placed between two transparent plastic layers and pressed (liver squash);¹³ worms were sexed and counted. A confirmation experiment with four mice was conducted in the same way, employing the post treatment timepoints of 60, 66, 78 and 85 h. To study whether the bioactivity of Ro 15-5458 was dependent on the development of the parasite, groups of four *S. mansoni*-infected mice were given single oral doses of 12.5 or 50 mg/kg Ro 15-5458 at days –2, 0, 1, 7, 14, 21, 28, 35, 42 and 49 post infection. Infected but untreated mice served as controls in all experiments.

S. haematobium and *S. japonicum*

To study the dose–response relationship of Ro 15-5458 in adult *S. haematobium* infections, groups of three to four hamsters were treated orally with single doses of 20 and 25 mg/kg, 6 months after infection. For *S. japonicum*, on day 35 post infection, 50 and 100 mg/kg Ro 15-5458 were administered to groups of four mice by oral gavage. Sixteen and 21 days after treatment, respectively, hamsters and mice were euthanized with CO₂. Worms were removed by picking, sexed and counted, and the worm burden reduction was calculated.¹⁹ Infected but untreated animals served as controls in all experiments.

In vivo PK studies in mice

Ro 15-5458 (50 mg/kg) was orally administered to non-fasted Swiss outbred mice ($n=6$) at a dose volume of 10 mL/kg. Blood samples were collected via submandibular bleeding (approximately 120 μ L; conscious sampling) at 1, 3, 7, 24, 30 and 48 h with three mice per timepoint and a maximum of three samples from each mouse. Blood was collected in polypropylene Eppendorf tubes containing heparin as an anticoagulant and a stabilization cocktail (Complete, Sigma-Aldrich) to minimize the potential for *ex vivo* compound degradation in blood/plasma samples. Once collected, blood samples were centrifuged (14 100 g) and the supernatant plasma was removed and stored at –80°C until analysis by LC-MS.

Samples were assayed against a 12-point calibration curve prepared in blank mouse plasma and processed together with the study samples. Samples and calibration standards were precipitated with a 2-fold volume of acetonitrile followed by vortex mixing and centrifugation (14 100 g, 3 min). The supernatant was separated and 2 μ L was injected onto the column [Phenomenex Kinetex PFP column (50 \times 2.1 mm, 2.6 μ m)] for LC-MS analysis. A Waters Xevo TQD coupled to a Waters Acquity UPLC with positive electrospray ionization in multiple-reaction monitoring mode was used for detection. A gradient cycle time of 4 min and a flow rate of 0.4 mL/min were employed. The mobile phase consisted of an acetonitrile/water gradient with 0.005 M ammonium formate. The plasma concentration versus time profile was defined by the average plasma concentration at each sample time.

Data analysis

The *in vitro* activity against NTS and adult *S. mansoni* was calculated in Microsoft Excel using the mean viability values (\pm SD) of Ro 15-5458 in relation to the control values. CompuSyn software (version 1.0; ComboSyn Inc., 2007) was used to calculate EC₅₀ values. The worm burden reduction (WBR) (*in vivo*) was determined based on the percentage of worm burden in infected, treated rodents compared with infected, untreated rodents, which served as controls,²⁰ and a Kruskal–Wallis test was employed for statistical significance in R (version 3.5.1). GraphPad Prism (Version 8.2.1) was used to calculate ED₅₀ values and to generate graphs. PK parameters were calculated using non-compartmental methods (PKSolver Version 2.0).

Results

In vitro activity of Ro 15-5458 against *S. mansoni* and *S. japonicum*

NTS exposed to 100 μ M Ro 15-5458 for 72 h died; however, lower concentrations were not lethal. An EC₅₀ of 33 μ M was calculated. Adult *S. mansoni* worms were exposed to 10 and 100 μ M Ro 15-5458 with and without the addition of albumin (45 g/L) for 72 h. EC₅₀ values of 85 and >100 μ M were calculated for worms incubated without and with albumin, respectively, suggesting a decrease in activity due to protein binding. An EC₅₀ of 65 μ M was obtained when performing a phenotypic readout on adult *S. japonicum* worms (without albumin). Results are summarized in Table 1.

When *S. mansoni* and *S. japonicum* were incubated for 48 h with 100 μ M Ro 15-5458, then washed, and left in medium alone, the worms died after an additional 7 days. At 10 μ M, the same experiment induced slowed motility and an inability of the worms to adhere to the plate over the remaining 10 days of the incubation.

Ro 15-5458 is stable when incubated with mouse and human microsomes, and human hepatocytes

In both test systems, the *in vitro* intrinsic clearance data suggested that the hepatic clearance of Ro 15-5458 is very low (Tables 2 and 3), according to commonly used classification bands to categorize compounds as low, medium or high clearance.

Table 1. *In vitro* results

Species, development stage	Concentration(s) tested (μ M)	Outcome
<i>S. mansoni</i> , NTS	1–100 μ M (6 dilutions)	EC ₅₀ =33 μ M
<i>S. mansoni</i> , adult worms	100, 10, 0 μ M	EC ₅₀ =85 μ M
<i>S. mansoni</i> , adult worms (+ albumin)	100, 10, 0 μ M	EC ₅₀ >100 μ M
<i>S. mansoni</i> , adult worms (long term)	100 μ M for 48 h, then medium only	Worms died after an additional 7 days of incubation in medium only.
<i>S. japonicum</i> , adult worms	100, 10, 0 μ M	EC ₅₀ =65 μ M

Identification of glucuronidated and de-ethylated metabolites produced by human hepatocytes *in vitro*

Metabolic profiling of Ro 15-5458 incubated with human hepatocytes identified two metabolites, a glucuronidated product (mol. wt = 569.67 Da, P + C₆H₈O₆) and a de-ethylated product, (mol. wt = 365.50 Da, P - C₂H₄) (Figure 1). The relative concentration of the metabolites was estimated based on the UV peak area relative to that of the parent peak (Figure S1). The de-ethylated metabolite accounted for approximately 6.6% of the total peak area, with the parent Ro 15-5458 accounting for approximately 90% of the total peak area (Table 4).

In vivo dose–response relationship against *S. mansoni*, *S. haematobium* and *S. japonicum*

Single oral doses of Ro 15-5458 were significantly effective in mice harbouring *S. mansoni* (juvenile, $P=0.0024$ for all doses tested; adult, $P=0.0016$ for all doses tested) and hamsters infected with *S. haematobium* ($P=0.0076$ for all doses tested) (Table 5). Against juvenile *S. mansoni*, of the five doses tested, the highest, 50 and 100 mg/kg, produced WBRs of 93.5% and 99%, respectively. Lower doses were ineffective. The ED₅₀ value was 15 mg/kg. Better activity was observed in animals harbouring adult parasites. Doses of 12.5 and 25 mg/kg resulted in total WBRs of 100% and 98.7%, respectively, with an ED₅₀ value of 5.3 mg/kg. For *S. haematobium*, doses of 20 and 25 mg/kg resulted in total WBRs of 68% and 87%, respectively. In contrast, in mice infected with adult *S. japonicum* Ro 15-5458 lacked activity after a dose of 50 mg/kg. In the 100 mg/kg treatment group ($n=4$), three mice died 4 h after treatment. In two subsequent experiments at the same dose, low efficacy was observed, but without the previously noted toxicity.

Table 2. Metabolic stability in mouse and human microsomes

Microsome species	$t_{1/2}$ (min) ^a	CL _{int, in vitro} (μL/min/mg protein) ^b	Clearance classification
Human	>255	<7	low
Mouse	>255	<7	low

^a $t_{1/2}$ (degradation half-life)= $\ln 2/k$.

^bCL_{int} = CL_{int, in vitro} × liver mass (g)/body weight (kg) × microsomal protein mass (mg)/liver mass (g).

Table 3. Metabolic stability in human hepatocytes

Compound ID	Cell density (×10 ⁶ cells/mL)	Human hepatocytes		
		k_e ^a	$t_{1/2}$ (min)	<i>in vitro</i> CL _{int} (μL/min/10 ⁶ cells)
Ro 15-5458	0.5	0.0076	91.2	15.2
7-Ethoxycoumarin ^b		0.0229	30.3	45.7
7-Hydroxycoumarin ^c		0.0372	18.6	74.4

^a k_e is the elimination rate constant.

^b7-Ethoxycoumarin is a cytochrome P450 substrate.

^c7-Hydroxycoumarin is a metabolite standard (the enzymatic product of 7-ethoxycoumarin).

Hepatic shift (*S. mansoni*)

The onset of the efficacy of Ro 15-5458, indicated by a shift in the distribution of worms from the mesenteric veins to the liver, is illustrated in Figure 2. In the first experiment, Ro 15-5458 acted slowly; at 8, 24, 48 h after a 17.5 mg/kg dose, all worms were still present in the mesenteric veins. By 72 h, the worm count in the mesenteric veins had decreased by 80% relative to non-treated controls. In the second experiment using the same dose, no worms had shifted to the liver 60 h after treatment. By 66 h, only a few worms had shifted to the liver (dead), while most of the worms were still

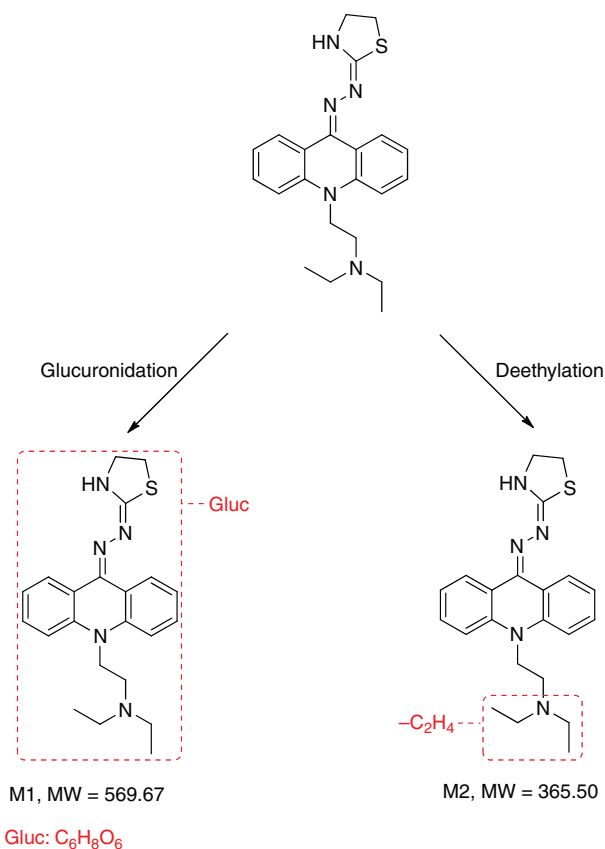


Figure 1. Metabolic products of Ro 15-5458 after incubation with human hepatocytes *in vitro*. This figure appears in colour in the online version of JAC and in black and white in the printed version of JAC.

Table 4. Metabolites of Ro 15-5458 in human hepatocytes

Metabolite code	[M + H] ⁺ m/z	LC-MS retention time (min)	Relative abundance (UV peak area) ^a	Metabolic pathway
M1	570.24	7.38	2.87%	glucuronidation, (P + C ₆ H ₈ O ₆)
M2	366.17	10.38	6.63%	de-ethylation, (P - C ₂ H ₄)
Parent (Ro-15-5458)	394.21	10.99	90.50%	NA

NA, not applicable.

^aSemi-quantitative data calculated by UV peak areas of the metabolites and parent in samples under UV wavelength at 254–460 nm.

Table 5. Dose–response relationships of Ro 15-5458 against various species and developmental stages of the schistosome parasite

Stage (age of infection)	Dose (mg/kg)	No. of animals used	No. of animals cured	Mean number of worms (SD)					total WBR % (SD)	P value (Kruskal–Wallis)
				liver	MV	total	males	females		
<i>S. mansoni</i> juvenile (21 days old)	control 1	8	–	0.6 (1.4)	33.8 (9.1)	34.4 (9.9)	17.4 (5.0)	17.0 (5.1)	–	–
	control 2 ^c	4	–	NA	NA	43.6 (5.3)	21.8 (5.3)	21.8 (5.3)	–	–
	6.25	4	0	1.3 (1.5)	18.0 (2.9)	19.3 (3.3)	10.8 (2.1)	8.5 (1.9)	44.0 (9.6)	0.002
	12.5	4	0	0.0 (0.0)	19.3 (5.6)	19.3 (5.6)	9.8 (2.6)	9.5 (3.0)	44.0 (16.4)	
	25	4 ^a	0	2.7 (2.1)	26.3 (10.0)	29.0 (10.8)	17.0 (5.0)	12.0 (6.1)	19.2 (27.4)	
	50	4	2	1.0 (1.4)	1.3 (1.9)	2.3 (2.6)	0.5 (1.0)	1.8 (2.1)	93.5 (7.7)	
<i>S. mansoni</i> adult (49 days old)	100 ^c	4	2	NA	NA	0.5 (0.6)	0.5 (0.6)	0.0 (0.0)	99.0 (0.5)	0.02
	control	8	–	0.0 (0.0)	19.9 (8.1)	19.9 (8.1)	10.0 (4.1)	9.9 (4.1)	–	–
	6.25	4	0	3.0 (2.2)	10.0 (10.7)	13.0 (9.7)	5.8 (3.8)	7.3 (6.0)	43.6 (32.0)	0.002
	12.5	4	4	0.0 (0.0)	0.0 (0.0)	0.0 (0.0)	0.0 (0.0)	0.0 (0.0)	100.0 (0.0)	
	25	4	4	0.0 (0.0)	0.3 (0.5)	0.3 (0.5)	0.0 (0.0)	0.3 (0.5)	98.7 (2.5)	
<i>S. haematobium</i> adult (6 months old)	control	4	–	4.0 (3.3)	36.0 (13.0)	18.5 (8.3)	21.5 (5.8)	18.5 (8.3)	–	–
	20	4	1	0.5 (1.0)	12.3 (10.2)	12.8 (10.2)	6.5 (5.3)	6.3 (4.9)	68.1 (25.6)	0.025
<i>S. japonicum</i> adult (35 days old)	25	3	2	0.0 (0.0)	5.3 (9.3)	5.3 (9.3)	2.7 (4.6)	2.7 (4.6)	86.7 (23.1)	
	control	6	–	0.3 (0.8)	17.5 (7.1)	17.8 (6.6)	8.8 (3.1)	9.0 (3.9)	–	–
	control ^d	4	–	4.0 (4.3)	25.5 (10.0)	29.5 (13.4)	14.8 (6.7)	14.8 (6.7)	–	–
	control ^e	4 ^a	–	0.0 (0.0)	18.0 (6.9)	18.0 (6.9)	9.0 (3.5)	9.0 (3.5)	–	–
	50	4	0	4.8 (1.0)	21.0 (7.0)	25.8 (7.8)	12.5 (3.4)	13.3 (4.6)	0.0 (0.0)	>0.05
	100	4 ^b	0	NA	NA	NA	NA	NA	NA	NA
	100 ^d	5	0	2.2 (3.4)	14.6 (11.0)	16.8 (13.8)	8.6 (7.0)	8.2 (6.8)	43.0 (46.9)	>0.05
	100 ^e	5	0	3.5 (1.9)	11.8 (4.2)	15.3 (5.9)	7.8 (3.0)	7.5 (2.9)	20.8 (25.0)	>0.05

MV, mesenteric veins; NA, not applicable. Total WBR (%) = 100% – 100% × (WB_{treated animals}/WB_{control animals}), whereby negative WBR values were set to zero before averaging.

A P value of ≤0.05 was considered as significant.

^aOne mouse was not infected and was excluded from the analysis.

^bThree mice died 4 h after treatment; the last mouse was sacrificed at the same timepoint because of poor general condition.

^cExperiment was performed at the CDIPD-UCSD; worms were recovered by reverse perfusion of the hepatic portal and mesenteric veins.

^dSecond experiment, new animal batch used.

^eThird experiment, new animal batch used.

in the mesenteric veins (alive). The worm numbers in the mesenteric veins had decreased by 44% and 76% relative to non-treated controls 78 and 85 h after treatment.

Effect of Ro 15-5458 on *S. mansoni* adults *ex vivo*

Mice infected with 42-day-old adult *S. mansoni* were administered a single oral dose of 15 mg/kg Ro 15-5458. After 22 h, and before

the hepatic shift had commenced, worms were recovered and incubated *in vitro*, as described.¹⁵ From the ninth day onwards, exposed adult male worms displayed a progressively more intense corkscrew-like coiling along the long axis (Video S1) relative to non-treated controls (Video S2). Also, both the oral and ventral sucker, and the intervening neck region became withered and rigid (Figure S2) in contrast to non-treated controls (Figure S3).

Stage specificity of single oral 12.5 and 50 mg/kg Ro 15-5458 in mice infected with *S. mansoni*

Doses of 50 and 12.5 mg/kg Ro 15-5458 were tested to understand the compound's efficacy against the parasite residing in the skin (day 1), lungs (day 7) and in the mesenteric system as juveniles (days 14 and 21) and adults (day 49) (Figure 3). At 50 mg/kg, all developmental stages of *S. mansoni* were affected. High total WBRs of 82%, 100%, 92%, 94% and 99% were observed for treatments occurring on days 1, 7, 14, 21 and 49 post infection. Lower efficacy was measured when 12.5 mg/kg was administered. Nevertheless, statistically significant worm burden reductions for

all development stages were recorded for treatment doses of 12.5 mg/kg ($P=0.019$) and 50 mg/kg ($P<0.001$) when compared with untreated control animals.

PK in mice

Following oral administration of Ro 15-5458 (50 mg/kg) to male Swiss outbred mice, high plasma concentrations were detectable at the first sampling timepoint (1 h) post-dose, indicating rapid absorption (Figure 4). The maximum plasma concentration (C_{max}) of 20.66 μM (8.13 $\mu\text{g}/\text{mL}$) was measured at 3 h post-dose (t_{max}) and the apparent elimination half-life was approximately 5 h. The area under the plasma concentration–time curve (AUC_{0-48h}) was approximately 254 $\mu\text{M}\cdot\text{h}$ (100 $\mu\text{g}\cdot\text{h}/\text{mL}$) and the clearance (CL/F) was 8.3 mL/min/kg (Table 6). Additionally, to determine the extent of protein binding, an experiment using mouse plasma was performed (Method S2). The unbound fraction (f_u) was low and had a value of 0.021 ± 0.001 , which correlates well with the observed clearance *in vivo*.²¹

Discussion

Praziquantel is globally employed in preventive chemotherapy campaigns to millions of people each year.²² A recent review⁵

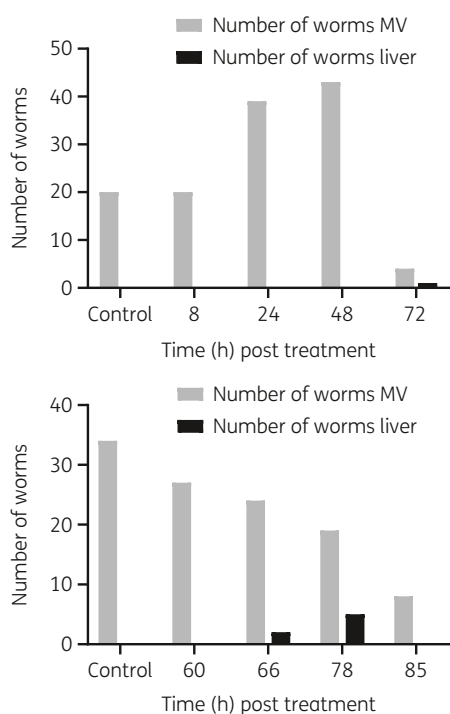


Figure 2. Hepatic shift of *S. mansoni* in mice 49 days after treatment with 17.5 mg/kg Ro 15-5458. Numbers of worms alive in the mesenteric veins (MV) and number of dead worms in the liver are shown from two individual experiments. Each bar shows the number of worms found in one mouse.

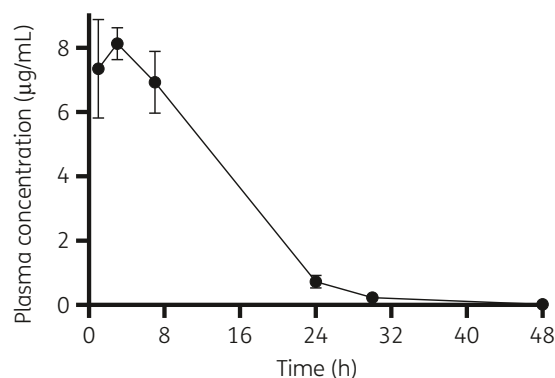


Figure 4. Plasma concentration–time curve of Ro 15-5458 in male Swiss outbred mice following oral administration of 50 mg/kg. Means and SD from three mice are shown.

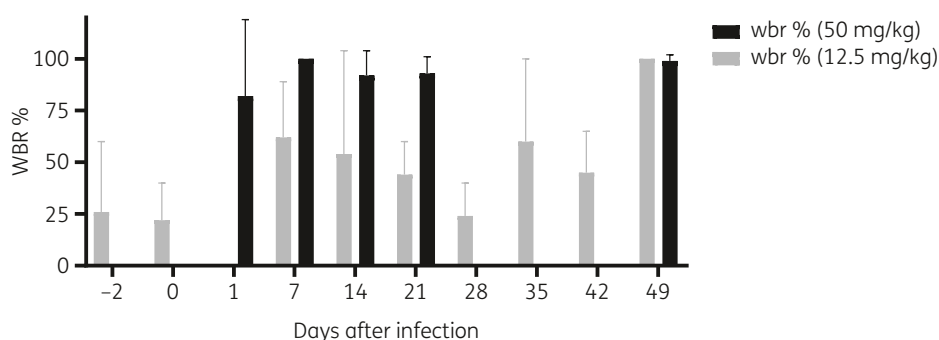


Figure 3. Stage-specific efficacy of Ro 15-5458 in *S. mansoni*-infected mice. Mice ($n=4$) were treated once orally with 12.5 mg/kg Ro 15-5458 on days –2, 0, 7, 14, 21, 28, 35, 42 and 49, and with 50 mg/kg on days 1, 7, 14, 21 and 49 post infection. Treatment on days 21 and 49 post infection was performed in the course of the dose–response study. For the *S. mansoni*-infected mice group treated on day 49 post infection, 25 mg/kg instead of 50 mg/kg served as the highest dose. Acquired data were integrated in the stage specificity study for the statistical analysis and generation of the displayed figure. Average worm burden reductions (WBRs %) were calculated 21–49 days post treatment (means and SD are presented).

Table 6. PK parameters in non-infected mice

PO dose	C _{max} (μM/μg/mL)	t _{max} (h)	AUC (μM·h/μg·h/mL)	t _{1/2} (h)	CL/F (mL/min/kg)
50 mg/kg (n=6)	20.66/8.13	3	254/100	4.9	8.3

Data presented are based on the mean concentration versus time data.

Experiments were performed at Monash University; mice were not fasted prior to drug administration.

stated the pressing need for new treatment options, but lamented the fact that none seemed to be on the horizon. It is against this background that we re-examined the *in vivo* efficacy of the largely forgotten Ro 15-5458, which was discovered in the early 1980s.⁷ 9-Acridanone hydrazones were reported to be active in rodents infected with *S. mansoni*,^{23–25} *S. haematobium*²⁶ and *S. japonicum*.⁷ Three doses of Ro 15-5458 (10, 15 and 20 mg/kg) were tested in a mouse model of chronic *S. mansoni* infection and each was effective (WBR >83.6%).²⁷ Subsequently, Ro 15-5458 was evaluated in primates, revealing high efficacy with no apparent toxicity.^{9,10,24,28,29} Baboons were cured of *S. mansoni* infections when treated with 50 and 25 mg/kg, whereas 12.5 mg/kg led to a WBR of 35%.^{8,9} In Cebus monkeys, doses of 50, 25 and 12.5 mg/kg cured infection.¹⁰ In contrast, higher and multiple doses of praziquantel were required to achieve cure in infected primates. For example, in *S. japonicum*-infected Vervet monkeys, cure was only obtained with five daily doses of 50 mg/kg praziquantel.³⁰

Here, we confirmed the high efficacy of Ro 15-5458 against *S. mansoni* in the mouse model. Adult *S. mansoni* infections were more susceptible to Ro 15-5458 than juvenile worm infections, with respective ED₅₀ values of 5.3 mg/kg and 15 mg/kg. Nevertheless, Ro 15-5458 had significant activity against immature parasites: high WBRs of 80%–100% were obtained when infected mice were treated with 50 mg/kg on days 1, 7, 14 and 21 after infection. Thus, in contrast to the well-established variable efficacy of praziquantel,^{31,32} Ro 15-5458 is active throughout the parasite's development.

We also confirmed activity in *S. haematobium*-infected hamsters and determined an ED₅₀ value of 17 mg/kg. We expected Ro 15-5458 to act in a similar manner in *S. japonicum*-infected mice. However, at doses up to 100 mg/kg, no significant WBRs were noted. Higher doses could not be tested as toxicity was observed. These findings are contrary to published results which showed significant efficacy.⁷ It is possible that different strains of *S. japonicum* are variously susceptible to treatment. Moreover, of the three medically important schistosomes studied here, *S. japonicum* infections are the most pathogenic³³ and this might have exacerbated any underlying toxicity of Ro 15-5458.

The *in vitro* data for *S. mansoni* NTS and adults, and *S. japonicum* adult worms indicate that Ro 15-5458 is a slow-acting compound and that high concentrations are necessary for worm death. Worms collected from mice after a single oral dose of 15 mg/kg Ro 15-5458 demonstrated a progressive corkscrew phenotype with withered suckers and neck region, which *in vivo* would conceivably hinder the parasite's ability to maintain its position in the mesenteric system as well as feed on host blood. The low levels of metabolism observed with both microsomes and hepatocytes, and the low clearance after oral

administration, do not support a role for active metabolites in the mode of action of Ro 15-5458.

We investigated the hepatic shift caused by Ro 15-5458 by dissecting *S. mansoni*-infected mice at different timepoints after treatment. The shift only became apparent at the 66 h timepoint and was notable for the loss of worms from the mesenteric system. The slowness of onset of the liver shift induced by Ro 15-5458 contrasts markedly with that for praziquantel which occurs 30 min after drug treatment.³⁴

We conclude that Ro 15-5458 has excellent antischistosomal properties against all development stages of *S. mansoni* and a favourable PK profile that supports single oral dosing. The lack of activity against *S. japonicum* identified here requires further investigation, given that a broad-spectrum antischistosomal drug is desirable.

Acknowledgements

We are grateful to the Swiss National Science Foundation and the U.S. National Institutes of Health for financial support. *Schistosoma japonicum*- (Philippine isolate) infected Swiss Webster mice and *Schistosoma haematobium*- (Egyptian isolate) infected LVG hamsters were provided by the NIAID Schistosomiasis Resource Center and distributed through BEI Resources under the NIH-NIAID Contracts HHSN272201700014I and HHSN27220100005I, respectively. The *S. mansoni* life cycle at the CDIPD was supported in part by snails and/or hamsters provided by the NIAID Schistosomiasis Resource Center that were distributed through BEI Resources under the NIH-NIAID Contract HHSN272201700014I.

Funding

This research was supported by the Swiss National Science Foundation (320030_175585/1) and the U.S. National Institutes of Health (NIH; AI116723-01). Research at the CDIPD was funded in part by R21AI126296 and OPP1171488 from the NIH and the Bill and Melinda Gates Foundation, respectively. Anh P. Ta was a 2017–2018 recipient of a UC San Diego Skaggs School of Pharmacy and Pharmaceutical Sciences post-sophomore year training program fellowship.

Transparency declarations

None to declare.

Supplementary data

Material S1, Methods S1 and S2, Figures S1, S2 and S3 and Videos S1 and S2 are available as [Supplementary data](#) at JAC Online.

References

- 1 Gryseels B, Polman K, Clerinx J et al. Human schistosomiasis. *Lancet* 2006; **368**: 1106–18.
- 2 Colley DG, Bustinduy AL, Secor WE et al. Human schistosomiasis. *Lancet* 2014; **383**: 2253–64.
- 3 King CH, Dangereld-Char M. The unacknowledged impact of chronic schistosomiasis. *Chronic Illn* 2008; **4**: 65–79.
- 4 Hotez PJ, Brindley PJ, Bethony JM et al. Helminth infections: the great neglected tropical diseases. *J Clin Invest* 2008; **118**: 1311–21.
- 5 Bergquist R, Utzinger J, Keiser J. Controlling schistosomiasis with praziquantel: how much longer without a viable alternative? *Infect Dis Poverty* 2017; **6**: 74.
- 6 Caffrey CR. Chemotherapy of schistosomiasis: present and future. *Curr Opin Chem Biol* 2007; **11**: 433–9.
- 7 Stohler HR, Montavon M. 9-Acridanone-hydrazones, a novel class of broad spectrum schistosomicidal agents. *XI International Congress for Tropical Medicine and Malaria* 1984. Calgary, p. 148.
- 8 Sturrock RF, Otieno M, James ER et al. A note on the efficacy of a new class of compounds, 9-acridanone-hydrazones, against *Schistosoma mansoni* in a primate—the baboon. *Trans R Soc Trop Med Hyg* 1985; **79**: 129–31.
- 9 Sturrock RF, Bain J, Webbe G et al. Parasitological evaluation of curative and subcurative doses of 9-acridanone-hydrazone drugs against *Schistosoma mansoni* in baboons, and observations on changes in serum levels of anti-egg antibodies detected by ELISA. *Trans R Soc Trop Med Hyg* 1987; **81**: 188–92.
- 10 Coelho PM, Pereira LH. *Schistosoma mansoni*: preclinical studies with 9-acridanone-hydrazones in *Cebus* monkeys experimentally infected. *Rev Inst Med Trop S Paulo* 1991; **33**: 50–7.
- 11 Eshete F, Bennett JL. *Schistosoma mansoni*: biochemical characteristics of the antischistosomal effects of Ro 15-5458. *Exp Parasitol* 1990; **71**: 69–80.
- 12 Eshete F, Bennett JL. The schistosomicidal compound Ro 15-5458 causes a reduction in the RNA content of *Schistosoma mansoni*. *Mol Biochem Parasitol* 1991; **45**: 1–8.
- 13 Lombardo FC, Pasche V, Panic G et al. Life cycle maintenance and drug-sensitivity assays for early drug discovery in *Schistosoma mansoni*. *Nat Protoc* 2019; **14**: 461–81.
- 14 Brombacher U, Link H, Montavon M. Schistosomicidal acridanone hydrazones. United States Patent 4,711,889/1986.
- 15 Abdulla M-H, Ruelas DS, Wolff B et al. Drug discovery for schistosomiasis: hit and lead compounds identified in a library of known drugs by medium-throughput phenotypic screening. *PLoS Negl Trop Dis* 2009; **3**: e478.
- 16 Pasche V, Laleu B, Keiser J. Early antischistosomal leads identified from *in vitro* and *in vivo* screening of the Medicines for Malaria Venture Pathogen Box. *ACS Infect Dis* 2018; **5**: 102–10.
- 17 Basch PF. Cultivation of *Schistosoma mansoni* *in vitro*. I. Establishment of cultures from cercariae and development until pairing. *J Parasitol* 1981; **67**: 179–85.
- 18 Keiser J, Panic G, Vargas M et al. Aryl hydantoin Ro 13-3978, a broad-spectrum antischistosomal. *J Antimicrob Chemother* 2015; **70**: 1788–97.
- 19 Xiao S-H, Keiser J, Chollet J et al. *In vitro* and *in vivo* activities of synthetic trioxolanes against major human schistosome species. *Antimicrob Agents Chemother* 2007; **51**: 1440–5.
- 20 Panic G, Vargas M, Scandale I et al. Activity profile of an FDA-approved compound library against *Schistosoma mansoni*. *PLoS Negl Trop Dis* 2015; **9**: e0003962.
- 21 Smith DA, Di L, Kerns EH. The effect of plasma protein binding on *in vivo* efficacy: misconceptions in drug discovery. *Nat Rev Drug Discov* 2010; **9**: 929–39.
- 22 WHO. Crossing the billion. Lymphatic filariasis, onchocerciasis, schistosomiasis, soil-transmitted helminthiasis and trachoma: preventive chemotherapy for neglected tropical diseases. 2017.
- 23 Kamel G, Metwally A, Guirguis F et al. Effect of a combination of the new antischistosomal drug Ro 15-5458 and praziquantel on different strains of *Schistosoma mansoni* infected mice. *Arzneimittelforschung* 2000; **50**: 391–4.
- 24 Pereira LH, Coelho PM, Costa JO et al. Activity of 9-acridanone-hydrazone drugs detected at the pre-postural phase, in the experimental schistosomiasis *mansoni*. *Mem Inst Oswaldo Cruz* 1995; **90**: 425–8.
- 25 Rawi S, Youssef OA, Metwally A et al. Parasitological evaluation of Ro 15-9268, a 9-acridanone-hydrazone derivative against *Schistosoma mansoni* in mice, and observations on changes in serum enzyme levels. *Parasitol Res* 2014; **113**: 437–46.
- 26 Guirguis FR. Efficacy of praziquantel and Ro 15-5458, a 9-acridanone-hydrazone derivative, against *Schistosoma haematobium*. *Arzneimittelforschung* 2003; **53**: 57–61.
- 27 Metwally A, Abdel Hadi A, Mikhail EG et al. Study of the efficacy of the new antischistosomal drug 10-[2-(diethylamino)ethyl]-9-acridanone-(thiazolidin-2-ylidene) hydrazone against an Egyptian strain of *S. mansoni* in mice. *Arzneimittelforschung* 1997; **47**: 975–9.
- 28 Coelho PM, Pereira LH, de Mello RT. Antischistosomal activity of acridanone-hydrazones in *Cebus* monkeys experimentally infected with the SJ strain of *Schistosoma mansoni*. *Rev Soc Bras Med Trop* 1995; **28**: 179–83.
- 29 Sulaiman SM, Ali HM, Homeida MM et al. Efficacy of a new Hoffmann-La Roche compound (Ro 15-5458) against *Schistosoma mansoni* (Gezira strain, Sudan) in vervet monkeys (*Cercopithecus aethiops*). *Trop Med Parasitol* 1989; **40**: 335–6.
- 30 James C, Webbe G, Nelson G. Susceptibility to praziquantel of *Schistosoma haematobium* in baboon (*Papio anubis*) and of *Schistosoma japonicum* in vervet monkey (*Cercopithecus aethiops*). *Z Parasitenkd* 1977; **52**: 179–94.
- 31 Xiao SH, Catto BA, Webster LT Jr. Effects of praziquantel on different developmental stages of *Schistosoma mansoni* *in vitro* and *in vivo*. *J Infect Dis* 1985; **151**: 1130–7.
- 32 Pica-Mattoccia L, Cioli D. Sex- and stage-related sensitivity of *Schistosoma mansoni* to *in vivo* and *in vitro* praziquantel treatment. *Int J Parasitol* 2004; **34**: 527–33.
- 33 Cheever AW. A review: *Schistosoma japonicum*: the pathology of experimental infection. *Exp Parasitol* 1985; **59**: 1–11.
- 34 Meister I, Ingram-Sieber K, Cowan N et al. Activity of praziquantel enantiomers and main metabolites against *Schistosoma mansoni*. *Antimicrob Agents Chemother* 2014; **58**: 5466–72.

CHAPTER VII: PRAZIQUANTEL PHARMACOKINETICS IN *O.FELINEUS*
INFECTED PATIENTS

**Pharmacokinetics of ascending doses of praziquantel in adults infected with
Opisthorchis felineus in Western Siberia, Russian Federation**

Alexandra Probst,^{a,b} Daniela Hofmann,^{a,b} Olga S. Federova,^c Sofia V. Mazeina,^c Tatiana S.
Sokolova,^c Ekatarina Golovach,^c Jennifer Keiser,^{a,b}

^a Swiss Tropical and Public Health Institute, Allschwil, Switzerland



^b University of Basel, P.O. Box CH-4003, Basel, Switzerland

^c Siberian State Medical University, 634050, Tomsk, Russian Federation

*Corresponding author: jennifer.keiser@swisstph.ch



Pharmacokinetics of Ascending Doses of Praziquantel in Adults Infected with *Opisthorchis felineus* in Western Siberia, Russian Federation

Alexandra Probst,^{a,b} Daniela Hofmann,^{a,b} Olga S. Fedorova,^c Sofia V. Mazeina,^c  Tatiana S. Sokolova,^c Ekaterina Golovach,^c  Jennifer Keiser^{a,b}

^aSwiss Tropical and Public Health Institute, Allschwil, Switzerland

^bUniversity of Basel, Basel, Switzerland

^cSiberian State Medical University, Tomsk, Russia

ABSTRACT Opisthorchiasis due to the liver fluke *Opisthorchis felineus* is highly prevalent in rural regions of Western Siberia, causing severe liver and bile duct maladies. Praziquantel administered as a three-dose regimen is the only drug used to treat *O. felineus*-infected individuals. A simpler single-dose treatment might serve as an alternative. The aim of this study was to compare the pharmacokinetic (PK) properties of single, ascending doses of praziquantel compared to multiple dosing in patients infected with *O. felineus* to contribute to updated treatment guidelines. Dried blood spots (DBSs) of 110 adults were collected at 11 time points post-drug administration at single oral doses of 20, 40, and 60 mg/kg, as well as 3 × 20 mg/kg (4 h dosing interval). DBS samples were analyzed using a validated liquid chromatography-tandem mass spectrometry (LC-MS/MS) method, and PK parameters were obtained for *R*-, *S*-, and *R-trans*-4-OH-praziquantel employing noncompartmental analysis. We observed the highest drug exposure for all analytes when the triple-dose scheme was used; area under the concentration-time curve from 0 to 24 h (AUC_{0–24}) values of 8.04, 27.75, and 36.38 μg/mL·h were obtained, respectively. Maximal plasma concentrations (C_{max}) values of 1.72, 4.89, and 2.69 μg/mL were calculated for *R*-, *S*-, and *R-trans*-4-OH-praziquantel, respectively, when patients were given a single 60-mg/kg dose, and they peaked at 1.5 and 2 h for the enantiomers and at 3 h for the metabolite. The herein-generated PK data, together with results that will be obtained from the integrated efficacy study, lay the groundwork for a possibly optimized treatment scheme for *O. felineus*-infected patients.

KEYWORDS praziquantel, pharmacokinetics, *Opisthorchis felineus*, dried blood spots, anthelmintic, LC-MS/MS, opisthorchiasis

Opisthorchiasis is a major foodborne trematodiasis, which, upon dietary consumption of raw or undercooked fish infested with metacercariae of the liver fluke *Opisthorchis felineus*, affects the hepatobiliary system of humans (1). The prevalence is especially high in rural areas of Western Siberia (i.e., in the Russian Federation, Siberia, Ukraine, and Kazakhstan), where it is estimated that 12.5 million individuals are at risk of infection with *O. felineus*, of which 1.6 million are infected (2–4). Due to growing tourist activity and migration, it has been shown that the number of infected humans has increased and spread to new areas outside Western Siberia (5). Humans infected with *O. felineus* may present with mild or severe symptoms. Left untreated, opisthorchiasis can lead to severe hepatobiliary morbidities such as acute or chronic cholangitis, pancreatitis, cholecystitis, hepatic abscesses, and obstruction of the bile ducts (1). Of concern is the carcinogenic potential of *O. felineus*; evidence of a risk of acquiring cholangiocarcinoma (CCA) has been reported (5–7). In the Russian Federation, praziquantel is the only drug that is officially registered for the treatment of opisthorchiasis.

Copyright © 2022 American Society for Microbiology. All Rights Reserved.

Address correspondence to Jennifer Keiser, jennifer.keiser@swisstph.ch.

The authors declare no conflict of interest.

Received 13 April 2022

Returned for modification 20 May 2022

Accepted 16 August 2022

Published 12 September 2022

TABLE 1 Participant characteristics for subjects recruited in the Russian Federation^a

Characteristic	Data for patients given praziquantel dose (mg/kg) of:				Total
	20	40	60	3 × 20	
No. of participants	28	26	28	28	110
Female (no. [%])	71	85	78	82	78
Age (yrs)	49 (39, 58)	49 (40, 59)	42 (36, 52)	54 (47, 58)	49 (41, 57)
Ht (cm)	164 (158, 172)	166 (158, 172)	164 (157, 170)	165 (160, 171)	164 (158, 172)
Wt (kg)	75 (66, 84)	70 (62, 89)	70 (65, 87)	80 (74, 90)	76 (65, 87)
BMI	27 (24, 32)	25 (23, 35)	28 (24, 30)	30 (26, 34)	28 (24, 32)

^aResults are shown as medians with first and third quartiles in parentheses unless indicated otherwise.

According to clinical guidelines, different doses of praziquantel are suggested for the treatment of the infection with *O. felineus*. The detailed treatment scheme is divided into 3 stages, employing pretreatment, anthelmintic therapy (praziquantel), and rehabilitation; the whole cycle takes about 3 months to be accomplished. For adults, praziquantel treatment options are 50, 60, and 75 mg/kg, divided into 3 intakes with dose intervals of 4 to 6 h (8).

Praziquantel is available as a racemic mixture (*R* and *S* enantiomer) and is metabolized via the cytochrome P450 system to the main metabolite *R-trans-4-OH-praziquantel* (9). Recently, the activity of both the enantiomer, as well as the main metabolite, was studied *in vitro*, and it was shown that *R-praziquantel* exhibited the highest activity in both juvenile and adult worms of *O. felineus* (10). There are 17 metabolites of praziquantel that were identified using different *in vitro* and *in vivo* techniques, as summarized by Zdesenko and Mutapi in a recent review (9). Of these, eight are distinguishable mono-oxidized metabolites, two are dehydrogenated mono-oxidized metabolites, three are di-oxidized metabolites, and four are glucuronide metabolites. The metabolic pathway of praziquantel to its main metabolite, 4-OH-praziquantel, was described by Nleya and colleagues (11), further highlighting the favorable formation of *trans-4-OH-praziquantel* to the *cis-4-OH-praziquantel* isomer. However, it is not known what drug component (enantiomer[s] or metabolite[s]) is driving the efficacy of praziquantel in *O. felineus*-infected patients.

Metabolism and pharmacokinetic (PK) data of praziquantel are available in the context of schistosomiasis treatment, with a recent review presenting the variable drug exposure in humans and animal models (9). Other PK studies have been conducted in healthy volunteers and *Opisthorchis viverrini*-infected individuals from Lao PDR, respectively (12–14). However, to date, not a single PK study was conducted in *O. felineus*-infected individuals. These data would yield important information about optimized, simpler dosing strategies.

In the framework of a randomized, controlled, single-blinded dose-finding trial in Tomsk, Siberia, we conducted a PK study using dried blood spot (DBS) sampling with the aim of elucidating the PK parameters of praziquantel in *O. felineus*-infected adults in the different treatment groups. We analyzed the kinetic disposition of both praziquantel enantiomers and its main metabolite, *R-trans-4-OH-praziquantel*, using noncompartmental analysis (NCA).

RESULTS

Participants' characteristics are summarized in Table 1. All participants were adults (78% female), aged 27 to 65, with a median body mass index (BMI) of 28. A total of 1,210 DBS samples were analyzed from 110 adults infected with *O. felineus*. Four hundred seventy-five measurements were under the lower limit of quantification (LLOQ) for *R-praziquantel* (39.3%), 258 were under the LLOQ for *S-praziquantel* (21.3%), and 112 were under the LLOQ for *R-trans-4-OH-praziquantel* (9.3%). Of the DBS samples, 0.7% were randomly chosen for incurred sample reanalysis. For *R-praziquantel*, 83% deviated less than 20% from the initial analyzed concentration; for *S-praziquantel* and *R-trans-4-OH-praziquantel*, 81% and 84% were within the acceptable range, respectively. The PK parameters are summarized in Table 2, and concentration versus time profiles of ascending doses are illustrated in Fig. 1 for all analytes.

The highest maximal blood concentration (C_{max}) values increased with ascending doses, and medians of 1.18, 2.32, and 2.69 $\mu\text{g/mL}$ for *R-trans-4-OH-praziquantel*; 0.75, 1.06, and 1.72 $\mu\text{g/mL}$ for *R-praziquantel*; and 1.76, 2.91, and 4.89 $\mu\text{g/mL}$ for *S-praziquantel*, respectively,

TABLE 2 PK parameters of Praziquantel (PZQ) in *O. felineus*-infected patients^a

Dose (mg/kg)	Analyte	C _{max} (μg/mL)	AUC _{0-24h} (μg·h/mL)	T _{max} (h)	t _{1/2} (h)
20	<i>R-trans</i> -4-OH-PZQ	1.18 (0.82–1.29)	10.29 (6.73–12.32)	2.50 (2.50–3.00)	4.59 (3.40–6.37)
	<i>R</i> -PZQ	0.75 (0.26–1.28)	1.38 (0.30–2.49)	1.00 (0.50–2.00)	1.21 (0.72–3.40)
	<i>S</i> -PZQ	1.76 (1.01–2.63)	3.79 (2.36–8.49)	1.00 (0.50–2.00)	2.29 (1.62–3.37)
40	<i>R-trans</i> -4-OH-PZQ	2.32 (1.69–2.57)	19.89 (14.55–29.28)	3.00 (2.50–3.00)	5.07 (4.42–7.15)
	<i>R</i> -PZQ	1.06 (0.65–1.57)	2.50 (1.61–4.65)	1.50 (1.00–2.00)	1.88 (1.06–2.34)
	<i>S</i> -PZQ	2.91 (1.92–3.78)	8.96 (5.94–15.18)	1.50 (1.00–2.00)	3.23 (1.71–4.09)
60	<i>R-trans</i> -4-OH-PZQ	2.69 (2.32–3.17)	31.90 (24.54–37.33)	3.00 (2.88–6.00)	6.25 (4.82–8.14)
	<i>R</i> -PZQ	1.72 (1.18–3.32)	5.91 (4.22–8.37)	1.50 (1.00–2.00)	2.42 (1.55–4.31)
	<i>S</i> -PZQ	4.89 (3.37–6.58)	19.80 (13.28–31.04)	2.00 (1.50–2.50)	3.29 (2.49–4.75)
3 × 20	<i>R-trans</i> -4-OH-PZQ	2.66 (1.98–3.12)	36.38 (28.47–42.72)	12.00 (10.00–12.00)	6.19 (5.38–8.97)
	<i>R</i> -PZQ	1.20 (0.69–2.01)	8.04 (4.23–12.09)	6.00 (5.00–10.00)	3.44 (3.02–3.82)
	<i>S</i> -PZQ	3.35 (1.90–4.16)	27.75 (13.54–37.65)	5.50 (2.75–10.00)	3.63 (3.32–4.34)

^aResults are shown as medians with interquartile ranges.

were obtained for patients treated with 20, 40, and 60 mg/kg praziquantel, respectively. At a single dose of 60 mg/kg, the C_{max} values were observed for *S*-praziquantel, with a median of 4.89 μg/mL (interquartile range [IQR], 3.37 to 6.58 μg/mL), followed by *R-trans*-OH-praziquantel at 2.69 μg/mL (IQR, 2.32 to 3.17 μg/mL) and *R*-praziquantel at 1.72 μg/mL (IQR, 1.18 to 3.32 μg/mL). Patients treated with three doses of 20 mg/kg (total of 60 mg/kg) had lower median C_{max} values (2.66, 1.20, and 3.35 for *R-trans*-4-OH-praziquantel, *R*-praziquantel, and *S*-praziquantel, respectively) than those receiving a single oral 60-mg/kg dose. The area under the concentration-time curve (AUC) also correlated with the dose; the highest values were obtained for the group of patients treated with three doses of 20 mg/kg. *R-trans*-4-OH-praziquantel had the highest AUC, with a median of 36.38 μg/mL (IQR, 28.47 to 42.72 μg/mL), followed by *S*-praziquantel with 27.75 μg/mL (IQR, 13.54 to 37.65 μg/mL) and *R*-praziquantel with 8.04 μg/mL (IQR, 4.23 to 12.09 μg/mL). The median time to reach C_{max} (T_{max}) values were similar in the three groups that received a single dose of praziquantel, ranging between 1 h and 3 h postdosing. However, T_{max} values for all analytes were shifted to later time points when the 60-mg/kg dose was given in three single 20-mg/kg intakes (with 4 h intervals). The metabolite *R-trans*-4-OH-praziquantel reached C_{max} at 12 h (IQR, 10.00 to 12.00 h) after the first dose. Large variations in T_{max} values were observed for both enantiomers, with medians of 6 h (IQR, 5.00 to 10.00 h) and 5.5 h (IQR, 2.75 to 10.00 h) for *R*- and *S*-praziquantel, respectively. For all analytes, the statistical significance of C_{max} and AUC was calculated between the treatment groups (Fig. 2), and a significant difference was found for both enantiomers as well as the metabolite when comparing a single 20-mg/kg dose versus a single 60-mg/kg dose.

DISCUSSION

Praziquantel is the drug of choice for the treatment of opisthorchiasis. Clinical guidelines in the Russian Federation suggest the use of different multiple doses of praziquantel, yet it remains unclear which of the suggested doses to apply. Moreover, a single dose of praziquantel is the recommended treatment in preventive chemotherapy, which was shown to be efficacious in *O. viverrini* infections (15). To our knowledge, the dosing schema has never been truly optimized, and neither the correlation of dose and efficacy nor the PK behavior of praziquantel in *O. felineus*-infected patients has been studied to date. For the first time, we conducted a PK study in patients infected with *O. felineus* that were treated with different dosing schema of praziquantel: group 1 received a single 20-mg/kg dose, group 2 received a single 40-mg/kg dose, group 3 received a single 60-mg/kg dose, and group 4 was treated with three doses of 20 mg/kg given in intervals of 4 h. We studied the drug disposition of the two enantiomers, *R*- and *S*-praziquantel, as well as the *R-trans*-OH-praziquantel metabolite in a previously established and validated DBS method (16). Noncompartmental modeling was used in this study; however, the data could be integrated in a next step in a recently established population PK model based on data from *O. viverrini*-infected adults and *Schistosoma mansoni*- and *Schistosoma haematobium*-infected children (17).

High variability between individuals of the same treatment group was observed for

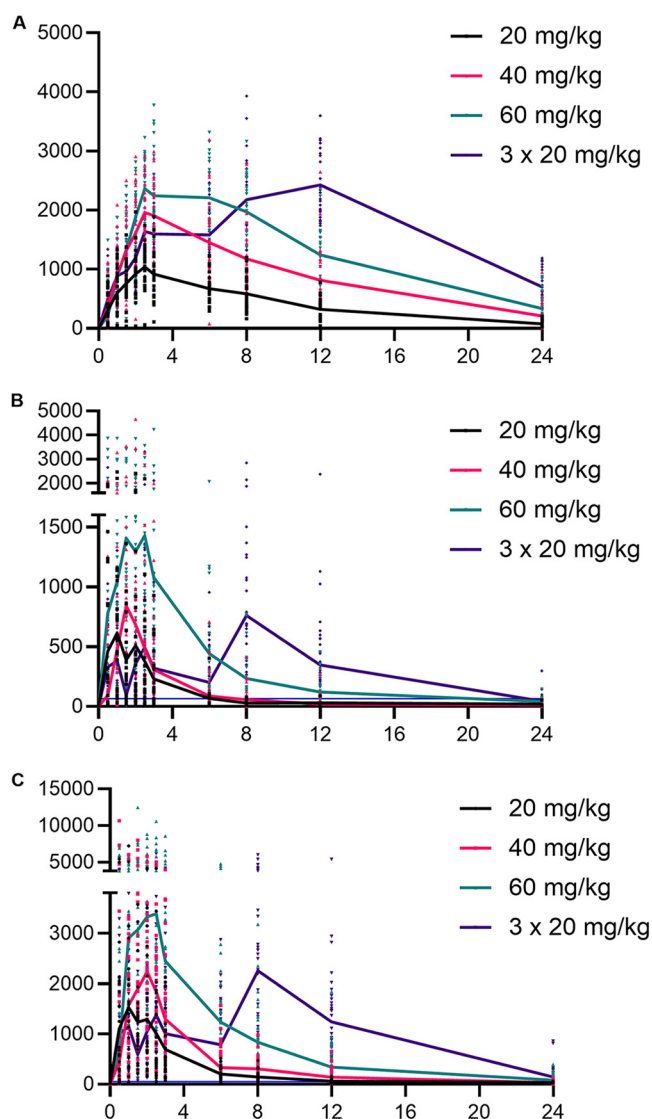


FIG 1 Concentration-time profiles of ascending doses of praziquantel. Graphs are shown for *R-trans-4-OH-praziquantel* (A), *R-praziquantel* (B), and *S-praziquantel* (C), respectively. Symbols capture individual values, while the curve describes the mean value. Table 1 additionally contains interquartile ranges of all PK parameters. The actual LLOQs were 64.5 ng/mL and 51.6 ng/mL for *R-* and *S-praziquantel*, respectively, and are indicated by a blue horizontal line.

all patient samples analyzed. Previous studies observed similar findings and attributed them to host factors such as the involvement of the cytochrome P450 system (CYP) in the first-pass metabolism of praziquantel, as well as external factors like drug-drug interactions or food intake (altered bioavailability) (9, 18, 19). Also, multiple dosages such as given to the participants of group 4 in our study can add to variability, mainly due to differences in the onset of absorption and elimination of the drug.

A previously published study by us examined the PK disposition of praziquantel in *O. viverrini*-infected patients (14). Nine patients were treated with three doses of 25 mg/kg (total of 75 mg/kg), and sampling was performed within a 24 h frame, similar to our study. Comparing the results of both groups of triple-dosed patients, we observed that the median C_{max} values for *R-praziquantel* (1.20; IQR, 0.69 to 2.01 $\mu\text{g/mL}$) and *S-praziquantel* (3.35; IQR, 1.90 to 4.16 $\mu\text{g/mL}$) were approximately six and four times higher in the *O. felineus*-infected patients than patients infected with *O. viverrini* (*R-praziquantel*, C_{max} 0.2; IQR, 0.1 to 1.1 $\mu\text{g/mL}$; and *S-praziquantel*, C_{max} 0.9; IQR, 0.6 to 2.3 $\mu\text{g/mL}$). Similar observations were made for the AUC values. On the contrary, the metabolite *R-trans-OH-praziquantel* displayed a 2.5 to 5 times

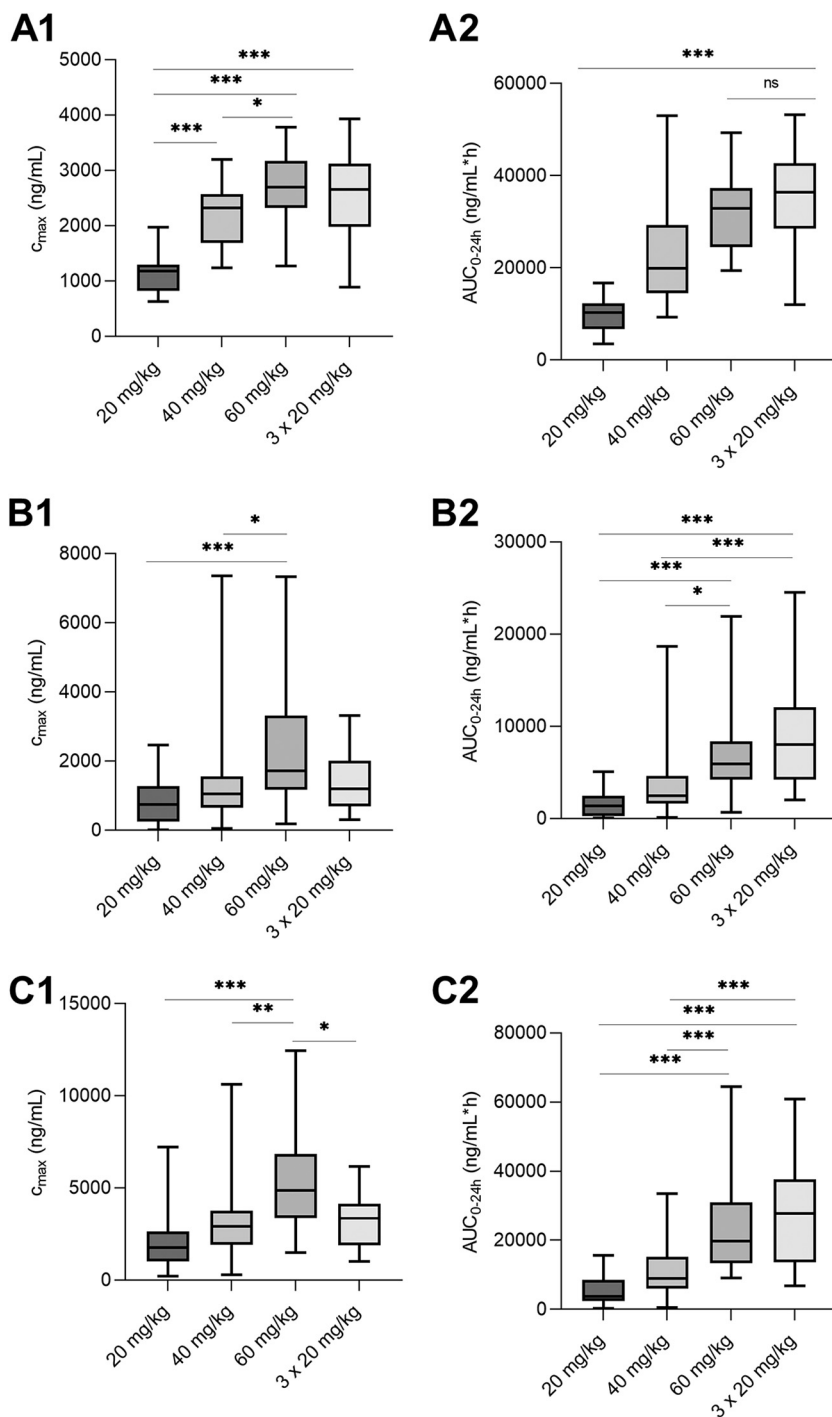


FIG 2 C_{max} (A1, B1, and C1) and AUC_{0-24} (A2, B2, and C2) of ascending doses of praziquantel in *O. felineus*-infected individuals. Graphs are shown for *R-trans*-4-OH-praziquantel and *R*- and *S*-praziquantel, respectively (top down). The median and minimum to maximum are illustrated. *, $P < 0.05$; **, $P < 0.01$; ***, $P < 0.001$.

lower C_{max} and AUC value, respectively, in the *O. felineus* cohort. This may be due to differences in genetic polymorphism of liver enzymes that are involved in the metabolism of praziquantel. In this respect, also, differences in ethnic populations may play a role (Lao PDR versus Russian Federation) (9). However, the sample size of both studies limits further interpretation. Half-life values of 3.3 and 6.4 h previously observed for *S*-praziquantel and *R-trans*-OH-praziquantel, respectively, in *O. viverrini*-infected patients is consistent with the half-life of *S*-praziquantel of 3.6 h and *R-trans*-OH-praziquantel of 6.2 h in our study (14).

Another study that examined the kinetic disposition of *R*-praziquantel, *S*-praziquantel,

and metabolites in nine healthy volunteers after a single oral dose of 1,500 mg (corresponds to 25 mg/kg for an individual weighing 60 kg) observed a 2.5 to 3 times lower exposure of the enantiomers and the *R-trans*-OH-praziquantel metabolite than we did. Median $AUC_{0-\infty}$ values were 0.52, 1.54, and 4.63 $\mu\text{g/mL}\cdot\text{h}$ for *R*-praziquantel, *S*-praziquantel, and *R-trans*-OH-praziquantel, respectively, whereas *O. felineus*-infected patients in group 1 (single oral 20-mg/kg dose) had median $AUC_{0-\infty}$ values (not shown in Table 1) of 1.67, 4.29, and 10.81, respectively (12). A difference in drug exposure in infected versus noninfected individuals was suggested by several studies (20–22), observing higher exposure in infected patients. Our study supports these findings. However, irrespectively of the dose (and infection status), *S*-praziquantel exposure was approximately three times higher than *R*-praziquantel exposure in our study and thus corresponds to previous findings (12, 23–26). Finally, except for *R*-praziquantel, half-life values were longer in *O. felineus*-infected versus noninfected individuals. Although our study observed differences in exposure parameters compared to both *O. viverrini*-infected patients as well as healthy study subjects, it is not fully clear how these findings correlate with praziquantel's efficacy. More studies (in animal models and opisthorchiasis patients) are needed with respect to connecting exposure values to the pathology of the disease. In particular, the location of the adult worms (biliary duct) needs to be considered, raising the question of whether C_{max} or/and AUC levels need to be maintained in the plasma or in the biliary ducts to drive efficacy.

As observed in previous studies, patient samples had double peaks in the PK profiles. This may be due to a possible reuptake of the drug during the passage through the gastrointestinal tract as well as potential precipitation (17, 27). Additionally, from a technical point of view, we were surprised to get different curve shapes of *R-trans*-OH-praziquantel in patient DBS samples versus laboratory DBS samples that served as calibration line and quality control samples, respectively, and were prepared by spiking venous blood with the analytes. All patient samples had double peaks in the chromatogram, whereas laboratory samples displayed only a single peak. This may be a matrix effect due to (i) differences in composition of capillary versus venous blood (from donors), (ii) the first drop(s) of blood containing fat or other contaminants on the skin, or (iii) the drying of the DBS cards being influenced by temperature and humidity. Such phenomena have been previously reported for, e.g., the drug albendazole (28).

A limitation of our study is that the large majority of our study participants were female (78%) with a median BMI of 28. Gender and weight were found, for many drugs, to influence PK properties (29–31). Though, to our knowledge, no information is available on whether these factors influence praziquantel disposition, it is worth highlighting that the population in this study differs from populations in previous studies, which also might explain the differences observed. Further studies are necessary to elucidate sex-, weight-, and age-related differences in the pharmacokinetics of praziquantel.

Conclusion. Using four different dosages of praziquantel, we have described the PK parameters in infected *O. felineus* patients in the Russian Federation. Exposure metrics, AUC, and C_{max} were positively correlated with dose. While AUC was highest in the $3 \times 20\text{-mg/kg}$ dose, the 60-mg/kg dose presented the highest C_{max} . Comparing our data with previously studied healthy volunteers, infection status seems to influence drug exposure. Our results in combination with the results from the efficacy study will be pivotal to establishing evidence-based dosing recommendations for praziquantel regarding *O. felineus* infections.

MATERIALS AND METHODS

Chemicals and reagents. Racemic (rac) praziquantel was obtained from Sigma-Aldrich (Buchs, Switzerland). *R*-praziquantel, *S*-praziquantel, and *R-trans*-4-OH-praziquantel were the product of Merck KgaA (Darmstadt, Germany). The internal standard praziquantel-d11 was purchased from Toronto Research Chemicals (Toronto, Canada). LC-MS-grade chemicals and solvents, including acetonitrile, isopropanol, formic acid, ammonium formate, and ammonium acetate, were purchased from Sigma-Aldrich (Buchs, Switzerland). Water was purified using a Milli-Q Advantage A10 (Merck, Darmstadt, Germany) purification system. Whatman 903 Proteinsaver cards were purchased from Sigma-Aldrich (Buchs, Switzerland). Human blood for preparation of calibrators and quality control (QC) samples was obtained in lithium heparin-coated vacutainer tubes from the local blood donation center (Basel, Switzerland). Praziquantel tablets (Biltricide; Bayer; 600 mg) were purchased in the local pharmacy.

LC-MS/MS equipment and operating conditions. A validated LC-MS/MS method described by Meister et al. and revalidated by Kovac et al. was used (16, 27). In brief, chromatographic separation was achieved by first loading the analytes onto a column trapping system (Halo C_{18} ; 4.6 by 5 mm; Optimize Technologies, Oregon City, OR, USA) to remove the remaining matrix and then eluting to a chiral Lux Cellulose-2 column (150 by 2 mm, 3 μ m; Phenomenex, CA, USA). Mobile phase A, containing 10 mM ammonium acetate with 0.015% formic acid, served as a loading solution at a flow rate of 0.35 mL/min. After a loading time of 1 min, a mixture of 2 mM ammonium formate and acetonitrile (1:4; mobile phase B) was used for the elution to the main column at a flow rate ascending to 0.45 mL/min at 3 min and remaining steady until 9.49 min. From 9.5 to 10.5 min, mobile phase A was used at a flow rate of 1 mL/min to reequilibrate the trapping system. A mixture of isopropanol and purified water (50:50) was used to clean the autosampler syringe, including the injection valve in between sample injections.

Study design and ethical considerations. The DBS sample collection was performed in the frame of a PK and dose-finding randomized controlled, single-blind study of praziquantel against *O. felineus* in infected adults (18 to 65 years), as assessed by the presence of eggs in the stool (O. S. Fedorova, J. Keiser, unpublished data). Ethical approval of the clinical trial was obtained from the Ethics Committee of Siberian State Medical University, which granted clearance on 29 May 2017 (reference no. 5308). The trial is registered at ISRCTN (<https://www.isrctn.com/ISRCTN10577372>). All participants gave informed consent. The study was carried out in Tomsk between June 2016 and March 2018 at the clinics of the Siberian State Medical University. The study physician carried out a clinical and physical examination and assessed the medical history of the participants. The safety and tolerability of the interventions were evaluated by clinical examinations and assessment of adverse events. Efficacy and safety data, as well as detailed information on inclusion and exclusion criteria, randomization procedure, and diagnostic methods, will be published elsewhere.

Three groups of each 28, 26, and 28 *O. felineus*-infected patients were treated with one oral dose of 20 mg/kg, 40 mg/kg, and 60 mg/kg, respectively. Another group of 28 patients was treated with three oral doses of 20 mg/kg praziquantel, with the second and third doses administered 4 and 8 h after the first dose, respectively. A placebo group was included in the study.

DBS sample collection and storage. A sterile one-way finger pricker (e.g., Accu-Check Softclix Pro; Roche, Switzerland) was used to obtain capillary blood at 0, 0.5, 1, 1.5, 2, 2.5, 3, 6, 8, 12, and 24 h after treatment with 20 mg/kg, 40 mg/kg, and 60 mg/kg of praziquantel (single oral dose) and at 0, 1, 2, 4, 5, 6, 7, 8, 10, 12, and 24 h after treatment with three doses of 20 mg/kg praziquantel given in intervals of 4 h. Quadruplets of a drop of blood at each time point were taken and transferred onto the DBS cards, dried for approximately 1 h, and stored afterward in plastic bags with desiccant. The cards were transferred to Basel, Switzerland, and kept at -20°C until further processing.

Sample procession. Sample procession was conducted based on previously published methods (14, 16, 27). Stock solutions of the analytes were prepared in acetonitrile to obtain 1.0-mg/mL concentrations for *R*- and *S*-praziquantel, a 10-mg/mL concentration for *trans*-4-OH-praziquantel, and a 1.25-mg/mL concentration for praziquantel-d11. They were stored at -20°C . For *R*- and *S*-praziquantel, QC samples at four concentrations of 10 ng/mL (LLOQ), 17.5 ng/mL (low QC [lQC]), 175 ng/mL (medium QC [mQC]), and 1,750 ng/mL (high QC [hQC]), respectively, as well as eight CLs covering the range of 10 ng/mL to 2,500 ng/mL, were prepared by spiking blood with the corresponding working solutions. The calibration line samples of *trans*-OH-praziquantel covered a range of 100 ng/mL to 25,000 ng/mL, and the QC samples were similarly prepared by spiking six different blanks to obtain LLOQ and low, middle, and high concentrations. The final concentration of organic solvent in the spiked blood samples was $<4.2\%$.

Disks of 6 mm in diameter were punched from the DBS samples and extracted with 200 μ L of extraction solution containing 400 ng/mL internal standard. Samples were shaken in a thermomixer for 20 min at 20°C and 1,400 rpm (Eppendorf Thermomixer C; Hamburg, Germany), and sonicated for 40 min. Thereafter, samples were filtered (2- μ m polyvinylidene difluoride [PVDF]-membrane 96-well filter plate [Corning Life Sciences, CA, USA]) by centrifugation (10 min at $2,250 \times g$, 20°C).

Data analysis. Drug concentration was calculated by interpolation from the calibration curve. The Excel add-in PKSolver (32) using noncompartmental analysis was utilized to calculate PK parameters for each patient. Maximum drug concentrations (C_{\max}) and the time to reach C_{\max} (T_{\max}) were observed values. The area under the curve was determined until the last measurement (AUC_{0-24}) using the linear trapezoidal rule. The elimination half-life ($t_{1/2}$) was estimated by the equation $t_{1/2} = \ln(2)/\lambda_z$, where λ_z was determined by performing a regression of the natural logarithm of the concentration values during the elimination period. The half-life was only estimated for patients who had a single peak in concentration and where the elimination phase was well estimated by the algorithm because of praziquantel's erratic absorption. The drug oral clearance (CL/F) and the apparent volume of distribution (V/F) were not evaluated. Statistical analysis was performed with Microsoft Excel and GraphPad Prism version 8.2.1 (GraphPad, CA, USA), respectively. Kruskal-Wallis analysis followed by Dunn's posttest was performed using the software R studio Version 4.0.3 to compare PK parameters (C_{\max} , AUC_{0-24}) between treatment arms.

ACKNOWLEDGMENTS

This work was supported by the Swiss National Science Foundation (no. 320030_175585).

We are thankful to all patients from the Russian Federation for participating in our study. We further thank the research team from the Siberian State Medical University, and we are grateful to Anna Kovshirina for helping with the sample procession.

We have no conflicts of interest to declare.

REFERENCES

- Pozio E, Armignacco O, Ferri F, Gomez Morales MA. 2013. *Opisthorchis felineus*, an emerging infection in Italy and its implication for the European Union. *Acta Trop* 126:54–62. <https://doi.org/10.1016/j.actatropica.2013.01.005>.
- Keiser J, Utzinger J. 2005. Emerging foodborne trematodiasis. *Emerg Infect Dis* 11:1507–1514. <https://doi.org/10.3201/eid1110.050614>.
- Keiser J, Utzinger J. 2009. Food-borne trematodiasis. *Clin Microbiol Rev* 22:466–483. <https://doi.org/10.1128/CMR.00012-09>.
- Petney TN, Andrews RH, Saijuntha W, Wenz-Mucke A, Sithithaworn P. 2013. The zoonotic, fish-borne liver flukes *Clonorchis sinensis*, *Opisthorchis felineus* and *Opisthorchis viverrini*. *Int J Parasitol* 43:1031–1046. <https://doi.org/10.1016/j.ijpara.2013.07.007>.
- Fedorova OS, Kovshirina YV, Kovshirina AE, Fedotova MM, Deev IA, Petrovskiy FI, Filimonov AV, Dmitrieva AI, Kudiyakov LA, Saltykova IV, Odermatt P, Ogorodova LM. 2017. *Opisthorchis felineus* infection and cholangiocarcinoma in the Russian Federation: a review of medical statistics. *Parasitol Int* 66:365–371. <https://doi.org/10.1016/j.parint.2016.07.010>.
- Fedorova OS, Fedotova MM, Zvonareva OI, Mazeina SV, Kovshirina YV, Sokolova TS, Golovach EA, Kovshirina AE, Konovalova UV, Kolomeets IL, Gutor SS, Petrov VA, Hattendorf J, Ogorodova LM, Odermatt P. 2020. *Opisthorchis felineus* infection, risks, and morbidity in rural Western Siberia, Russian Federation. *PLoS Negl Trop Dis* 14:e0008421. <https://doi.org/10.1371/journal.pntd.0008421>.
- Pakharukova MY, Mordvinov VA. 2016. The liver fluke *Opisthorchis felineus*: biology, epidemiology and carcinogenic potential. *Trans R Soc Trop Med Hyg* 110:28–36. <https://doi.org/10.1093/trstmh/trv085>.
- Bronstein AM, Ozeretskovskaya NN, Panteleeva EI, Plushcheva GL, Gitsu GA. 1988. An analysis of 4 strategies for the praziquantel treatment of persons infested with *Opisthorchis felineus* under conditions excluding reinfection. *Med Parazitol (Mosk)* 19–24. <https://pubmed.ncbi.nlm.nih.gov/3252134/>.
- Zdesenko G, Mutapi F. 2020. Drug metabolism and pharmacokinetics of praziquantel: a review of variable drug exposure during schistosomiasis treatment in human hosts and experimental models. *PLoS Negl Trop Dis* 14:e0008649. <https://doi.org/10.1371/journal.pntd.0008649>.
- Avustinovich DF, Tsyganov MA, Pakharukova MY, Chulakov EN, Dushkin AV, Krasnov VP, Mordvinov VA. 2020. Effectiveness of repeated administration of praziquantel with disodium glycyrrhizinate and two enantiomers of praziquantel on *Opisthorchis felineus* (Rivolta, 1884). *Acta Parasitol* 65:156–164. <https://doi.org/10.2478/s11686-019-00149-2>.
- Nleya L, Thelgingwani R, Li X-Q, Cavallin E, Isin E, Nhachi C, Masimirembwa C. 2019. The effect of ketoconazole on praziquantel pharmacokinetics and the role of CYP3A4 in the formation of X-OH-praziquantel and not 4-OH-praziquantel. *Eur J Clin Pharmacol* 75:1077–1087. <https://doi.org/10.1007/s00228-019-02663-8>.
- Lima RM, Ferreira MAD, de Jesus Ponte Carvalho TM, Dumêt Fernandes BJ, Takayanagui OM, Garcia HH, Coelho EB, Lanchote VL. 2011. Albendazole-praziquantel interaction in healthy volunteers: kinetic disposition, metabolism and enantioselectivity. *Br J Clin Pharmacol* 71:528–535. <https://doi.org/10.1111/j.1365-2125.2010.03874.x>.
- Na Bangchang K, Karbwang J, Pungpak S, Radomyos B, Bunnag D. 1993. Pharmacokinetics of praziquantel in patients with opisthorchiasis. *Southeast Asian J Trop Med Public Health* 24:717–723.
- Meister I, Kovac J, Duthaler U, Odermatt P, Huwyler J, Vanobberghen F, Sayasone S, Keiser J. 2016. Pharmacokinetic study of praziquantel enantiomers and its main metabolite R-trans-4-OH-praziquantel in plasma, blood and dried blood spots in *Opisthorchis viverrini*-infected patients. *PLoS Negl Trop Dis* 10:e0004700. <https://doi.org/10.1371/journal.pntd.0004700>.
- Sayasone S, Meister I, Andrews JR, Odermatt P, Vonghachack Y, Xayavong S, Sengngam K, Phongluxa K, Hattendorf J, Bogoch II, Keiser J. 2017. Efficacy and safety of praziquantel against light infections of *Opisthorchis viverrini*: a randomized parallel single-blind dose-ranging trial. *Clin Infect Dis* 64:451–458. <https://doi.org/10.1093/cid/ciw785>.
- Meister I, Leonidova A, Kovač J, Duthaler U, Keiser J, Huwyler J. 2016. Development and validation of an enantioselective LC-MS/MS method for the analysis of the anthelmintic drug praziquantel and its main metabolite in human plasma, blood and dried blood spots. *J Pharm Biomed Anal* 118:81–88. <https://doi.org/10.1016/j.jpba.2015.10.011>.
- Falcoz C, Guzy S, Kovač J, Meister I, Coulibaly J, Sayasone S, Wesche D, Lin YW, Keiser J. 2022. R-praziquantel integrated population pharmacokinetics in preschool- and school-aged African children infected with *Schistosoma mansoni* and *S. haematobium* and Lao adults infected with *Opisthorchis viverrini*. *J Pharmacokinet Pharmacodyn* 49:293–310. <https://doi.org/10.1007/s10928-021-09791-8>.
- Olliaro P, Delgado-Romero P, Keiser J. 2014. The little we know about the pharmacokinetics and pharmacodynamics of praziquantel (racemate and R-enantiomer). *J Antimicrob Chemother* 69:863–870. <https://doi.org/10.1093/jac/dkt491>.
- Murray M. 2006. Altered CYP expression and function in response to dietary factors: potential roles in disease pathogenesis. *Curr Drug Metab* 7: 67–81. <https://doi.org/10.2174/138920006774832569>.
- Mandour ME, el Turabi H, Homeida MM, el Sadig T, Ali HM, Bennett JL, Leahy WJ, Harron DW. 1990. Pharmacokinetics of praziquantel in healthy volunteers and patients with schistosomiasis. *Trans R Soc Trop Med Hyg* 84:389–393. [https://doi.org/10.1016/0035-9203\(90\)90333-a](https://doi.org/10.1016/0035-9203(90)90333-a).
- el Guiniady MA, el Touny MA, Abdel-Bary MA, Abdel-Fatah SA, Metwally A. 1994. Clinical and pharmacokinetic study of praziquantel in Egyptian schistosomiasis patients with and without liver cell failure. *Am J Trop Med Hyg* 51:809–818. <https://doi.org/10.4269/ajtmh.1994.51.809>.
- Ofori-Adjei D, Adjepon-Yamoah KK, Lindström B. 1988. Oral praziquantel kinetics in normal and *Schistosoma haematobium*-infected subjects. *Ther Drug Monit* 10:45–49. <https://doi.org/10.1097/00007691-198810010-00008>.
- Bagchus WM, Bezuidenhout D, Harrison-Moench E, Kourany-Lefoll E, Wolna P, Yalokinoglu O. 2019. Relative bioavailability of orally dispersible tablet formulations of Levo- and Racemic praziquantel: two phase I studies. *Clin Transl Sci* 12:66–76. <https://doi.org/10.1111/cts.12601>.
- Meister I, Ingram-Sieber K, Cowan N, Todd M, Robertson MN, Meli C, Patra M, Gasser G, Keiser J. 2014. Activity of praziquantel enantiomers and main metabolites against *Schistosoma mansoni*. *Antimicrob Agents Chemother* 58:5466–5472. <https://doi.org/10.1128/AAC.02741-14>.
- Bonate PL, Wang T, Passier P, Bagchus W, Burt H, Lüpfer C, Abila N, Kovac J, Keiser J. 2018. Extrapolation of praziquantel pharmacokinetics to a pediatric population: a cautionary tale. *J Pharmacokinet Pharmacodyn* 45: 747–762. <https://doi.org/10.1007/s10928-018-9601-1>.
- Lima RM, Ferreira MAD, Ponte T, Marques MP, Takayanagui OM, Garcia HH, Coelho EB, Bonato PS, Lanchote VL. 2009. Enantioselective analysis of praziquantel and trans-4-hydroxypraziquantel in human plasma by chiral LC-MS/MS: application to pharmacokinetics. *J Chromatogr B Analyt Technol Biomed Life Sci* 877:3083–3088. <https://doi.org/10.1016/j.jchromb.2009.07.036>.
- Kovač J, Meister I, Neodo A, Panic G, Coulibaly JT, Falcoz C, Keiser J. 2018. Pharmacokinetics of praziquantel in *Schistosoma mansoni*- and *Schistosoma haematobium*-infected school- and preschool-aged children. *Antimicrob Agents Chemother* 62:e02253-17. <https://doi.org/10.1128/AAC.02253-17>.
- Schulz JD, Neodo A, Coulibaly JT, Keiser J. 2019. Pharmacokinetics of albendazole, albendazole sulfoxide, and albendazole sulfone determined from plasma, blood, dried-blood spots, and Mitra samples of hookworm-infected adolescents. *Antimicrob Agents Chemother* 63:e02489-18. <https://doi.org/10.1128/AAC.02489-18>.
- Greenblatt DJ, von Moltke LL. 2008. Gender has a small but statistically significant effect on clearance of CYP3A substrate drugs. *J Clin Pharmacol* 48:1350–1355. <https://doi.org/10.1177/0091270008323754>.
- Florida M, Giuliano M, Palmisano L, Vella S. 2008. Gender differences in the treatment of HIV infection. *Pharmacol Res* 58:173–182. <https://doi.org/10.1016/j.phrs.2008.07.007>.
- Schwartz JB. 2007. The current state of knowledge on age, sex, and their interactions on clinical pharmacology. *Clin Pharmacol Ther* 82:87–96. <https://doi.org/10.1038/sj.cpt.6100226>.
- Zhang Y, Huo M, Zhou J, Xie S. 2010. PKSolver: an add-in program for pharmacokinetic and pharmacodynamic data analysis in Microsoft Excel. *Comput Methods Programs Biomed* 99:306–314. <https://doi.org/10.1016/j.cmpb.2010.01.007>.

CHAPTER VIII: DISCUSSION

8. Rationale and objectives

While many milestones in the fight against Neglected Tropical Diseases (NTDs) have been reached, there are at least 1.76 billion people still requiring interventions against NTDs (WHO 2020). Schistosomiasis and opisthorchiasis affect the poorest populations, living in rural areas. Without access to medical interventions, these infectious diseases can easily develop to chronic malignancies, bearing a huge burden not only for the individuals but also for entire communities (Hotez and Kamath 2009; Utzinger and Keiser 2013; Fedorova et al. 2020).

WHO's roadmap for NTDs aims for the elimination of schistosomiasis as a public health problem by 2030. Critical actions need to be implemented, such as targeted snail control, reliable diagnostic tests and preventive chemotherapy for all populations in need, to mention a few (WHO 2020). With praziquantel being the only drug available for the treatment of schistosomiasis, it will be challenging to reach the WHO 2030 goals. Endowed with a good safety profile and active against all *Schistosoma* species, praziquantel is not efficacious against the developing stages of the worm. This presents a major drawback of the drug of choice and thus, treating an entire population with praziquantel never results in 100% effectiveness (Cioli et al. 2014). Moreover, with respect to the abundant use of praziquantel, questions attributed to resistance development arise (Crellen et al. 2016).

Praziquantel is the drug of choice, not only for schistosomiasis but also for opisthorchiasis. Yet, treatment against opisthorchiasis is even less established, with no standardized treatment schemes present.

The two main aims of this thesis were to (re-)discover potent antischistosomal drugs as alternatives to praziquantel and to lay the groundwork for a standardized treatment scheme for opisthorchiasis due to *O. felineus*. The first aim was carried out by following-up on the SAR program of promising antischistosomal pyridobenzimidazoles (PBIs) by testing a 3rd generation drug set (Chapter III). We further investigated the antischistosomal activity and

pharmacokinetic properties of SF₅-containing *N,N'*-diarylureas (Chapter IV) and we explored different extracts and fractions of the medicinal plants *Artemisia annua* and *Artemisia afra* against newly transformed schistosomula and adult *S. mansoni* (Chapter V). Moreover, with the characterization of the largely forgotten lead candidate, Ro 15-5458, we pursued drug rescuing (Chapter VI). The second aim was accomplished by investigating the pharmacokinetic properties of ascending doses of praziquantel in *O. felineus* infected patients from Western Siberia (Chapter VII).

Since the obtained results and outcomes have been discussed in detail within the manuscripts presented, this discussion focusses on the lessons learned, including challenges that were encountered during presented studies and opportunities that arouse from these, both in the field of schistosomiasis as well as opisthorchiasis.

The original discussion on schistosomiasis has been modified and complemented, and was published as a manuscript in 'Advances in Parasitology' after the oral examination (Sub-Chapter 8.1).

SUB-CHAPTER 8.1: A WAY FORWARD FOR ANTISCHISTOSOMAL DRUGS

Improving translational power in antischistosomal drug discovery

Alexandra Probst,^{a,b} Stefan Biendl,^{a,b} Jennifer Keiser,^{a,b}

^a Swiss Tropical and Public Health Institute, Allschwil, Switzerland




^b University of Basel, P.O. Box CH-4003, Basel, Switzerland

^c Siberian State Medical University, 634050, Tomsk, Russian Federation

*Corresponding author: jennifer.keiser@swisstph.ch

Published in *Advances in Parasitology*, 2022; 117, 43-73

Improving translational power in antischistosomal drug discovery

Alexandra Probst^{a,b,†} , Stefan Biendl^{a,b,†} ,
and Jennifer Keiser^{a,b,*} 

^aSwiss Tropical and Public Health Institute, Department of Medical Parasitology and Infection Biology, Basel, Switzerland

^bUniversity of Basel, Basel, Switzerland

*Corresponding author: e-mail address: jennifer.keiser@swisstph.ch

Contents

1. Filling the drug pipeline for schistosomiasis	2
2. Evaluating the importance of <i>S. mansoni</i> isolate origin for early antischistosomal drug discovery	3
3. The <i>S. mansoni</i> mouse model for drug efficacy testing	5
4. Infection intensity of the patent <i>S. mansoni</i> mouse model	8
5. Pharmacokinetic/pharmacodynamic (PK/PD) relationship of selected drugs	10
5.1 No correlation between praziquantel exposure and <i>in vivo</i> efficacy	10
5.2 Chronic <i>S. mansoni</i> infection influences exposure parameters of drugs	16
5.3 Prolonged drug exposure well above <i>in vitro</i> potency not always correlates with good <i>in vivo</i> efficacy	19
5.4 Special cases	21
6. Concluding remarks	22
Acknowledgements and funding	23
References	23

Abstract

Schistosomiasis is a poverty-associated tropical disease caused by blood dwelling trematodes that threaten approximately 10% of the world population. Praziquantel, the sole drug currently available for treatment, is insufficient to eliminate the disease and the clinical drug development pipeline is empty. Here, we review the characteristics of the patent *Schistosoma mansoni* mouse model used for *in vivo* antischistosomal drug discovery, highlighting differences in the experimental set-up across research groups and their potential influence on experimental results. We explore the pharmacokinetic/pharmacodynamic relationship of selected drug candidates, showcasing opportunities

† Contributed equally (joint first authorship).

to improve the drug profile to accelerate the transition from the early drug discovery phase to new clinical candidates.



1. Filling the drug pipeline for schistosomiasis

Schistosomiasis, a disease with a tremendous global burden, is caused by the blood dwelling trematodes of the genus *Schistosoma*. Associated with poverty, approximately 10% of the world population is at risk for an infection with one of the three clinically important species, *Schistosoma haematobium*, *Schistosoma japonicum* and *Schistosoma mansoni* (King, 2010; WHO, 2020). Praziquantel (PZQ) is the sole drug currently available for the treatment of schistosomiasis (Colley et al., 2014; WHO, 2020). Ever since its discovery by Bayer AG, Leverkusen and Merck KGaA, Darmstadt decades ago, praziquantel has been the key contributor to control schistosomiasis (within preventive chemotherapy campaigns) by reducing the disease morbidity (Spangenberg, 2021). However, praziquantel is far from being a perfect drug. The fact that it is rarely curative coupled to the main drawback of the drug, which is its inactivity against developing infections, call for a better understanding of the underlying mechanisms of drug action (only recently, a transient receptor (TRP) channel in *S. mansoni* has been discovered (*Sm*.TRP_{PZQ}) (Park and Marchant, 2020)), as well as the discovery and development of new drugs in the fight against schistosomiasis (Panic and Keiser, 2018; Spangenberg, 2021).

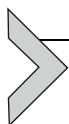
With the aim to eliminate schistosomiasis as a public health problem by 2030 (WHO, 2020), the drug discovery landscape has gained momentum over the past few years, with research efforts mainly driven by academic institutions. Different research groups all over the globe have brought promising drug candidates forward, as recently summarized (Dziwornu et al., 2020). Despite the preclinical pipeline being filled with several drug candidates (repurposed, rescued and new chemotypes), many gaps remain in the understanding of the profile of a compound required for the treatment of schistosomiasis.

To facilitate the discovery of novel antischistosomal drugs this review aims to increase our understanding of key elements of the schistosome drug discovery process, including the predictive pharmacology of lead compounds as well as the experimental setup used. We first summarize characteristics on the most commonly used *in vivo* model, the *S. mansoni* mouse model. Moreover, we highlight new findings on praziquantel, filling some

BOX 1 Highlights

- Praziquantel activity against *ex vivo* adult *S. mansoni* isolates of South American and Western African origin does not differ significantly.
- Academic research groups distributed over only a few public institutions drive *in vivo* drug efficacy research on *S. mansoni*. Biologic variability of mouse strain and gender as well as parasite isolates origin offer the advantage of obtaining a broader coverage of naturally occurring pathogen and host disease variability.
- Infection intensity of the patent *S. mansoni* mouse model follows a linear correlation to the number of cercariae *s.c.* injected per mouse.
- Praziquantel plasma exposure does not correlate with the *in vivo* efficacy in juvenile *S. mansoni*-infected mice.
- Chronic *S. mansoni* infection influences exposure parameters of drugs.
- No general rules apply regarding the correlation between *in vivo* drug efficacy and kinetic disposition; experimental differences must be taken in account when evaluating PK/PD relationship.

remaining knowledge gaps of the drug of choice. Lastly, we aim to shed light on the required pharmacokinetic/pharmacodynamic (PK/PD) relationship analysing the correlation between kinetic disposition and *in vivo* drug efficacy of selected candidates. A better understanding of the profile of a compound required for antischistosomal treatment and the available tools might help to accelerate the transition from the early drug discovery phase to the preclinical stage and eventually pave the way for a new clinical candidate (Box 1).

**2. Evaluating the importance of *S. mansoni* isolate origin for early antischistosomal drug discovery**

Phenotypic activity screens of compound libraries against *S. mansoni* are still the mainstay in antischistosomal drug discovery to provide small drug-like molecules as starting points for drug development programs (Biendl et al., 2021; Pasche et al., 2018). Recent multicenter activity screens of the same drug libraries, however, resulted in only limited overlap in identified hit compounds between different laboratories and these inconsistencies were proposed to be caused by differences in the parasite strain among others (Maccesi et al., 2019; Panic et al., 2015). To examine the hypothesis of differences in *S. mansoni* strains driving outcomes of

antischistosomal drug activity tests, we evaluated the phenotypic response of adult schistosomes, derived from two different isolate origins, to praziquantel in the same laboratory. Such an evaluation allows excluding differences in assay methodology and read-out (and weighing thereof, see below) which are the main drivers of inter-laboratory inconsistencies. We selected isolates from South America (Brazil) and Western Africa (Liberia), to cover a large spatial distance of isolate origin (see Methods in Supplementary Material in the online version at <https://doi.org/10.1016/bs.apar.2022.05.002>).

Following exposure to praziquantel, viability of *ex vivo* adult *S. mansoni* of both isolates decreased rapidly. The fast onset of action resulted in high double-digit to low triple-digit nanomolar EC_{50} values after 1 h of drug exposure, independent of isolate origin (Fig. 1, Table S1 in Supplementary Material in the online version at <https://doi.org/10.1016/bs.apar.2022.05.002>). Drug activity did not improve significantly for prolonged exposure times. In summary, we did not observe significant differences of praziquantel or (*R*)-praziquantel activity against both tested isolates for any evaluation time point (Fig. 1). Therefore, we hypothesize that there is not sufficient reason to expect

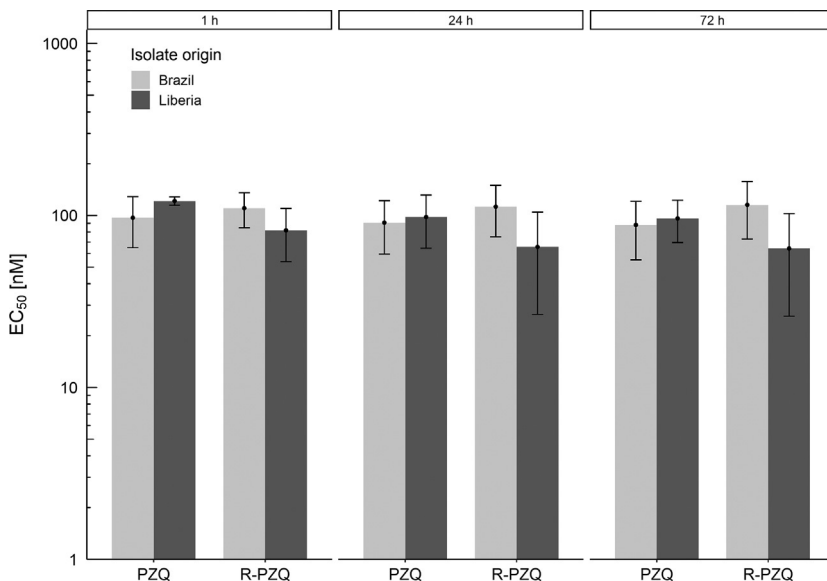


Fig. 1 Praziquantel (PZQ) and (*R*)-Praziquantel (R-PZQ) *in vitro* activity against adult *S. mansoni* from isolates of Brazilian and Liberian origin after 1, 24 and 72 h of drug exposure. Each point represents the mean EC_{50} value, and the error bars represent the 95% confidence interval of the mean.

differences in the response of new compounds on different isolates. Thus, we believe that for early antischistosomal drug discovery it is sufficient to initially screen compounds against single isolates only. However, for compounds that have further advanced the antischistosomal drug discovery cascade, characterization of *in vitro* and *in vivo* drug activity against multiple strains offers additional value, to potentially identify compound specific effects. Recent studies of different isolates and strains at the genomic and transcriptomic levels showed remarkable differences (Berger et al., 2021; Doyle and Cotton, 2019; Gower et al., 2013; Stroehlein et al., 2022)—some of these might have an influence on drug sensitivity. Hence, further studies evaluating the effect of such differences on drug efficacy are required.



3. The *S. mansoni* mouse model for drug efficacy testing

Academic research groups distributed over only a few public institutions drive *in vivo* drug efficacy research on *S. mansoni*. Besides high research activity in Brazil, where *S. mansoni* still presents a public health concern, and Egypt, where Theodor Bilharz first described *Schistosoma* parasites, for example, groups at Swiss TPH, LSHTM and the University of California continuously publish evaluations of new or repurposed compounds in the *S. mansoni* mouse model. We collected and summarized characteristics of host mice, *S. mansoni* infection and evaluation methods employed by key institutions driving antischistosomal drug discovery, to allow appraisal and comparisons of results generated in these laboratories (Table 1).

Generally, young animals are infected shortly after purchase and acclimatization to improve susceptibility to infection. Further, there is good accordance between research groups on infection duration to achieve juvenile and adult (patent infection) worm life stages reflecting the parasite life cycle in the host organism.

We identified three main variations influencing mouse model characteristics of the various laboratories and complicating direct comparability of experimental results. First, utilization of mice of different strain and gender. All research groups use other but similar general purpose mouse strains (e.g. NMRI, Swiss Webster), with the exception of researchers at LSHTM and TBRI both employing CD1 mice (Botros et al., 2020; Gardner et al., 2021). However, researchers at TBRI utilize male mice, while most other groups, including the group at LSHTM, utilize female mice in their studies due to their increased susceptibility to infection (Eloi-Santos et al., 1992; Nakazawa et al., 1997). The effect of mice strain on experimental end-points remains

Table 1 The *S. mansoni* mouse model for drug efficacy testing.

Institution	Host				Infection					Evaluation			Ref.
	Strain	Age at infection [weeks]	Sex	Animals per group	Isolate origin	Route	Intensity [number of cercariae]	Duration [weeks]		post treatment [weeks]	Worm recovery	Egg burden	
Swiss TPH	NMRI	4	f	4	Liberia	<i>s.c.</i>	100	49	21	2–3	Perfusion (j.), Picking (ad.)	No	<i>a)</i>
LSHTM	CD1	5	f	5	Puerto Rico	<i>s.c.</i>	150	42	21	1–2	Perfusion	No	<i>b)</i>
UCSD/ UCSF	Swiss webster	3–6	f	3–6	Puerto Rico	<i>s.c.</i>	140–150	≥42	21	2	Perfusion	Yes	<i>c)</i>
TBRI	CD1	NR	m	10	Egypt	imm.	80	49	21	1d-2	Perfusion	Yes	<i>d)</i>
UNG	Balb/c, Swiss	3	NR	3–10	Brazil (BH)	imm., <i>s.c.</i>	70–80	≥42	21	2–3	Perfusion, Picking	Yes	<i>e)</i>
FIOCRUZ	Albino	NR	f	10	Brazil (LE)	<i>s.c.</i>	100	45	NR	1d-2	Perfusion	Yes	<i>f)</i>

The table summarizes characteristics of host mice, *S. mansoni* infection and evaluation methods employed by key institutions working on antischistosomal drug discovery and development.

Abbreviations: Swiss TPH: Swiss Tropical and Public Health Institute, Basel, Switzerland; LSHTM: London School of Hygiene and Tropical Medicine, London, United Kingdom; UCSD: Skaggs School of Pharmacy and Pharmaceutical Sciences, University of California San Diego, San Diego, USA; UCSF: University of California San Francisco, San Francisco, USA; TBRI: Theodor Bilharz Research Institute, Giza, Egypt; UNG: Universidade Guarulhos, Guarulhos, Brazil; FIOCRUZ: Laboratory of Schistosomiasis, Rene Rachou Research Center Fiocruz, Belo Horizonte, Brazil; BH: Belo Horizonte; imm.: tail (UNG) or body (TBRI) immersion; *s.c.*: subcutaneous; ad.: adult; j.: juvenile; Perfusion: reverse perfusion of the hepatic portal system; m: male; f: female; d: day; Ref.: Reference; NR: not reported.

References: (a): (Biendl et al., 2021; Lombardo et al., 2019a; Probst et al., 2020b). (b): (Gardner et al., 2021). (c): (Wolfe et al., 2018). (d): (Botros et al., 2020). (e): (de Moraes et al., 2014; Silva et al., 2017, 2021; Xavier et al., 2020). (f): (Castro et al., 2018; Katz et al., 2013).

largely unknown, but is likely to influence susceptibility to infection, parasite and disease development as well as drug pharmacokinetics (Bickle et al., 1980; Cheever et al., 1987), similar to mouse gender. Finally, insufficient reporting of mouse characteristics occasionally impedes complete appraisal of individual study methodology (Katz et al., 2013; Silva et al., 2021; Xavier et al., 2020).

Second, utilization of parasites of different isolate origin (described above) as well as infection route and dose. Although mouse body or tail immersion into a cercariae suspension was predominantly used, especially by groups from the Middle East and South America (Botros et al., 2020; de Moraes et al., 2014; Silva et al., 2017), *s.c.* infection nowadays is most commonly employed, likely due to the ease of application and higher control over the quantity of introduced parasites (Gardner et al., 2021; Lombardo et al., 2019a; Silva et al., 2021). Infection intensity varies between 70 and 150 applied cercariae per mouse rendering an optimized trade-off between worm yield and severity of disease responsibly for disease burden and stress of the animal subject.

Third, worm recovery methodology and drug effect evaluation. Worm burden reduction (WBR) is consensually considered as the main read-out for drug effect evaluation. Additionally, most groups, except the European groups at LSHTM and Swiss TPH, evaluate drug effect on egg reduction rate. Differential weighing of such additional read-outs in drug effect evaluation can provoke minor deviations in conclusions arising from consistent experimental results. Further, to accurately determine worm burden, worms need to be removed exhaustively from sacrificed mice and counted. While reverse perfusion of the hepatic portal system is the mainstay of adult worm recovery and the only practicable methodology for the recovery of the smaller juvenile worms, direct picking of adult worms from their dwelling site after mouse dissection provides equivalent results and offers an alternative procedure that is less time sensitive and offers the advantage that the hepatic shift can be determined. While most other of these identified variations are likely to affect experimental results only slightly, differences in mouse strain and gender are gateways for biologic variability potentially resulting in discrepancies between laboratories. However, especially the later differences in addition to utilization of parasite isolates of different origin offer the advantage of obtaining a broader coverage of naturally occurring pathogen and host disease variability and might thus improve translatability of laboratory examinations to real-world environments.



4. Infection intensity of the patent *S. mansoni* mouse model

As mentioned above, WBR is the main efficacy read-out employed in *in vivo* studies evaluating antischistosomal drug activity. Calculation of the WBR is based on the absolute worm count in infected and treated mice compared to infected, but untreated (vehicle control) mice (see for example Methods, 2.6 Data analysis in Supplementary Material in the online version at <https://doi.org/10.1016/bs.apar.2022.05.002>). Thus, the worm load of experimental mice might impact efficacy results and their statistical significance.

To better understand the underlying biological variation and statistical distribution of infection intensities achieved by *s.c.* infection with *S. mansoni* cercariae, we reanalysed adult worm yields from control mice studied in experiments conducted in our group during the last decade of continued research activity (see Methods in Supplementary Material in the online version at <https://doi.org/10.1016/bs.apar.2022.05.002>).

Infection intensity of the patent *S. mansoni* mouse model follows a linear correlation to the number of cercariae injected per mouse, where roughly every fourth *s.c.* injected cercarium develops into an adult worm (Fig. 2). At the most commonly employed infection dose for many years for drug activity studies in our laboratory of 100 cercariae per mouse, (Biendl et al., 2021; Probst et al., 2020b) our *S. mansoni* mouse model yields 22 adult worms on average. Adult worm infection intensity increases on average by 28 adults for every additional 100 cercariae injected, and this rate remains stable up to the maximally tested dose of 400 cercariae per mouse (Table S2 in Supplementary Material in the online version at <https://doi.org/10.1016/bs.apar.2022.05.002>). Our linear model is in good accordance with observations from other groups working in the field (see Table 1) (Castro et al., 2018; Gardner et al., 2021; Wolfe et al., 2018; Xavier et al., 2020). For other infection doses frequently employed in these laboratories, namely, 80 and 150 cercariae per mouse, our linear model estimates yields of *ca.* 17 and 36 adult worms, respectively. Notably, infection by whole body or tail appears to yield higher worm counts compared to *s.c.* infection (Botros et al., 2020; Silva et al., 2017).

Furthermore, our analysis revealed considerable variability/variation even at the most commonly employed infection dose of 100 cercariae, with yields ranging between 5 and 71 adult worms (interquartile range: 14,

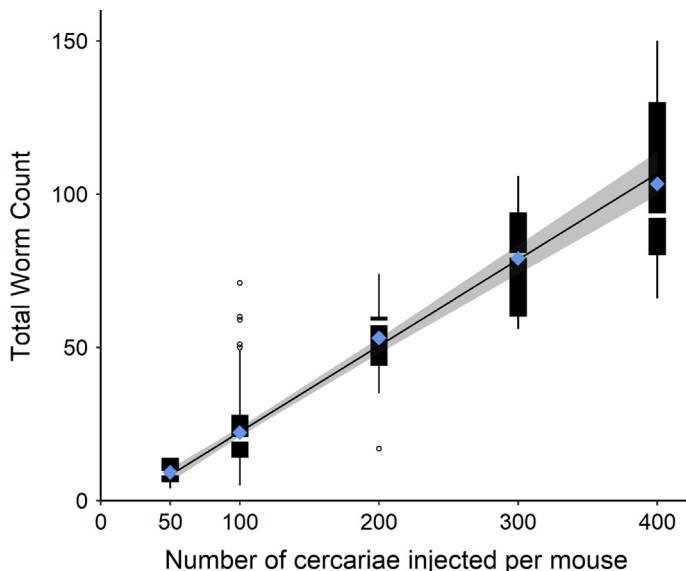


Fig. 2 Infection intensity of the patent *S. mansoni* mouse model. Boxplot depicting total worm count (worm burden) per mouse extracted from mice ($n = 9, 245, 23, 6, 6$) infected by s.c. injection of cercariae (50, 100, 200, 300, 400, respectively). Diamond points in light blue represent the mean of the distribution. The median is depicted as dividing white space between the 25th and 75th percentile in black. The whiskers extend to the minimum or maximum value in the data or to a maximal distance from the quartiles of $\pm 1.5 \times$ interquartile range (IQR) respectively. Dots represent potential outliers. The line represents the linear fit and the grey area shows the 95% confidence area of the fit.

$n = 245$). Factors acting as underlying causes for biological variability need to be carefully considered during experiment planning to improve comparability between studies. These factors include mouse age at infection linked to immune system maturity as well as mouse stress levels at infection and during worm development. Typically, young mice are infected after at least 1 week of acclimatization and before reaching an age of 6 weeks to improve susceptibility to infection (Lombardo et al., 2019a; Silva et al., 2021; Wolfe et al., 2018). Besides mouse acclimatization, training of the experimenter conducting infection is essential to reduce variation at infection. Finally, based on our experimental experience over the last decade, we suspect batch-to-batch variations in cercarial viability and virulence to be a key driver of inter-experiment variability that can seldom be detected or assessed prior to mouse infection.



5. Pharmacokinetic/pharmacodynamic (PK/PD) relationship of selected drugs

While it is well-known that PK/PD studies are often employed in the drug discovery pipeline for the majority of drugs, it has not been established whether there is a PK/PD correlation in the *S. mansoni* rodent models. The location of the worms should be kept in mind when discussing pharmacokinetics. While the adult worms are found in the mesenteric veins of the intestine (*S. mansoni* and *S. japonicum*) or the urinary plexus surrounding the bladder (*S. haematobium*), juvenile worms travel through the inferior vena cava to the heart, the left lung (and back to the heart) before entering the abdominal aorta and finally locating to the portal vasculature, where the parasites mature (Nation et al., 2020).

In the following section, we analyse and compare different drug candidates that were characterized by us and other research groups with regard to the relationship between pharmacokinetics and *in vivo* efficacy (Table 2) to better understand PK/PD relationships.

5.1 No correlation between praziquantel exposure and *in vivo* efficacy

As a Class II drug (Biopharmaceutical Classification System, BCS), praziquantel possess high permeability and a limited solubility, it undergoes slow absorption in the gut lumen and is marked by extensive first-pass metabolism in the liver by the cytochrome P450 system (Lindenberg et al., 2004). Praziquantel is rapidly cleared and has a short half-life (Olliaro et al., 2014). *In vitro*, the drug is fast acting and has an IC₅₀ value of approximately 0.1 μM after 72 h. Several years ago, our research group reported on the PK/PD relationship of praziquantel in the *S. mansoni* mouse model (Abla et al., 2017). Briefly, racemic praziquantel, given at a single oral dose of 400 mg/kg, resulted in worm burden reductions of 84–100% and the same applies for the levo enantiomer, which is consistent with the *R*-praziquantel being the pharmacologically active form of the drug (Abla et al., 2017; Lombardo et al., 2019b; Meister et al., 2014). Contrary, the *S*-praziquantel enantiomer, responsible for most of the bitter taste of the tablet (Meyer et al., 2009), did not reduce the worm burden in infected *S. mansoni* mice (WBR = 18%) (Meister et al., 2014). Abla and colleagues reported that plasma exposures of the active enantiomer were increased by 10- to 20-fold when 1-aminobenzotriazole (ABT), a pan-CYP inhibitor

Table 2 PK/PD relationship of antischistosomal compounds.

Chemical class	ID	Dose p.o. (mg/kg)	WBR (%)	T _{1/2} (h)	T _{max} (h)	C _{max} (μM)	AUC _{0-t} (μM ² h)	<i>In vitro</i> IC ₅₀ (μM) ^a	Mouse model: infected (gender, strain)	<i>In vitro</i> intr. Cl. (μL/ min/mg protein)	<i>In vitro</i> met. Stability (% rem.) ^b	<i>In vitro</i> cytotox. (μM) (cellline)	cLogP	violation of Limpinski's rule of 5	References	
Pyrazino-isoquinoline	PZQ	400	97			6.3 ^c	11.4 ^c	0.16	Yes (f, NMRI)				3.4	0	a)	
			84			11.7 ^c	12.0 ^c									
			100					0.10								
	PZQ	400	94													
	R-PZQ		100													
	S-PZQ		18													
	R-PZQ		84	3.3	0.8	8.6	20.2	0.06								
S-PZQ			4.7	0.8	1.6	5.8	18.9									
Aryl-methanols	a	200	72–80	183	12	19	1501	11	Yes (f, NMRI)			11.8 (L6)	3.7	0	b)	
				34	12	27	1332		No (f, NMRI)							
	b		83–93	182	24	14	2027	6	Yes (f, NMRI)			9.7 (L6)	4.4	0		
				72	48	19	2128		No (f, NMRI)							
Ozonides	c	400		39	2	459	22,463	66	No (f, NMRI)				4.8	0	c)	
				80					Yes (f, NMRI)							
9-acridanone hydrazone	d	100	96	17	0.5	4.6	127	85	Yes (f, Swiss Webster)	< 7 (HML)/< 7 (MLM)			4	0	d)	
		100 (i.p.)	99	20	0.5	6.3	126									
		50		5	3	21	254		No (m, Swiss outbreed)							
		12.5	100						Yes (f, NMRI)							
		25	99													

Continued

Table 2 PK/PD relationship of antischistosomal compounds.—cont'd

Chemical class	ID	Dose p.o. (mg/kg)	WBR (%)	T _{1/2} (h)	T _{max} (h)	C _{max} (μM)	AUC _{0-t} (μM*h)	<i>In vitro</i> IC ₅₀ (μM) ^a	Mouse model: infected (gender, strain)	<i>In vitro</i> intr. Cl. (μL/ min/mg protein)	<i>In vitro</i> met. Stability (% rem.) ^b	<i>In vitro</i> cytotox. (μM) (cellline)	cLogP	violation of Limpinski's rule of 5	References
Pyridobenz-imidazoles (1st gen.)	e	400	59					2.4	Yes (f, NMRI)		70 (MLM, 30 min)	9.6 (CHO)	5.6	1	e)
		20		3.2	2.3	1.2	12		No (NA, NA)						
		2 (i.v.)			6.6			5							
Pyridobenz-imidazoles (2nd gen.)	f	400	69					0.4	Yes (f, NMRI)		84 (MLM, 30 min) /	4.3 (CHO)	6.7	1	f)
		20		0.3	3	0.3	2 ^d		No (NA, C57B1/6)		97 (HML, 30 min)				
		2 (i.v.)			2.6			90 ^d							
N,N'-Diarylureas	g	400	15		24	22	389	0.3	Yes (f, NMRI)		80 (MLM, 60 min)	5.8 (L6)	5.3	1	g)
		100	24		24	12	209	0.3			70 (MLM, 60 min)	3.3 (L6)	5.5	1	
	i		36		24	25	353	0.3			105 (MLM, 60 min)	2.9 (L6)	5.5	1	
		20			113	24	8	500		No (f, NMRI)					
	j	400	0		25	3	171	691	0.1	Yes (f, NMRI)		63 (MLM, 60 min)	3.3 (L6)	4.6	0
N,N'-Diarylureas	k	100	40	11	4	31	394	0.2	Efficacy: yes (f, NMRI), PK: no (m, Swiss outbreak)	10 (HML) / 7 (MLM)		> 100 (U-20S, HEK293, HC-04)	5.8	1	h)
		20		10	4	40	953	0.9		<7 (HML) / <7 (MLM)			3.3	0	

	m	0	13	25	679	0.5	<7 (HML) / 12 (MLM)	6.2	1				
	n	37	2.7	4	31	216	0.9	<7 (HML) / 12 (MLM)	4.4	0			
	o	0			27	989	0.5	<7 (HML) / <7 (MLM)	6.1	1			
	p	50	18	7.5	56	1486	0.7	<7 (HML) / <7 (MLM)	4.7	0			
	q	2	2.3	2	20	175	3.3	<7 (HML) / <7 (MLM)	3.2	0			
	r	2			55	2273	0.8	<7 (HML) / 16 (MLM)	5.1	1			
Hydantoins	s	100			124	2740	>100	No (m, Swiss outbreak)	8 (HML) / <7 (MLM)	non-toxic up to 30 µM (L6)	2.1	0	i)
					95			Yes (f, NMRI)					
	t				30	1	488	1360	Efficacy: yes (f, NMRI), PK: no (m, Swiss outbreak)	<7 (HML) / <7 (MLM)	0	0	
	u				100	7	155	6480		<7 (HML) / <7 (MLM)	0.6	0	

Continued

Table 2 PK/PD relationship of antischistosomal compounds.—cont'd

Chemical class	ID	Dose p.o. (mg/kg)	WBR (%)	T _{1/2} (h)	T _{max} (h)	C _{max} (μM)	AUC _{0-t} (μM*h)	<i>In vitro</i> IC ₅₀ (μM) ^a	Mouse model: infected (gender, strain)	<i>In vitro</i> intr. Cl. (μL/ min/mg protein)	<i>In vitro</i> met. Stability (% rem.) ^b	<i>In vitro</i> cytotox. (μM) (cellline)	cLogP	violation of Limpinski's rule of 5	References	
Thiosulfuric acids	v	100	51 (m) / 83 (f)						Yes (f, Swiss Webster)	0.15–0.19 (MLM)		non-toxic up to 40 μM (BESM, C2C12, HuH-7)	2	0	j)	
		400	74 (m) / 100 (f)													
		100		1.3	0.5	2.4	4.9		No (f, Swiss Webster)							
		15 (i.v.)					8.7									
		m/z 210	100		5.8	4.0										
		m/z 210	15 (i.v.)			0.08										
Imidazo-pyrazines (and triazol-pyridines)	w	6.25	98			1.3 (24h conc)			Yes (f, CD1), juvenile infection		90 (MH, 90 min) 105 (HH, 90 min)		6.7	2	k)	
					90	1.9 (24h conc)	0.01	Yes (f, CD1), adult infection								
		0.5 (i.v.)		23.4		4.5 (inf.)		No (m, Swiss albino)								
		2.5				0.5 (24h conc.)										

Benzo-phenone	x	300 (for 5 days)	43–56				Yes (f, albino)	7.8	1	<i>l)</i>
		15	6.1	1	7	68.3	Yes (m, Swiss albino)			
			1.7	1.1	11.4	43.9	No (m, Swiss albino)			

^a*In vitro* assay, readout at 72h post-incubation.

^bMLM = mouse liver microsomes, HLM = human liver microsomes, MH = mouse hepatocytes, HH = human hepatocytes.

^cC_{max} and AUC of R-PZQ were measured.

^dAUC_{0-inf} was reported.

PK data (exact values) in infected *S. mansoni* were not published previously.

References: (a): (Abla et al., 2017; Lombardo et al., 2019b; Meister et al., 2014). (b): (Ingram et al., 2012; Ingram et al., 2013; Keiser et al., 2009). (C): (Keiser et al., 2012; Leonidova et al., 2016). (d): (Probst et al., 2020b). (e): (Okombo et al., 2017). (f): (Mayoka et al., 2019). (g): (Probst et al., 2021). (h): (Wu et al., 2018). (i): (Keiser et al., 2015; Wang et al., 2014; Wang et al., 2016). (j): (Wolfe et al., 2018). (k): (Gardner et al., 2021). (l): (Castro et al., 2018).

was administered prior to praziquantel, however, the increased total exposure was not predictive for the *in vivo* efficacy. The authors further evaluated the exposure levels of praziquantel given after a pre-treatment with dexamethasone (DEX), a CYP-inhibitor. Despite a 10-fold decrease in systemic plasma exposure the *in vivo* efficacy was maintained. These results led to the conclusion that the estimated portal vein concentration (in contrast to the systemic concentration), is a good predictor for the efficacy of praziquantel in the adult *S. mansoni* mouse model (Abla et al., 2017). Lombardo and colleagues, in another study, presented exposure parameters not only for R-praziquantel but also for the S-enantiomer, which had a 3.5 times lower AUC as well as a 5 times lower c_{\max} but reached the maximal concentration at the same time (t_{\max}) as its counterpart (Lombardo et al., 2019b). Also here, no correlation between exposure parameters and activity was observed, confirming S-praziquantel's lack of efficacy.

It is possible that the reason for the lack of efficacy of praziquantel against juvenile worms is due to a low concentration of praziquantel at the worm location sites. We therefore investigated whether pre-treatment with ABT and DEX, results in increased/decreased efficacy of praziquantel in mice infected with juvenile *S. mansoni* worms (7- and 21-days after infection) (Table 3). Without pre-treatment, a single oral 400 mg/kg dose of praziquantel resulted in the expected, low median WBRs of 27 and 43% at day 7 and 21 post-infection, respectively, when compared to infected but untreated controls. The same dose usually results in approximately 80–100% WBRs when adult *S. mansoni* infected mice are treated with praziquantel (Meister et al., 2014). WBRs did not change significantly, when ABT or DEX were administered prior to praziquantel (Table 3). Plasma exposure values were not measured, as we expected to achieve similar levels as determined by Abla and colleagues (Abla et al., 2017) irrespective of the time point of infection. Our findings suggest that despite increasing praziquantel plasma exposure efficacy against juvenile infections cannot be improved. Moreover, our results support findings from an old study by Gönnert and Andrews that demonstrated that even at a high concentration of 1000 mg/kg praziquantel, juvenile *S. mansoni* infections could not be cleared (Gönnert and Andrews, 1977) in experimentally infected mice (Fig. 3).

5.2 Chronic *S. mansoni* infection influences exposure parameters of drugs

Many factors influence the efficacy of a drug. As such, host, parasite and drug-related factors are important contributors in either increasing or

Table 3 PZQ efficacy studies in infected *S. mansoni* (juvenile) with and without the CYP inhibitor/inducer, ABT/DEX

Pre-treatment:		Start of pre-treatment (days after infection)	Treatment: PZQ dose (p.o., mg/kg)	Start of treatment (days after infection)	WBR % (median, range) ^c	Nr of mice included in analysis
Pre-treatment: ABT dose (p.o., mg/kg) ^a	DEX dose (i.p., mg/ kg) ^b					
					0	8
			400	7	27 (7–48)	4
50		7	400	7 (+2h)	39 (27–48)	4
	100 (i.p.)	7–9	400	10	46 (27–59)	4
			400	21	43 (27–59)	4
50		21	400	21 (+2h)	46 (27–59)	4
	100 (i.p.)	21–23	400	24	56 (38–69)	4

^aABT = 1-aminobenzotriazole.

^bDEX = dexamethasone.

^cWBR = worm burden reduction.

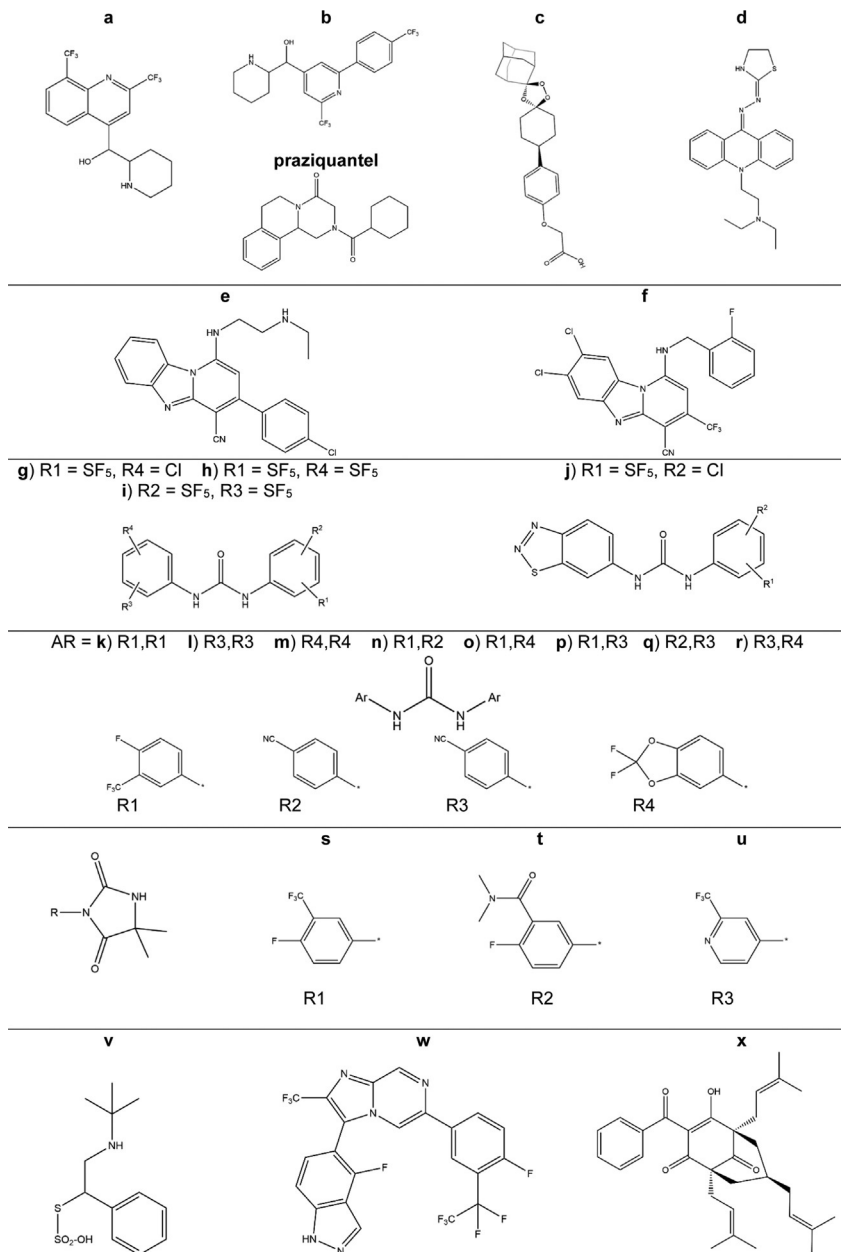


Fig. 3 Chemical structures of compounds a – x and praziquantel.

decreasing the *in vivo* efficacy. Given that the liver and thus hepatic metabolism are strongly affected by chronic schistosomiasis due to *S. mansoni* infections, an increase or a decrease of total plasma concentration may be assumed depending on the drug and its active form (parent compound or metabolite). We identified data of five experimental compounds, which compared PK profiles of infected *vs* non-infected groups of mice namely, mefloquine (a) (Ingram et al., 2013), enpiroline (b) (Ingram et al., 2013), Ro 15-5458 (d) (Probst et al., 2020b), a *N,N'* diarylurea (i) (Probst et al., 2021) and the natural compound 7-epiclusianone (7-epi) (x) (Castro et al., 2018). The studies reported a considerable increase in half-life (exposure time) for all compounds when infected mice received drug treatment. However, while the observed AUC (measured systemic exposure) was not affected when (a) and (b) were administered to infected mice, there was a decrease in AUC for (d) and (i) and an increase for (x) when administered to infected mice. Given the two-sided influence (increase and decrease in exposure parameters) of herein presented drugs, it would be interesting to study how far the infection status (e.g. the degree of inflammation of the gut wall) influences drug absorption (leading to delayed peaking of the drug).

5.3 Prolonged drug exposure well above *in vitro* potency not always correlates with good *in vivo* efficacy

While the infection status of mice employed in the above-mentioned PK studies was responsible for differences observed in some of the drug related exposure parameters, this was not the case for all studies analysed, exemplified by the imidazopyrazines (w). Moreover, neither mouse gender nor mouse strain appeared to play a role in influencing exposure parameters of (w). Plasma concentrations 24h after drug administration seemed to be predictive for the efficacy of the imidazopyrazines in the mouse model given it was at least fivefold higher when compared to the *in vitro* adult worm blood potency. Although it was not possible to determine whether AUC or plasma concentration after 24h better correlated with the *in vivo* efficacy, the study demonstrated that for this series of compounds it was important to achieve plasma concentrations after 24h in the animal model at least fivefold higher than the calculated blood potency *in vitro* (Gardner et al., 2021).

Two other drug classes represented by the drug candidates (c) and (e, f), which were first studied for their antimalarial activity, show—to some extent—a correlation between exposure and *in vivo* activity. On one hand, a prolonged drug exposure with plasma levels well above the *in vitro* IC₅₀

value is likely responsible for the *in vivo* efficacy of the ozonide (c); on the other hand, investigations on the pyridobenzimidazoles (PBIs) (e) and (f) point to suboptimal drug exposure due to solubility-limited absorption.

OZ418 (c), a synthetic alternative to the antimalarial drug artemisinin, demonstrated significant worm killing against the three main *Schistosoma* species, and most importantly, the juvenile stage of the infection (Keiser et al., 2012; Panic and Keiser, 2018; Xiao et al., 2007). OZ418 reached maximal concentration levels after approximately 2 h post-dosing in non-infected mice, and had an extensive half-life ($t_{1/2} = 39$ h) (Leonidova et al., 2016). The slow clearance and hence the prolonged drug circulation as well as the fact that plasma levels ($AUC = 22,463 \mu\text{M}$) remained above the IC_{50} value ($66 \mu\text{M}$) observed for *S. mansoni in vitro* is most probably responsible for the *in vivo* efficacy (Leonidova et al., 2016). Similar to OZ418, worm-killing driven by the antimalarial mefloquine (a) is rather exposure-dependent (AUC) than c_{max} driven (Ingram et al., 2013).

First studied against *P. falciparum* (Ndakala et al., 2011), three series of PBIs (Mayoka et al., 2019; Okombo et al., 2017; Probst et al., 2020a) have been evaluated for their potential against *S. mansoni in vitro* and in experimentally infected mice (Mayoka et al., 2019; Okombo et al., 2017; Probst et al., 2020a). In short, these studies found potent *in vitro* activities against NTS and adult *S. mansoni*. Worm burden reductions of 60% and 70% were obtained for the best compounds from the first and second generation PBIs, respectively, after a single oral 400 mg/kg dose. Further, both studies engaged in PK evaluations and reported solubility-limited absorption (delayed peaking of plasma concentration) and a short half-life due to high hepatic clearance (Mayoka et al., 2019; Okombo et al., 2017). While the first set of PBIs, exemplified by (e) observed high variability in oral bioavailability ($F = 25$ (14–42) %), the second generation PBIs, exemplified by (f) reported bioavailability being lower than 1%. This together with the high clearance rate of tested drugs, suggests that exposure is insufficient and thus the compounds fail to exhaust their worm-killing potential. As no PK study was conducted along the efficacy studies for third generation PBIs (Probst et al., 2020a), no conclusion on the PK/PD relationship can be drawn from the latest investigations.

On the other hand, two studies that evaluated the antischistosomal properties of the diarylureas (g–j) (Probst et al., 2021) and (k–r) (Wu et al., 2018) found no correlation between *in vivo* efficacy and exposure parameters. Interestingly, with exception of (j), drug absorption for all tested *N*, *N'*-diarylureas was delayed (most likely due to low aqueous solubility)

and c_{\max} was only reached 24 h after administration, irrespective of the infection status and dose (i) (Probst et al., 2021). Wu and coworkers (Wu et al., 2018) found only low and moderate *in vivo* efficacy of diarylureas with WBRs ranging from 0% to 50% after single oral doses of 100 mg/kg. PK parameters were only investigated in non-infected mice. Although c_{\max} values were an order of magnitude greater than IC_{50} values obtained *in vitro* no correlation between exposure and *in vivo* efficacy was found. While Wu and colleagues argue that even though high plasma concentrations are maintained over a prolonged period, the drug might not be available in its unbound form to exert its effect at the site of action.

5.4 Special cases

For the hydantoin Ro 13-3978 (s) and its analogues (t, u) PK studies were performed separate from efficacy studies, using non-infected mice. While Ro 13-3978 was quickly absorbed, the clearance process was saturated, and high drug exposure was observed over 24 h. Two derivatives, which are quickly metabolized to Ro 13-3978 (rapid decline in parent concentration and thus low c_{\max} and AUC values), confirmed the drug's excellent *in vivo* efficacy with comparable WBRs. With other compounds, exemplified by (u), reaching high exposure rates over a prolonged time (similar to (s)), the hydantoins' antischistosomal drug action seems to be rather exposure dependent than c_{\max} driven ((t) reached the highest maximal plasma concentration but was the least effective drug with regard to WRB) (Wang et al., 2016). However, compared to all herein discussed drugs, the hydantoins present a unique class of antischistosomal lead candidates: they are highly efficacious *in vivo* but completely lack *in vitro* activity. Therefore, a host-mediated mechanism of action involving cell recruitment is proposed (Panic et al., 2017), which requires further experimental confirmation.

A drug that showed no activity *in vitro* against *S. mansoni* but possessed a broad efficacy spectrum against all developmental stages of the parasite *in vivo*, is TPT sulfonate (v), a thiosulfate drug. In fact, not the parent compounds, but a non-toxic metabolite (TP thiol, *m/z* 210) is responsible for its antischistosomal activity (Wolfe et al., 2018). In a PK study, non-infected mice were dosed with TPT orally (100 mg/kg) and intravenously (15 mg/kg), respectively. The drug was shown to be rapidly absorbed ($t_{\max} = 0.5$ h for the parent compound (p.o.), 4 h (p.o.) and 0.08 h (i.v.) for the *m/z* 210 metabolite) and extensively metabolized (non-CYP-mediated, first-pass metabolism) (Box 2).

BOX 2 Outstanding Questions

- Do compounds that have further advanced the antischistosomal drug discovery cascade act differently against *S. mansoni* of different isolate origin and can we deduct information on drug mechanism of action from potential differences?
- What is the influence of mouse strain and gender on drug efficacy and drug pharmacokinetics in the patent *S. mansoni* mouse model?
- How can suspect batch-to-batch variations in cercarial viability and virulence be detected, assessed or reduced prior to mouse infection to limit inter-experiment variability of infection intensity?
- Are extrapolated portal vein concentrations more predictive of an optimal *in vivo* efficacy than systemic plasma concentrations for antischistosomal drugs in general?
- Which PK parameter(s) correlate best with the *in vivo* efficacy and is it possible to establish a rule of thumb to decide early on advancing antischistosomal drug candidates in the pipeline according to their PK profile?
- For which drug candidates would a PK assessment in infected mice be more predictive than in healthy mice?



6. Concluding remarks

With early antischistosomal drug discovery gaining momentum in recent years, translation of isolated *in vitro* and early *in vivo* experimental findings to a generalizable desired molecular product profile becomes increasingly important. To guide appraisal and comparison of findings generated by the key drivers of *in vivo* antischistosomal drug efficacy research, we summarized characteristics of the *S. mansoni* mouse model. Patent infection intensity follows a linear correlation to the number of *s.c.* injected cercariae and is well understood, however, causes for batch-to-batch variations in cercarial viability and virulence as well as the influence of mouse strain and gender on drug efficacy and drug pharmacokinetics remains largely unknown (see outstanding questions).

From the studies analysed, a trend towards prolonged drug exposure, but not a generally high systemic plasma exposure (c_{\max}) seem to be predictive for an optimal activity. The maximal concentration as such may not be driving the *in vivo* efficacy; however, some of the herein presented findings suggest that the measured plasma concentrations need to be maintained above

the *in vitro* IC₅₀ values for a prolonged time period. In this regard it would be interesting to study by which factor and for how long the drug concentration need to be above the *in vitro* IC₅₀ value or whether the plasma concentration at 24 h post-dosing (as proposed by [Gardner et al., 2021](#)) offers a better prediction/approach. Further, looking at extrapolated portal vein concentrations could be interesting, knowing that at least for praziquantel's efficacy this parameter appears to be crucial in *S. mansoni* infected mice.

Circadian changes, both in the parasite as well as in the host, represent a factor that was not discussed in this review (as none of the analysed studies contained further information or experiments covering this point) but may have an influence on the pharmacokinetics and pharmacodynamics. Although a recent study identified daily rhythms in the transcriptomes of adult *S. mansoni*, it was surprising to learn that some of the core clock genes (conserved across a wide range of animals) were lacking ([Rawlinson et al., 2021](#)). However, the potential involvement of the 24-h rhythmic environment of the mammalian host in metabolism and pharmacokinetic processes and thus chrono-efficacy or chrono-toxicity ([Dong et al., 2020](#)) must be kept in mind when discussing PK/PD relationships of antischistosomal drugs. In order to obtain more information on interesting leads early in the discovery process, PK studies could be integrated when first entering animal testing with hits identified from *in vitro* studies. Not only would this approach reduce the use of animals following the 3R rule (as the same group of mice is used for efficacy and PK evaluation) but allows to study the drug of interest in a more realistic setting. Further, time course and exposure levels in infected animals may give a hint on unexpected outcomes such as toxicity. Finally, these studies can inform on dosing and administration strategies and together with data on physical-chemical properties (e.g. solubility, permeability, etc.), SAR programs, *in vitro* studies (activity, cytotoxicity, metabolism) and *in vivo* evaluations (efficacy), pave the way to new and/or optimized antischistosomal drugs.

Acknowledgements and funding

We gratefully acknowledge financial support from the Swiss National Science Foundation (No. 320030_175585).

References

Abla, N., Keiser, J., Vargas, M., Reimers, N., Haas, H., Spangenberg, T., 2017. Evaluation of the pharmacokinetic-pharmacodynamic relationship of praziquantel in the *Schistosoma mansoni* mouse model. *PLoS Negl. Trop. Dis.* 11 (9), e0005942.

- Berger, D.J., Crellen, T., Lamberton, P.H.L., Allan, F., Tracey, A., Noonan, J.D., Kabatereine, N.B., Tukahebwa, E.M., Adriko, M., Holroyd, N., Webster, J.P., Berriman, M., Cotton, J.A., 2021. Whole-genome sequencing of *Schistosoma mansoni* reveals extensive diversity with limited selection despite mass drug administration. *Nat. Commun.* 12 (1), 4776.
- Bickle, Q., Long, E., James, E., Doenhoff, M., Festing, M., 1980. *Schistosoma mansoni*: influence of the mouse host's sex, age, and strain on resistance to reinfection. *Exp. Parasitol.* 50 (2), 222–232.
- Biendl, S., Haberli, C., Keiser, J., 2021. Discovery of novel antischistosomal scaffolds from the open access pandemic response box. *Expert Rev. Anti Infect. Ther.*, 1–9.
- Botros, S.S., El-Lakkany, N.M., Seif El-Din, S.H., William, S., Sabra, A.N., Hammam, O.A., de Koning, H.P., 2020. The phosphodiesterase-4 inhibitor roflumilast impacts *Schistosoma mansoni* ovipositing in vitro but displays only modest antischistosomal activity in vivo. *Exp. Parasitol.* 208, 107793.
- Castro, A.P., Kawano, T., Spelta, L.E.W., de Castro, A.T., Pereira, N.A., Couto, F.F.B., Dos Santos, M.H., Boralli, V.B., Marques, M.J., 2018. In vivo schistosomicidal activity of 7-epiclusianone and its quantification in the plasma of healthy and *Schistosoma mansoni* infected mice using UPLC-MS/MS. *Phytomedicine* 38, 66–73.
- Cheever, A.W., Duvall, R.H., Hallack Jr., T.A., Minker, R.G., Malley, J.D., Malley, K.G., 1987. Variation of hepatic fibrosis and granuloma size among mouse strains infected with *Schistosoma mansoni*. *Am. J. Trop. Med. Hyg.* 37 (1), 85–97.
- Colley, D.G., Bustinduy, A.L., Secor, W.E., King, C.H., 2014. Human schistosomiasis. *Lancet* 383 (9936), 2253–2264.
- de Moraes, J., de Oliveira, R.N., Costa, J.P., Junior, A.L., de Sousa, D.P., Freitas, R.M., Allegretti, S.M., Pinto, P.L., 2014. Phytol, a diterpene alcohol from chlorophyll, as a drug against neglected tropical disease schistosomiasis mansoni. *PLoS Negl. Trop. Dis.* 8 (1), e2617.
- Dong, D., Yang, D., Lin, L., Wang, S., Wu, B., 2020. Circadian rhythm in pharmacokinetics and its relevance to chronotherapy. *Biochem. Pharmacol.* 178, 114045.
- Doyle, S.R., Cotton, J.A., 2019. Genome-wide approaches to investigate anthelmintic resistance. *Trends Parasitol.* 35 (4), 289–301.
- Dziwornu, G.A., Attram, H.D., Gachuhi, S., Chibale, K., 2020. Chemotherapy for human schistosomiasis: how far have we come? What's new? Where do we go from here? *RSC Med. Chem.* 11 (4), 455–490.
- Eloi-Santos, S., Olsen, N.J., Correa-Oliveira, R., Colley, D.G., 1992. *Schistosoma mansoni*: mortality, pathophysiology, and susceptibility differences in male and female mice. *Exp. Parasitol.* 75 (2), 168–175.
- Gardner, J.M.F., Mansour, N.R., Bell, A.S., Helmby, H., Bickle, Q., 2021. The discovery of a novel series of compounds with single-dose efficacy against juvenile and adult *Schistosoma* species. *PLoS Negl. Trop. Dis.* 15 (7), e0009490.
- Gönnert, R., Andrews, P., 1977. Praziquantel, a new broad-spectrum antischistosomal agent. *Z. Parasitenkd.* 52 (2), 129–150.
- Gower, C.M., Gouvas, A.N., Lamberton, P.H., Deol, A., Shrivastava, J., Mutombo, P.N., Mbuh, J.V., Norton, A.J., Webster, B.L., Stothard, J.R., Garba, A., Lamine, M.S., Kariuki, C., Lange, C.N., Mkoji, G.M., Kabatereine, N.B., Gabrielli, A.F., Rudge, J.W., Fenwick, A., Sacko, M., Demele, R., Lwambo, N.J., Tchuente, L.A., Rollinson, D., Webster, J.P., 2013. Population genetic structure of *Schistosoma mansoni* and *Schistosoma haematobium* from across six sub-Saharan African countries: implications for epidemiology, evolution and control. *Acta Trop.* 128 (2), 261–274.
- Ingram, K., Ellis, W., Keiser, J., 2012. Antischistosomal activities of mefloquine-related arylmethanols. *Antimicrob. Agents Chemother.* 56 (6), 3207–3215.

- Ingram, K., Duthaler, U., Vargas, M., Ellis, W., Keiser, J., 2013. Disposition of mefloquine and enpiroline is highly influenced by a chronic *Schistosoma mansoni* infection. *Antimicrob. Agents Chemother.* 57 (9), 4506–4511.
- Katz, N., Couto, F.F., Araujo, N., 2013. Imatinib activity on *Schistosoma mansoni*. *Mem. Inst. Oswaldo Cruz* 108 (7), 850–853.
- Keiser, J., Chollet, J., Xiao, S.H., Mei, J.Y., Jiao, P.Y., Utzinger, J., Tanner, M., 2009. Mefloquine—an aminoalcohol with promising antischistosomal properties in mice. *PLoS Negl. Trop. Dis.* 3 (1), e350.
- Keiser, J., Ingram, K., Vargas, M., Chollet, J., Wang, X., Dong, Y., Vennerstrom, J.L., 2012. In vivo activity of aryl ozonides against *Schistosoma* species. *Antimicrob. Agents Chemother.* 56 (2), 1090–1092.
- Keiser, J., Panic, G., Vargas, M., Wang, C., Dong, Y., Gautam, N., Vennerstrom, J.L., 2015. Aryl hydantoin Ro 13-3978, a broad-spectrum antischistosomal. *J. Antimicrob. Chemother.* 70 (6), 1788–1797.
- King, C.H., 2010. Parasites and poverty: the case of schistosomiasis. *Acta Trop.* 113 (2), 95–104.
- Leonidova, A., Vargas, M., Huwyler, J., Keiser, J., 2016. Pharmacokinetics of the antischistosomal lead ozonide OZ418 in uninfected mice determined by liquid chromatography–tandem mass spectrometry. *Antimicrob. Agents Chemother.* 60 (12), 7364–7371.
- Lindenberg, M., Kopp, S., Dressman, J.B., 2004. Classification of orally administered drugs on the World Health Organization model list of essential medicines according to the biopharmaceutics classification system. *Eur. J. Pharm. Biopharm.* 58 (2), 265–278.
- Lombardo, F.C., Pasche, V., Panic, G., Endriss, Y., Keiser, J., 2019a. Life cycle maintenance and drug-sensitivity assays for early drug discovery in *Schistosoma mansoni*. *Nat. Protoc.* 14, 461–481.
- Lombardo, F.C., Perissutti, B., Keiser, J., 2019b. Activity and pharmacokinetics of a praziquantel crystalline polymorph in the *Schistosoma mansoni* mouse model. *Eur. J. Pharm. Biopharm.* 142, 240–246.
- Maccesi, M., Aguiar, P.H.N., Pasche, V., Padilla, M., Suzuki, B.M., Montefusco, S., Abagyan, R., Keiser, J., Mourão, M.M., Caffrey, C.R., 2019. Multi-center screening of the pathogen box collection for schistosomiasis drug discovery. *Parasit. Vectors* 12 (1), 493.
- Mayoka, G., Keiser, J., Häberli, C., Chibale, K., 2019. Structure–activity relationship and in vitro absorption, distribution, metabolism, excretion, and toxicity (ADMET) studies of N-aryl 3-trifluoromethyl pyrido[1,2-a]benzimidazoles that are efficacious in a mouse model of schistosomiasis. *ACS Infect. Dis.* 5 (3), 418–429.
- Meister, I., Ingram-Sieber, K., Cowan, N., Todd, M., Robertson, M.N., Meli, C., Patra, M., Gasser, G., Keiser, J., 2014. Activity of praziquantel enantiomers and main metabolites against *Schistosoma mansoni*. *Antimicrob. Agents Chemother.* 58 (9), 5466–5472.
- Meyer, T., Sekljic, H., Fuchs, S., Bothe, H., Schollmeyer, D., Miculka, C., 2009. Taste, a new incentive to switch to (R)-praziquantel in schistosomiasis treatment. *PLoS Negl. Trop. Dis.* 3 (1), e357.
- Nakazawa, M., Fantappie, M.R., Freeman, G.L., Jr., Eloi-Santos, S., Olsen, N.J., Kovacs, W.J., Secor, W.E., Colley, D.G., 1997. *Schistosoma mansoni*: susceptibility differences between male and female mice can be mediated by testosterone during early infection. *Exp. Parasitol.* 85 (3), 233–240.
- Nation, C.S., Da'dara, A.A., Marchant, J.K., Skelly, P.J., 2020. Schistosome migration in the definitive host. *PLoS Negl. Trop. Dis.* 14 (4), e0007951.
- Ndakala, A.J., Gessner, R.K., Gitari, P.W., October, N., White, K.L., Hudson, A., Fakorede, F., Shackelford, D.M., Kaiser, M., Yeates, C., Charman, S.A., Chibale, K., 2011. Antimalarial Pyrido[1,2-a]benzimidazoles. *J. Med. Chem.* 54 (13), 4581–4589.

- Okombo, J., Singh, K., Mayoka, G., Ndubi, F., Barnard, L., Njogu, P.M., Njoroge, M., Gibbard, L., Brunschwig, C., Vargas, M., Keiser, J., Egan, T.J., Chibale, K., 2017. Antischistosomal activity of pyrido[1,2-a]benzimidazole derivatives and correlation with inhibition of beta-hematin formation. *ACS Infect. Dis.* 3 (6), 411–420.
- Olliaro, P., Delgado-Romero, P., Keiser, J., 2014. The little we know about the pharmacokinetics and pharmacodynamics of praziquantel (racemate and R-enantiomer). *J. Antimicrob. Chemother.* 69 (4), 863–870.
- Panic, G., Keiser, J., 2018. Acting beyond 2020: better characterization of praziquantel and promising antischistosomal leads. *Curr. Opin. Pharmacol.* 42, 27–33.
- Panic, G., Vargas, M., Scandale, I., Keiser, J., 2015. Activity profile of an FDA-approved compound library against *Schistosoma mansoni*. *PLoS Negl. Trop. Dis.* 9 (7), e0003962.
- Panic, G., Ruf, M.T., Keiser, J., 2017. Immunohistochemical investigations of treatment with Ro 13-3978, praziquantel, oxamniquine, and mefloquine in *Schistosoma mansoni*-infected mice. *Antimicrob. Agents Chemother.* 61 (12).
- Park, S.K., Marchant, J.S., 2020. The journey to discovering a flatworm target of praziquantel: a Long TRP. *Trends Parasitol.* 36 (2), 182–194.
- Pasche, V., Laleu, B., Keiser, J., 2018. Early antischistosomal leads identified from *in vitro* and *in vivo* screening of the Medicines for Malaria Venture Pathogen Box. *ACS Infect Dis.* 5 (1), 102–110.
- Probst, A., Chisanga, K., Dziwornu, G.A., Haeberli, C., Keiser, J., Chibale, K., 2020a. Expanding the activity profile of pyrido[1,2-a]benzimidazoles: synthesis and evaluation of novel N1-1-Phenylethanamine derivatives against *Schistosoma mansoni*. *ACS Infect. Dis.* 7 (5), 1032–1043.
- Probst, A., Häberli, C., Siegel, D., Huang, J., Vigneron, S., Ta, A.P., Skinner, D.E., El-Sakkary, N., Momper, J.D., Gangoiti, J., Dong, Y., Vennerstrom, J.L., Charman, S.A., Caffrey, C.R., Keiser, J., 2020b. Efficacy, metabolism and pharmacokinetics of Ro 15-5458, a forgotten schistosomicidal 9-acridanone hydrazone. *J. Antimicrob. Chemother.* 75 (10), 2925–2932.
- Probst, A., Pujol, E., Häberli, C., Keiser, J., Vázquez, S., 2021. *In vitro*, *in vivo*, and ADME evaluation of SF(5)-containing *N,N'*-diarylureas as antischistosomal agents. *Antimicrob. Agents Chemother.* 65 (10) (Aac0061521).
- Rawlinson, K.A., Reid, A.J., Lu, Z., Driguez, P., Wawer, A., Coghlan, A., Sankaranarayanan, G., Buddenborg, S.K., Soria, C.D., McCarthy, C., Holroyd, N., Sanders, M., Hoffmann, K.F., Wilcockson, D., Rinaldi, G., Berriman, M., 2021. Daily rhythms in gene expression of the human parasite *Schistosoma mansoni*. *BMC Biol.* 19 (1), 255.
- Silva, M.P., de Oliveira, R.N., Mengarda, A.C., Roquini, D.B., Allegretti, S.M., Salvadori, M.C., Teixeira, F.S., de Sousa, D.P., Pinto, P.L.S., da Silva Filho, A.A., de Moraes, J., 2017. Antiparasitic activity of nerolidol in a mouse model of schistosomiasis. *Int. J. Antimicrob. Agents* 50 (3), 467–472.
- Silva, M.P., Silva, T.M., Mengarda, A.C., Salvadori, M.C., Teixeira, F.S., Alencar, S.M., Luz Filho, G.C., Bueno-Silva, B., de Moraes, J., 2021. Brazilian red propolis exhibits antiparasitic properties *in vitro* and reduces worm burden and egg production in a mouse model harboring either early or chronic *Schistosoma mansoni* infection. *J. Ethnopharmacol.* 264, 113387.
- Spangenberg, T., 2021. Alternatives to praziquantel for the prevention and control of schistosomiasis. *ACS Infect. Dis.* 7 (5), 939–942.
- Stroehlein, A.J., Korhonen, P.K., Lee, V.V., Ralph, S.A., Mentink-Kane, M., You, H., McManus, D.P., Tchuente, L.T., Stothard, J.R., Kaur, P., Dudchenko, O., Aiden, E.L., Yang, B., Yang, H., Emery, A.M., Webster, B.L., Brindley, P.J., Rollinson, D., Chang, B.C.H., Gasser, R.B., Young, N.D., 2022. Chromosome-level genome of *Schistosoma haematobium* underpins genome-wide explorations of molecular variation. *PLoS Pathog.* 18 (2), e1010288.

- Wang, C., Zhao, Q., Min, J., Muniyan, S., Vargas, M., Wang, X., Dong, Y., Guy, R.K., Lin, M.-F., Keiser, J., Vennerstrom, J.L., 2014. Antischistosomal versus antiandrogenic properties of aryl hydantoin Ro 13-3978. *Am. J. Trop. Med. Hyg.* 90 (6), 1156–1158.
- Wang, C., Zhao, Q., Vargas, M., Jones, J.O., White, K.L., Shackleford, D.M., Chen, G., Saunders, J., Ng, A.C., Chiu, F.C., Dong, Y., Charman, S.A., Keiser, J., Vennerstrom, J.L., 2016. Revisiting the SAR of the antischistosomal aryl hydantoin (Ro 13-3978). *J. Med. Chem.* 59 (23), 10705–10718.
- WHO, 2020. Ending the neglect to attain the sustainable development goals: A road map for neglected tropical diseases 2021–2030. WHO.
- Wolfe, A.R., Neitz, R.J., Burlingame, M., Suzuki, B.M., Lim, K.C., Scheideler, M., Nelson, D.L., Benet, L.Z., Caffrey, C.R., 2018. TPT sulfonate, a single, oral dose schistosomicidal prodrug: In vivo efficacy, disposition and metabolic profiling. *Int. J. Parasitol. Drugs Drug Resist.* 8 (3), 571–586.
- Wu, J., Wang, C., Leas, D., Vargas, M., White, K.L., Shackleford, D.M., Chen, G., Sanford, A.G., Hemsley, R.M., Davis, P.H., Dong, Y., Charman, S.A., Keiser, J., Vennerstrom, J.L., 2018. Progress in antischistosomal N,N'-diaryl urea SAR. *Bioorg. Med. Chem. Lett.* 28 (3), 244–248.
- Xavier, R.P., Mengarda, A.C., Silva, M.P., Roquini, D.B., Salvadori, M.C., Teixeira, F.S., Pinto, P.L., Morais, T.R., Ferreira, L.L.G., Andricopulo, A.D., de Moraes, J., 2020. H1-antihistamines as antischistosomal drugs: *in vitro* and *in vivo* studies. *Parasit. Vectors* 13 (1), 278.
- Xiao, S.-H., Keiser, J., Chollet, J., Utzinger, J., Dong, Y., Endriss, Y., Vennerstrom, J.L., Tanner, M., 2007. *In vitro* and *in vivo* activities of synthetic trioxolanes against major human schistosome species. *Antimicrob. Agents Chemother.* 51 (4), 1440–1445.

8.2 Insights into praziquantel pharmacokinetics of *O. felineus* infected patients

Although praziquantel is the drug of choice for the treatment of opisthorchiasis and thus widely used in *O. felineus* infected patients, very little is known about its disposition. Moreover, until recently, only limited knowledge on the *in vitro* activity and *in vivo* efficacy was available. Studies investigating these questions have shown that PZQ leads to tegumental destruction of the worm, inducing contractions of the musculature and subsequent paralysis. Single oral doses of 400 mg/kg led to worm burden reductions of 70-80 % in hamsters harboring acute and chronic infections (Pakharukova et al. 2015). Avgustinovich and coworkers launched comparative *in vitro* studies, exploring the activity of racemic praziquantel, *R*-PZQ and *S*-PZQ *in vitro*. They found that *R*-PZQ exhibited the highest activity towards both, juvenile and adult worms of *O. felineus* (Avgustinovich et al. 2020).

Given that no standardized treatment scheme for *O. felineus* infected patients is available, it was our aim to compare the PK properties of single ascending doses of PZQ in contrast to multiple doses. Our study was embedded in a randomized controlled, single-blinded dose finding trial in Tomsk, Siberia. Summarizing, we found a positive correlation of exposure metrics (AUC, c_{max}) and dose (20, 40 60 and 3x20 mg/kg). Highest systemic drug exposure (AUC) was reported for patients treated with three doses of 20 mg/kg, while a single oral 60 mg/kg dose led to highest maximal plasma concentration (c_{max}). Also, drug exposure seemed to be influenced by the infection status as suggested by several studies (Lima et al. 2011; Mandour et al. 1990; el Guiniady et al. 1994; Ofori-Adjei, Adjepon-Yamoah, and Lindström 1988). Interestingly, a study by Meister and colleagues found that, on one hand, exposure levels of *R*- and *S*-PZQ were lower, and on the other hand, the *R-trans*-OH-PZQ levels were higher in patients that were infected with *O. viverrini* in contrast to the results obtained from our study with *O. felineus* patients (Meister et al. 2016). These results might be explained by the infection intensity, genetic polymorphisms of liver enzymes involved in drug metabolism (patients from Southeast Asia vs. Russian Federation), as well as more obvious factors, such as the use of different formulations or food effects (Zdesenko and Mutapi 2020). However, in

order to contribute to updated treatment guidelines and to inform on dosing strategies, efficacy results need to be analyzed first. In this regard, it will be interesting to see whether not only dose and exposure metrics correlate, but also to study the correlation of infection intensity and systemic exposure as well as the occurrence of adverse drug reactions.

References

- Avgustinovich, D. F., M. A. Tsyganov, M. Y. Pakharukova, E. N. Chulakov, A. V. Dushkin, V. P. Krasnov, and V. A. Mordvinov. 2020. 'Effectiveness of Repeated Administration of Praziquantel with Disodium Glycyrrhizinate and Two Enantiomers of Praziquantel on *Opisthorchis felinus* (Rivolta, 1884)', *Acta Parasitol*, 65: 156-64.
- Cioli, D., L. Pica-Mattocchia, A. Basso, and A. Guidi. 2014. 'Schistosomiasis control: praziquantel forever?', *Mol Biochem Parasitol*, 195: 23-9.
- Crellen, T., M. Walker, P. H. Lamberton, N. B. Kabatereine, E. M. Tukahebwa, J. A. Cotton, and J. P. Webster. 2016. 'Reduced Efficacy of Praziquantel Against *Schistosoma mansoni* Is Associated With Multiple Rounds of Mass Drug Administration', *Clin Infect Dis*, 63: 1151-59.
- el Guiniady, M. A., M. A. el Touny, M. A. Abdel-Bary, S. A. Abdel-Fatah, and A. Metwally. 1994. 'Clinical and pharmacokinetic study of praziquantel in Egyptian schistosomiasis patients with and without liver cell failure', *Am J Trop Med Hyg*, 51: 809-18.
- Fedorova, O. S., M. M. Fedotova, O. I. Zvonareva, S. V. Mazeina, Y. V. Kovshirina, T. S. Sokolova, E. A. Golovach, A. E. Kovshirina, U. V. Konovalova, I. L. Kolomeets, S. S. Gutor, V. A. Petrov, J. Hattendorf, L. M. Ogorodova, and P. Odermatt. 2020. 'Opisthorchis felinus infection, risks, and morbidity in rural Western Siberia, Russian Federation', *PLoS Negl Trop Dis*, 14: e0008421.
- Hotez, P. J., and A. Kamath. 2009. 'Neglected tropical diseases in sub-saharan Africa: review of their prevalence, distribution, and disease burden', *PLoS Negl Trop Dis*, 3: e412.
- Lima, R. M., M. A. D. Ferreira, T. M. de Jesus Ponte Carvalho, B. J. Dumêt Fernandes, O. M. Takayanagui, H. H. Garcia, E. B. Coelho, and V. L. Lanchote. 2011. 'Albendazole-praziquantel interaction in healthy volunteers: kinetic disposition, metabolism and enantioselectivity', *Br J Clin Pharmacol*, 71: 528-35.
- Mandour, M. E., H. el Turabi, M. M. Homeida, T. el Sadig, H. M. Ali, J. L. Bennett, W. J. Leahey, and D. W. Harron. 1990. 'Pharmacokinetics of praziquantel in healthy volunteers and patients with schistosomiasis', *Trans R Soc Trop Med Hyg*, 84: 389-93.
- Meister, I., J. Kovac, U. Duthaler, P. Odermatt, J. Huwyler, F. Vanobberghen, S. Sayasone, and J. Keiser. 2016. 'Pharmacokinetic Study of Praziquantel Enantiomers and Its Main Metabolite R-trans-4-OH-PZQ in Plasma, Blood and Dried Blood Spots in *Opisthorchis viverrini*-Infected Patients', *PLoS Negl Trop Dis*, 10: e0004700.
- Ofori-Adjei, D., K. K. Adjepon-Yamoah, and B. Lindström. 1988. 'Oral praziquantel kinetics in normal and *Schistosoma haematobium*-infected subjects', *Ther Drug Monit*, 10: 45-9.
- Pakharukova, M. Y., A. G. Shilov, D. S. Pirozhkova, A. V. Katokhin, and V. A. Mordvinov. 2015. 'The first comprehensive study of praziquantel effects in vivo and in vitro on European liver fluke *Opisthorchis felinus* (Trematoda)', *Int J Antimicrob Agents*, 46: 94-100.
- Utzinger, J., and J. Keiser. 2013. 'Research and development for neglected diseases: more is still needed, and faster', *Lancet Glob Health*, 1: e317-8.
- WHO. 2020. "Ending the neglect to attain the Sustainable Development Goals: A road map for neglected tropical diseases 2021–2030." <https://www.who.int/publications/i/item/9789240010352>.

Zdesenko, G., and F. Mutapi. 2020. 'Drug metabolism and pharmacokinetics of praziquantel: A review of variable drug exposure during schistosomiasis treatment in human hosts and experimental models', *PLoS Negl Trop Dis*, 14: e0008649.